Order Number 9207094

Estimation of clearances and impact forces of mechanical systems using vibro-impact response

Lin, Shao-Quan, Ph.D.

City University of New York, 1991

U·M·I
300 N. Zeeb Rd.
Ann Arbor, MI 48106

A

ESTIMATION OF CLEARANCES AND IMPACT FORCES OF MECHANICAL SYSTEMS USING VIBRO-IMPACT RESPONSE

by

SHAO-QUAN LIN

A dissertation submitted to the Graduate Faculty in Engineering in partial fulfillment of the requirements for the degree of Doctor of Philosophy, The City University of New York.

1991

This manuscript has been read and accepted for the Graduate Faculty in Engineering in satisfaction of the dissertation requirement for the degree of Doctor of Philosophy.

24th May 91
Date

C Bapat
Chair of Examining Committee

5/29/91
Date

Gerald G. Lowen
Executive Officer

Professor Charusheel N. Bapat

Professor Stephen Cowin

Professor Gerald G. Lowen

Professor Ali M. Sadegh

Professor M. Senator

Supervisory Committee

The City University of New York

Abstract

ESTIMATION OF CLEARANCES AND IMPACT FORCES
OF MECHANICAL SYSTEMS USING VIBRO-IMPACT RESPONSE

by

Shao-Quan Lin

Advisor: Professor Charusheel N. Bapat

Increasing clearances in many mechanical and industrial systems are closely related to wear. Hence accurate estimation of clearances and impact forces is extremely important in system monitoring and preventive maintenance. Three novel approaches are developed in this dissertation to estimate clearances and impact forces in situ by measuring and using vibro-impact responses of these systems. The describing function approach and the optimization approach are developed for a system under a deterministic excitation and the spectral analysis approach is developed for a system under a random excitation. These three approaches are presented and tested using a single degree of freedom impact oscillator model. Extension of these approaches to a continuous beam-stop system is presented to illustrate the applicability to other complex systems with clearances. Computer programs based on these approaches were developed to estimate clearances and impact forces. Both computer simulated experiments and physical experiments were conducted to test these approaches. The estimates obtained using vibroimpact responses from the mechanical analogues of an impact oscillator and a beam-stop system and from a

computer program to simulate an impact oscillator agreed well with actual clearances and impact forces. The effects of input amplitude and frequency, stiffness and clearance size, asymmetry, and damping on estimation of clearances are studied and guidelines are developed for practical use.

ACKNOWLEDGMENTS

I wish to express my sincere appreciation to my adviser Professor Charusheel N. Bapat for his support and guidance throughout the course of this research.

My appreciation also goes to Professors Stephen Cowin, Gerald G. Lowen, Ali M. Sadegh and M. Senator for serving on my Supervisory Committee. I specially wish to thank Professor Gerald G. Lowen for his encouragement and constant help.

This research was partially supported by the PSC-CUNY and an Engineering Research Equipment Grant, No MSM-8506495, from the National Science Foundation of the U.S.A.

TO MY FAMILY

TABLE OF CONTENTS

CHAPTER I.	INTRODUCTION	1
CHAPTER II.	ESTIMATION OF CLEARANCES AND IMPACT FORCES FOR SYSTEMS UNDER A DETERMINISTIC EXCITATION	7
2.1	INTRODUCTION	7
2.2	AN IMPACT OSCILLATOR MODEL	8
2.3	DESCRIBING FUNCTION APPROACH	13
2.4	OPTIMIZATION APPROACH	20
2.5	EXPERIMENTS AND COMPUTATIONS	22
2.5.1	SIMULATION USING A DIGITAL COMPUTER	22
2.5.2	EXPERIMENTS USING A MECHANICAL ANALOGUE	24
2.5.3	COMPUTATION PROCEDURE	29
2.6	RESULTS AND DISCUSSION	30
2.7	CONCLUSIONS	72
CHAPTER III.	ESTIMATION OF CLEARANCES FOR SYSTEMS UNDER A RANDOM EXCITATION	73
3.1	INTRODUCTION	73
3.2	THEORY	74
3.3	EXPERIMENTS AND COMPUTATIONS	83
3.3.1	SIMULATION USING A DIGITAL COMPUTER	83

3.3.2	EXPERIMENTS USING A MECHANICAL ANALOGUE	84
3.3.3	COMPUTATION PROCEDURE	86
3.4	RESULTS AND DISCUSSION	87
3.5	CONCLUSIONS	106
CHAPTER IV.	ESTIMATION OF CLEARANCES AND IMPACT FORCES FOR A BEAM-STOP SYSTEM	109
4.1	INTRODUCTION	109
4.2	MODEL OF A BEAM-STOP SYSTEM	110
4.3	ESTIMATION OF CLEARANCE AND IMPACT FORCES	115
4.4	EXPERIMENTS	120
4.4.1	EXPERIMENTAL SETUP	120
4.4.2	FREQUENCY RESPONSE FUNCTIONS	121
4.4.3	ESTIMATION PROCEDURE	125
4.5	RESULTS AND DISCUSSION	127
4.6	CONCLUSIONS	147
CHAPTER V.	CONCLUSIONS	148
APPENDIX A.	FORCED VIBRATION OF A BEAM SUPPORTED AT MANY LOCATIONS	150
A1.	UNDER A BASE EXCITATION	153
A2.	UNDER A CONCENTRATED FORCE EXCITATION	154

APPENDIX B.	THE EFFECT OF DAMPING ON VIBRATION OF BEAM AT RESONANCE	156
B1.	UNDER A BASE EXCITATION	156
B2.	UNDER THE EXCITATION OF A CONCENTRATED FORCE	158
APPENDIX C.	COMPUTER PROGRAMS	160
C1.	Program IOSIMU	160
C2.	Program DFA	167
C3.	Program OPA	171
C4.	Program SPASIMU	176
C5.	Program SPAEX	182
C6.	Program HB	188
C7.	Program HF	195
C8.	Program BMDFA	202
C9.	Program BMOPA	207
C10.	Program BMSPA	213
C11.	Function ER	220
C12.	Subroutine FFT	222
C13.	Subroutine POWELL	225
C14.	Subroutine DSCPOW	227
REFERENCES		231

LIST OF TABLES

TABLE 1. The clearance estimation results and values of intermediate variables of the case of Figure 10. The actual clearances were $d_1 = d_2$ 1.19 mm. 33

TABLE 2. Estimation of clearances when actual clearances were nonidentical. The parameters were: $d_1 = 1.80 \pm 0.05$ mm and $d_2 = 0.64 \pm 0.05$ mm, and stop springs with stiffness $k_1 = 11906 \pm 100$ N/m and $k_2 = 11748 \pm 100$ N/m. 51

TABLE 3. Estimation of clearances in case of a one sided stop. The parameters were: (a) strong stop: $k_2 = 11748 \pm 100$ N/m and $d_2 = 0.64 \pm 0.05$ mm, (b) weak stop: $k_2 = 1643 \pm 50$ N/m and $d_2 = 1.27 \pm 0.05$ mm. 54

TABLE 4. The effect of weak springs $k_1 = 1675 \pm 50$ N/m and $k_2 = 1643 \pm 50$ N/m. (a) Practically identical clearances, $d_1 = d_2 = 1.27 \pm 0.05$ mm. (b) Nonidentical clearances, $d_1 = 0.71 \pm 0.05$ mm and $d_2 = 1.27 \pm 0.05$ mm. 56

TABLE 5. The comparison of estimated clearances with actual values for an oscillator with nonidentical stiffnesses and gaps. The parameters were $k_1 = 11748 \pm 100$ N/m, $k_2 = 1643 \pm 50$ N/m, $d_1 = 1.63 \pm 0.05$ mm and $d_2 = 1.27 \pm 0.05$ mm. 59

TABLE 6. Estimation of clearances using data from mechanical experiments when clearances and support springs were practically identical. The actual clearances were: $d_1 = 1.22 \pm 0.05$ mm and $d_2 = 1.19 \pm 0.05$ mm. 91

TABLE 7. Estimation of clearances using computer simulated data when clearances and support springs were practically identical. The actual clearances were: $d_1 = 1.22$ mm and $d_2 = 1.19$ mm. 92

TABLE 8. Comparison of actual clearances to its estimates based on data from mechanical experiments. 96

TABLE 9. Comparison of actual clearances to its estimates based on data from computer simulation. 103

TABLE 10. Comparison of natural frequencies obtained from experiments and calculations. 124

TABLE 11. Estimates of clearances based on data from mechanical experiments under sinusoidal excitation. The system parameters were $x_1 = 435$ mm, $x_2 = 549$ mm, $k_1 = k_2 = 11600 \pm 100$ N/m and $d_1 = d_2 = 0.64 \pm 0.05$ mm. 135

TABLE 12. Estimates of clearances based on data from mechanical experiments under sinusoidal excitation. The system parameters were $x_1 = 435$ mm, $x_2 = 549$ mm, $k_1 = k_2 = 11600 \pm 100$ N/m and $d_1 = d_2 = 0.25 \pm 0.05$ mm. 139

TABLE 13. Estimates of clearances based on data from mechanical experiments under sinusoidal excitation. The system parameters were $x_1 = 435$ mm, $x_2 = 549$ mm, $k_1 = k_2 = 11600 \pm 100$ N/m and asymmetric clearances $d_1 = 0.25 \pm 0.05$ mm and $d_2 = 0.64 \pm 0.05$ mm, i.e. a overall clearance $d_1+d_2 = 0.89 \pm 0.1$ mm. 143

TABLE 14. Estimates of clearances based on data from mechanical experiments under sinusoidal excitation. The system parameters were $x_1 = 361$ mm, $x_2 = 549$ mm, $k_1 = k_2 = 11600 \pm 100$ N/m and $d_1 = d_2 = 0.71 \pm 0.05$ mm. 146

LIST OF FIGURES

FIGURE 1.	Some mechanical and industrial structures containing clearances.	2
FIGURE 2.	A model of an impact oscillator.	7
FIGURE 3.	Block diagram of an impact oscillator.	9
FIGURE 4.	(a) Feedback representation of an impact oscillator. (b) Its decomposition into a two input one output system and a dead-zone nonlinearity.	12
FIGURE 5.	(a) The relation between the input y(t) and an impact force u(t) for the dead-zone nonlinearity and (b) their temporal variation.	15
FIGURE 6.	Isolated stop-clearance nonlinearity with measured y(t) and u(t) calculated using equation (2.32).	21
FIGURE 7.	Mechanical analogue of an impact oscillator and attached transducers.	25
FIGURE 8.	Experimental instrumentation.	26
FIGURE 9.	Experimental and theoretical frequency response function of the oscillator without stops.	28
FIGURE 10.	The traces of b(t), x(t) and y(t). (a) Mechanical experiment; (b) Computer simulation. The system parameters were m = 0.1061 kg, c = 0.7127 Ns/m, k_0 = 1746 N/m, $k_1 = k_2$ = 11663 N/m, $d_1 = d_2$ = 1.19 mm and b(t) = 0.687sin40πt mm.	32

FIGURE 11. The frequency spectra B(f) and Y(f). (a) Mechanical experiment; (b) Computer simulation. The system parameters were identical to those reported in Figure 10. 35

FIGURE 12. The frequency spectra U(f). (a) Mechanical experiment; (b) Computer simulation; (c) The $\hat{U}(f)$ which is the Fourier transform of the $\hat{u}(t)$ from the mechanical experimental data. The system parameters were identical to those reported in Figure 10. 37

FIGURE 13. The temporal distribution of impact forces u(t). (a) Measured using an impedance head, (b) Estimated using the experimental data in the describing function approach, (c) Calculated using experimental data in equation (2.32), (d) Calculated using computer generated data in equation (2.32), (e) Estimated using experimental data and the optimization approach, and (f) Filtering measured y(t) and calculated u(t) of Figure (c) above 200 Hz. The system parameters were identical to those reported in Figure 10. 38

FIGURE 14. The objective function $J(\hat{d}_1, \hat{d}_2)$ as a function of $\hat{d}_1$ by fixing $\hat{d}_2$ = 1.19 mm, (a) using mechanical experimental data and (b) using computer simulated data. The system parameters were identical to those reported in Figure 10. 39

FIGURE 15. The effect of varying the input base amplitude |b(t)| on the clearance estimation. (a) Estimation of clearance d_1. (b) Estimation of clearance d_2. The main system parameters are identical to those given in Figure 10. The results in this and other figures are presented by:
Data from experiment;
○ Describing Function Approach,
□ Optimization Approach.
Data from computer simulation;
△ Describing Function Approach,
◇ Optimization Approach.
Averages of corresponding estimates are represented by corresponding blocked symbols. 43

FIGURE 16. The y(t), Y(f) and U(f) of one case of Figure 15 where |b(t)| = 3.515 mm. (a) Mechanical experiment and (b) Computer Simulation. 44

FIGURE 17.	The effect of varying the input base amplitude |b(t)| on the impact force estimation. (a) Estimated impact force $\hat{u}(t)$ from the optimization approach. (b) Measured impact force. The main system parameters are identical to those given in Figure 10.	46
FIGURE 18.	The effect of varying the input frequency of the sinusoidal input on the clearance estimation. |b(t)| = 1.4 mm. (a) Estimation of clearance d_1 and (b) Estimation of clearance d_2. The main system parameters are identical to those given in Figure 10 and Symbols are same as those used in Figure 15.	47
FIGURE 19.	The effect of varying the input frequency of the sinusoidal input on the impact force estimation. (a) Estimated impact force $\hat{u}(t)$ from the optimization approach. (b) Measured impact force. The main system parameters are identical to those given in Figure 10.	49
FIGURE 20.	(a) The trace y(t) and (b) the frequency spectrum Y(f) for a case considered in Table 2 column 3. The b(t) was 1.58sin(50πt) mm.	52
FIGURE 21.	The impact force, (a) u(t) obtained using equation (2.32) and (b) $\hat{u}(t)$ estimated using the optimization approach. Parameters are same as those of Table 3 and b(t) was 0.71sin50πt mm.	55
FIGURE 22.	The spectra of (a) U(f), (b) $\hat{U}(f)$ and impact force (c) u(t) and (d) $\hat{u}(t)$. The parameters were $k_1 = 1675 \pm 50$ N/m, $k_2 = 1643 \pm 50$ N/m, $d_1 = d_2 = 1.27 \pm 0.05$ mm, and b(t) = 0.54sin50πt mm.	58
FIGURE 23.	(a) The y(t), (b) Y(f), (c) u(t) and (d) $\hat{u}(t)$ for a system when oscillator was hitting only one side. The input was 0.15sin40πt mm and other parameters are identical to those of Table 5.	60
FIGURE 24.	(a) The y(t), (b) Y(f), (c) u(t) and (d) $\hat{u}(t)$ for a system when oscillator was hitting both sides. The input was 0.71sin40πt mm and other parameters are identical to those of Table 5.	61

FIGURE 25.	Effect of dimensionless amplitude of excitation, β. System parameters were $\zeta = 0.25$, $s_1 = s_2 = 10$, $\delta = 1$ and $\lambda = 0.8$. Symbols in Figures 25-31 are same as those of Figure 15.	64
FIGURE 26.	Effect of excitation frequency ratio λ. System parameters were $\zeta = 0.25$, $s_1 = s_2 = 10$, $\delta = 1$ and $\beta = 3.2$.	65
FIGURE 27.	Effect of stiffness ratio. System parameters were $\zeta = 0.25$, $s_1 = s_2$, $\delta = 1$, $\beta = 1$ and $\lambda = 1.6$.	66
FIGURE 28.	Effect of unequal stop stiffnesses. System parameters were $\zeta = 0.15$, $s_1 = 10$, $\delta = 1$, $\beta = 1$ and $\lambda = 2.5$.	67
FIGURE 29.	Effect of unequal clearances. System parameters were $\zeta = 0.15$, $s_1 = s_2 = 10$, $\beta = 3$, $\lambda = 2.5$ and dimensionless clearance corresponding to d_1 is 1.0.	68
FIGURE 30.	Effect of primary system damping ratio, ζ. System parameters were $s_1 = s_2 = 10$, $\delta = 1$, $\beta = 1$ and $\lambda = 2.5$.	69
FIGURE 31.	Effect of adding noise to system output. System parameters were $\zeta = 0.15$, $s_1 = s_2 = 10$, $\delta = 1$, $\beta = 3$ and $\lambda = 0.8$.	71
FIGURE 32.	Experimental instrumentation.	85
FIGURE 33.	Sample records from mechanical experiment, (a) Base excitation b(t), (b) System response y(t). The system parameters were m = 0.1061 kg, k_0 = 1746 N/m, c = 0.7127 Ns/m, $k_1 = k_2 = 11600 \pm 100$ N/m, $d_1 = 1.22 \pm 0.05$ mm and $d_2 = 1.19 \pm 0.05$ mm.	89
FIGURE 34.	The spectra (a) $S_y(\omega)$ and (b) $S_{yu}(\omega)$ corresponding to the sample shown in Figure 33. The (c) and (d) represents respectively the $S_y(\omega)$ and $S_{yu}(\omega)$ obtained using all ten samples.	90

FIGURE 35.	(a) Force excitation g(t), (b) system response y(t), and spectra (c) $S_y(\omega)$ and (d) $S_{yu}(\omega)$ using 1 sample from computer simulation. The system parameters were m = 0.1061 kg, k_0 = 1746 N/m, c = 0.7127 Ns/m, $k_1 = k_2$ = 11600 N/m, d_1 = 1.22 mm and d_2 = 1.19 mm.	94
FIGURE 36.	The spectra from computer simulation. (a) $S_y(\omega)$ and (b) $S_{yu}(\omega)$ using 10 records, (c) $S_y(\omega)$ and (d) $S_{yu}(\omega)$ using 100 records. The system parameters were the same as those of Figure 35.	95
FIGURE 37.	Sample records of system response y(t) of the case in Table 8, row 2.	97
FIGURE 38.	Sample records of system response y(t). (a) Mechanical experiment and (b) Computer simulation. The system parameters were m = 0.1061 kg, k_0 = 1746 N/m, c = 0.7127 Ns/m, $k_1 = k_2$ = 1750 N/m, d_1 = 0.81 mm and d_2 = 1.52 mm.	98
FIGURE 39.	The spectra of the same system of Figure 38 estimated using 10 records. (a) $S_y(\omega)$ and (b) $S_{yu}(\omega)$ from mechanical experiments, (c) $S_y(\omega)$ and (d) $S_{yu}(\omega)$ from computer simulation.	99
FIGURE 40.	Sample records of system response y(t). (a) Mechanical experiment and (b) Computer simulation. The system parameters were m = 0.1061 kg, k_0 = 1746 N/m, c = 0.7127 Ns/m, k_1 = 1750 N/m, k_2 = 11600 N/m, d_1 = 0.81 mm and d_2 = 1.45 mm.	101
FIGURE 41.	The cross spectra $S_{yu}(\omega)$ of the same system of Figure 40. (a) Estimated using 10 records from mechanical experiments, (b) Estimated using 10 records from computer simulation and (c) Estimated using 100 records from computer simulation.	102
FIGURE 42.	The effect of varying the intensity of random excitation on the clearance estimation.	104
FIGURE 43.	The effect of identical spring stiffnesses of stops on the clearance estimation. The $d_1 = d_2$ = 1.2 mm and σ_g = 10 N.	105

FIGURE 44.	The effect of clearance size on the clearance estimation. The clearances were identical i.e. $d_1 = d_2$ and the input was $\sigma_g = 3d_1k_0$ N.	107
FIGURE 45.	The effect of varying damping coefficient on the clearance estimation. The clearances were $d_1 = d_2 = 1.2$ mm and $\sigma_g = 10$ N.	108
FIGURE 46.	A cantilever beam with a pair of stops.	111
FIGURE 47.	Decomposition of the beam-stop system into two systems (a) and (b).	112
FIGURE 48.	(a) Block diagram of the beam-stop system and (b) its decomposition.	114
FIGURE 49.	Experimental setup for the beam-stop system.	121
FIGURE 50.	Frequency response function $H_{b2}(f)$. (a) From deterministic experiment, O , and from calculations, - - - -. (b) From random experiment, —— .	123
FIGURE 51.	Frequency response functions.	124
FIGURE 52.	The traces of b(t) and $y_2(t)$. The system parameters were $x_1 = 435$ mm, $x_2 = 549$ mm, $k_1 = k_2 = 11600 \pm 100$ N/m, $d_1 = d_2 = 0.64 \pm 0.05$ mm and $b(t) = 0.98\sin(38\pi t)$ mm.	129
FIGURE 53.	The frequency spectra B(f) and $Y_2(f)$. The system parameters were identical to those reported in Figure 52.	130
FIGURE 54.	The frequency spectra U(f), $\hat{U}(f)$ and $Y_1(f)$. The system parameters were identical to those reported in Figure 52.	131
FIGURE 55.	The traces of u(t) and $y_1(t)$. The system parameters were identical to those reported in Figure 52.	132

FIGURE 56.	The estimated and measured impact forces u(t). (a) Estimated using experimental data and the optimization approach. (b) Measured using an impedance head. The system parameters were identical to those reported in Figure 52.	133
FIGURE 57.	(a) Estimated impact force $\hat{u}(t)$ from the optimization approach. (b) Measured impact force. The system parameters were identical to those given in Table 11.	138
FIGURE 58.	Typical measured system excitation b(t) and response $y_2(t)$ and their spectra. The system parameters were identical to those given in Table 12.	140
FIGURE 59.	(a) The power spectrum $S_{y1}(f)$ and (b) The cross spectrum $S_{y1u}(f)$. The system parameters were identical to those reported in Table 12.	141
FIGURE 60.	(a) The sinusoidal excitation b(t) and (b) the response $y_2(t)$ of a beam-stop system with asymmetric clearances. The system parameters were identical to those reported in Table 13 and $b(t) = 0.69\sin(38\pi t)$ mm.	144
FIGURE 61.	(a) The random excitation b(t) and (b) the response $y_2(t)$ of a beam-stop system with asymmetric clearances. The system parameters were identical to those reported in Table 13.	145

CHAPTER I.

INTRODUCTION

Clearances exist in many mechanical and industrial structures. In heat exchangers and nuclear piping systems, clearances are incorporated between tubes and baffle plates and between pipe and snubbers (positioned along the length) to control large amplitude displacements and to allow the thermal expansion, respectively [1]. In kinematic pairs of mechanisms and machines such as ball and roller bearings, meshing gears, cams and robot arms the existence of clearance is the result of manufacturing tolerances and/or many times is essential for functioning [2-6]. Control system devices and precision mechanisms possess clearances as motion limiting constraints or as deadspace nonlinearities. In vibration isolation mounts for mechanical systems, clearances allow the equipment to function freely without impacts over a designed displacement range but limits the accidental maximum displacement. Many times, clearances are incorporated in relays, slider-crank mechanisms, valves, pumps and many measuring devices to allow the required motion for their functioning. Clearances may exist for lubrication purpose or may develop in many mechanical systems and linkages due to wear [7]. Some of these systems are shown in Figure 1.

Vibrating members of systems with clearances impact, produce noise, excite vibrations at higher frequencies and accelerate wear. The wear in turn will enlarge the clearances and results in a loss of precision, performance, and stability. On the other hand, since clearances are closely related to wear and system failure, they could be used as an important monitoring parameter to reach an accurate assessment of the system's health

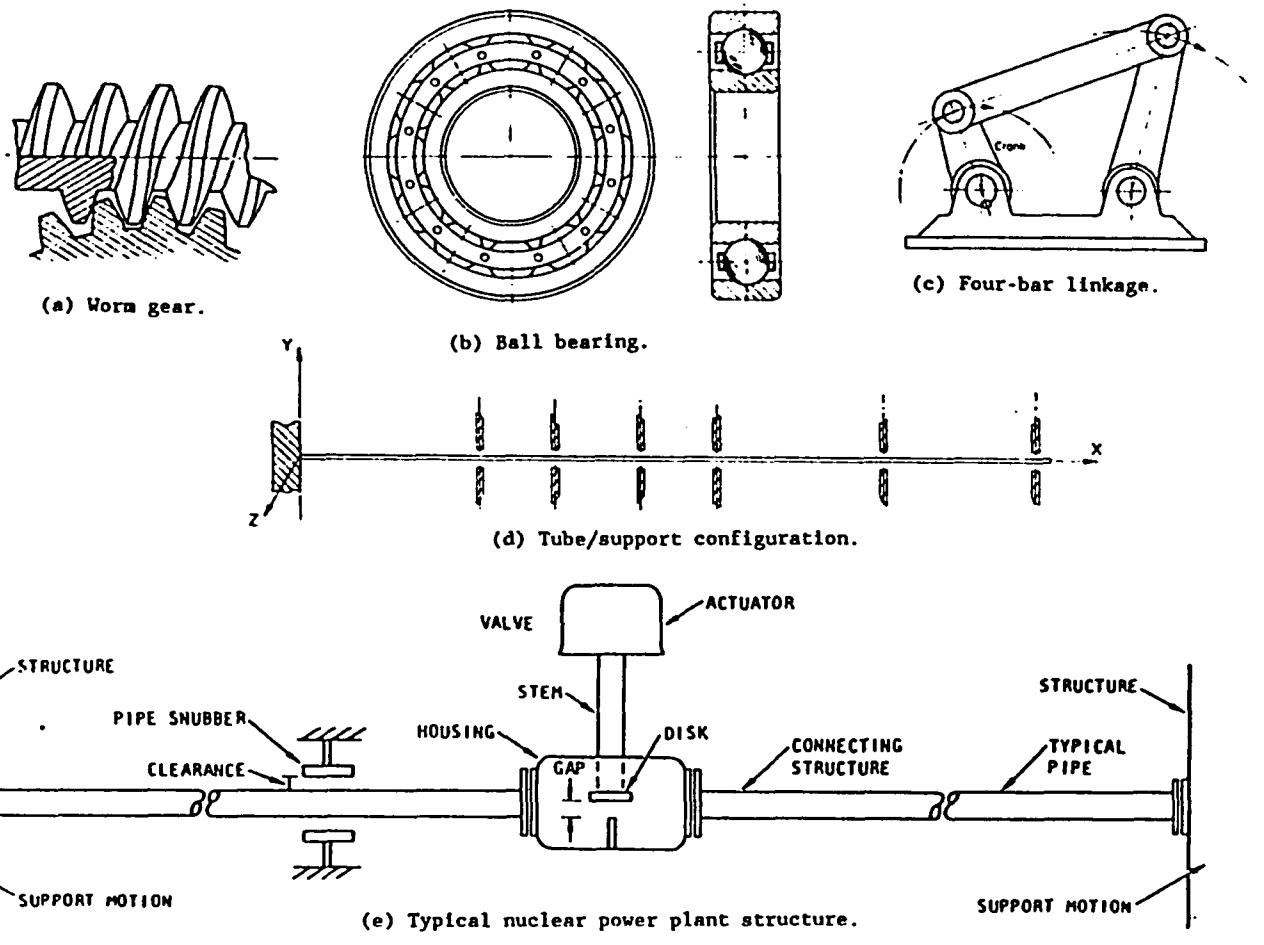

Figure 1. Some mechanical and industrial structures containing clearances.

[8,9]. As an example, the flow-induced vibrations of heat exchanger tubes cause impact/fretting wear at the highly vulnerable tube-baffle interfaces and clearances continue to increase with time due to tube thinning and hole enlargement which eventually leads to heat exchanger tube failures [10-14]. It was reported that tube support plates were the most common location for tube failures, accounting for 41.8% of the defects [14]. Indian Point 2 Reactor in USA reported [14] that twenty-six steam generator tubes were plugged in one year because of reduced tube diameter at the support plates. Since a single tube leak may result in extended and costly power plant failure and repairs, an early warning of failures is of vital importance. The danger of tube failure grows with increase in clearance and as such clearance can be used as an important monitoring parameter to indicate time scales for critical damage to occur. Additionally, the impact forces due to the clearances could also be used to estimate the wear rate [15,16].

The locations where clearances are usually present are inside the system and hence clearances could not be measured directly without the disassembly of the system, which in most cases is impractical. Stoppage only to measure clearances could be extremely expensive in lost production or service. As such several on-line approaches are under development to accurately determine clearances, but special transducers based on ultrasonic, eddy-current, or fiber-optics principle need to be installed into the system as an integral part of the clearance [8]. These approaches are accurate but need access to put the transducers into the system and this limits the use of these approaches to already fabricated systems. Additionally, these transducers are quite expensive and this limits their application to specialized and expensive systems and they also do not provide any hint of the developed impact forces.

The aim of the research presented is to develop techniques of on-line, in-situ clearance and impact force estimation using vibro-impact response. It is assumed that the system with unknown clearances is excited by known deterministic or random forces and vibration signals are picked up at some convenient locations. The unknown clearances and the impact forces will be estimated from the vibration signals with reliability and precision. This is an "inverse" problem, which is extremely important in engineering and science and indeed important to mankind in general as man has always been seeking knowledge of a physical system beyond that which is directly observable. In an inverse problem, the structure or some parameters of the system are unknown, the hidden features of the system are to be extracted from the measurement of the input and output of the system. When the structure of the system is known, and only some parameters are unknown and to be found, this inverse problem is known as a parameter estimation problem. The present problem is one of this type as clearances of the system are considered unknown and need to be estimated. Generally, an inverse problem is more difficult to solve than a direct problem. An inverse problem can only be solved on the knowledge of the corresponding direct problem. The difficulty of our clearance estimation problem is further aroused from the inherent nonlinearity because of impacting due to clearances. Parameter estimation is a modern and exciting discipline that is growing rapidly [17-22], however only few papers have been published on clearance and impact force estimation problem. Whiston [15,16] presented a technique of estimating impact force by remote vibration analysis for a beam-stop system. The impact force is considered as an external force and was estimated using an inverse transfer function (the so called Timoshenko transfer function). However, its application to estimate clearances and impact forces of a vibrating system colliding repeatedly is unclear. Cempel [23,24] suggested that the coherence function between a deriving force and a mechanism's

structural vibration, and a harmonic index can be used as a measure of the overall clearances in kinematic pairs. This study only gives a qualitative measure and does not estimate actual clearances and impact forces.

An impact oscillator model is chosen to develop clearance and impact force estimation approaches because of the oscillator's wide applicability and simplicity. At the same time it contains almost all basic response features of a system with clearances. The simple impact oscillator model is a reasonable approximation for many real systems such as measuring devices, fuel gages, torsional gear systems with shafts, piston and cylinder, fuel density meters, dead-space nonlinearity in control systems and elastic members with joint clearances, etc. Impact pair, which can be an idealized model for bearings, gears, cams, and mechanism joints, can also be considered as a special case of this system where the main spring and damper are very weak [25]. Additionally many continuous systems such as a beam-stop system can be reduced to an impact oscillator model when only the first mode is considered [26-33]. Dubowsky and Freudensten formulated an elastic mechanical joint with clearances to an impact pair model [34]. They suggested that for common coupling the surface compliance could be represented by a linear spring rate. They believed that the simple, elastic, impact-pair model exhibits a variably dynamic characteristic which are representative of mechanical systems with clearances [35]. Masri [26] reduced a cantilever beam with a stop to a single-degree-of-freedom system (an impact oscillator) and derived a steady state solution under harmonic excitations. Late this work was extended by Anderson and Masri [31] to material nonlinearity and to impulsive base acceleration. Chen et al. [32] studied a force excited beam supported at the ends and with a motion limiting stop at the midpoint. A solution method determining the steady state motion was developed by reducing the system to an impact oscillator model. Galhoud, Masri and Anderson [33] derived an exact solution for the steady state motion of

a viscous damped two-degree-of-freedom impact oscillator with non-symmetric clearances, under the action of harmonic excitation. A four-bar linkage with a clearance was also shown to be dynamically equivalent to an impact oscillator in terms of generalized coordinates [36]. Dynamics of systems with piecewise-linear characteristic as the impact oscillator were studied by many investigators [37-41].

Three novel clearance and impact force estimation approaches are presented in this dissertation. Two approaches, the describing function approach and the optimization approach are developed for systems under a deterministic excitation. These two approaches are presented and are tested using a single degree of freedom impact oscillator model in Chapter 2. A third approach, the spectral analysis approach, is developed for systems under random excitation, which is presented in Chapter 3 together with the testing results. The needed vibro-impact response of an impact oscillator was obtained using an approach of simulation of motion on a digital computer and using a mechanical analogue. The comparison of estimated quantities with actual values indicated a good agreement. The application of these clearance estimation approaches to a continuous beam-stop system is presented in Chapter 4 to illustrate that the three estimation approaches developed on an impact oscillator model can be easily extended to other more complex systems with clearances. A mechanical analogue of the beam-stop model was used to generate the needed vibro-impact response and the estimated quantities were again shown to agree with the actual values.

CHAPTER II.

ESTIMATION OF CLEARANCES AND IMPACT FORCES FOR SYSTEMS UNDER A DETERMINISTIC EXCITATION

2.1 INTRODUCTION

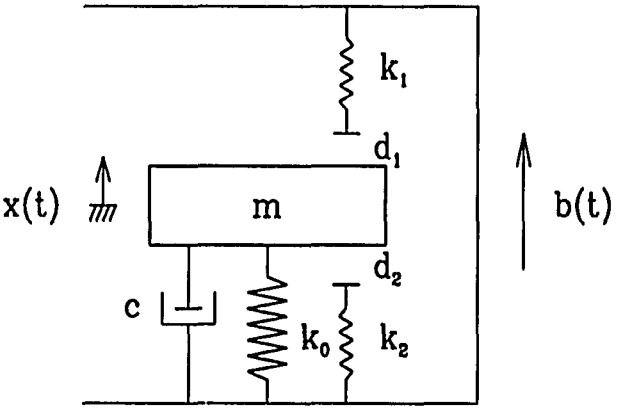

Figure 2. A model of an impact oscillator.

Two approaches to estimate clearances and impact forces for systems under a deterministic excitation will be developed in this chapter using an example of an impact oscillator model shown in Figure 2 with two asymmetric motion limiting stops with nonidentical spring stiffnesses. The impact oscillator is chosen because of its wide applicability and simplicity, and also because it contains almost all the basic features of systems with clearances. The response of an impact oscillator is inherently nonlinear due to its collisions with stops. Without the stops, it is simply a single degree of freedom linear

oscillator. It could be suggested that an impact oscillator can be seen as a combination of a linear part and a nonlinear part of clearances and stops. Most systems with clearances can be decomposed in such a way. This common feature connects the impact oscillator model to other systems with clearances and makes the approaches derived here immediately applicable on other systems with clearances. It will be seen that such decomposition takes advantage of the well developed linear analysis techniques to a maximum extent and greatly reduces the complexity of clearance and impact force estimation.

The next section gives the system representation of an impact oscillator model. In Sections 2.3 and 2.4 the theory of the describing function approach and the optimization approach to estimate clearances and impact forces is presented. The predictions of these approaches were compared with actual values using vibro-impact responses obtained by simulating the motion using a digital computer and from physical experiments conducted using a mechanical analogue of an impact oscillator. The experiments and computations are described in Section 2.5. The results of mechanical and computer simulated experiments are reported and discussed in Section 2.6. The comparison of estimated quantities with actual values indicates a good agreement and shows that the approaches presented are promising.

2.2 AN IMPACT OSCILLATOR MODEL

Consider an impact oscillator model shown in Figure 2 with a known mass, m, a linear spring with stiffness, k_0, and a viscous damper with damping constant c. The d_1 and d_2 are the unknown clearances (to be estimated) between the oscillator and the two elastic stops. The corresponding spring stiffnesses of stop springs k_1 and k_2, respectively, are assumed known. Let b(t) be the known external base excitation and x(t) be the absolute

displacement of the mass measured from the static equilibrium position. Let $y(t)=x(t)-b(t)$ be the relative displacement between the mass and the base. The differential equation of motion of mass m can be written as

$$m\ddot{y}(t)+c\dot{y}(t)+k[y(t)]=-m\ddot{b}(t), \tag{2.1}$$

where

$$k(y) = \begin{cases} k_0 y+(y+d_2)k_2 & -\infty < y \le -d_2, \\ k_0 y & -d_2 < y < d_1, \\ k_0 y+(y-d_1)k_1 & d_1 \le y < \infty, \end{cases} \tag{2.2}$$

and superscript dot represents differentiation with respect to time t. The above equations remain essentially the same when mass m is excited by an external force g(t). In that case, y(t) and $-m\ddot{b}(t)$ will be, respectively, replaced by x(t) and g(t) in the above equations.

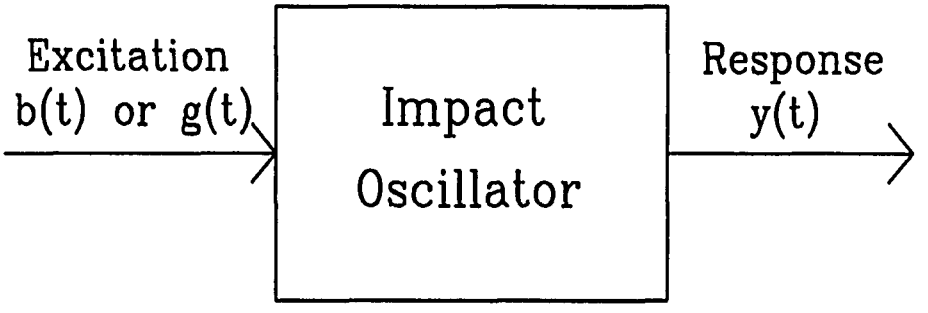

Figure 3. Block diagram of an impact oscillator.

With k(y) defined by equation (2.2), equation (2.1) is clearly a nonlinear differential equation describing a nonlinear system given by the block diagram of Figure 3. It is assumed throughout that the system excitation and response are available and to be used in the estimation of clearances and impact forces. The inherent nonlinearity of the system makes such estimation difficult. A different way of looking at and presenting the system in the following will greatly simplify the problem.

Equations (2.1) and (2.2) can be rearranged by separating intermittently produced impact forces u[y(t)] generated by the stops out of k[y(t)] and transferring to the right hand side as

$$m\ddot{y}(t)+c\dot{y}(t)+k_0y(t)=-m\ddot{b}(t)-u[y(t)], \tag{2.3}$$

where

$$u[y(t)] = \begin{cases} k_2(y(t)+d_2) & -\infty < y(t) \le -d_2, \\ 0 & -d_2 < y(t) < d_1, \\ k_1(y(t)-d_1) & d_1 \le y(t) < \infty. \end{cases} \tag{2.4}$$

Fourier transform of both sides of equation (2.3) yields

$$(k_0-m\omega^2+ic\omega)Y(\omega)=m\omega^2B(\omega)-U(\omega), \tag{2.5}$$

where Y(ω), B(ω) and U(ω) are the Fourier transforms of y(t), b(t) and u[y(t)], respectively. The definitions of forward and inverse Fourier transforms are

$$X(\omega)=\int_{-\infty}^{+\infty}x(t)e^{-j\omega t}dt \tag{2.6}$$

and

$$x(t)=\frac{1}{2\pi}\int_{-\infty}^{+\infty}X(\omega)e^{j\omega t}d\omega. \tag{2.7}$$

Solving the equation (2.5) for Y(ω) gives

$$Y(\omega) = H(\omega)\,[m\omega^2 B(\omega) - U(\omega)] = m\omega^2 H(\omega)B(\omega) - H(\omega)U(\omega), \tag{2.8}$$

where

$$H(\omega) = \frac{1}{(k_0 - m\omega^2 + ic\omega)}. \tag{2.9}$$

The H(ω) is the frequency response function of a single degree of freedom oscillator and is defined as the ratio of the Fourier transformed displacement and external force [42,43].

Equations (2.3) and (2.4) or alternatively equations (2.8), (2.9) and (2.4) totally define the impact oscillator. A block diagram of a feedback system shown in Figure 4(a) can be constructed from these equations. The feedback representation of the system reveals more clearly the physical property of the impact oscillator. The mass vibrates under the base excitation and hits the stop springs to produce the impact force which is fed back to the single degree of freedom oscillator. Careful examination of equation (2.8) and Figure 4(a) reveals that the response of an impact oscillator can be considered as a combination of a linear response $m\omega^2 H(\omega)B(\omega)$ due to the external excitation b(t) and a nonlinear response $H(\omega)U(\omega)$ due to the impact forces. The straight-forward element of the feedback system is linear and the nonlinearity is only due to the nonlinear force deflection characteristics of the clearance-stop system (also called a dead-zone nonlinearity [44]), which is the feedback element. The u[y(t)] can be considered as a stops generated quasi-input. Then the complete impact oscillator can be further considered as a system made up of two parts as shown in Figure 4(b): a two input one output linear subsystem defined by equation (2.8) or (2.3) and an isolated dead-zone nonlinearity defined by equation (2.4). This decomposition is very advantageous since instead of dealing with the nonlinear system of Figure 3 as a whole, now well developed techniques of linear analysis can be used on the linear subsystem and nonlinear analysis is restricted to

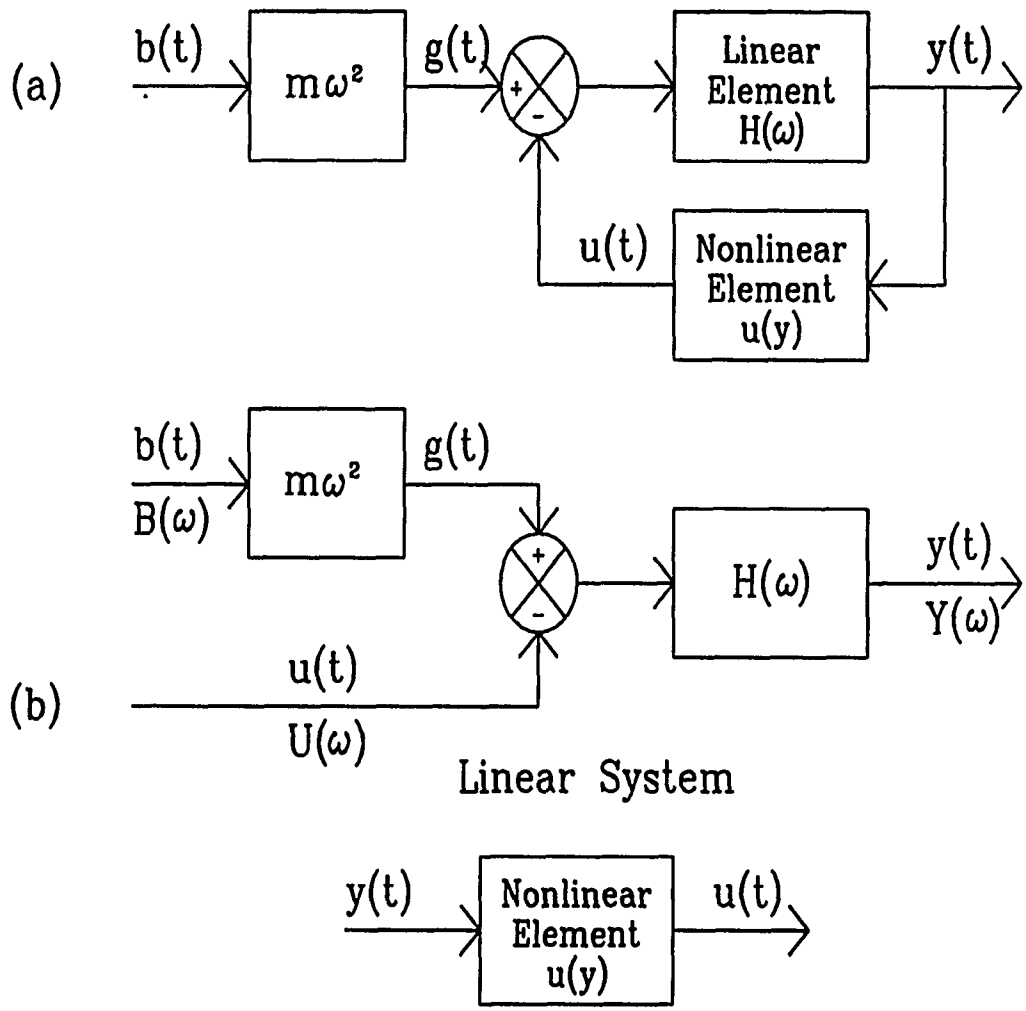

Figure 4. (a) Feedback representation of an impact oscillator. (b) Its decomposition into a two input one output system and a dead-zone nonlinearity.

a relatively simple nonlinearity. This greatly reduces the complexity of clearance and impact force estimation. Many other vibro-impact systems with clearances may be represented by block diagrams similar to Figure 4(a) and could be decomposed to linear subsystem(s) and nonlinear element(s) as Figure 4(b). The estimation approaches presented in this chapter and Chapter 3 using an example of an impact oscillator can be applied to many other systems with clearances. This will be illustrated using a beam-stop system in Chapter 4.

In the following two clearance estimation approaches, the describing function approach and the optimization approach, are presented.

2.3 DESCRIBING FUNCTION APPROACH

A linear system excited by a sinusoidal force reaches a steady-state and its response has the same frequency as the excitation frequency. However, when a nonlinear system is excited sinusoidally, the output contains other harmonics in addition to the fundamental sinusoidal component. In many cases by properly adjusting the input, the other harmonics can be made negligible compared to the fundamental component. Then the nonlinear element can be approximately characterized by the ratio of a fundamental harmonic component of the output to the input and is called a describing function. To account for the phase information, generally this ratio is expressed in the form of a complex number [44,45]. Similarly, describing functions for higher frequency components could be considered. However, the probable improvement at the cost of simplicity was felt to be insignificant. The theory developed to estimate clearances and impact forces based on the describing function method is described next. First the theoretical expressions for two describing functions in terms of clearances will be determined. These two theoretical

expressions will be equated to the experimentally obtained values. This leads to two coupled nonlinear equations whose solutions lead to the estimates of the unknown clearances.

Consider a clearance estimation problem of an impact oscillator shown in Figure 2. Let the base displacement be sinusoidal with amplitude B and circular frequency Ω. It is assumed that the system has reached a steady periodic state. The relation between the output u(t) and the input y(t) of the isolated dead-zone nonlinearity and their temporal variations are shown in Figure 5(a) and 5(b) respectively. Considering only the first two term of the Fourier series expansion, the y(t) can be expressed as

$$y(t) = Y_0 + Y_1 \sin \Omega t. \tag{2.10}$$

The Y_0 represents a d.c. shift of the oscillator, possible under repeated collisions. The two term approximation seems drastic, however it can be seen from the block diagram of Figure 4(a) and the frequency response function given by equation (2.9), that the resonantly excited lightly damped oscillator acts as a low pass filter and as such the higher frequency components in y(t) due to impact force u(t) are drastically attenuated as compared to the first two. The impact force u(t) can be expanded into a Fourier series as

$$u(t) = U_0 + \sum_{n=1}^{\infty} A_n \cos(n\Omega t) + B_n \sin(n\Omega t) = U_0 + \sum_{n=1}^{\infty} U_n \sin(n\Omega t + \phi_n), \tag{2.11}$$

where

$$U_n = \sqrt{A_n^2 + B_n^2} \quad \text{and} \quad \tan \phi_n = \frac{A_n}{B_n}. \tag{2.12}$$

The constant term U_0 of u(t) can be obtained as

$$U_0 = \frac{1}{2\pi} \int_0^{2\pi} u[y(t)] d(\Omega t). \tag{2.13}$$

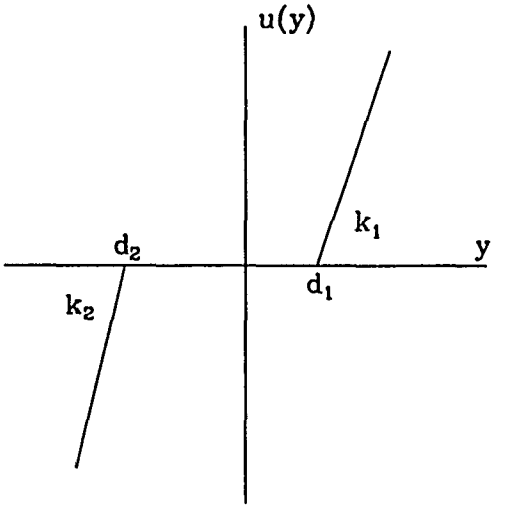

(a)

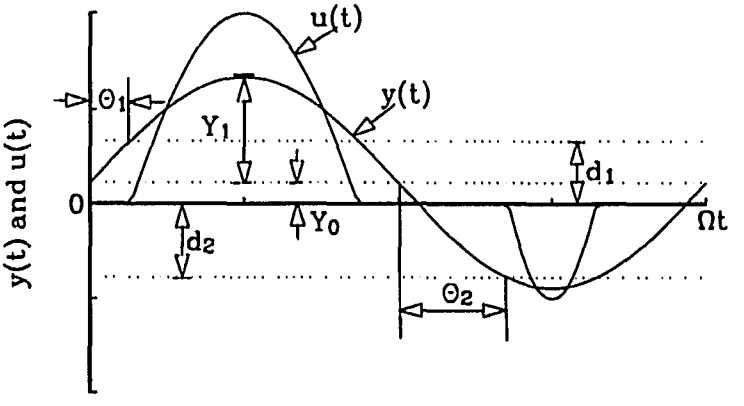

(b)

Figure 5. (a) The relation between the input y(t) and an impact force u(t) for the dead-zone nonlinearity and (b) their temporal variation.

Using the dead-zone nonlinear function given by equation (2.4) and substituting y(t) given by equation (2.10), U_0 can be calculated in view of Figure 5(b) as

$$U_0 = \frac{1}{2\pi}\left[\int_{\theta_1}^{\pi-\theta 1} k_1(Y_0 + Y_1\sin(\Omega t) - d_1)d(\Omega t) + \int_{\pi+\theta_2}^{2\pi-\theta 2} k_2(Y_0 + Y_1\sin(\Omega t) + d_2)d(\Omega t)\right]$$

$$= \frac{Y_1}{2\pi}\{k_1[-(\pi - 2\theta_1)\sin\theta_1 + 2\cos\theta_1] + k_2[(\pi - 2\theta_2)\sin\theta_2 - 2\cos\theta_2]\}, \qquad (2.14)$$

where θ_1 and θ_2 are the phase angles when the mass hits stop 1 and stop 2 respectively and are identified in Figure 5(b). The θ_1 and θ_2 satisfy

$$d_1 = Y_0 + Y_1\sin\theta_1, \quad \text{and} \quad d_2 = -Y_0 + Y_1\sin\theta_2, \qquad (2.15)$$

respectively. Similarly, A_1 and B_1 can be found as,

$$A_1 = \frac{1}{\pi}\int_0^{2\pi} u[y(t)]\cos(\Omega t)d(\Omega t)$$

$$= \frac{1}{\pi}\left[\int_{\theta_1}^{\pi-\theta_1} k_1(Y_0 + Y_1\sin(\Omega t) - d_1)\cos(\Omega t)d(\Omega t) + \int_{\pi+\theta_2}^{2\pi-\theta_2} k_2(Y_0 + Y_1\sin(\Omega t) + d_2)\cos(\Omega t)d(\Omega t)\right]$$

$$= 0 \qquad (2.16)$$

and

$$B_1 = \frac{1}{\pi}\int_0^{2\pi} u[y(t)]\sin(\Omega t)d(\Omega t)$$

$$= \frac{1}{\pi}\left[\int_{\theta_1}^{\pi-\theta_1} k_1(Y_0 + Y_1\sin(\Omega t) - d_1)\sin(\Omega t)d(\Omega t) + \int_{\pi+\theta_2}^{2\pi-\theta_2} k_2(Y_0 + Y_1\sin(\Omega t) + d_2)\sin(\Omega t)d(\Omega t)\right]$$

$$= \frac{Y_1}{2\pi}[k_1(\pi - 2\theta_1 - \sin 2\theta_1) + k_2(\pi - 2\theta_2 - \sin 2\theta_2)]. \qquad (2.17)$$

The amplitude U_1 and the phase shift ϕ_1 of the fundamental harmonic can be expressed as

$$U_1 = \sqrt{A_1^2 + B_1^2} = |B_1| \quad \text{and} \quad \phi_1 = \tan^{-1}\left(\frac{A_1}{B_1}\right) = 0. \qquad (2.18)$$

Using equations (2.10)-(2.18), the relations between U_0, U_1 and Y_0, Y_1 can be expressed as two ratios,

$$N_0 = \frac{U_0}{Y_1} = \frac{1}{2\pi}\{k_1[(2\theta_1 - \pi)\sin\theta_1 + 2\cos\theta_1] - k_2[(2\theta_2 - \pi)\sin\theta_2 + 2\cos\theta_2]\}, \tag{2.19}$$

$$N_1 = \frac{U_1 e^{i\phi_1}}{Y_1} = \frac{1}{2\pi}[k_1(\pi - 2\theta_1 - \sin 2\theta_1) + k_2(\pi - 2\theta_2 - \sin 2\theta_2)], \tag{2.20}$$

which are the describing functions for this impact oscillator. It should be noted that for the impact oscillator the N_0 is always real, however in general N_1 can be a complex number. But as $\phi_1 = 0$ the N_1 is also real in this case and this fact will be used later to develop a simplified expression. The N_0 and N_1 are functions of θ_1 and θ_2 which in turn are functions of two unknown clearances d_1 and d_2 as given by equation (2.15). Substituting experimentally obtained N_0 and N_1 into the left hand sides of equations (2.19) and (2.20) respectively and solving these two nonlinear equations give θ_1 and θ_2. Using these θ_1 and θ_2 and measured Y_0 and Y_1 into equation (2.15) the clearances d_1 and d_2 can be easily calculated.

The procedure to determine N_0 and N_1 experimentally using y(t) and b(t) is explained below. The Y_0 and Y_1 can be obtained from the Fourier transform $Y(\omega)$ of y(t) as

$$Y_0 = Y(0) \quad \text{and} \quad Y_1 = |Y(\Omega)|. \tag{2.21}$$

The U_0 and U_1 can be found from the known system excitation b(t) and response y(t) as follows. Solving equation (2.8) for $U(\omega)$ gives

$$U(\omega) = m\omega^2 B(\omega) - \frac{Y(\omega)}{H(\omega)}. \tag{2.22}$$

Substitute $\omega = 0$ and $\omega = \Omega$ respectively into the above equation to obtain U_0 and U_1 as

$$U_0 = U(0) = -\frac{Y(0)}{H(0)}, \tag{2.23}$$

$$U_1 e^{i\phi_1} = U(\Omega) = m\Omega^2 B(\Omega) - \frac{Y(\Omega)}{H(\Omega)}. \tag{2.24}$$

The experimental values of N_0 and N_1 can be found using equations (2.21)-(2.24) as

$$N_0 = \frac{U_0}{Y_1} = -\frac{Y(0)}{H(0)\,|\,Y(\Omega)\,|}, \tag{2.25}$$

$$N_1 = \frac{U_1 e^{i\phi_1}}{Y_1} = \frac{m\Omega^2 B(\Omega)}{Y(\Omega)} - \frac{1}{H(\Omega)}. \tag{2.26}$$

To find N_1 using equation (2.26) needs somewhat difficulty to obtain phase information in addition to the amplitude information which could be obtained with relative ease using a narrow band filter and a vibration meter. A simplified approach which needs no phase information is possible and is described next. Substituting $1/H(\Omega) = (k_0 - m\Omega^2) + ic\Omega$ and noting that N_1 in the present case must be real, the magnitudes of both sides of equation (2.26) could be equated to give

$$\sqrt{(N_1 + k_0 - m\Omega^2)^2 + (c\Omega)^2} = m\Omega^2 \frac{|\,B(\Omega)\,|}{|\,Y(\Omega)\,|}. \tag{2.27}$$

Solving the above equation for N_1 gives

$$N_1 = m\Omega^2 - k_0 \pm \sqrt{\frac{(m\Omega^2\,|\,B(\Omega)\,|)^2}{|\,Y(\Omega)\,|^2} - (c\Omega)^2}, \tag{2.28}$$

which needs no phase information. The two values of N_1 leads to non-uniqueness, however practical considerations will be required to choose the proper sign and will be considered later in the section on results and discussion. The basic procedure of clearance estimation remains the same as discussed before.

When clearance-stop nonlinearity is symmetric, i.e. $k_1 = k_2 = k$ and $d_1 = d_2 = d$, and if experimental response y(t) is also symmetric then $Y_0 = U_0 = N_0 = 0$ and $\theta_1 = \theta_2 = \theta$. Substituting these special values in equation (2.20) leads to a simplified expression,

$$N_1 = \frac{k}{\pi}(\pi - 2\theta - \sin 2\theta). \tag{2.29}$$

Equation (2.29) is a single nonlinear equation in a single unknown θ which can be numerically solved to a desired accuracy. Then the identical clearances can be calculated using equation (2.15) and using Y_0=0, as

$$d = d_1 = d_2 = Y_1 \sin\theta. \tag{2.30}$$

Once clearances d_1 and d_2 are estimated, then impact forces can be estimated by using experimentally obtained y(t) in equation (2.4) or, using only Y_0 and Y_1 as

$$u(t) = \begin{cases} k_1(Y_0 + Y_1\sin(\Omega t) - d_1) & \theta_1 \le \Omega t \le \pi - \theta_1 \\ 0 & \pi - \theta_1 < \Omega t < \pi + \theta_2 \\ k_2(Y_0 + Y_1\sin(\Omega t) + d_2) & \pi + \theta_2 \le \Omega t \le 2\pi - \theta_2 \end{cases}. \tag{2.31}$$

The validity and limitations of using two term approximation and its relationship to the severity of nonlinearity will be discussed later. However, intuition suggests that the estimation of clearances and impact forces based on describing function approach will be accurate only when response y(t) is reasonably represented by $Y_0 + Y_1\sin\Omega t$. Extreme distortion of y(t) from sinusoidal output due to strong interactions between oscillator and very stiff stops and/or extreme asymmetry, (i.e., $k_1, k_2 >> k_0$ and/or $d_1/d_2 >> 1$, $k_1 >> k_2$ etc.) will invalidate the basic assumptions of this approach and the estimates would be suspect. Another approach, which overcomes the above limitations and is based on minimizing a functional, is presented in what follows.

2.4 OPTIMIZATION APPROACH

Assume that under the known input b(t), the system response is y(t) which produces an impact force u(t). Then U(ω) in frequency domain can be obtained experimentally using equation (2.22) and using Fourier transforms of measured b(t) and y(t). Taking inverse Fourier transform of U(ω) will give the periodic impact force in time domain as

$$u(t) = F^{-1}\left[m\omega^2 B(\omega) - \frac{Y(\omega)}{H(\omega)}\right], \tag{2.32}$$

where F^{-1} indicate an inverse Fourier transformation. The calculation of u(t) given by equation (2.32) involves no approximation. However, some errors may be introduced from the practical bandwidth limitations of the measuring equipment such as an accelerometer, a vibration meter, an impedance head or a data acquisition system, and due to the numerical evaluation of Fourier and inverse Fourier transforms of y(t) and of U(ω), respectively.

Now consider an isolated stop-clearance nonlinearity with measured y(t) and calculated u(t) as shown in Figure 6. The best estimates $\hat{d}_1$ and $\hat{d}_2$, respectively, of clearances d_1 and d_2, could be obtained from minimizing an objective function (a time averaged sum of squares of deviations) J,

$$J(\hat{d}_1,\hat{d}_2) = \begin{cases} \frac{1}{T}\int_0^T \{\hat{u}[y(t),\hat{d}_1,\hat{d}_2] - u(t)\}^2 dt + [k_1(\hat{d}_1 - y_{max})]^2 & \hat{d}_1 > y_{max}, \\ \frac{1}{T}\int_0^T \{\hat{u}[y(t),\hat{d}_1,\hat{d}_2] - u(t)\}^2 dt & \hat{d}_1 \le y_{max} \text{ and } \hat{d}_2 \le -y_{min}, \\ \frac{1}{T}\int_0^T \{\hat{u}[y(t),\hat{d}_1,\hat{d}_2] - u(t)\}^2 dt + [k_2(\hat{d}_2 + y_{min})]^2 & \hat{d}_2 > -y_{min}, \end{cases}$$

(2.33)

where y_{max} and y_{min} are the maximum and minimum values of y(t), $t \in [0,T]$, respectively. The $\hat{u}[y(t),\hat{d}_1,\hat{d}_2]$ could be obtained by substituting measured y(t) and assumed $\hat{d}_1$ and $\hat{d}_2$ in equation (2.4). The T represents the time duration of the sample and should preferably include at least a few cycles of motion to average out small external uncontrolled disturbances such as an exciter fan noise, building vibrations etc. $J(\hat{d}_1,\hat{d}_2)$ being the sum of squares is always positive and will be zero when estimated values coincide with actual values. The search for the minimum of J should be limited within the range $0 \le \hat{d}_1 \le y_{max}$ and $0 \le \hat{d}_2 \le -y_{min}$. The search for the estimates $\hat{d}_1$ and $\hat{d}_2$ using function J where terms $[k_1(\hat{d}_1 - y_{max})]^2$ and $[k_2(\hat{d}_2 + y_{min})]^2$were included was found to be better behaved than without these terms. Once clearances are estimated, the impact forces can be estimated using equation (2.4).

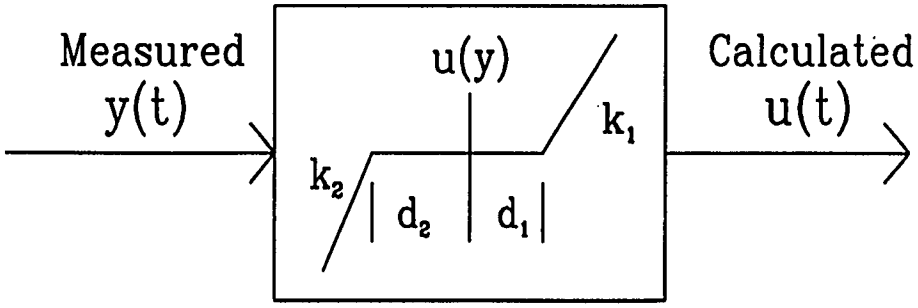

Figure 6. Isolated stop-clearance nonlinearity with measured y(t) and u(t) calculated using equation (2.32).

2.5 EXPERIMENTS AND COMPUTATIONS

Two approaches described in the last sections to estimate clearances and impact forces need the response y(t) and the knowledge of the basic oscillator parameters m, k_0, c, k_1, k_2 and external excitation b(t). The response y(t) was obtained by simulating the motion using a digital computer and from physical experiments conducted using a mechanical analogue of an impact oscillator. Computer simulated experiments are convenient, economical and flexible enough to independently vary any parameter of interest. However, the real world complications such as higher resonances, nonlinearities, unavoidable friction, practical limitations on producing pure sinusoidal input, measuring errors, filtering properties of accelerometers, vibration meters and their frequency band limitations are not easy to reproduce in the computer simulation. Hence additional experiments were performed using a mechanical model. The details of these two ways of generating y(t) are given next.

2.5.1 SIMULATION USING A DIGITAL COMPUTER

A computer program was developed, which used exact solution of differential equation (2.1) with piecewise linear spring stiffness properties given by equation (2.2). An exact solution can be obtained for the displacement of the mass between the ith and (i+1)th change over conditions (2.2) with the knowledge of displacement $y(t_i)$ and velocity $\dot{y}(t_i)$ at the instant of the ith change over. The displacement of m between cross over time intervals t_i and t_{i+1} can be written as

$$y(t) = Y_{pj}\sin(\Omega t' + \psi_j) + e^{-\frac{c}{2m}t'} Y_{cj}\sin\left(\sqrt{\frac{s_j}{m} - \left(\frac{c}{2m}\right)^2}\, t' + \alpha_j\right) + Q_j,$$

$$0 \le t' \le t_{i+1} - t_i, \tag{2.34}$$

where

$$\begin{cases} s_1 = k_0 + k_1 & Q_1 = \dfrac{k_1}{s_1} d_1 & y(t) \geq d_1 \\ s_0 = k_0 & Q_0 = 0 & -d_2 < y(t) < d_1, \\ s_2 = k_0 + k_2 & Q_2 = -\dfrac{k_2}{s_2} d_2 & y(t) \leq -d_2 \end{cases}$$

$$Y_{pj} = \frac{m\Omega^2 A}{\sqrt{(s_j - m\Omega^2)^2 + c^2\Omega^2}}, \qquad \psi_j = \phi_i - \tan^{-1}\frac{c\Omega}{s_j - m\Omega^2},$$

$$Y_{cj} = \sqrt{\frac{(2mV_{0e} + c\,y_{0e})^2}{4ms_j - c^2} + y_{0e}^2}, \qquad \alpha_j = \tan^{-1}\left(\frac{y_{0e}\sqrt{4ms_j - c^2}}{2mV_{0e} + c\,y_{0e}}\right),$$

with

$$\phi_i = \Omega t_i + \phi_0 (\mathrm{mod}\, 2\pi), \qquad y_{0e} = y(t_i) - Q_j - Y_{pj}\sin\psi_j, \qquad V_{0e} = \dot{y}(t_i) - Y_{pj}\Omega\cos\psi_j.$$

The t_{i+1} can be obtained by solving a transcendental equation (2.34) by substituting

$$y(t_{i+1}) = \begin{cases} d_1 & y(t) > d_1 \\ d_1 \text{ or } d_2 & -d_2 < y(t) < d_1 \\ d_2 & y(t) < -d_2 \end{cases} \tag{2.35}$$

in the left hand side of equation (2.34). A computer program is developed to obtain the complete temporal behavior of this system and is given in Appendix C. The iterative procedure to determine t_{i+1} was continued until the absolute value of the difference between $y(t_{i+1})$ given by (2.35) and the right hand side of equation (2.34) was less than 10^{-13}. The value of $\dot{y}(t_{i+1})$ is obtained by substituting $t' = t_{i+1} - t_i$ and $t = t_{i+1}$ in the time derivation of equation (2.34). Then $y(t_{i+1})$ and $\dot{y}(t_{i+1})$ are the initial conditions for the next region. This process starts with given initial conditions $y(t_0)$, $\dot{y}(t_0)$ and ϕ_0, and is repeated to find the change over conditions every time the motion of the mass enters the next linear region until the system reaches a steady state, which can be seen as the repetition of the so

obtained change over conditions. In my computer simulated experiments, the process was started with zero initial conditions and repeated until the completion of 400 cycles of external force, which ensured that in most of the cases the system reached a steady state. The temporal behavior of this system was obtained using a double precision arithmetic on a VAXstation 2000 digital computer. The values of input parameters m, k_0, c, k_1, k_2 and b(t) used in the digital simulation were those obtained from the mechanical experiment or used as an external excitation respectively.

2.5.2 EXPERIMENTS USING A MECHANICAL ANALOGUE

An experimental model of an impact oscillator shown in Figure 7 was built. Three heat treated and ground steel rods fastened to the base plate and the top plate forms the frame of the structure. A linear bearing together with an aluminium arm, which was clamped on the bearing, constitutes the mass of the oscillator. The mass moved freely along the rod which indicated that the sliding/rolling friction was negligible. The main spring (coil diameter = 1.70 mm, outside diameter = 18.29 mm, number of turns = 11 and material = music wire) connected the mass to the base plate. Two other springs were fixed on the brackets which were clamped to the other two rods and these springs represented the elastic stops. The gaps between main mass and these stops were adjustable. An accelerometer was mounted on the main mass bracket to measure the absolute displacement, x(t). The whole assembly was fixed to the electromagnetic shaker using the base plate. The base input, b(t), was measured using an accelerometer. A force transducer was connected to one of the stop springs to measure the impact force. Compensation for the added mass on the impedance head can be achieved by subtracting $m_{extra}\omega^2 b(t)$ from

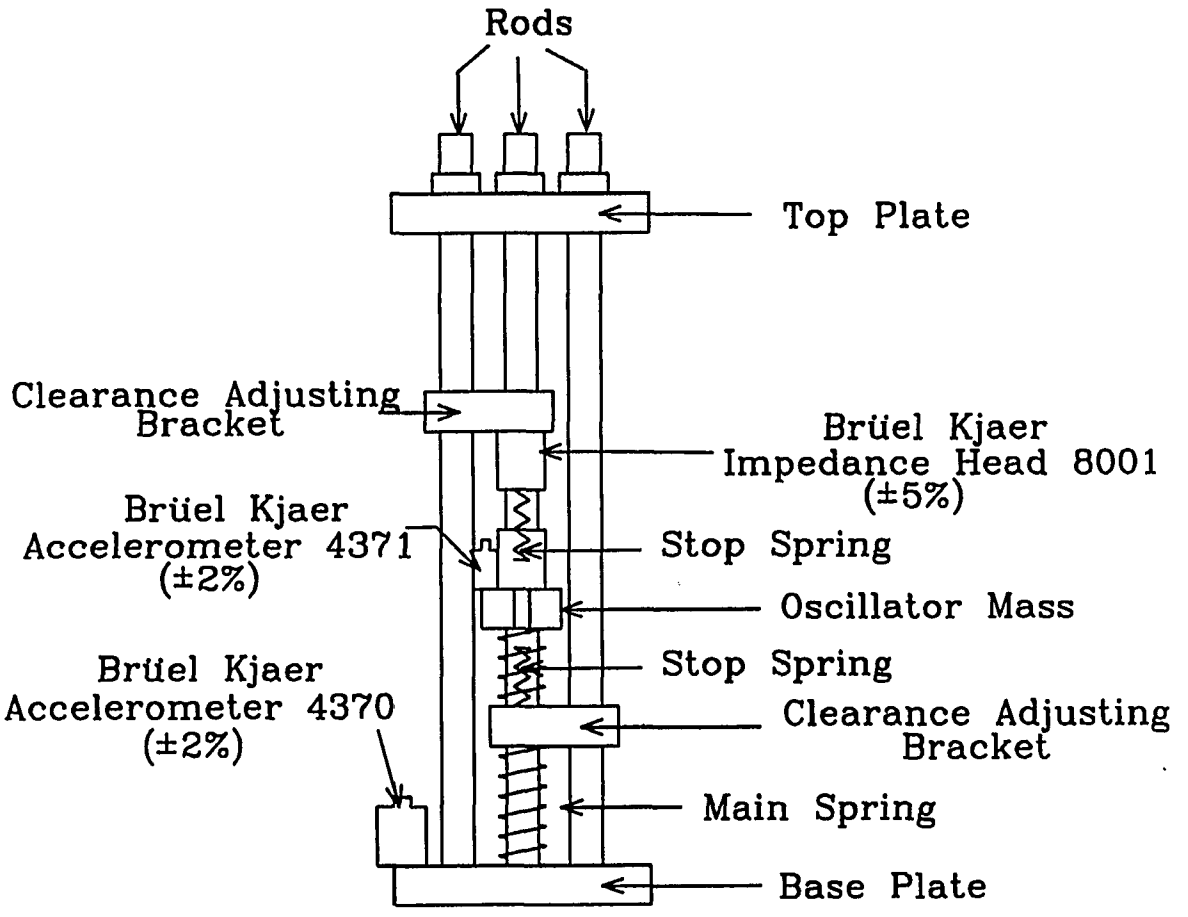

Figure 7. Mechanical analogue of an impact oscillator and attached transducers.

the impact force. The m_{extra} was found to be 10.95 g. This experimental set up ensured that mass moved only along the rod (i.e. uniaxially) with little damping and simulated the single-degree-of-freedom oscillator reasonably well.

The experimental instrumentation is shown in Figure 8. The exciter, which was controlled by signals generated by the exciter control and amplified by the power

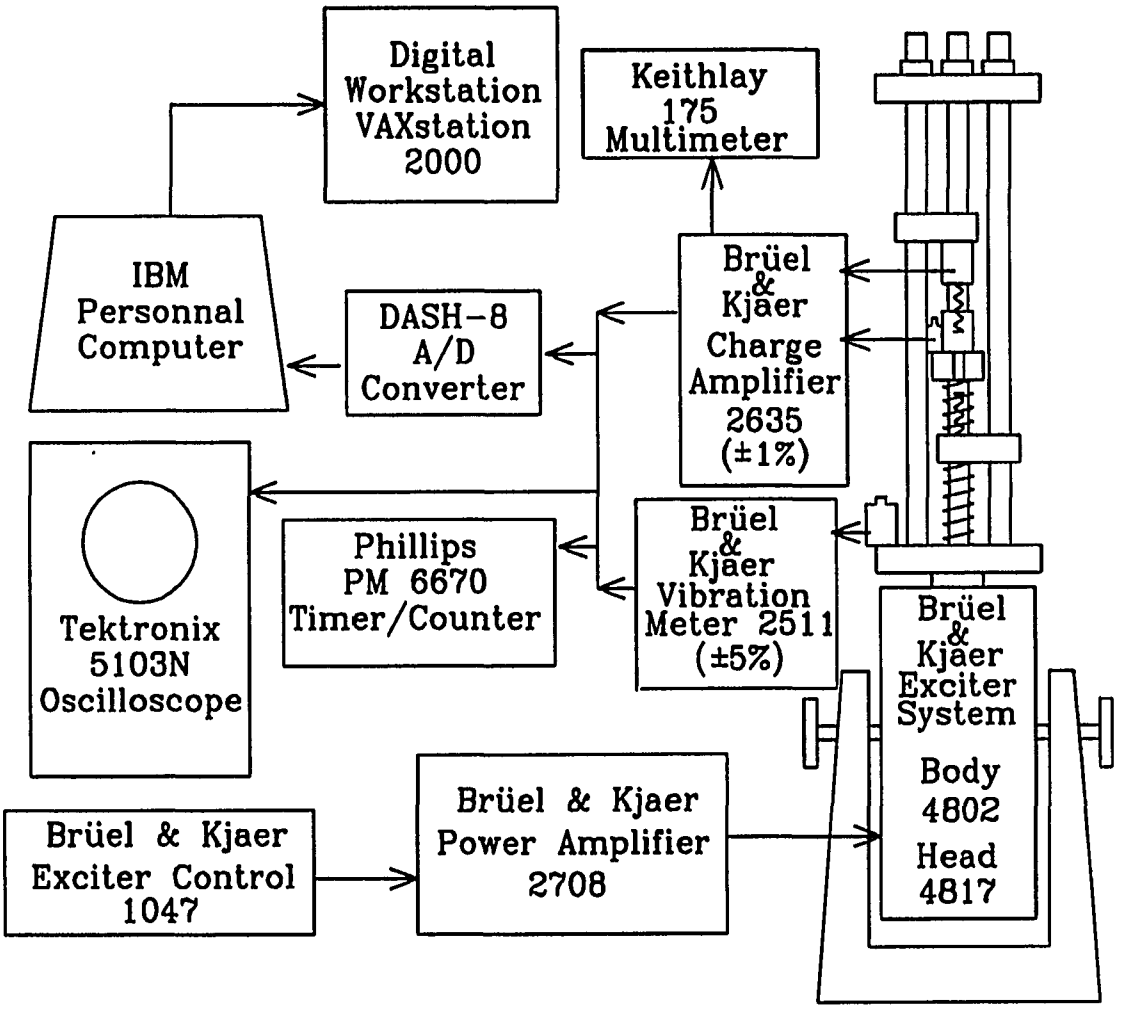

Figure 8. Experimental instrumentation.

amplifier, provided a sinusoidal base excitation to the impact oscillator. The amplitude and frequency of the excitation can be adjusted by the exciter control and the power amplifier. The sinusoidal input displacement b(t) and the output x(t), which was amplified using a charge amplifier, were measured using a vibration meter and a multimeter

respectively and were displayed on a four channel storage oscilloscope. The phase difference between the output and the input was measured using a high resolution timer/counter. The b(t) and x(t) were digitized using a A/D converter and were stored on a floppy disk. The A/D converter performed the conversion on one channel at one time and scanned other channels in sequence. Hence, the sampled discrete data will be $b_n = b(n\nabla t)$ and $x_n = x(n\nabla t + \nabla t/2)$ where ∇t was taken as 1/1024 second and the sample duration was 1 second. The full scale input to the A/D converter was limited in +5v to -5v with a resolution of 0.00244 volts [46]. Hence proper amplification was used so that as far as possible full dynamic range of A/D converter was used to reduce the error of quantization without overloading.

The values of m and k_0 were found to be 0.1061 kg and 1746 N/m, respectively. The mass m includes the mass of the linear bearing, the attached bracket and the accelerometer. Without stop springs, the experimental model is an analogue of a single degree of freedom oscillator. By measuring the base displacement b(t) and the mass displacement x(t) at various frequencies and finding the ratio of amplitude of relative displacement y(t) to that of b(t), the frequency response function under base excitation of the oscillator was obtained experimentally, which is shown as the scattered points in Figure 9. The theoretical frequency response function under base excitation is [47],

$$H_b(\omega) = \frac{k_0 + ic\omega}{k_0 - m\omega^2 + ic\omega}. \tag{2.36}$$

The damping constant c was found by fitting the theoretical frequency response, with m and k_0 given above, that best fitted the experimental data. The damping constant c was found to be 0.7127 Ns/m and the resonant frequency was 20.4 Hz. The free vibration and the forced vibration test confirmed the validity of the above values. Using these m, k_0 and c values, the theoretical frequency response was calculated and is shown also in Figure 9

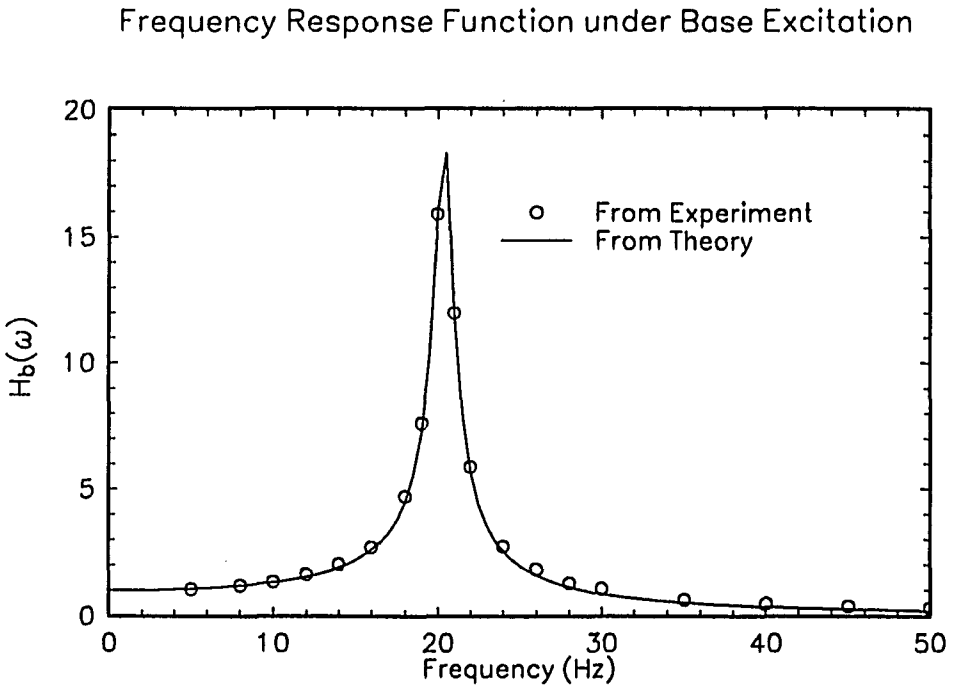

Figure 9. Experimental and theoretical frequency response function of the oscillator without stops.

by the continuous curve. A few groups of stop springs were used and their values of stiffness are reported in the section of results. The frequency of the sinusoidal excitation was kept in the resonant range in order to excite the motion of the mass with sufficient amplitude to ensure that the mass hits the stops without overloading the exciter and triggering the automatic shut down. The frequency and amplitude of the external sinusoidal excitation was controlled by the exciter control and the power amplifier. The system was allowed to settle and readings were taken only after it settled. The

experimentally obtained relative displacement y(t) in a discrete form was obtained from sampled b_n and x_n using the time shift property of Fourier transform as

$$y_n = y(n\nabla) = F^{-1}\left\{e^{-j\frac{\omega\nabla t}{2}} F[x(n\nabla t + \nabla t/2)] - F[b(n\nabla t)]\right\}. \quad (2.37)$$

Computational procedure to estimate clearances and impact forces was identical for data obtained using the mechanical experiment and the computer simulation and is detailed next.

2.5.3 COMPUTATION PROCEDURE

The computation procedures of estimation of impact forces and clearances based on the describing function approach and the optimization approach which use sinusoidal input are described here. All computations were performed using a double precision arithmetic on a VAXstation 2000 digital computer.

The Fourier transforms $B(\omega)$ and $Y(\omega)$ were obtained from the digitized b(t) and y(t) using a FFT [48-50] subroutine. The $B(\Omega)$, $Y(0)$ (Y_0) and $Y(\Omega)$ (Y_1) needed for the describing function approach were obtained from $B(\omega)$ and $Y(\omega)$. Then describing functions N_0 and N_1 were obtained using equations (2.25) and (2.26). Substituting these experimentally obtained values in the left hand sides of equations (2.19) and (2.20) generates two nonlinear equations in two unknowns θ_1 and θ_2. These equations were iteratively solved until the minimum of the differences between the right and the left hand sides was found. The estimates of d_1 and d_2 were obtained using calculated θ_1, θ_2, Y_0 and Y_1 into equation (2.15). A somewhat approximate value of N_1 was found from equation (2.28) when a simplified approach was used, however the other procedure remained the same.

For the purpose of clearance estimation, there is no need to calculate the impact force u(t) when the describing function approach is used. If impact force estimation is also desired, it can be done by using equation (2.4) or more approximately using equation (2.31) after the clearances have been estimated. However, in using the optimization approach the impact force u(t) must first be calculated from experimentally obtained data. The Fourier transform $U(\omega)$ of the impact force u(t) was obtained using equation (2.22). The periodic impact force u(t) needed for the optimization approach was obtained by inverse Fourier transform (equation (2.32)). The optimization approach estimates $\hat{d}_1$ and $\hat{d}_2$ such that the estimated impact force $\hat{u}(t)$ and "actual" u(t) calculated from experimentally obtained data using equation (2.32) match. The optimal estimates $\hat{d}_1$ and $\hat{d}_2$ were found by searching for the minimum of J given by equation (2.33). The time duration T used for the minimization of functional J was one second. The Powell method [51,52], which was designed specially for minimizing a sum of squares and entirely avoids all derivatives and their approximations [17,51-54], was used to search for the minimum and iterative computations were started using $\hat{d}_1 = \hat{d}_2 = 0$.

2.6 RESULTS AND DISCUSSION

The comparison of estimated clearances with actual ones based on the describing function approach and the optimization approach is presented here. First a typical case is presented to show the step by step detail of these approaches. Afterwards the effects of asymmetry in stop stiffnesses and gaps, the amplitude and frequency of input and advantages and limitations of these two approaches are considered.

As an example, consider an impact oscillator under a sinusoidal excitation, $b(t) = 0.687\sin(40\pi t)$ mm, contacting stops with support springs constants $k_1 = k_2 = 11663 \pm 100$ N/m and gaps $d_1 = d_2 = 1.19 \pm 0.05$ mm. The b(t) and x(t) measured from the mechanical

experiment and y(t) obtained from them by equation (2.37) are shown in Figure 10(a). The corresponding time histories obtained using the digital simulation approach are shown in Figure 10(b). Similarity between (a) and (b) of Figure 10 suggests that both the mechanical analogue and the computer simulation simulated the impact oscillator well. Clearances were estimated using b(t) and y(t) of Figure 10 by the computer programs (Appendix C) based on the describing function approach and the optimization approach. The estimates of d_1 and d_2 as well as the values of intermediate variables N_0, N_1, θ_1 and θ_2 are tabulated in Table 1. For a symmetric system when the response y(t) is dominated by its fundamental harmonic as the present case, clearances can also be estimated by the describing function approach using directly the reading of measuring instruments with the help of a hand calculator. Results obtained by this way are reported as Simplified Approach in Table 1 row 2 and is presented first. The comparison of actual gaps to estimated values indicates that predictions are accurate.

When the output x(t) is dominated by the fundamental harmonic the |y(t)| can be approximated by

$$| y(t) | = \sqrt{(| x(t) | \cos\phi - | b(t) |)^2 + (| x(t) | \sin\phi)^2}. \qquad (2.38)$$

The |x(t)| and phase angle ϕ between x(t) and b(t) were measured using a multimeter and a phase meter respectively. The measured values of |x(t)|, ϕ and |y(t)| calculated by equation (2.38) were 2.02 mm, -7° and 1.32 mm, respectively. The response was nearly symmetric and hence $N_0 = Y_0/U_0 \approx 0$ and N_1 was found out from equation (2.28) using the + sign in that expression. The value corresponding to the other sign was negative and was rejected. As this system is nearly symmetric, the calculated value is substituted in equation (2.29).

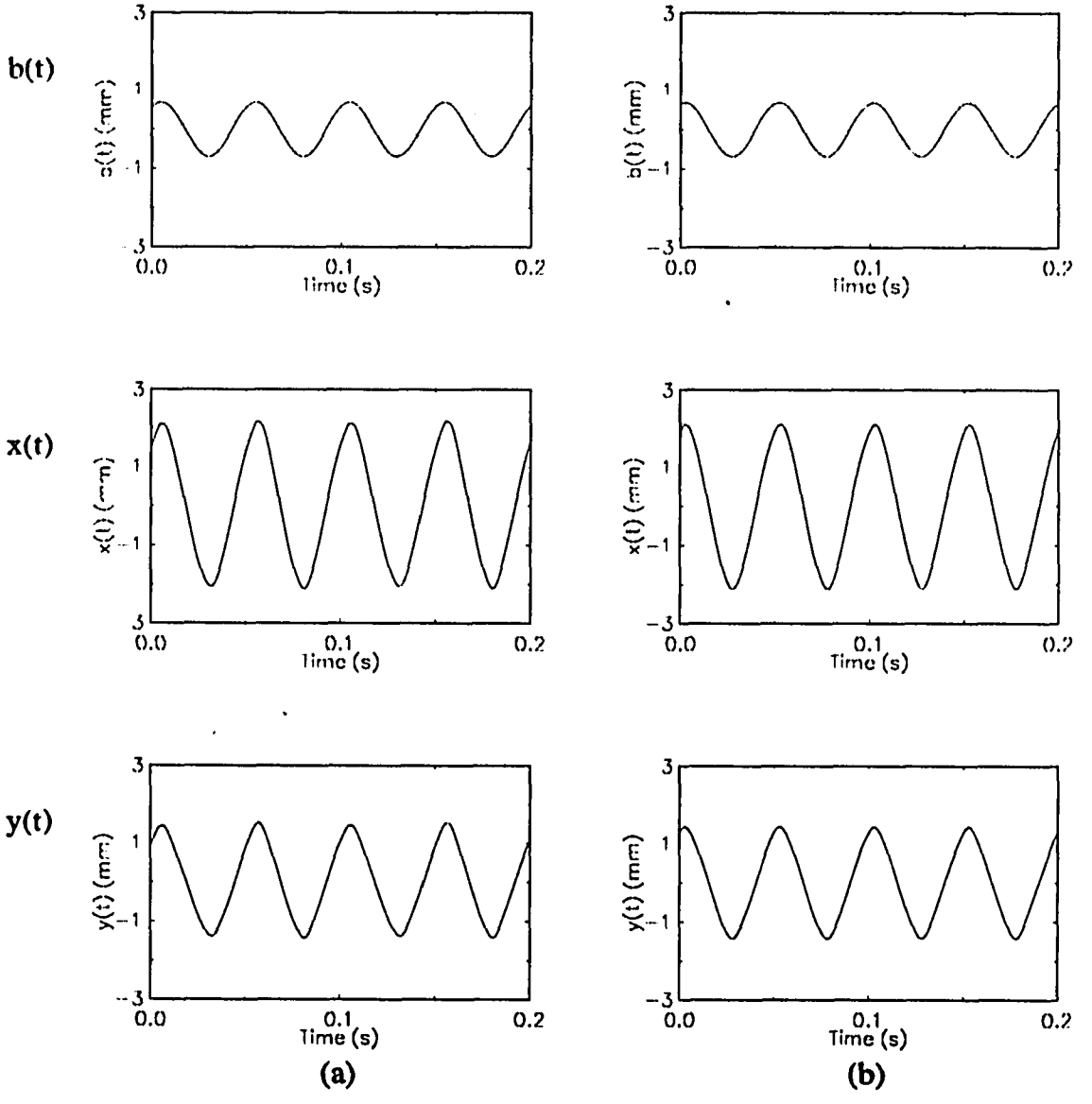

Figure 10. The traces of b(t), x(t) and y(t). (a) Mechanical experiment; (b) Computer simulation. The system parameters were m = 0.1061 kg, c = 0.7127 Ns/m, k_0 = 1746 N/m, $k_1 = k_2$ = 11663 N/m, $d_1 = d_2$ = 1.19 mm and b(t) = 0.687sin40πt mm.

TABLE 1

The clearance estimation results and values of intermediate variables of the case of Figure 10. The actual clearances were $d_1 = d_2$ 1.19 mm.

			N_0	N_1	θ_1	θ_2	d_1 (mm)	d_2 (mm)
Describing Function Approach	Mechanical Experiment	Simplified Approach	0	818	58°		1.12	
		General Approach	12	777+74i	58°	59°	1.12	1.15
	Computer Simulation		0	782+2i	58°	58°	1.14	1.14
Optimization Approach	Computer Simulation						1.19	1.19
	Mechanical Experiment						1.20	1.20
		Filtered y(t) & u(t) above 200 Hz					1.16	1.25

The resulting equation was quite simple and solved for θ with the help of a hand calculator. The estimate of identical clearances was then obtained by equation (2.30) as 1.12 mm which is quite close to the exact values of 1.19 mm.

Corresponding estimates obtained using the general computer program based on the describing function approach are reported in Table 1 row 3 as General Approach and were accurate. The b(t) and x(t) shown in Figure 10(a) were sampled and inputted to the computer program. The B(f) and Y(f), $f = \omega/2\pi$, shown in Figure 11(a) were found next. The B(20), Y(0) and Y(20) needed for the application of the describing function approach were obtained from B(f) and Y(f). They were:

B(20) = 0.556 - i0.404 mm, Y(0) = -0.00926 mm and Y(20) = 0.910 - i0.975 mm.

N_0 and N_1 were then found by equations (2.25) and (2.26) and are reported in Table 1. In theory N_1 must be real, however in reality due to experimental noise and errors the value came out to be a complex number. However, the imaginary part of N_1 was very small compared with the real part and its effect on the estimation of clearances was negligible. The estimates obtained using the real part of N_1 or modules of N_1 were quite similar. For symmetric systems, the N_0 should be zero, however in reality due to some unavoidable asymmetry and also experimental noise and errors, the N_0 came out to be a small number. This resulted in that the estimates of d_1 and d_2 were not identical, however they were very close. The corresponding estimates based on the computer simulation data were quite accurate (Table 1, row 4). Comparing the B(f) and Y(f) from computer simulation, shown in Figure 11(b), with those from mechanical experiment, it can be seen that the corresponding spectra contained the same components but the computer generated data were purer and free from noise. From the results reported in Table 1, it can be inferred that when the fundamental component dominates the response, the estimates of clearances

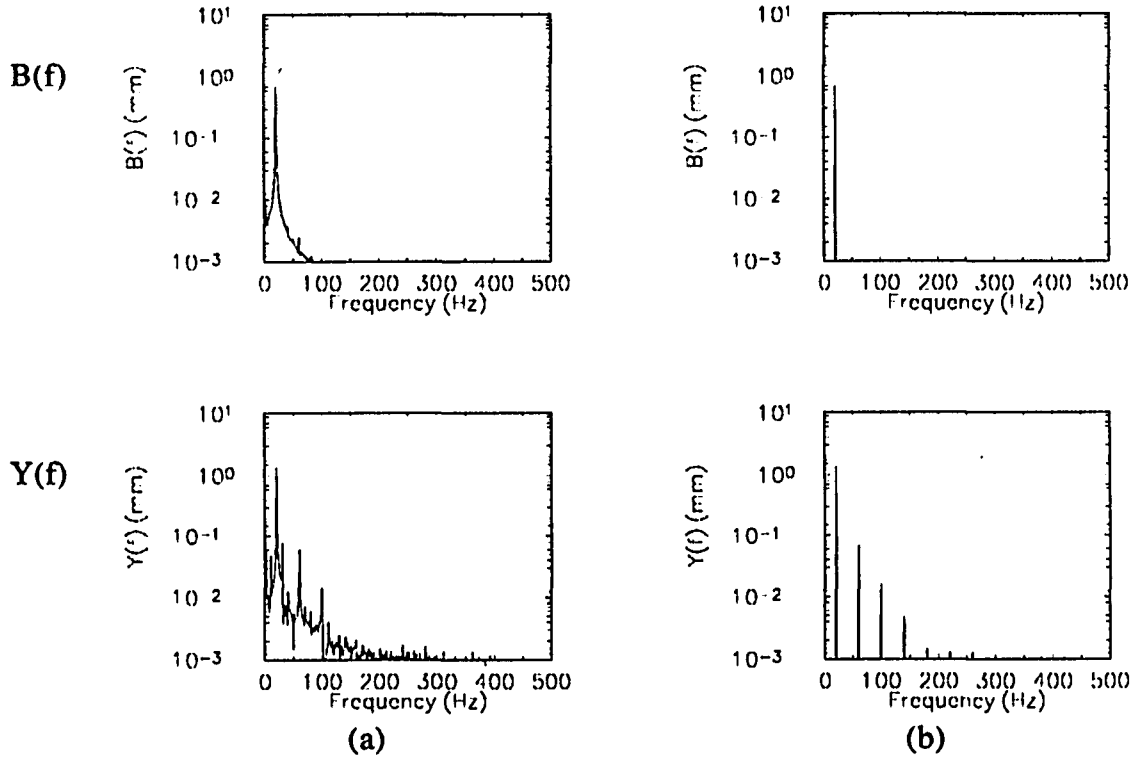

Figure 11. The frequency spectra B(f) and Y(f). (a) Mechanical experiment; (b) Computer simulation. The system parameters were identical to those reported in Figure 10.

obtained using the describing function approach will be reasonably accurate.

The estimation of clearances based on the optimization approach needs further processing of data of Figure 11, which is presented in Figure 12 and Figure 13(c), (d) and (e). The U(f) shown in Figure 12 were obtained from the corresponding B(f) and Y(f) of Figure 12. For comparison, the $\hat{U}(f)$ obtained by Fourier transforming the optimal estimate $\hat{u}(t)$ using the mechanical experimental data is also shown in Figure 12. Comparison of the U(f) shown in Figure 12(a) with those shown in Figure 12(b) reveals significant differences presented in high frequencies. This difference resulted due to the

multiplication of Y(f) by $H^{-1}(f)$ (see equation (2.32)). The unavoidable small amplitude but high frequency noise resulting from the cooling fan of the shaker, measuring equipment, quantization error in analogue to digital conversion and due to numerical errors introduced in the Fourier transform of y(t), Y(f), gets multiplied by the very large high frequency components of $H^{-1}(f)$. Computer generated data does not contain most of this high frequency noise and hence the resulting U(f) contains very little high frequency noise (see Figure 12(b)). By inverse FFT, the u(t) was obtained from the related U(f). Figure 13(c) and (d) show the u(t) from mechanical experiment and computer simulation respectively. Due to the high frequency components in the U(f), the u(t) obtained from mechanical experiment looked very noisy. The u(t) obtained by filtering experimentally obtained U(f) above 200 Hz is shown in Figure 13(f). The objective function could be constructed using the u(t) (equation (2.33)). Figure 14(a) shows the objective function $J(\hat{d}_1, \hat{d}_2)$ using mechanical experimental data as a function of $\hat{d}_1$ by fixing $\hat{d}_2$. The corresponding $J(\hat{d}_1, \hat{d}_2)$ using computer simulated data is shown in Figure 14(b). During the actual estimation, these curves of $J(\hat{d}_1, \hat{d}_2)$ were not really formed, only their minima were searched to find the best estimates of clearances. These estimates based on the data obtained using the computer simulation and the mechanical experiment are presented in Table 1 and indicates good agreement with the actual values. The high frequency noise in u(t) (mechanical experiment) did not prevent the optimization approach from giving an accurate clearance estimate and the effect of filtering y(t) and u(t) above 200 Hz was small (see last row of Table 1).

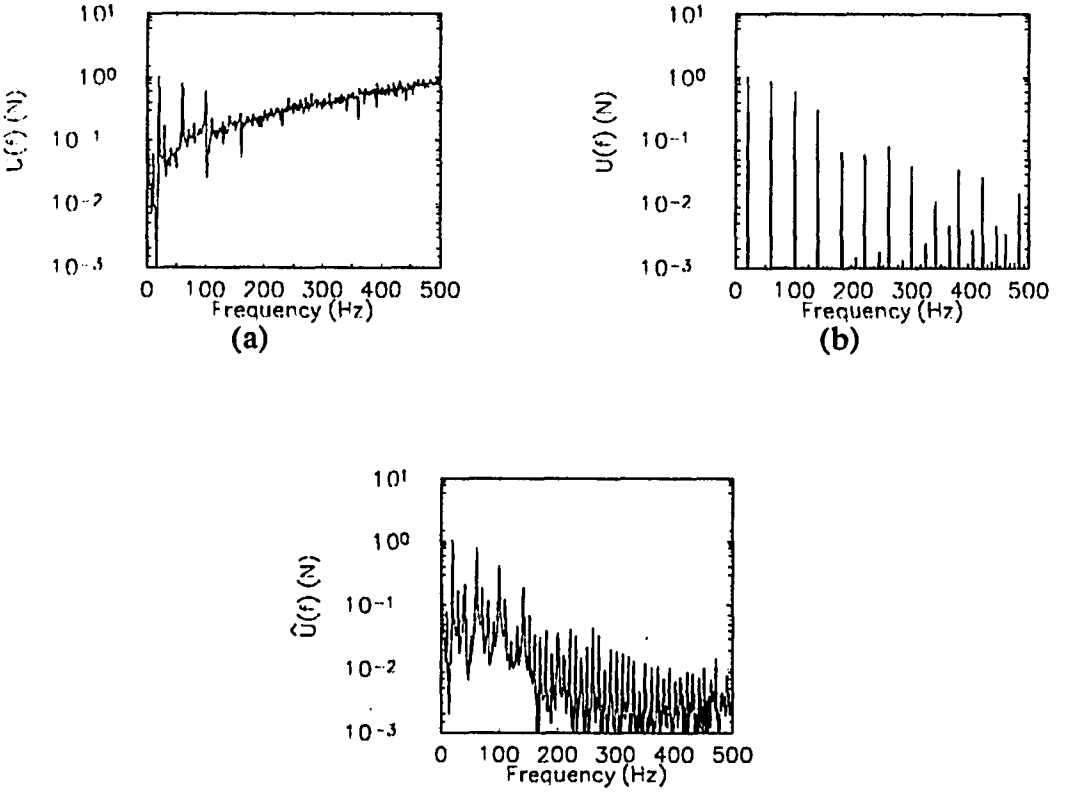

Figure 12. The frequency spectra U(f). (a) Mechanical experiment; (b) Computer simulation; (c) The $\hat{U}$(f) which is the Fourier transform of the $\hat{u}$(t) from the mechanical experimental data. The system parameters were identical to those reported in Figure 10.

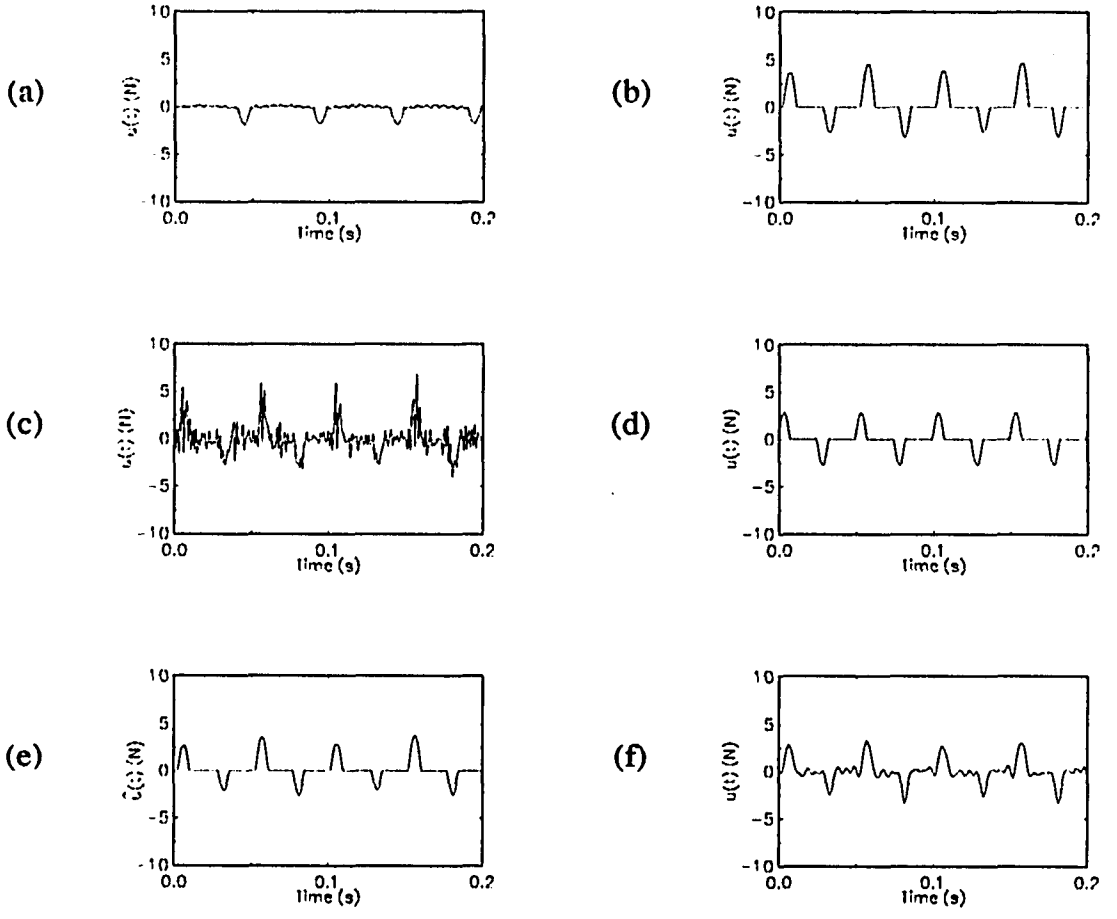

Figure 13. The temporal distribution of impact forces u(t). (a) Measured using an impedance head, (b) Estimated using the experimental data in the describing function approach, (c) Calculated using experimental data in equation (2.32), (d) Calculated using computer generated data in equation (2.32), (e) Estimated using experimental data and the optimization approach, and (f) Filtering measured y(t) and calculated u(t) of Figure (c) above 200 Hz. The system parameters were identical to those reported in Figure 10.

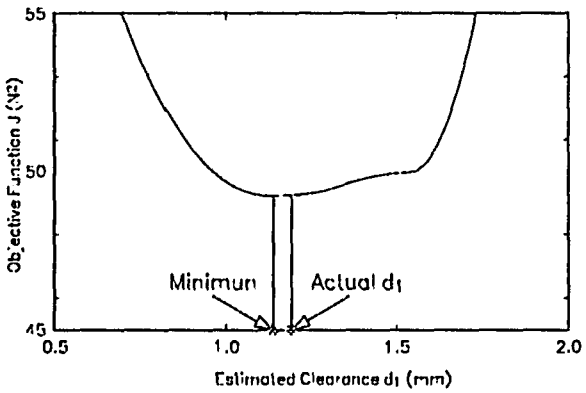

(a)

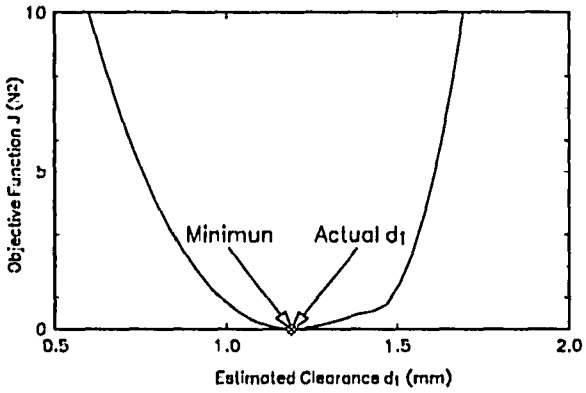

(b)

Figure 14. The objective function $J(\hat{d}_1, \hat{d}_2)$ as a function of $\hat{d}_1$ by fixing $\hat{d}_2 = 1.19$ mm, (a) using mechanical experimental data and (b) using computer simulated data. The system parameters were identical to those reported in Figure 10.

Estimates of impact forces based on the two approaches and the actual impact forces indicate that overall estimates are reasonable (see Figure 13). Only one impedance head was used and hence only impact force trace due to the stop spring on the positive displacement side was obtained (compare Figure 13(a) and 13(c)). The experimentally obtained impact force u(t) in Figure 13(a) looks very similar to the calculated u(t)s shown in Figure 13(b), (d), (e) and (f). The trace of the impact force calculated using equation (2.32), where experimental y(t) and b(t) were used to calculate B(f) and Y(f), shown in Figure 13(c) differs significantly from all other traces shown there. The significant differences occurred are essentially due to high frequencies present in (c). The source of the high frequency noise has been explained previously. Filtering experimentally obtained U(f) above 200 Hz indicates that the corresponding u(t) (Figure 13(f)) compares better with the measured u(t) (Figure 13(a)). The estimate $\hat{u}(t)$ of the impact force u(t) and its frequency transform $\hat{U}(f)$ (see Figure 12(c)) obtained using the optimization approach show few high frequency components as $\hat{u}(t)$ is obtained by minimizing the error in the mean square sense and minimization effectively filters out the high frequency components of the wide-band noise. In this sense, the $\hat{u}(t)$ is a better estimate of the impact force then the u(t). The peak values of u(t) obtained from the measured u(t) and estimated $\hat{u}(t)$ from the optimization approach are 1.8 N and 2.2 N, respectively and the agreement is reasonable. In view of the measurement and processing errors and the unavoidable noise, the estimates of clearances and impact forces should be considered very reasonable.

The effects of amplitude and frequency of excitation, unsymmetry in spring stiffnesses and gaps, and soft stop springs on the estimation based on these two approaches are studied using a total of seven combinations of stop springs and clearance sizes and

reported in what follows. The estimates based on the data from the mechanical experiments will be compared with and complemented by estimates using data generated using simulation on a digital computer.

The effect of the amplitude of input |b(t)| on the estimation based on the above mentioned approaches is shown in Figure 15. The results using the mechanical experimental data indicate that some scatter in the estimates is unavoidable and as such the average will give a better estimation and this figure confirms the conjecture. Within the range of the amplitude of excitation, the estimates obtained using the optimization approach are generally quite accurate especially those based on the computer simulation. The input amplitude had no noticeable effect on the estimation based on the optimization approach. To the contrary, there was a clear tendency of the estimates obtained using the describing function approach. The tendency was that as the amplitude of input became larger, the estimate became less accurate. The results obtained at |b(t)| = 3.52 mm produced somewhat larger error and hence corresponding y(t), Y(f) and U(f) are shown in Figure 16. This figure indicates that the response y(t) was quite complex. Even though the system was symmetric, the complex response y(t) was asymmetric. This is due to the nonlinearity of the present system. The estimates obtained using the describing function approach were not accurate as Y(f) and U(f) apparently indicate that the response and the impact forces were no longer dominated by the fundamental component and hence the describing function approach was not applicable as its basic assumption was violated. The results presented previously in Figure 10-13 were obtained with the identical system parameters as those of Figure 16 except under a smaller base excitation. Comparing the y(t), Y(f) and U(f) in Figure 16 with the corresponding figures in Figure 10-12 illustrates a larger excitation would excite more and stronger high frequency harmonics and make the

assumption of the describing function approach less satisfied. This explains the tendency displayed in Figure 15. The limitation of the describing function approach is that it works well for systems undergoing medium intensity impacts (see Figure 15). As opposed to this, even though the response was complex, the estimates obtained using the optimization approach based on the computer simulation are quite accurate. Additionally the responses obtained using mechanical experiment and computer simulation indicate that they were almost identical. The comparison of estimated impact forces and measured impact forces for all the mechanical experiment cases considered in Figure 15 is shown in Figure 17, and the agreement is reasonable. The accuracy of impact force estimation is closely related with the accuracy of the corresponding clearance estimation. The somewhat larger difference between the estimated and the measured u(t) in a few cases results from the multiplication of the small error in clearance estimation by the very high stop spring stiffness values and is unavoidable.

The effect of varying the frequency of the sinusoidal input on the estimates of clearances is shown in Figure 18 and the average values of estimated clearances are reasonably accurate. Except a small frequency range, which is likely around the resonant frequency of the impact oscillator, the excitation frequency seems to have little effect on the clearance estimation. The effect of varying the input frequency of the sinusoidal input on the impact force estimation is shown in Figure 19. The estimates match quite well with the measured ones.

(a)

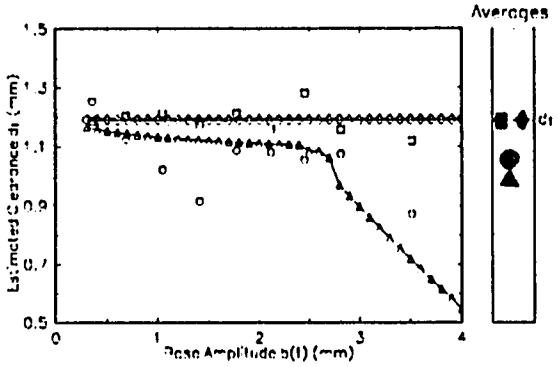

(b)

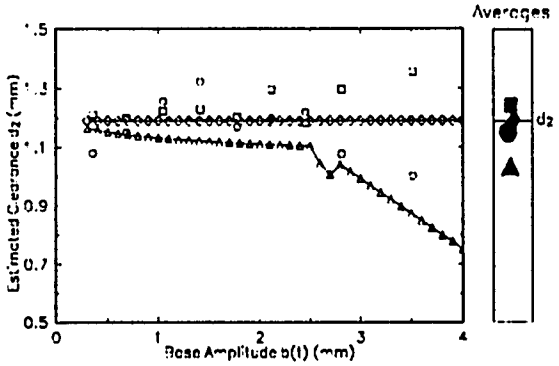

Figure 15. The effect of varying the input base amplitude |b(t)| on the clearance estimation. (a) Estimation of clearance d_1. (b) Estimation of clearance d_2. The main system parameters are identical to those given in Figure 10. The results in this and other figures are presented by: Data from experiment; ◯ Describing Function Approach, □ Optimization Approach. Data from computer simulation; △ Describing Function Approach, ◇ Optimization Approach. Averages of corresponding estimates are represented by corresponding blocked symbols.

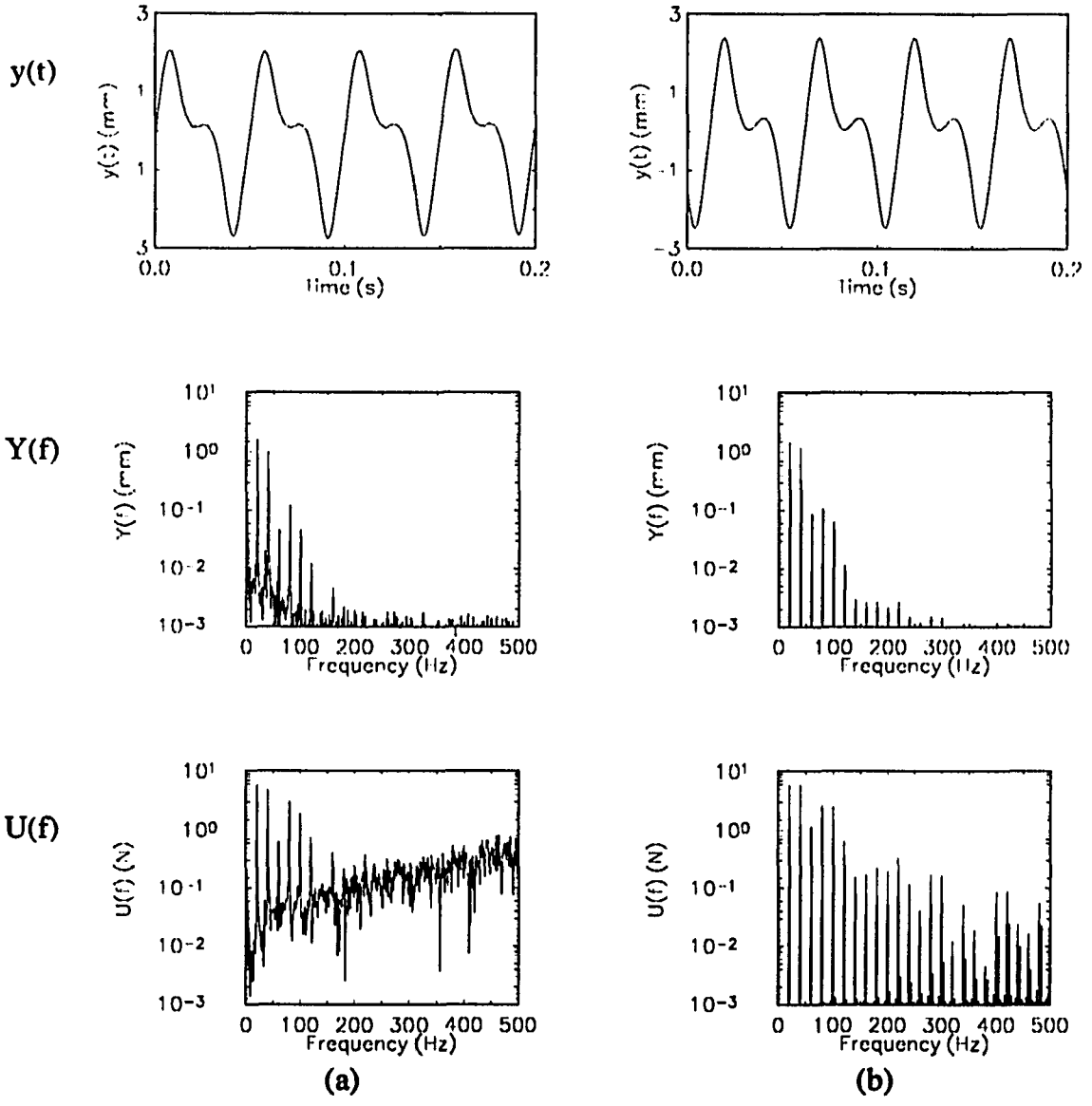

Figure 16. The y(t), Y(f) and U(f) of one case of Figure 15 where |b(t)| = 3.515 mm. (a) Mechanical experiment and (b) Computer Simulation.

|b(t)|=0.69 mm

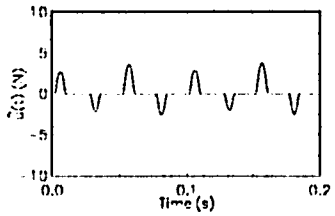

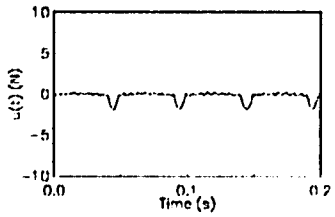

|b(t)|=1.45 mm

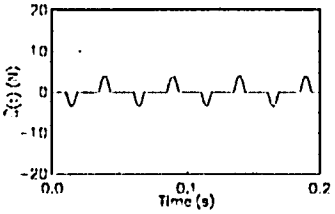

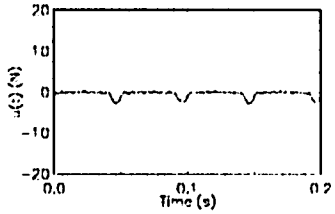

|b(t)|=1.41 mm

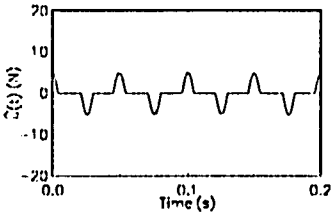

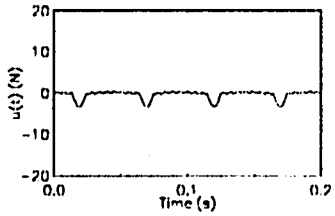

|b(t)|=1.78 mm

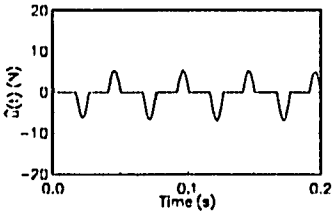

(a)

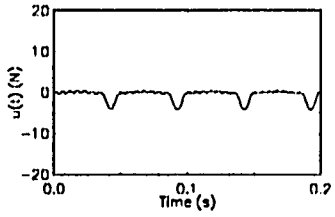

(b)

Continued on the next page.

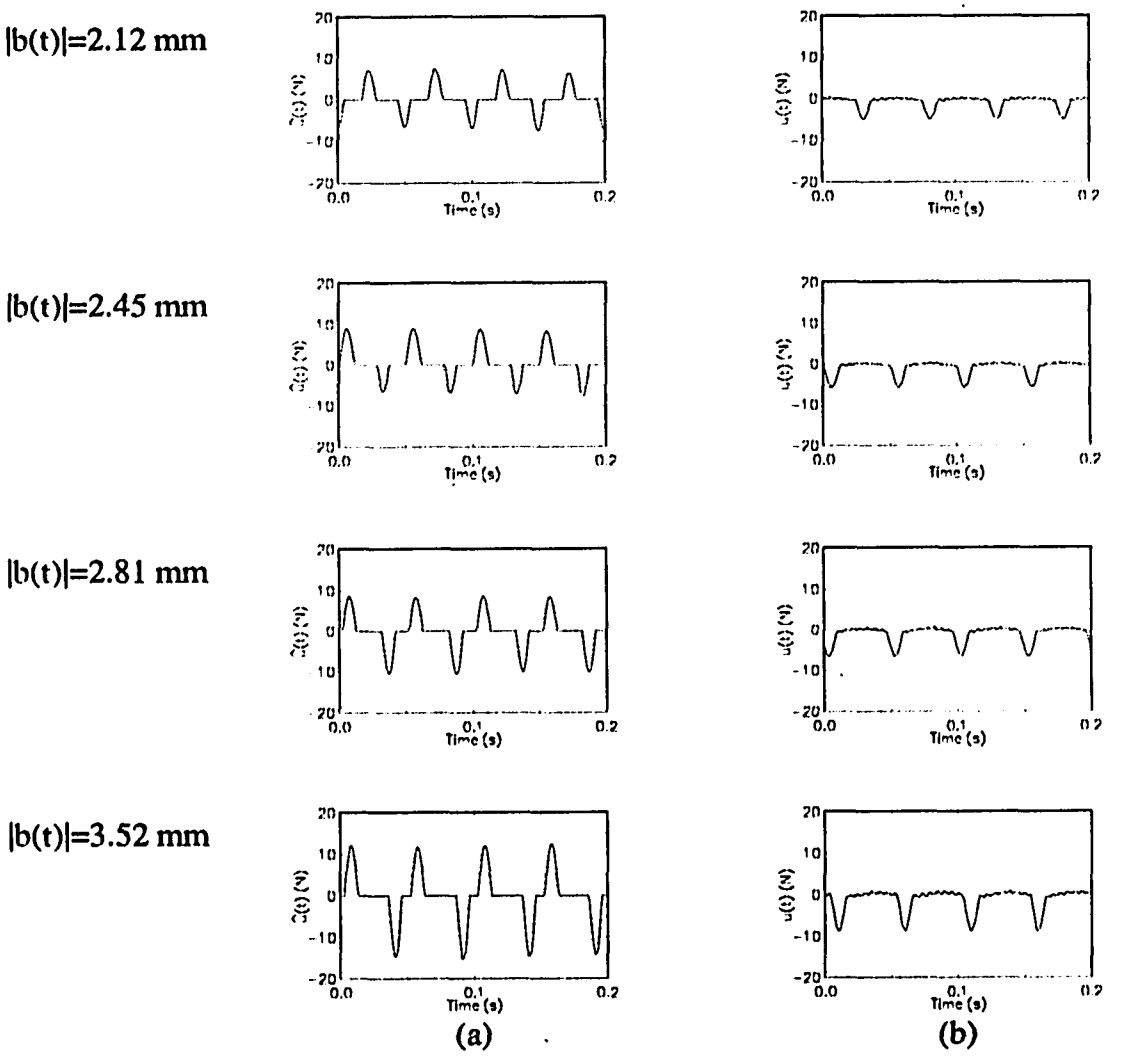

Figure 17. The effect of varying the input base amplitude |b(t)| on the impact force estimation. (a) Estimated impact force $\hat{u}(t)$ from the optimization approach. (b) Measured impact force. The main system parameters are identical to those given in Figure 10.

(a)

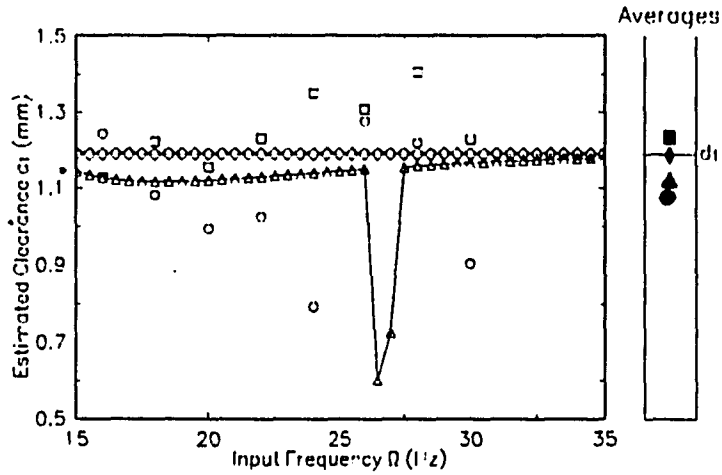

(b)

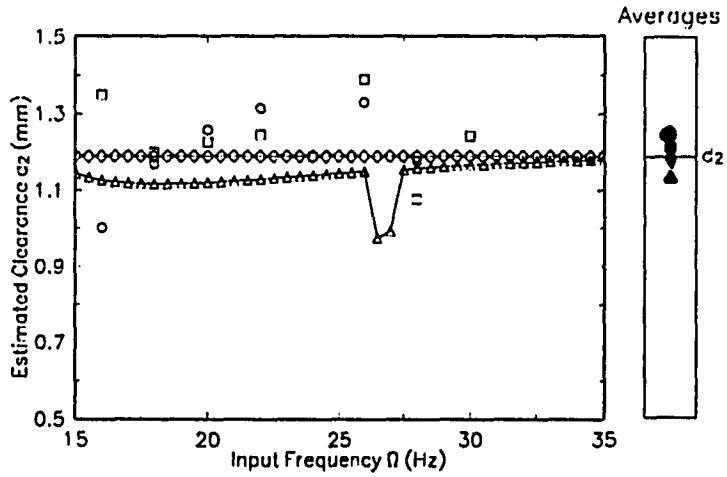

Figure 18. The effect of varying the input frequency of the sinusoidal input on the clearance estimation. $|b(t)| = 1.4$ mm. (a) Estimation of clearance d_1 and (b) Estimation of clearance d_2. The main system parameters are identical to those given in Figure 10 and Symbols are same as those used in Figure 15.

f=16 Hz

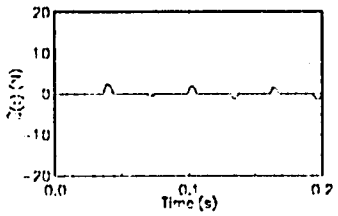

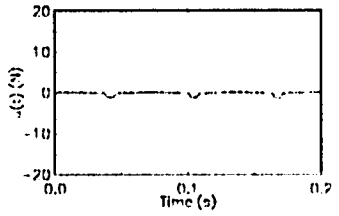

f=18 Hz

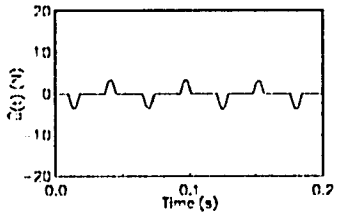

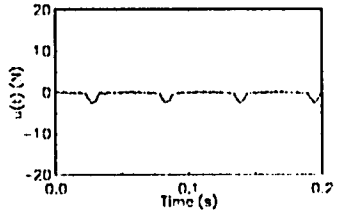

f=20 Hz

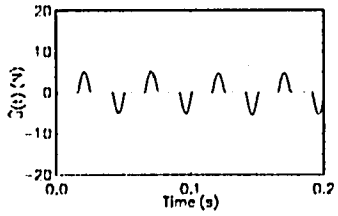

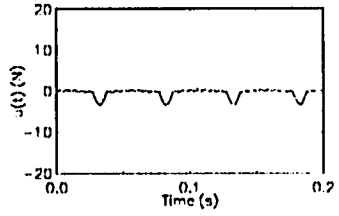

f=22 Hz

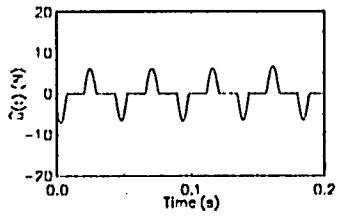

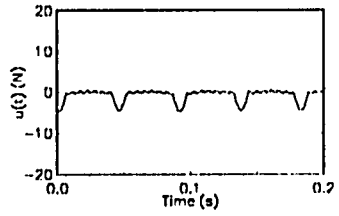

(a) (b)

Continued on the next page.

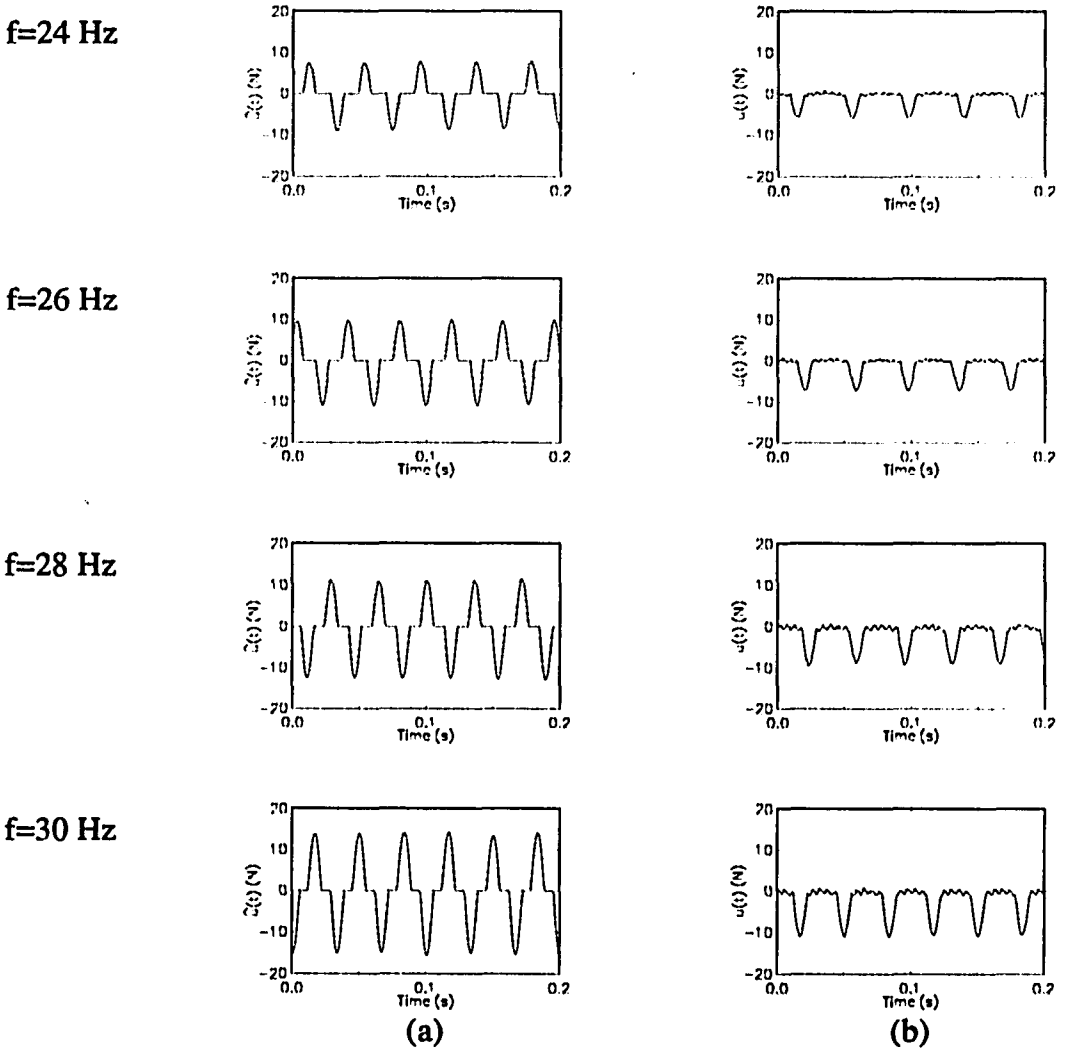

Figure 19. The effect of varying the input frequency of the sinusoidal input on the impact force estimation. (a) Estimated impact force $\hat{u}(t)$ from the optimization approach. (b) Measured impact force. The main system parameters are identical to those given in Figure 10.

Figures 15 and 18 indicate that the proper choice of the amplitude and the frequency of b(t) is important to ensure that collisions occur on both sides and the vibroimpact interaction is neither too weak nor too strong, which in turn ensure the accurate estimation. In case of a very weak interaction, the noise may predominate the small amplitude impact force and as such estimates based on both approaches will be less accurate. However, the indication of small values of (impact force on side one)/k_1 and (impact force on side two)/k_2 as compared to $y(t)_{max}$ and $y(t)_{min}$ respectively is that the clearance $d_1 \approx y(t)_{max}$ and $d_2 \approx -y(t)_{min}$. The very strong interaction leading to intense distortion, which indicates higher harmonics, should also be avoided as describing function approach is less accurate in this case. Then the best way is to adjust the input so that the distortion is reduced to an acceptable level. These two figures also indicate that the average values of clearances obtained by varying the input amplitude and frequency is the best way to estimate clearances.

The cases described above were symmetric. The results for estimation of clearances where gaps were significantly unsymmetric are presented in Table 2 and indicate a very reasonable agreement with actual values when the optimization approach was used. The agreement is better using the computer generated data than using the data from actual experiments. The estimates obtained using the describing function approach are reasonable in most cases except one, where base excitation b(t) was $1.58\sin(50\pi t)$ mm. Figure 20 shows the y(t) and Y(f) of this case. Generally, for a symmetric case, the response y(t) contains only odd order harmonics; but for an asymmetric case both even and odd harmonics are generated. This causes the assumption used in the describing function approach to be less satisfied and clearances estimation less accurate in asymmetric cases.

Figure 20 shows that the y(t) contained not only the even super harmonic at frequency 50 Hz but also strong sub-harmonics at frequencies 12.5 Hz and 37.5 Hz. That explains why the describing function approach did not work satisfactorily in that case.

TABLE 2

Estimation of clearances when actual clearances were nonidentical. The parameters were: $d_1 = 1.80 \pm 0.05$ mm and $d_2 = 0.64 \pm 0.05$ mm, and stop springs with stiffness $k_1 = 11906 \pm 100$ N/m and $k_2 = 11748 \pm 100$ N/m. In this and following tables,

D.F.A. = The Describing Function Approach.

Opt.A. = The Optimization Approach.

Input Frequency (Hz)			20	25	25	30	Average
Base Amplitude (mm)			1.61	0.77	1.58	0.77	
d_1 (mm)	Mechanical Experiment	D.F.A.	1.77	1.54	0.97	1.40	1.42
		Opt.A.	1.61	1.69	1.61	1.68	1.65
	Computer Simulation	D.F.A.	1.89	1.82	1.84	1.45	1.75
		Opt.A.	1.80	1.80	1.80	1.80	1.80
d_2 (mm)	Mechanical Experiment	D.F.A.	0.36	0.69	0.64	0.95	0.66
		Opt.A.	0.64	0.65	0.79	0.72	0.70
	Computer Simulation	D.F.A.	0.32	0.37	0.52	0.14	0.34
		Opt.A.	0.64	0.64	0.64	0.64	0.64

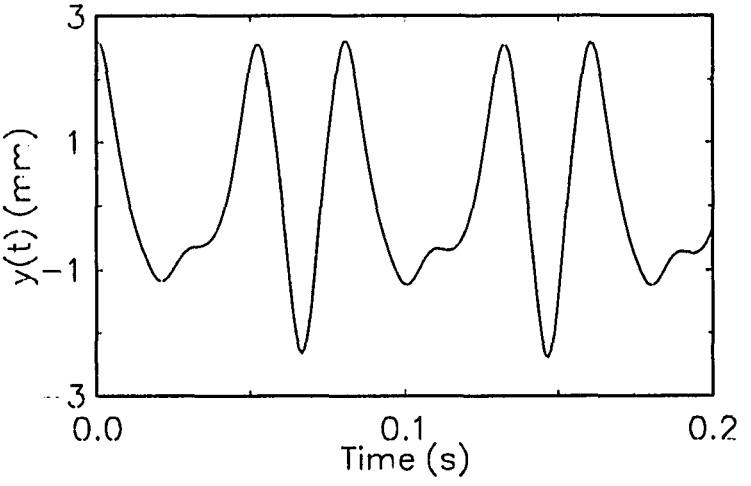

(a)

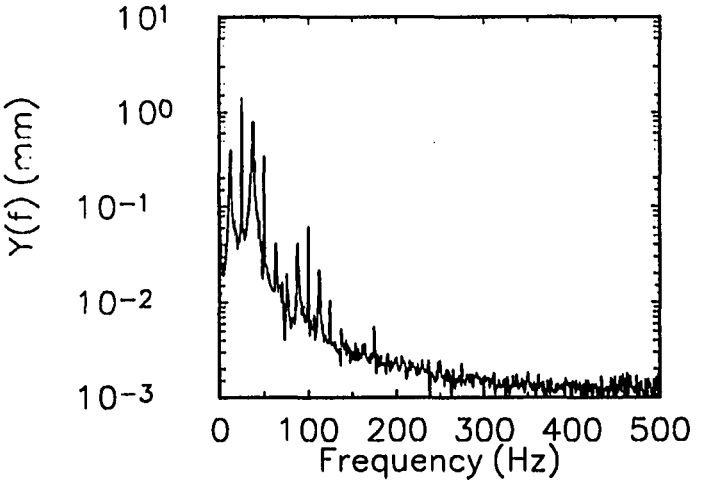

(b)

Figure 20. (a) The trace y(t) and (b) the frequency spectrum Y(f) for a case considered in Table 2 column 3. The b(t) was 1.58sin(50πt) mm.

The results obtained for a one sided stop with strong k_2, k_2/k_0 = 11748/1746 and gap = 0.64mm, and weak k_2, k_2/k_0 = 1643/1746 and gap = 1.27mm are presented in Table 3. The results indicate that the describing function approach failed in this case, however, the results obtained based on the optimization approach and using the experimental data and the computed data gave very good estimations. The corresponding u(t) obtained using the mechanical experimental data in equation (2.32) and the estimated $\hat{u}(t)$ obtained using the optimization approach for one of the cases of Table 3 are shown in Figure 21 and indicate a good agreement. The indication that u(t) and $\hat{u}(t)$ are only on the negative side additionally confirms that in fact the system was hitting stop only on one side. As discussed above, the high frequency noise in u(t) is mainly due to the inversion procedure involved in equation (2.32).

The effects of soft identical support springs, $k_0 \approx k_1 \approx k_2$, with identical and nonidentical gaps on the estimation of clearances are presented in Table 4(a) and 4(b) respectively. The results are quite reasonable in all these cases, however the estimates using the optimization approach are better. The describing function approach worked in these cases as nonlinearity was small and the Y(f) in these cases confirmed that the responses were dominated by the fundamental component. However, it was observed that experimentally obtained u(t) was somewhat contaminated by the noise amplified during the inversion process and hence it is better to use the estimate $\hat{u}(t)$ obtained during the optimization approach. U(f), $\hat{U}(f)$, u(t) and $\hat{u}(t)$ of one of the cases in Table 4 are shown in Figure 22 (a), (b), (c) and (d) respectively and they confirm the above observation.

TABLE 3

Estimation of clearances in case of a one sided stop. The parameters were: (a) strong stop: $k_2 = 11748 \pm 100$ N/m and $d_2 = 0.64 \pm 0.05$ mm, (b) weak stop: $k_2 = 1643 \pm 50$ N/m and $d_2 = 1.27 \pm 0.05$ mm.

(a) Estimated Clearance d_2 for strong stop cases

Input Frequency (Hz)		15	20	20	25	25	30	35	Average
Base Amplitude (mm)		1.45	0.70	1.42	0.15	0.71	0.40	0.71	
Mechanical	D.F.A.	0.54	0.83	1.26	1.29	1.88	2.78	1.41	1.43
Experiment	Opt.A.	0.55	0.61	0.62	0.63	0.64	0.60	0.63	0.61
Computer	D.F.A.	0.26	0.45	0.30	0.51	0.35	0.30	0.58	0.39
Simulation	Opt.A.	0.64	0.64	0.64	0.64	0.64	0.64	0.64	0.64

(b) Estimated Clearance d_2 for weak stop cases

Input Frequency (Hz)		20	25	30	35	Average
Base Amplitude (mm)		1.58	0.92	1.57	1.56	
Mechanical	D.F.A.	2.55	2.43	2.87	1.03	2.22
Experiment	Opt.A.	1.26	1.63	1.46	1.41	1.44
Computer	D.F.A.	1.16	1.21	1.24	1.26	1.22
Simulation	Opt.A.	1.27	1.27	1.27	1.27	1.27

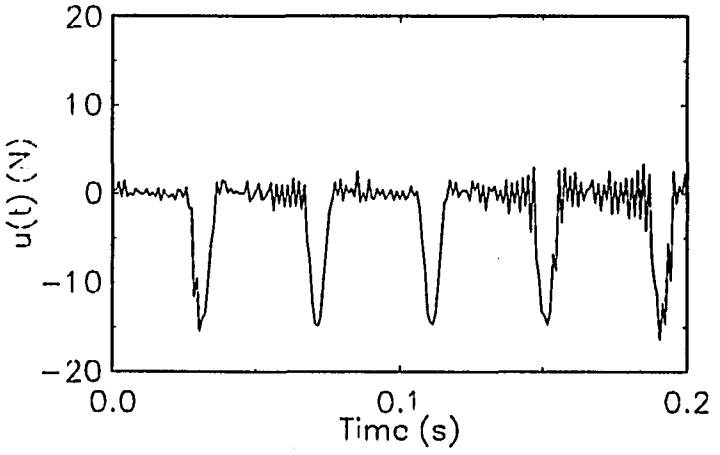

(a)

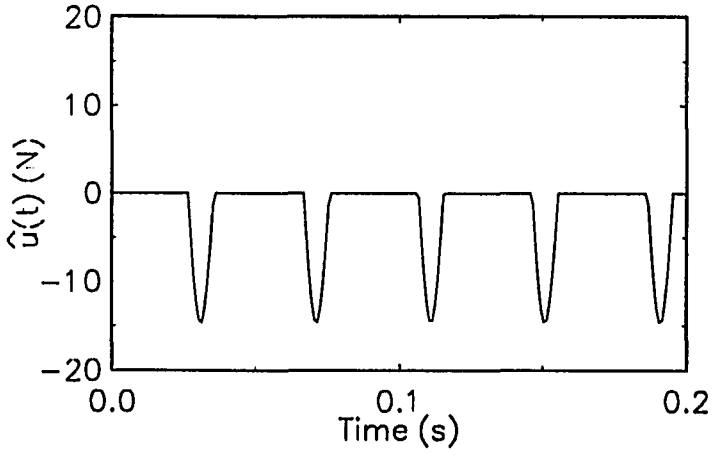

(b)

Figure 21. The impact force, (a) u(t) obtained using equation (2.32) and (b) $\hat{u}$(t) estimated using the optimization approach. Parameters are same as those of Table 3 and b(t) was 0.71sin50πt mm.

TABLE 4

The effect of weak springs $k_1 = 1675 \pm 50$ N/m and $k_2 = 1643 \pm 50$ N/m.

(a) Practically identical clearances, $d_1 = d_2 = 1.27 \pm 0.05$ mm

Input Frequency (Hz)			20	20	25	30	35	Average
Base Amplitude (mm)			0.70	1.44	0.54	0.85	1.44	
d_1 (mm)	Mechanical Experiment	D.F.A.	1.32	1.22	1.41	1.33	1.23	1.30
		Opt.A.	1.31	1.11	1.37	1.26	1.34	1.28
	Computer Simulation	D.F.A.	1.26	1.26	1.27	1.27	1.27	1.27
		Opt.A.	1.27	1.27	1.27	1.27	1.27	1.27
d_2 (mm)	Mechanical Experiment	D.F.A.	1.38	1.37	1.15	1.27	1.42	1.32
		Opt.A.	1.32	1.49	1.19	1.30	1.50	1.36
	Computer Simulation	D.F.A.	1.26	1.27	1.27	1.27	1.27	1.27
		Opt.A.	1.27	1.27	1.27	1.27	1.27	1.27

Table 4(b) please see the next page.

TABLE 4

(Continued)

(b) Nonidentical clearances, $d_1 = 0.71 \pm 0.05$ mm and $d_2 = 1.27 \pm 0.05$ mm

Input Frequency (Hz)			20	25	25	35	Average
Base Amplitude (mm)			0.72	0.44	1.30	0.71	
d_1 (mm)	Mechanical Experiment	D.F.A.	0.51	0.93	0.84	0.55	0.71
		Opt.A.	0.54	0.62	0.82	0.55	0.63
	Computer Simulation	D.F.A.	0.69	0.71	0.71	0.61	0.68
		Opt.A.	0.71	0.71	0.71	0.71	0.71
d_2 (mm)	Mechanical Experiment	D.F.A.	1.38	1.16	1.02	1.26	1.21
		Opt.A.	1.36	1.45	1.01	1.30	1.28
	Computer Simulation	D.F.A.	1.28	1.27	1.27	1.01	1.21
		Opt.A.	1.27	1.27	1.27	1.27	1.27

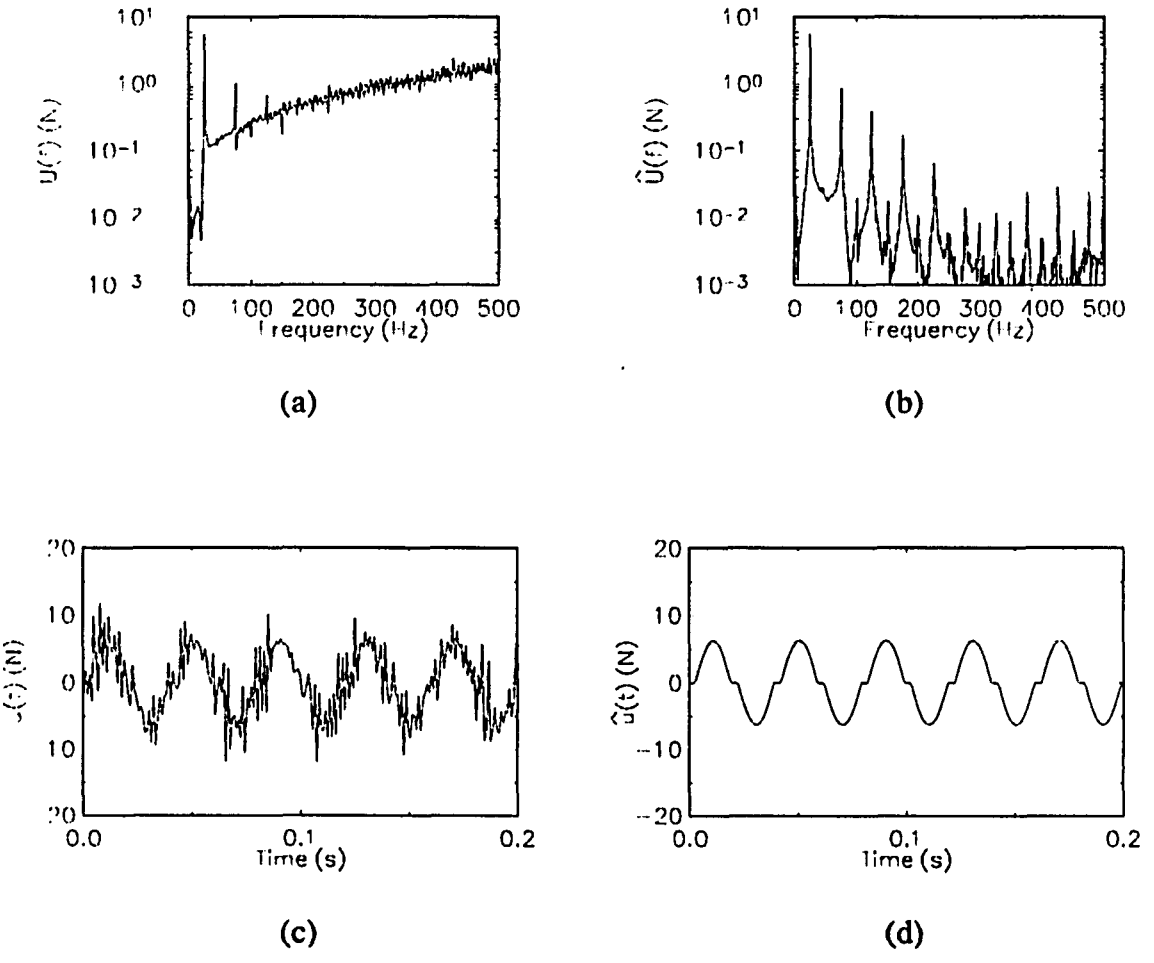

Figure 22. The spectra of (a) U(f), (b) $\hat{U}$(f) and impact force (c) u(t) and (d) $\hat{u}$(t). The parameters were $k_1 = 1675 \pm 50$ N/m, $k_2 = 1643 \pm 50$ N/m, $d_1 = d_2 = 1.27 \pm 0.05$ mm, and $b(t) = 0.54\sin 50\pi t$ mm.

The results for the case of asymmetric clearances and spring stiffnesses are presented in Table 5 and the agreement is reasonable. In such cases where gaps were quite different it is possible that for a given input system the mass may just hit a single stop. Such a situation is shown in Figure 23. Even though u(t) from the experiment was dominated by

the noise, the optimization approach was able to estimate the gap accurately and even to extract $\hat{u}(t)$ from the noisy u(t). The other gap was estimated as $|\, y(t)_{max} \,|$ and was not accurate. However, when the input amplitude was increased so that the system hits both stops, the estimates of clearances and impact forces were quite reasonable. Corresponding y(t), Y(f), u(t) and $\hat{u}(t)$ are shown in Figure 24 (a), (b), (c) and (d) respectively.

TABLE 5

The comparison of estimated clearances with actual values for an oscillator with nonidentical stiffnesses and gaps. The parameters were $k_1 = 11748 \pm 100$ N/m, $k_2 = 1643 \pm 50$ N/m, $d_1 = 1.63 \pm 0.05$ mm and $d_2 = 1.27 \pm 0.05$ mm.

Input Frequency (Hz)			20	20	25	Average
Base Amplitude (mm)			0.15	0.71	0.43	
d_1 (mm)	Mechanical Experiment	D.F.A.	1.55	1.79	1.94	1.76
		Opt.A.	1.67	1.66	1.70	1.68
	Computer Simulation	D.F.A.	1.55	1.52	1.48	1.52
		Opt.A.	1.54	1.63	1.63	1.60
d_2 (mm)	Mechanical Experiment	D.F.A.	1.34	0.88	0.71	0.98
		Opt.A.	1.34	1.33	1.42	1.36
	Computer Simulation	D.F.A.	1.25	1.30	1.31	1.29
		Opt.A.	1.27	1.27	1.27	1.27

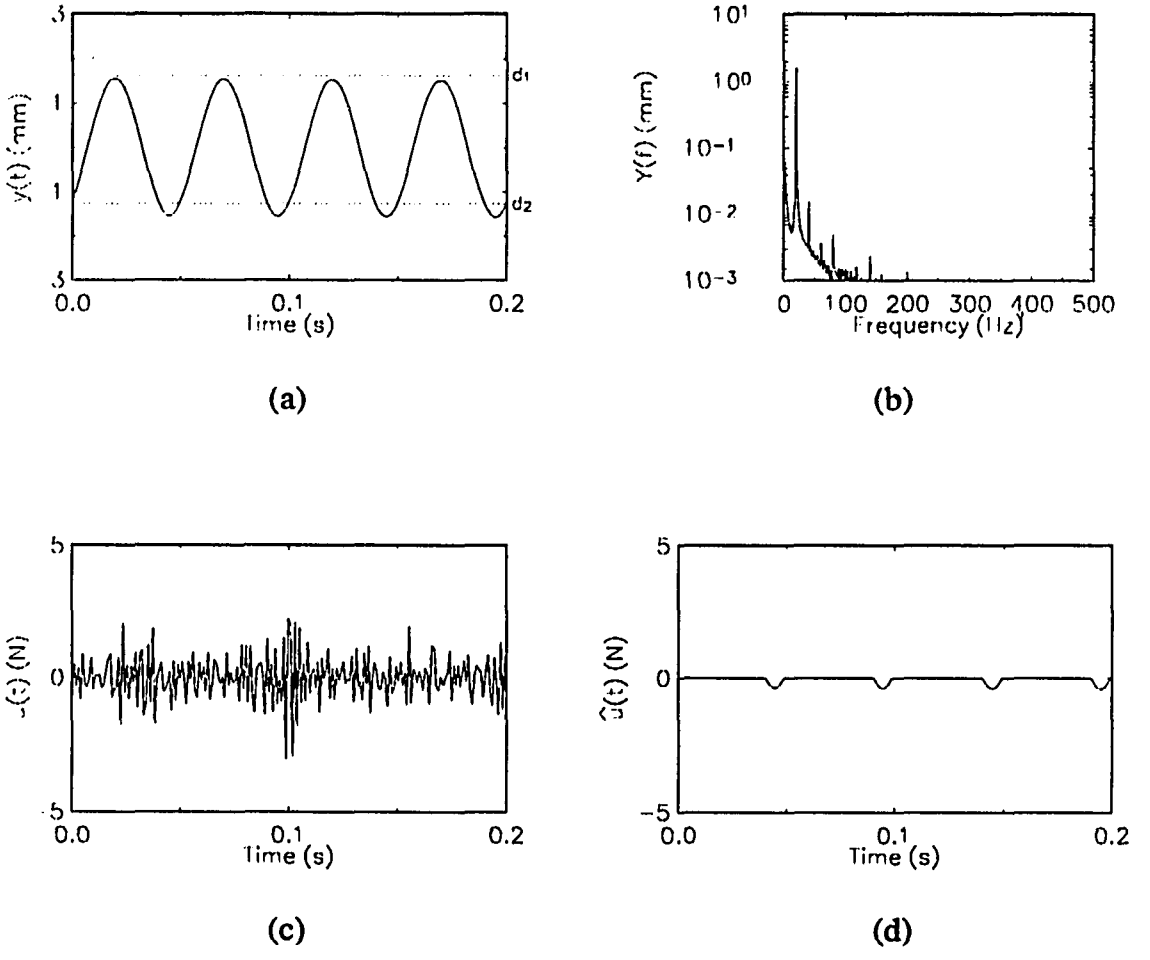

Figure 23. (a) The y(t), (b) Y(f), (c) u(t) and (d) $\hat{u}$(t) for a system when oscillator was hitting only one side. The input was 0.15sin40πt mm and other parameters are identical to those of Table 5.

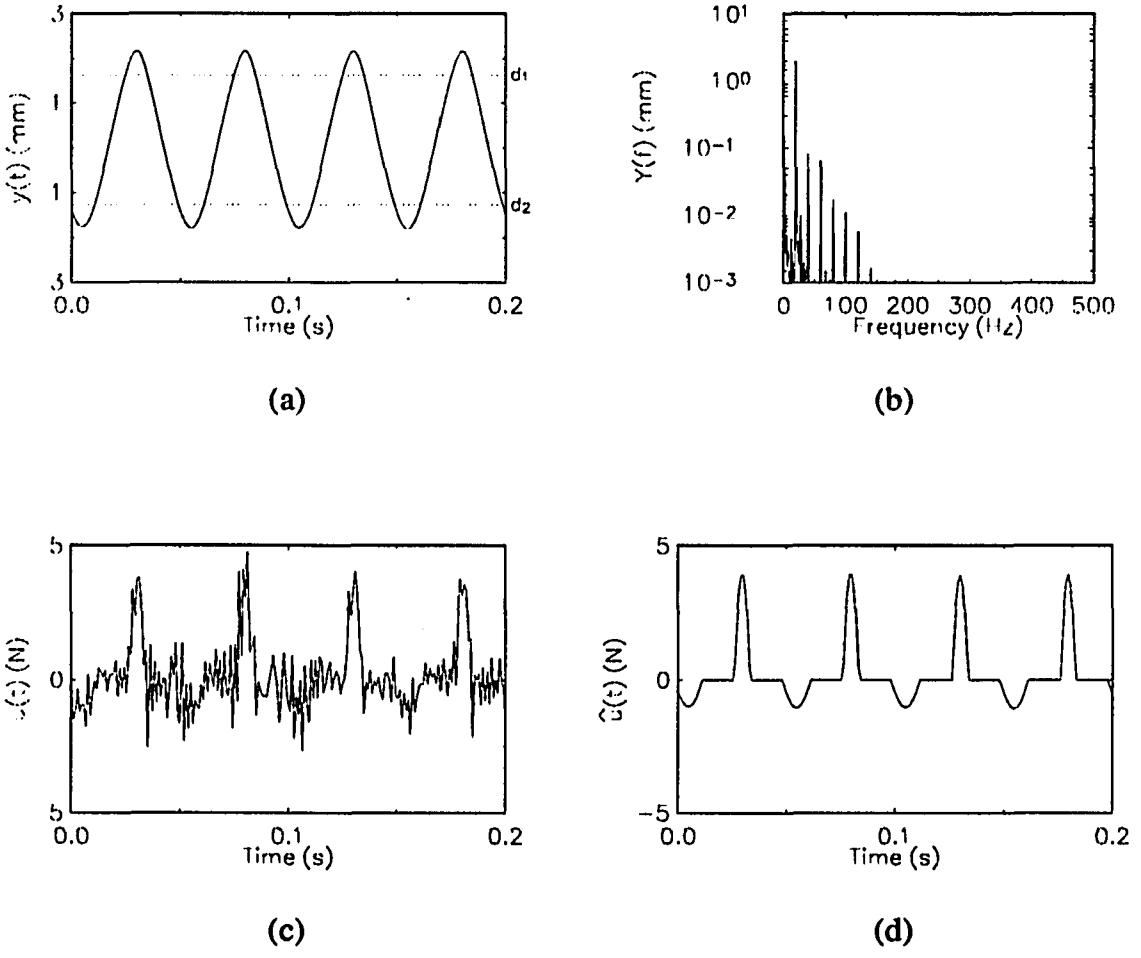

Figure 24. (a) The y(t), (b) Y(f), (c) u(t) and (d) $\hat{u}(t)$ for a system when oscillator was hitting both sides. The input was $0.71\sin 40\pi t$ mm and other parameters are identical to those of Table 5.

Extensive checking was done using the mechanical analogue where discrete and limited variations of parameters were possible. In addition to that, clearance estimates based on these two novel approaches presented in this chapter were further checked using

data generated by simulating motion on a digital computer. It is more preferable to express the system parameters in a dimensionless form. By introducing the following notations

$$\begin{aligned} \omega_n^2 &= \frac{k_0}{m}, & \zeta &= \frac{c}{2m\omega_n}, & w &= \frac{y}{d_1}, \\ \delta &= \frac{d_2}{d_1}, & s_1 &= \frac{k_1}{k_0}, & s_2 &= \frac{k_2}{k_0}, \\ \beta &= \frac{A}{d_1}, & \lambda &= \frac{\Omega}{\omega_n}, & \tau &= \omega_n t, \end{aligned} \tag{2.39}$$

the impact oscillator represented by equations (2.3) and (2.4) and under a sinusoidal excitation b(t) = B sin (Ωt) can be described in a dimensionless form as

$$\ddot{w}(\tau) + 2\zeta\dot{w}(\tau) + w(\tau) = \beta\lambda^2 \sin(\lambda\tau) - \begin{cases} s_2(w(\tau)+\delta) & -\infty < w(\tau) \le -\delta \\ 0 & -\delta < w(\tau) < 1 \\ s_1(w(\tau)-1) & 1 \le w(\tau) < \infty \end{cases}. \tag{2.40}$$

The system contains six independent parameters: the dimensionless base excitation amplitude β, the excitation frequency ratio λ, the stop stiffness ratios s_1 and s_2, the clearance ratio δ and the damping ratio ζ. The effects of changing these parameters on the clearance estimates are presented in Figure 25-30, respectively. For all situations, the optimization approach always gave very good estimates. It seems that using clean, noise-free input and output signals the optimization approach will work better and variation of various system parameters will not affect the estimation. By using the describing function approach, the overall estimates were also quite reasonable, but varying the system parameters did affect the accuracy of estimation. In the following, how and why these system parameters affect the clearance estimation using the describing function approach will be discussed. Figure 25 shows that when $\beta < 8$, the accuracy of estimation decreased as the base amplitude increased. But when β exceeded 8, the estimates suddenly

became very accurate. Non-dimensionalizing the system parameters of Figure 15, it can be seen that Figure 15 is a part of Figure 25 with $\beta < 3.4$. The reason for the tendency of decreasing accuracy was already explained when Figure 15 was discussed. When β is very large (relatively) the clearances are so small that the system behaves very similar to a linear system without clearances and with a combined spring stiffness $1+s_1(s_2)$. As a result, the response is again close to a sinusoidal, the assumption of the describing function approach is well satisfied and a good estimation is again obtained. Even though a large excitation may result in a good estimation, practically it may not be a good choice as it will also produce a large impact force which may damage the structure being investigated. Figure 26 shows that the excitation frequency had little effect on the accuracy of the describing function approach over most of the frequency range except when the frequency ratio λ was around 1, i.e. when the impact oscillator was excited near the resonant frequency of the corresponding simple oscillator without stops. Even though the computer simulated results shown in Figure 26 indicate that for the purpose of increasing accuracy, clearances should be estimated under excitation with frequency far away from the resonant frequency, practical considerations will force us to choose excitation frequency not far from the resonance in order to ensure that the mass hits the stops under acceptable excitation amplitude. Figure 27 shows the effects of the stiffness ratio of the stop. When stiffness ratios s_1 and s_2 are small, the clearances and stops have a smaller effect on the system and the system is close to a linear one. But when the stiffness ratios s_1 and s_2 become larger, more and stronger higher harmonics will be generated in the system output and the output differs considerably from a sinusoidal wave. Then the assumption of the describing function approach is less satisfied, and the clearance estimation based on this approach becomes less accurate. Figure 27 clearly indicates the limitation of the describing function approach that it can not be used for systems with very high support

stiffness. When unequal stop stiffnesses are under consideration, the asymmetry of the system which generate even order higher harmonics will affect estimation using the describing function approach. It is interesting to see from Figure 28 that when one side stop became harder ($s_2 >> s_1$) it only affected the estimation of the clearance on that side (clearance 2) and had little effect on the other clearance (clearance 1). Figure 29 shows that as one clearance increased the estimated clearance also followed the same trend and gave accurate values. Figure 30 shows that the damping ratio had little effect on the clearance estimation.

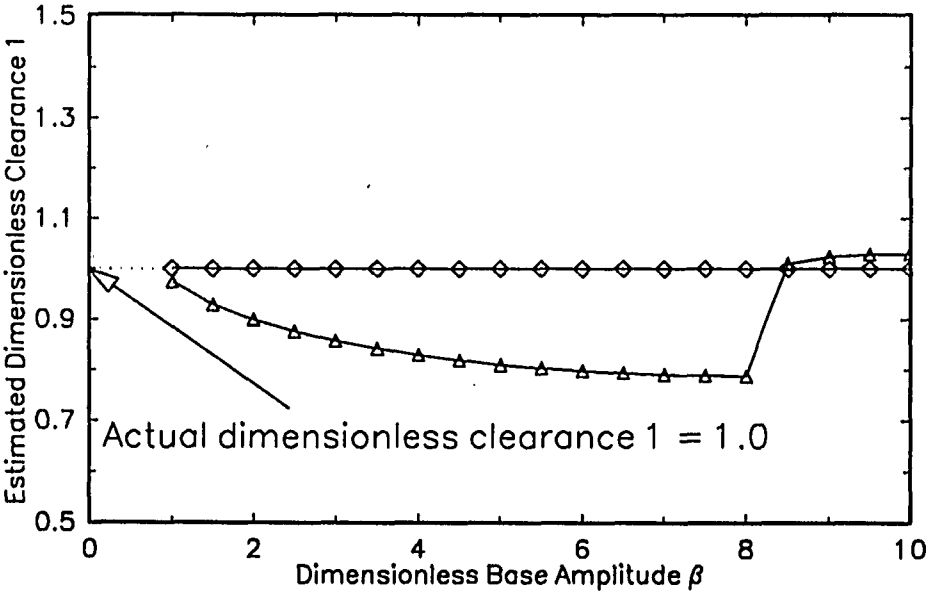

Figure 25. Effect of dimensionless amplitude of excitation, β. System parameters were $\zeta = 0.25$, $s_1 = s_2 = 10$, $\delta = 1$ and $\lambda = 0.8$. Symbols in Figures 25-31 are same as those of Figure 15.

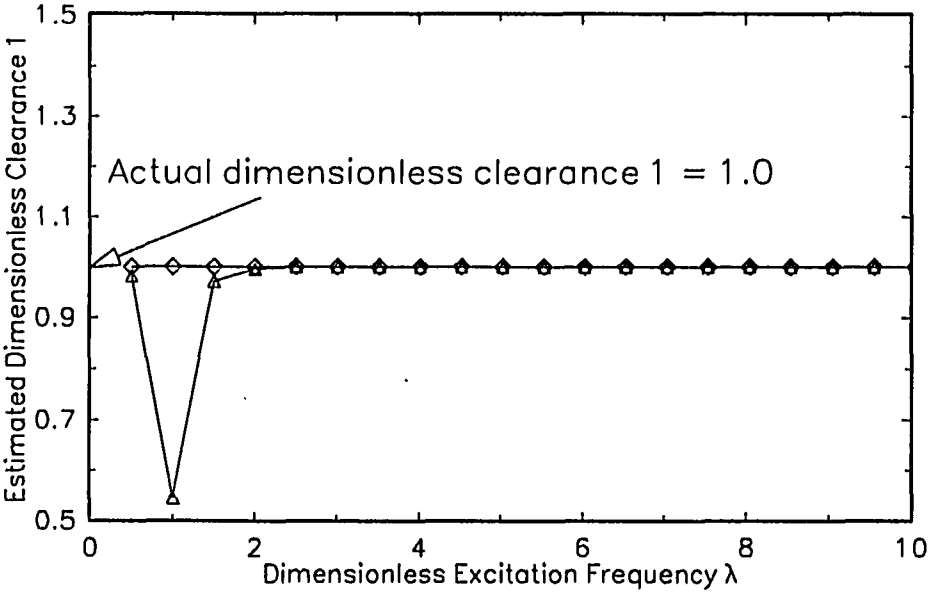

Figure 26. Effect of excitation frequency ratio λ. System parameters were $\zeta = 0.25$, $s_1 = s_2 = 10$, $\delta = 1$ and $\beta = 3.2$.

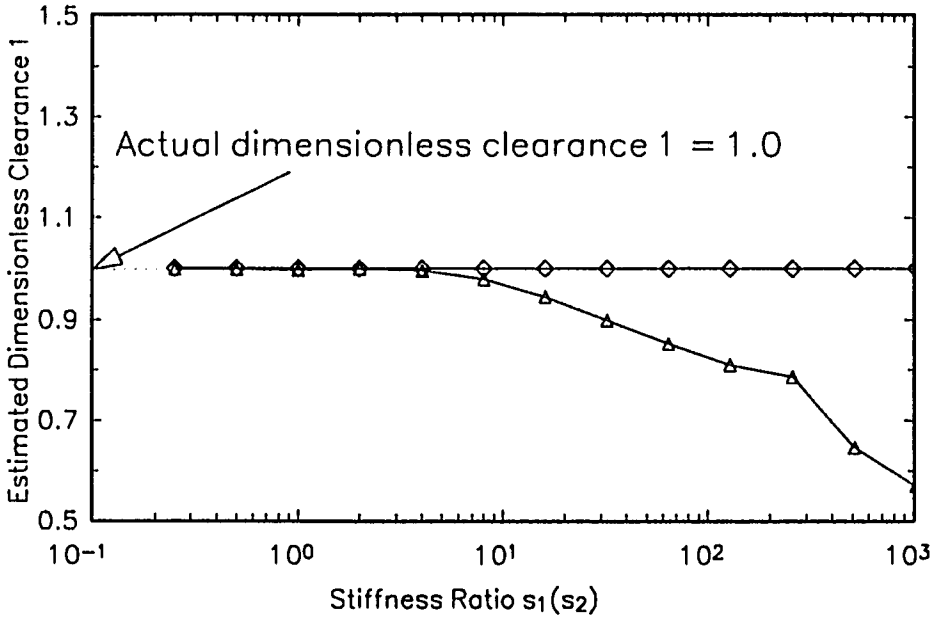

Figure 27. Effect of stiffness ratio. System parameters were $\zeta = 0.25$, $s_1 = s_2$, $\delta = 1$, $\beta = 1$ and $\lambda = 1.6$.

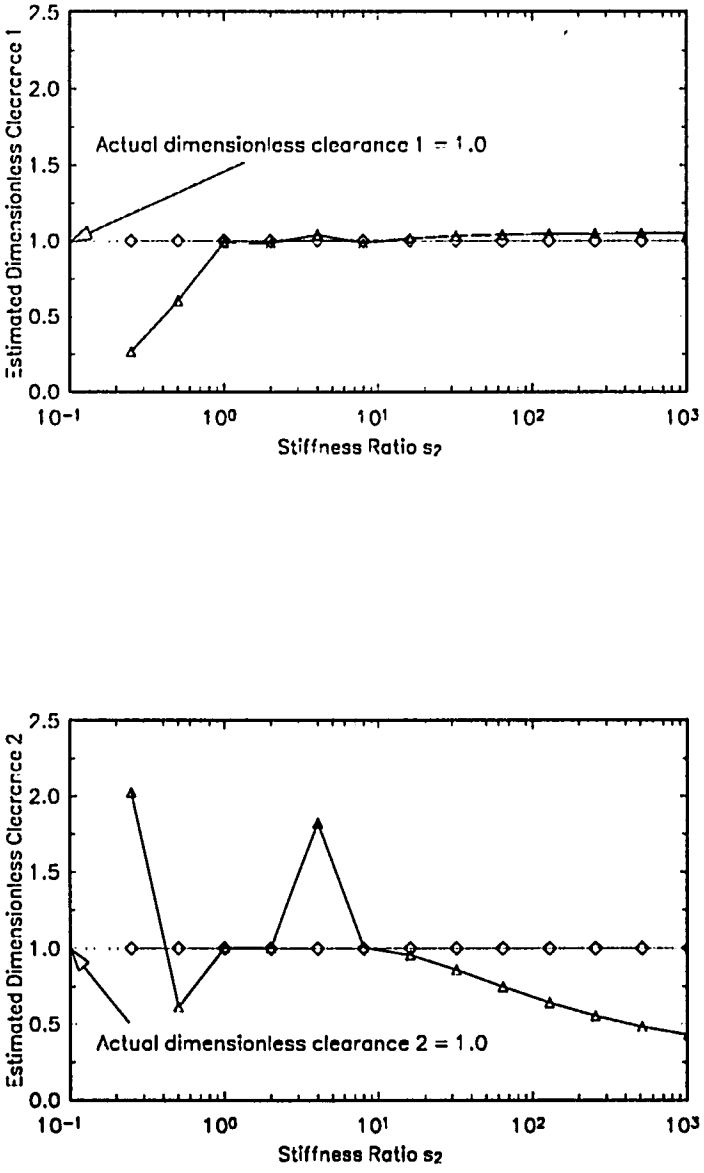

Figure 28. Effect of unequal stop stiffnesses. System parameters were $\zeta = 0.15$, $s_1 = 10$, $\delta = 1$, $\beta = 1$ and $\lambda = 2.5$.

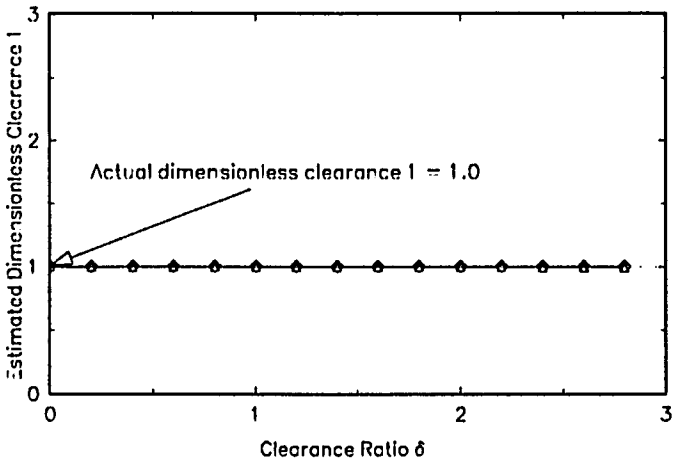

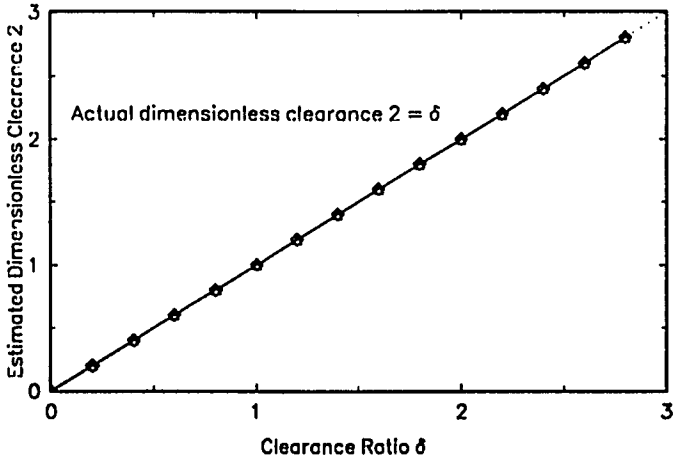

Figure 29. Effect of unequal clearances. System parameters were $\zeta = 0.15$, $s_1 = s_2 = 10$, $\beta = 3$, $\lambda = 2.5$ and dimensionless clearance corresponding to d_1 is 1.0.

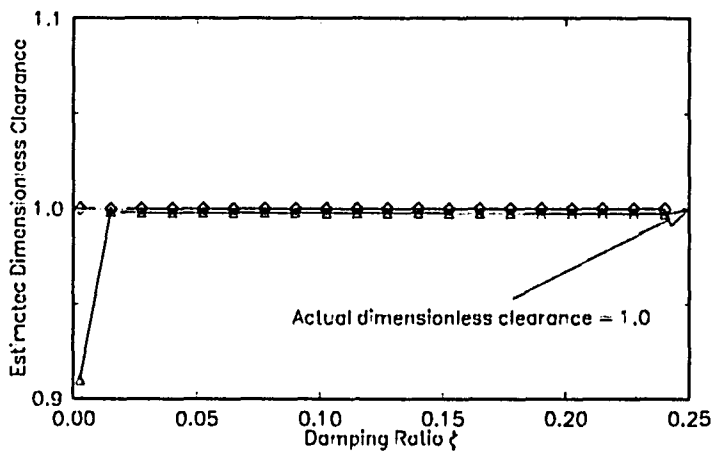

Figure 30. Effect of primary system damping ratio, ζ. System parameters were $s_1 = s_2 = 10$, $\delta = 1$, $\beta = 1$ and $\lambda = 2.5$.

In practice, a system response can only be measured with some measurement error. The effect of this measurement error on the performance of the clearances estimation approaches can be simulated by adding to y(t) a white noise with a certain noise-to-signal ratio. The effect of adding white noise to the output on the estimates was checked and is shown in Figure 31. In almost all cases reported above, the estimates obtained using the optimization approach were better than those obtained using the describing function approach. The estimates obtained with additional noise are somewhat surprising. Only in this case the estimates obtained using the describing function approach were better than those obtained using the optimization approach. This is due to the fact that the describing function approach only uses the constant term and the fundamental component of y(t) to perform the estimation. When the white noise has a zero mean value, it has little effect on

the constant term of y(t), and the fundamental component of y(t) is less susceptible to the noise. Hence the describing function approach is robust against the effects of the measurement noise. This property of the describing function approach makes it attractive for a practical application. Contrary to this, the optimization approach is more sensitive to measurement error. The main reason can be explained as follows. The first step of the optimization approach is estimating the impact force in frequency domain, which takes the following form when noise is considered

$$\hat{U}(\omega) = m\omega^2 B(\omega) - \frac{\hat{Y}(\omega)}{H(\omega)}, \tag{2.41}$$

where $\hat{Y}(\omega)$ is the spectrum of y(t) plus white noise N(ω).

The error in estimated $\hat{U}(\omega)$, DU(ω), due to the noise can be found by substituting $\hat{Y}(\omega)$ into (2.41) and noting the relation between the real Y(ω) and U(ω). We have

$$DU(\omega) = U(\omega) - \hat{U}(\omega) = \frac{N(\omega)}{H(\omega)}. \tag{2.42}$$

Since at high frequency H(ω) is very small, the high frequency parts of N(ω) will be greatly amplified when the polluted system response, Y(ω)+N(ω), is used to estimate the impact force. Using such inaccurate impact force in minimizing $J(\hat{d}_1, \hat{d}_2)$ to estimate clearances inevitably results in a larger error. Figure 31 shows the sensitivity of estimation using the optimization approach, however the effect of small percentage noise below 2% is negligible. For large noise/signal ratio the optimization approach does not work well. In real experiments with the mechanical analogue the system acts as a low pass filter and most of the results obtained using the optimization approach agree better with actual values than the results obtained using the describing function approach.

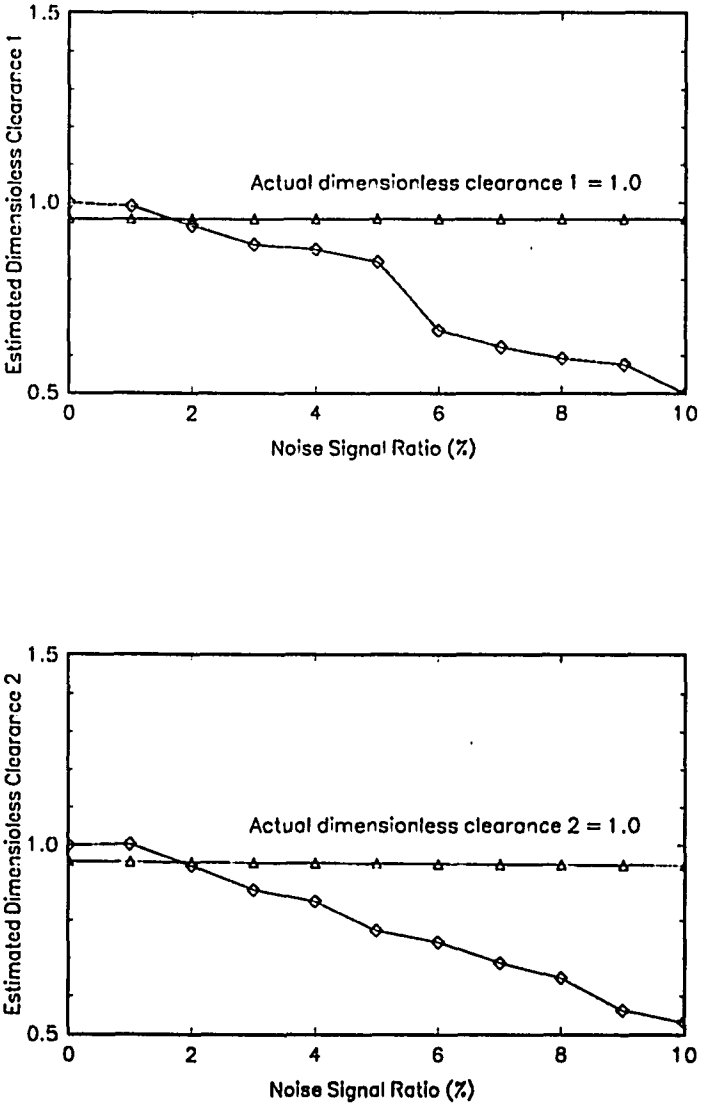

Figure 31. Effect of adding noise to system output. System parameters were $\zeta = 0.15$, $s_1 = s_2 = 10$, $\delta = 1$, $\beta = 3$ and $\lambda = 0.8$.

2.7 CONCLUSIONS

Two novel in situ clearance and impact force estimation approaches, one based on a describing function approach and the other on an optimization approach, are developed in this chapter for a harmonically excited vibroimpact system. The estimates obtained using data from the mechanical analogue of an impact oscillator and simulation using a digital computer were shown to agree with actual clearances and impact forces. The results obtained using describing function approach are more reliable when response was dominated by the fundamental harmonic. The optimization approach worked well for simple as well as complex motions. Proper adjustment of the input frequency and amplitude which produces response with medium intensity impacts with small distortion of the output from the first harmonic coupled with averaging estimates obtained under different excitations seems to be the best approach to estimate unknown clearances and impact forces. A simplified approach to estimate clearances in case of a symmetric system with the use of a vibration meter and a hand calculator is promising for the on site in situ application. Clearances in practical mechanical structures might have very small magnitudes. But due to the limited accuracy of the experimental instruments relatively larger clearances around 1 mm were used the experiments. Further experimental research is required when clearances are very small. Another novel clearance estimation approach for a randomly excited vibroimpact system is presented in the next chapter using again an impact oscillator model as an example.

CHAPTER III.

ESTIMATION OF CLEARANCES FOR SYSTEMS UNDER A RANDOM EXCITATION

3.1 INTRODUCTION

Two novel in situ clearance and impact force estimation approaches, one based on a describing function approach and the other on an optimization approach, were developed for harmonically excited systems in the last chapter. Here, a novel clearance estimation approach is presented for systems under random excitation. The potential advantage of this approach is that clearances could be estimated using normal operating conditions. The excitation to an operating system is more likely to be random than sinusoidal. As an example, turbulent flow produces random excitation to heat exchanger tubes and results in random vibration [12,55,56].

As in the last chapter, an impact oscillator model is chosen to develop the clearance estimation approach. Similar to Chapter 2, this impact oscillator is again treated as a linear subsystem coupled with an isolated nonlinear element as shown in Figure 4(b). Spectral analysis [20-22,57-60] is used to analyze the linear subsystem and hence this approach is called a Spectral Analysis Approach. Considering the nonlinear element, theoretical expressions are developed to relate the first two coefficients W_0 and W_1 of Chebyshev-Hermite expansion of nonlinear relation between u(t) and y(t) in terms of unknown clearances d_1 and d_2 and mean and variance of the random response y(t). A procedure to evaluate W_0 and W_1 from the measured y(t) and b(t) and calculated u(t) is then presented. Substitution of experimentally obtained values in the theoretical

expressions results in two coupled nonlinear equations in two unknown clearances and can be numerically solved. The theoretical prediction was checked using a single degree of freedom impact oscillator model. The needed vibro-impact response of an impact oscillator was obtained using an approach of simulation of motion on a digital computer and using a mechanical analogue. The comparison of estimated quantities with actual values indicated a reasonable agreement.

3.2 THEORY

The spectral analysis approach to estimate clearances is developed using an impact oscillator model shown in Figure 2 with two asymmetric motion limiting stops with nonidentical spring stiffnesses. Impact oscillator parameters are assumed known and have mass, m, linear spring with stiffness, k_0, and a viscous damper with damping constant c. The d_1 and d_2 are the unknown clearances between the oscillator and the two elastic stops. The corresponding spring stiffnesses k_1 and k_2, respectively, are assumed known. Let b(t) be the known random external base excitation and x(t) be the absolute displacement of the mass measured from the static equilibrium position. Let $y(t)=x(t)-b(t)$ be the relative displacement between the mass and the base. It is assumed that the b(t) is a stationary and ergotic stochastic process and so is y(t). The differential equation of motion of mass m take the same form as equations (2.3) and (2.4) derived in last chapter as

$$m\ddot{y}(t)+c\dot{y}(t)+k_0y(t)=-m\ddot{b}(t)-u[y(t)], \tag{3.1}$$

where

$$u[y(t)] = \begin{cases} k_2(y(t)+d_2) & -\infty < y(t) \le -d_2, \\ 0 & -d_2 < y(t) < d_1, \\ k_1(y(t)-d_1) & d_1 \le y(t) < \infty. \end{cases} \tag{3.2}$$

All variables in the above equations should be understood as stochastical processes. The equations essentially remain the same when mass m is excited by an external force g(t). In that case, y(t) and $-m\ddot{b}(t)$ will be, respectively, replaced by x(t) and g(t) in those equations.

Consider equations (3.1) and (3.2) separately. Equation (3.2) itself defines a dead-zone nonlinearity due to the nonlinear force deflection characteristics of the clearance-stop pair. With u[y(t)] on its right side being considered as a quasi-input, equation (3.1) represents a linear subsystem under two inputs: the base excitation b(t) and the stop produced impact force excitation u(t). So the complete impact oscillator can be decomposed into two parts: a two input one output linear subsystem and an isolated dead-zone nonlinearity (see Figure 4(b)). It will be seen that this decomposition is very advantageous as well developed techniques of linear spectral analysis can be used for the linear subsystem and a special nonlinear analysis is applied only to the isolated nonlinearity.

Consider first the isolated clearance-stop nonlinearity defined by equation (3.2). Even under Gaussian base excitation b(t), the y(t) and u(t) may still be non-Gaussian processes [57,58]. The second order joint probability density function $p(y_1, y_2)$ of the non-Gaussian process y(t) can be expressed as a series of Chebyshev-Hermite polynomials as [61-65]

$$p(y_1,y_2)=\frac{1}{2\pi\sigma_y^2}\exp\left\{-\frac{1}{2\sigma_y^2}[(y_1-m_y)^2+(y_2-m_y)^2]\right\}\left[\sum_{n=0}^{\infty}\frac{C_n}{(n!)^2}H_n\left(\frac{y_1-m_y}{\sigma_y}\right)H_n\left(\frac{y_2-m_y}{\sigma_y}\right)\right], \tag{3.3}$$

where $y_1=y(t)$, $y_2=y(t+\tau)$ and m_y and σ_y^2 are the mean value and the variance of y(t) respectively. The H_n are the Chebyshev-Hermite polynomials defined by [61],

$$H_n(x) = (-1)^n \exp\left(\frac{x^2}{2}\right)\frac{d^n}{dx^n}\left[\exp\left(-\frac{x^2}{2}\right)\right], \tag{3.4}$$

or by the recurrence relation,

$$\begin{cases} H_0(x) = 1, & H_1(x) = x \\ H_{n+1}(x) = xH_n(x) - nH_{n-1}(x) \end{cases} \tag{3.5}$$

The coefficients, C_n, n=1,2,..., which are functions of τ, are determined as follows. Multiplying both sides of equation (3.3) by $H_n\left(\frac{y_1-m_y}{\sigma_y}\right)H_n\left(\frac{y_2-m_y}{\sigma_y}\right)dy_1dy_2$ and integrating leads to

$$\int_{-\infty}^{\infty}\int_{-\infty}^{\infty} p(y_1,y_2)H_n\left(\frac{y_1-m_y}{\sigma_y}\right)H_n\left(\frac{y_2-m_y}{\sigma_y}\right)dy_1dy_2$$

$$= \int_{-\infty}^{\infty}\int_{-\infty}^{\infty}\frac{1}{2\pi\sigma_y^2}\exp\left\{-\frac{1}{2\sigma_y^2}[(y_1-m_y)^2+(y_2-m_y)^2]\right\}$$

$$\left[\sum_{i=0}^{\infty}\frac{C_i}{(i!)^2}H_i\left(\frac{y_1-m_y}{\sigma_y}\right)H_i\left(\frac{y_2-m_y}{\sigma_y}\right)\right]H_n\left(\frac{y_1-m_y}{\sigma_y}\right)H_n\left(\frac{y_2-m_y}{\sigma_y}\right)dy_1dy_2. \tag{3.6}$$

By virtue of the orthogonality of H_n,

$$\int_{-\infty}^{\infty}H_n\left(\frac{y-m_y}{\sigma_y}\right)H_m\left(\frac{y-m_y}{\sigma_y}\right)\frac{1}{\sqrt{2\pi}\sigma_y}\exp\left(-\frac{(y-m_y)^2}{2\sigma_y^2}\right)dy = \begin{cases} n! & m=n \\ 0 & m\neq n \end{cases}, \tag{3.7}$$

the right side of equation (3.6) simply becomes C_n. Writing the left side of equation (3.6) in the form of expectation [57,58], equation (3.6) gives the expression for C_n as

$$C_n = E\left\{H_n\left(\frac{y_1-m_y}{\sigma_y}\right)H_n\left(\frac{y_2-m_y}{\sigma_y}\right)\right\}. \tag{3.8}$$

Substituting the first two Chebyshev-Hermite polynomials into equation (3.8), gives the first two C_ns, as

$$C_0 = E[1] = 1, \quad C_1 = E\left[\left(\frac{y_1-m_y}{\sigma_y}\right)\left(\frac{y_2-m_y}{\sigma_y}\right)\right] = \rho_y(\tau), \tag{3.9}$$

where $\rho_y(\tau)$ is the autocovariance coefficient of response y(t) [57].

The nonlinear relation between the response y(t) and the impact force u(t) defined by equation (3.2) can also be expressed as a series of Chebyshev-Hermite polynomials, as

$$u(y) = \sum_{n=0}^{\infty} W_n H_n\left(\frac{y - m_y}{\sigma_y}\right), \tag{3.10}$$

where W_n are the constants which can be found by using the orthogonality of H_n. Multiplying both sides of equation (3.10) by $\frac{1}{\sqrt{2\pi}\sigma_y}\exp\left(-\frac{(y-m_y)^2}{2\sigma_y^2}\right)H_n\left(\frac{y-m_y}{\sigma_y}\right)dy$ and integrating gives

$$\int_{-\infty}^{\infty} \frac{1}{\sqrt{2\pi}\sigma_y}\exp\left(-\frac{(y-m_y)^2}{2\sigma_y^2}\right)H_n\left(\frac{y-m_y}{\sigma_y}\right)u(y)dy$$

$$= \int_{-\infty}^{\infty} \frac{1}{\sqrt{2\pi}\sigma_y}\exp\left(-\frac{(y-m_y)^2}{2\sigma_y^2}\right)H_n\left(\frac{y-m_y}{\sigma_y}\right)\sum_{i=0}^{\infty} W_i H_i\left(\frac{y-m_y}{\sigma_y}\right)dy. \tag{3.11}$$

Using the orthogonality of H_n, the above equation reduces to

$$\int_{-\infty}^{\infty} \frac{1}{\sqrt{2\pi}\sigma_y}\exp\left(-\frac{(y-m_y)^2}{2\sigma_y^2}\right)u(y)H_n\left(\frac{y-m_y}{\sigma_y}\right)dy = n!W_n. \tag{3.12}$$

W_n can be obtained as

$$W_n = \frac{1}{n!}\int_{-\infty}^{\infty} \frac{1}{\sqrt{2\pi}\sigma_y}\exp\left(-\frac{(y-m_y)^2}{2\sigma_y^2}\right)u(y)H_n\left(\frac{y-m_y}{\sigma_y}\right)dy. \tag{3.13}$$

The first two terms W_0 and W_1 can be found by substituting equation (3.2) and the first two Chebyshev-Hermite polynomials into equation (3.13) and integrating as

$$W_0 = \int_{-\infty}^{\infty} \frac{1}{\sqrt{2\pi}\sigma_y} \exp\left(-\frac{(y-m_y)^2}{2\sigma_y^2}\right) u(y)dy$$

$$= \frac{1}{\sqrt{2\pi}\sigma_y}\left[\int_{-\infty}^{-d_2} \exp\left(-\frac{(y-m_y)^2}{2\sigma_y^2}\right) k_2(y+d_2)dy + \int_{d_1}^{\infty} \exp\left(-\frac{(y-m_y)^2}{2\sigma_y^2}\right) k_1(y-d_1)dy\right]$$

$$= \frac{\sigma_y}{\sqrt{2\pi}}\left[k_1 \exp\left(-\frac{(d_1-m_y)^2}{2\sigma_y^2}\right) - k_2 \exp\left(-\frac{(d_2+m_y)^2}{2\sigma_y^2}\right)\right] +$$

$$\frac{1}{2}\left[k_2(m_y+d_2)erfc\left(\frac{d_2+m_y}{\sqrt{2}\sigma_y}\right) + k_1(m_y-d_1)erfc\left(\frac{d_1-m_y}{\sqrt{2}\sigma_y}\right)\right] \tag{3.14}$$

and

$$W_1 = \int_{-\infty}^{\infty} \frac{1}{\sqrt{2\pi}\sigma_y} \exp\left(-\frac{(y-m_y)^2}{2\sigma_y^2}\right) u(y)\left(\frac{y-m_y}{\sigma_y}\right)dy$$

$$= \frac{1}{\sqrt{2\pi}\sigma_y}\left[\int_{-\infty}^{-d_2} \exp\left(-\frac{(y-m_y)^2}{2\sigma_y^2}\right)\left(\frac{y-m_y}{\sigma_y}\right) k_2(y+d_2)dy +\right.$$

$$\left.\int_{d_1}^{\infty} \exp\left(-\frac{(y-m_y)^2}{2\sigma_y^2}\right)\left(\frac{y-m_y}{\sigma_y}\right) k_1(y-d_1)dy\right]$$

$$= \frac{\sigma_y}{2}\left[k_2 erfc\left(\frac{d_2+m_y}{\sqrt{2}\sigma_y}\right) + k_1 erfc\left(\frac{d_1-m_y}{\sqrt{2}\sigma_y}\right)\right]. \tag{3.15}$$

The erfc in the above equations is the complementary error function defined by

$$erfc(x) = \frac{2}{\sqrt{\pi}}\int_x^{\infty} e^{-u^2} du. \tag{3.16}$$

It can be observed that equations (3.14) and (3.15) relate W_0 and W_1 to unknown clearances, d_1 and d_2. When W_0 and W_1 have been estimated, d_1 and d_2 can be calculated by solving these two coupled nonlinear equations. Next, the two surprisingly simple equations to estimate W_0 and W_1 from the experimentally obtained data is presented in what follows.

The cross correlation function of y(t) and u(t), $R_{yu}(\tau)$, can be obtained using equations (3.3) and (3.10) as

$$R_{yu}(\tau) = E[y(t)u(t+\tau)]$$

$$= \int_{-\infty}^{\infty}\int_{-\infty}^{\infty} p(y_1, y_2) y_1 u(y_2) dy_1 dy_2$$

$$= \int_{-\infty}^{\infty}\int_{-\infty}^{\infty} \frac{1}{2\pi\sigma_y^2} \exp\left\{-\frac{1}{2\sigma_y^2}[(y_1 - m_y)^2 + (y_2 - m_y)^2]\right\} \times$$

$$\left[\sum_{n=0}^{\infty} \frac{C_n}{(n!)^2} H_n\left(\frac{y_1 - m_y}{\sigma_y}\right) H_n\left(\frac{y_2 - m_y}{\sigma_y}\right)\right] y_1 \sum_{n=0}^{\infty} W_n H_n\left(\frac{y_2 - m_y}{\sigma_y}\right) dy_1 dy_2. \tag{3.17}$$

Using the orthogonality relations between H_ns, the last expression reduces to

$$R_{yu}(\tau) = \int_{-\infty}^{\infty} \frac{1}{\sqrt{2\pi}\sigma_y} \exp\left[-\frac{1}{2}\left(\frac{y_1 - m_y}{\sigma_y}\right)^2\right]\left[\sum_{n=0}^{\infty} \frac{C_n}{(n!)} W_n H_n\left(\frac{y_1 - m_y}{\sigma_y}\right)\right] y_1 dy_1$$

$$= C_0 W_0 m_y + C_1 W_1 \sigma_y. \tag{3.18}$$

Substituting the values of C_0 and C_1 from equation (3.9) into above equation gives

$$R_{yu}(\tau) = m_y W_0 + \rho_y(\tau)\sigma_y W_1. \tag{3.19}$$

The relation between the autocovariance coefficient $\rho_y(\tau)$ and the autocorrelation function $R_y(\tau)$ is given by [57]

$$\rho_y(\tau) = \frac{R_y(\tau) - m_y^2}{\sigma_y^2}. \tag{3.20}$$

Substituting the last equation into equation (3.19) yields

$$R_{yu}(\tau) = m_y W_0 - \frac{m_y^2 W_1}{\sigma_y} + \frac{W_1}{\sigma_y} R_y(\tau). \tag{3.21}$$

By averaging both sides over τ and using the ergotic property of y(t) and u(t), the above equation becomes

$$\lim_{T_\tau\to\infty}\frac{1}{T_\tau}\int_0^{T_\tau}\left[\lim_{T\to\infty}\frac{1}{T}\int_0^{T} y(t)u(t+\tau)dt\right]d\tau$$

$$=m_y W_0-\frac{m_y^2 W_1}{\sigma_y}+\frac{W_1}{\sigma_y}\left\{\lim_{T_\tau\to\infty}\frac{1}{T_\tau}\int_0^{T}\left[\lim_{T\to\infty}\frac{1}{T}\int_0^{T} y(t)y(t+\tau)dt\right]d\tau\right\} \tag{3.22}$$

By changing the order of integration on both sides, the above equation reduces to

$$m_y m_u = m_y W_0-\frac{m_y^2 W_1}{\sigma_y}+\frac{W_1}{\sigma_y}m_y^2, \tag{3.23}$$

which leads to a very simple equation

$$W_0 \;=\; m_u. \tag{3.24}$$

The m_u in the above equation is the mean value of the impact force u(t).

Taking the Fourier transforms of both sides of Equation (3.21), the cross spectral density function of y(t) and u(t) can be expressed as

$$S_{yu}(\omega)=\left(m_y W_0-\frac{m_y^2 W_1}{\sigma_y}\right)\delta(\omega)+\frac{W_1}{\sigma_y}S_y(\omega), \tag{3.25}$$

where $\delta(\omega)$ is the Dirac delta function [66] and $s_y(\omega)$ is the power spectral density function of y(t). When $\omega\neq 0$, equation (3.25) reduces to

$$S_{yu}(\omega)=\frac{W_1}{\sigma_y}S_y(\omega), \qquad \omega\neq 0. \tag{3.26}$$

Solving equation (3.26) for W_1 leads to

$$W_1=\sigma_y\frac{S_{yu}(\omega)}{S_y(\omega)}, \qquad \omega\neq 0. \tag{3.27}$$

The value of W_1 given by equation (3.27) can be obtained at any frequency $\omega = \omega_1$. However, for better accuracy, the average value of W_1 could be found using a frequency range ($\omega_1 < \omega < \omega_2$) as

$$W_1 = \sigma_y \frac{\int_{\omega_1}^{\omega_2} S_{yu}(\omega) d\omega}{\int_{\omega_1}^{\omega_2} S_y(\omega) d\omega}. \tag{3.28}$$

Equations (3.24) and (3.28) together with equations (3.14) and (3.15) form the basis of the clearance estimation approach presented here. The approach of finding the values of m_y, σ_y, $S_y(\omega)$, m_u and $S_{yu}(\omega)$ from the base excitation b(t) and response y(t) is described next.

Assume that the time histories of b(t) and y(t) of time duration T, $0 \le t \le T$, are available. Since y(t) is assumed as an ergotic process, the mean m_y, variance σ_y^2, and power spectral density $S_y(\omega)$ can be estimated as

$$m_y = \lim_{T \to \infty} \frac{1}{T} \int_0^T y(t) dy = \lim_{T \to \infty} \frac{1}{T} Y(0, T), \tag{3.29}$$

$$\sigma_y^2 = \lim_{T \to \infty} \frac{1}{T} \int_0^T y(t)^2 dy - m_y^2, \tag{3.30}$$

and

$$S_y(\omega) = \lim_{T \to \infty} \frac{1}{T} E\{| Y(\omega, T) |^2\}, \tag{3.31}$$

where Y(ω,T) is a finite Fourier transform of y(t), $0 \le t \le T$, which is defined as

$$Y(\omega, T) = \int_0^T y(t) e^{-i\omega t} dt. \tag{3.32}$$

The mean value of the impact force, m_u, and the cross spectral density function of y(t) and u(t), $S_{yu}(\omega)$, can not be found directly form y(t). However, these can be obtained

by using the analysis of the linear subsystem defined by equation (3.1) as follows. Fourier transforming both sides of equation (3.1) yields

$$U(\omega,T)=m\omega^2B(\omega,T)-\frac{Y(\omega,T)}{H(\omega)}, \tag{3.33}$$

where

$$H(\omega)=\frac{1}{(k_0-m\omega^2+ic\omega)}. \tag{3.34}$$

The finite Fourier transforms B(ω,T) and Y(ω,T) can be obtained from the input b(t) and measured output y(t) respectively, and the U(ω,T) can be obtained by using equation (3.33). Both the m_u and the $S_{yu}(\omega)$ can then be obtained from U(ω,T) and Y(ω,T) as,

$$m_u=\lim_{T\to\infty}\frac{1}{T}U(0,T) \tag{3.35}$$

and

$$S_{yu}(\omega)=\lim_{T\to\infty}\frac{1}{T}E\{Y^*(\omega,T)U(\omega,T)\}. \tag{3.36}$$

One can also find the power spectral density function $S_u(\omega)$ of the impact force u(t) which gives important information about the power distribution in frequency domain of the impact force, according to the following equation

$$S_u(\omega)=\lim_{T\to\infty}\frac{1}{T}E\{|U(\omega,T)|^2\}. \tag{3.37}$$

In summary, clearances can be estimated using the spectral analysis approach as follows. Estimate the statistical properties m_y, σ_y, $S_y(\omega)$, m_u and $S_{yu}(\omega)$ from the experimentally obtained b(t) and y(t). The W_0 and W_1 can be obtained using the just mentioned values in equations (3.24) and (3.28), respectively. Substituting the values of

W_0 and W_1 into the left hand sides of equations (3.14) and (3.15) respectively, generates two coupled nonlinear equations in two unknowns d_1 and d_2 and can be solved using numerical iteration.

3.3 EXPERIMENTS AND COMPUTATIONS

The predictions from the clearance estimation approach described in the last section were tested using computer simulated experiments and physical experiments conducted using a mechanical analogue of an impact oscillator. Computer simulated experiments are convenient, economical and flexible enough to vary independently any parameter of interest. However, the real world complications are not easy to reproduce in the computer simulation. Hence additional experiments were performed using a mechanical analogue. In both experiments, system responses y(t) were generated using known random excitation and the spectral analysis approach presented above was used to estimate the clearances. The estimated clearances were compared with the actual values to validate the clearance estimation approach presented. The comparison indicates a reasonable agreement. The details of these two ways of generating y(t) are given next.

3.3.1 SIMULATION USING A DIGITAL COMPUTER

During computer simulations a random external force g(t) was generated and used instead of a base excitation b(t) (see equation (3.1)). A computer program based on a standard fourth-order Runge-Kutta method [67] was developed to solve equation (3.1) and is given in Appendix C. The temporal behavior of the impact oscillator was obtained using a double precision arithmetic on a VAXstation 2000 digital computer. The values of input parameters m, k_0, c, k_1 and k_2 used in the digital simulation were those obtained from the mechanical experiment. The amplitude of g(t) was adjusted such that the amplitude of

simulated response y(t) looked similar to that obtained from a mechanical experiment under a base excitation. The initial velocity and displacement were assumed zero for this simulation. The sampling time used was 1/1024 second and the sample duration was 1 second.

3.3.2 EXPERIMENTS USING A MECHANICAL ANALOGUE

The same experimental model of an impact oscillator shown in Figure 7 and detailed in the last chapter was used in the mechanical experiments. The experimental instrumentation shown in Figure 32 was very similar to that shown in Figure 8. The noise generator together with a filter was used instead of the exciter control to generate random input. The random input displacement b(t) and the output x(t), which were amplified using a vibration meter and a charge amplifier respectively, were digitized using a A/D converter and were stored on a floppy disk. The b(t) and x(t) were also displayed on a four channel storage oscilloscope. The A/D converter performed the conversion on one channel at one time and scanned other channels in sequence. Hence, the sampled discrete data will be $b_n = b(n\nabla t)$ and $x_n = x(n\nabla t + \nabla t/2)$. The ∇t was taken as 1/1024 second and the sample duration chosen was 1 second. The Nyquist frequency [21,22] by using this ∇t is 512 Hz which is well above the highest frequency of the signals processed in the experiments and so the "Aliasing Error" [21,22,48,59] was avoided. The sample duration of 1 second gave a frequency resolution of 1 Hz for all spectral quantities acquired during the signal processing. For each experiment, 10 samples were taken. Instruments were calibrated and proper amplification factors were selected to use the full dynamic range of these instruments.

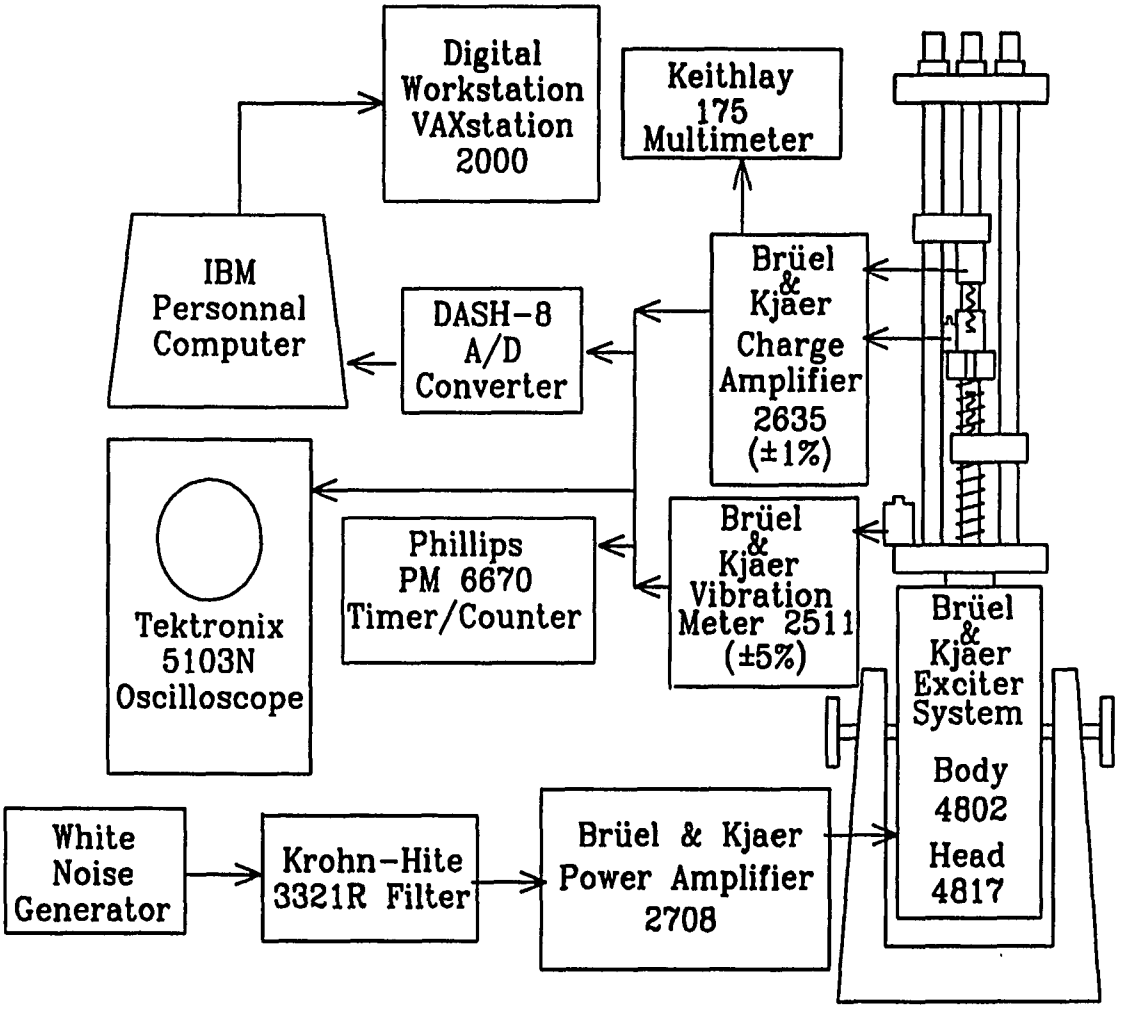

Figure 32. Experimental instrumentation.

The values of m, k_0, c and natural frequency were found to be 0.1061 kg, 1746 N/m, 20.4 Hz and 0.7127 Ns/m, respectively. The random signal generated by the noise generator was filtered above 300 Hz, which is about 15 times the natural frequency of the oscillator and well below the Nyquist frequency. In this frequency range, the random signal would have enough power in the resonant range in order to excite the motion of the

mass with sufficient amplitude to ensure that the mass hits the stops without overloading the exciter and triggering the automatic shut down. The experimentally obtained relative displacement y(t) in a discrete form was obtained from sampled b_n and x_n using the time shift property of Fourier transform (equation (2.37)). Computational procedure to estimate clearances and impact forces was identical for data obtained using the mechanical experiment and the computer simulation. The procedure is detailed next.

3.3.3 COMPUTATION PROCEDURE

The computation procedure of estimation of clearances based on the spectral analysis approach which uses random excitation is described next. All computations were performed using double precision arithmetic on a VAXstation 2000 digital computer. The clearance estimation procedure consists of the following three steps,

I. Calculate the statistical properties m_y, σ_y, $S_y(\omega)$, m_u and $S_{yu}(\omega)$ from the experimentally obtained records of b(t) and y(t);

II. Calculate W_0 and W_1 using the values of the above variables in equations (3.24) and (3.28), respectively;

III. Estimate clearances d_1 and d_2 by numerically solving equations (3.14) and (3.15).

Fourier transforms $B(\omega,T)$ (or $G(\omega,T)$ in the computer simulation) and $Y(\omega,T)$ were obtained from the digitized b(t) (or g(t)) and y(t) of duration T using a FFT [48-50] subroutine. The Fourier transform $U(\omega,T)$ of impact force u(t) was evaluated using equation (3.33). The spectra $S_y(\omega)$ and $S_{yu}(\omega)$ needed for the spectral analysis approach were obtained form $Y(\omega,T)$ and $U(\omega,T)$ using equations (3.31) and (3.36), respectively. The time duration of each sample was finite, i.e. 1 second. The expected value was estimated using spectral quantities for each sample record of the collection of records and

by averaging the results. The mean values m_y and m_u and the standard deviation σ_y were estimated using equations (3.29), (3.35) and (3.30) respectively. In these calculations, the integrals were replaced by sums and all records were included in the averaging. The W_0 and W_1 were obtained using equations (3.24) and (3.28), respectively. The frequency range ω_1 through ω_2, $\omega_1 = 2\pi$ and $\omega_2 = 512 \times 2\pi$, was considered in evaluating equation (3.28) and the integrals were replaced by sums. Substituting the calculated W_0 and W_1 into the left hand sides of equations (3.14) and (3.15) respectively, generates two nonlinear equations in two unknowns d_1 and d_2. These equations were iteratively solved by the Powell method [51-54] to obtain the estimates of d_1 and d_2.

3.4 RESULTS AND DISCUSSION

The comparison of estimated clearances with actual ones based on the spectral analysis approach is presented next. Several experiments, using the analogue of an impact oscillator shown in Figure 7 with different stop stiffnesses and clearances, were performed and the results are reported in what follows. Corresponding computer simulated experiments using the same system parameters as those of mechanical experiments were also performed and reported together with the mechanical experiment results. Additionally, taking the flexibility of computer simulations, the effects of excitation amplitude, spring stiffness and damping on the clearance estimation were further studied using a computer simulation approach and results are reported.

First a sample case is described in detail to illustrate the presented clearance estimation approach. Consider the analogue of an impact oscillator with m = 0.1061 kg, k_0 = 1746 N/m and c = 0.7127 Ns/m under random excitation contacting stops with support springs constants $k_1 = k_2 = 11600 \pm 100$ N/m and gaps $d_1 = 1.22 \pm 0.05$ mm and $d_2 = 1.19 \pm 0.05$ mm. These parameters are used throughout unless stated otherwise. From the

practical point of view this case can be considered symmetric. Ten sample records each of 1 second duration were obtained from the mechanical experiments. The random signal generated by the noise generator in mechanical experiments was close to white noise, however it had to go through the filter and the shaker in order to generate the input b(t). Due to this process, the high frequency components were filtered out. As an example, the first record of sampled b(t) and y(t) is shown in Figure 33. The spectra $S_y(\omega)$ and $S_{yu}(\omega)$ corresponding to the record shown in Figure 33 are shown in Figure 34(a) and 34(b), respectively. Estimation of $S_y(\omega)$ and $S_{yu}(\omega)$ obtained using a single record is less reliable. The spectra $S_y(\omega)$, $S_{yu}(\omega)$ obtained using all 10 records are shown in Figure 34(c) and 34(d). The comparison of these two figures to those on the left indicates that the use of ten samples smoothens these curves and is preferable. The W_1 was obtained using these $S_y(\omega)$ and $S_{yu}(\omega)$ in equation (3.28). The value of W_0 as a mean of the impact force u(t) was efficiently obtained using U(0,T) in equation (3.35). Using m_y, σ_y, W_0 and W_1 the estimates of clearances were obtained by solving coupled equations (3.14) and (3.15). The results obtained using each of the ten sampled input and output records are presented in Table 6. In the same table the values of W_0 and W_1 obtained using calculated m_y, σ_y and actual clearances in equations (3.14) and (3.15) respectively, are also presented using superscript *. The results indicate that W_0 and W_0^* and W_1 and W_1^* are reasonably close. In most of these cases, the estimates of clearances were quite acceptable, but variation did exist among these estimates. The means and deviations of estimates d_1 and d_2 are 1.18mm and 0.39mm, and 1.10 mm and 0.30 mm respectively. Clearly, estimation using an individual record of 1 second duration was not so desirable, but the estimated values obtained using 10 records were found to be quite reasonable. It can be concluded that the estimates based on the mechanical experiments compared well with actual clearances.

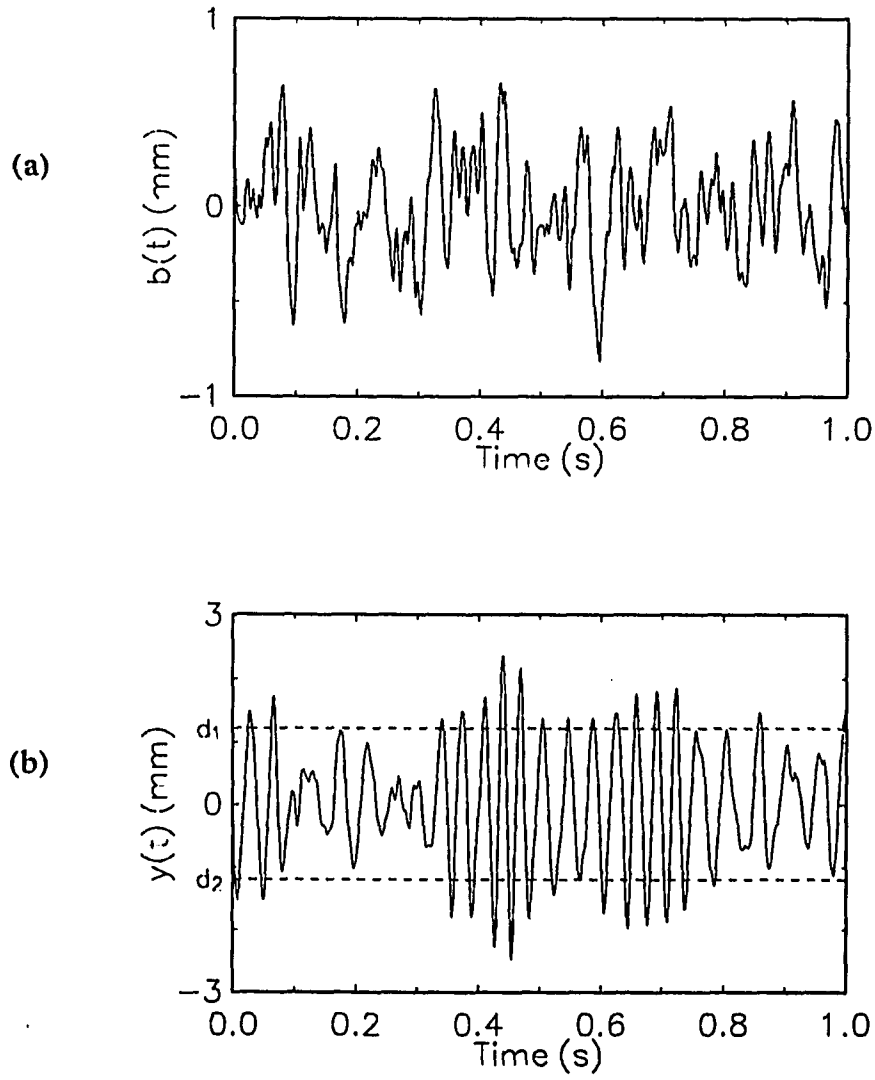

Figure 33. Sample records from mechanical experiment, (a) Base excitation b(t), (b) System response y(t). The system parameters were m = 0.1061 kg, k_0 = 1746 N/m, c = 0.7127 Ns/m, $k_1 = k_2$ = 11600±100 N/m, d_1 = 1.22±0.05 mm and d_2 = 1.19±0.05 mm.

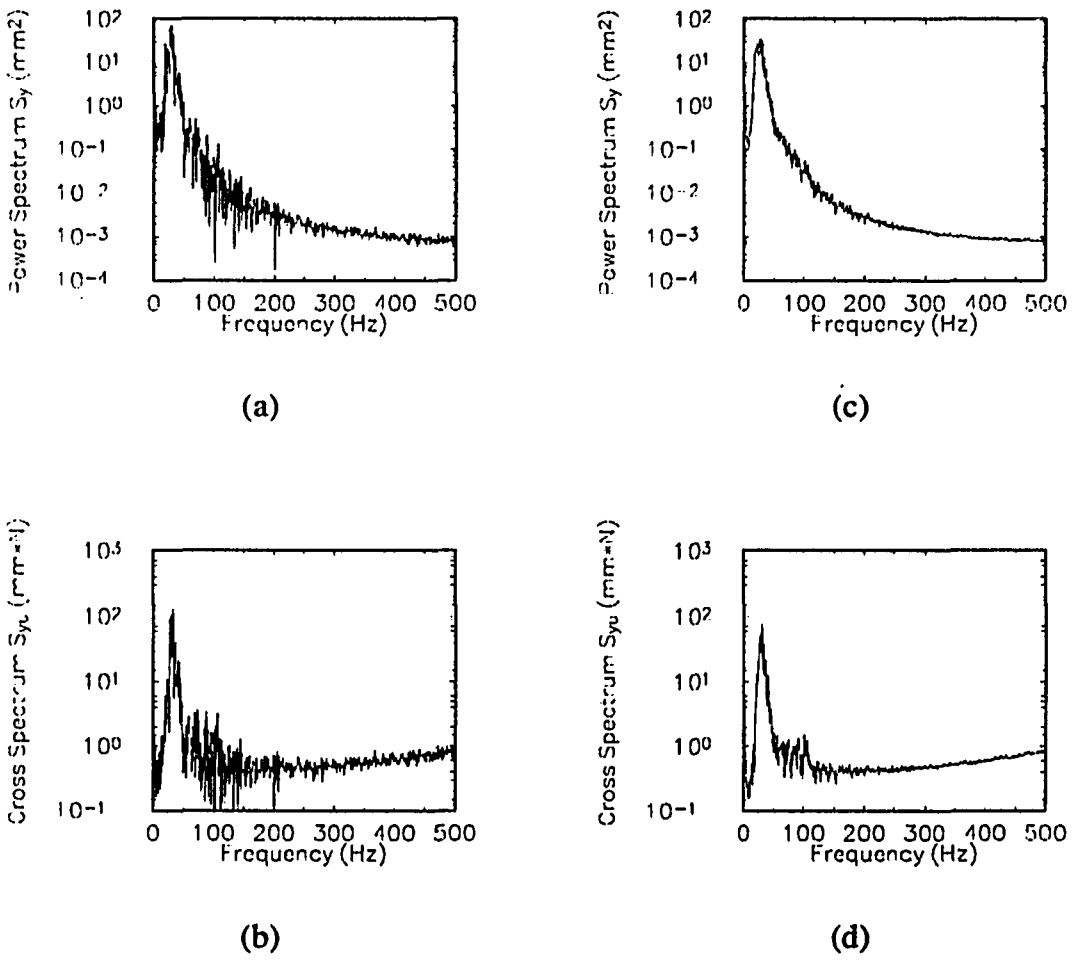

Figure 34. The spectra (a) $S_y(\omega)$ and (b) $S_{yu}(\omega)$ corresponding to the sample shown in Figure 33. The (c) and (d) represents respectively the $S_y(\omega)$ and $S_{yu}(\omega)$ obtained using all ten samples.

TABLE 6

Estimation of clearances using data from mechanical experiments when clearances and support springs were practically identical. The actual clearances were: $d_1 = 1.22 \pm 0.05$ mm and $d_2 = 1.19 \pm 0.05$ mm.

	m_y(mm)	σ_y(mm)	W_0^*	W_1^*	W_0	W_1	d_1(mm)	d_2(mm)
Record 1	0.009	0.919	-0.014	2.022	-0.015	2.181	1.18	1.15
Record 2	-0.024	0.609	-0.022	0.342	0.042	0.281	1.13	1.45
Record 3	-0.005	0.736	-0.024	0.868	0.009	0.988	1.15	1.17
Record 4	0.047	0.649	0.023	0.479	-0.082	0.986	1.08	0.88
Record 5	-0.061	1.225	-0.286	4.631	0.106	3.210	1.38	1.58
Record 6	-0.101	0.592	-0.058	0.313	0.176	0.700	0.74	1.26
Record 7	0.363	0.981	0.925	2.824	-0.634	1.810	2.25	0.73
Record 8	-0.059	0.826	-0.125	1.402	0.103	1.391	1.09	1.33
Record 9	-0.006	0.856	-0.039	1.584	0.010	2.999	0.88	0.89
Record 10	0.112	0.726	0.109	0.840	-0.195	2.466	0.93	0.60
Records 1-10	0.027	0.842	0.022	1.487	-0.048	1.744	1.18	1.08

TABLE 7

Estimation of clearances using computer simulated data when clearances and support springs were practically identical. The actual clearances were: $d_1 = 1.22$ mm and $d_2 = 1.19$ mm.

	m_y(mm)	σ_y(mm)	W_0^*	W_1^*	W_0	W_1	d_1(mm)	d_2(mm)
1 Record	0.010	0.780	-0.007	1.108	-0.028	0.863	1.34	1.27
10 Records	0.010	0.856	-0.009	1.580	-0.014	1.297	1.31	1.27
100 Records	0.008	0.879	-0.013	1.738	-0.008	1.426	1.31	1.28

The corresponding estimates obtained using a computer simulation approach are presented in Table 7. Here random force excitation g(t) was used instead of the random base excitation b(t). Corresponding g(t), y(t), $S_y(\omega)$ and $S_{yu}(\omega)$ of a single sample are shown in Figure 35(a) through 35(d) respectively. The g(t) shown in Figure 35(a) is quite different from the excitation b(t) shown in Figure 33(a). The g(t) generated by the computer as a random function was very close to a white noise, but the random signal generated by the noise generator in mechanical experiments had to go through the filter and the shaker in order to produce the b(t) and the high frequency components of it were filtered out. However, since the impact oscillator itself acts as a low pass filter and high frequency components in the excitation has little effect on the response, the response y(t) of computer simulation in Figure 35(b) as well as the spectra $S_y(\omega)$ and $S_{yu}(\omega)$ (Figure 35 (c) and (d)) are similar to the corresponding ones obtained in mechanical experiments

shown in Figures 33(b), 34(a) and 34(b). The $S_y(\omega)$ and $S_{yu}(\omega)$ obtained using 10 and 100 samples of 1 second duration are shown in Figure 36(a) through 36(d) respectively and these figures indicate similar smoothening to that observed in the mechanical experiments. A second peak appears in the $S_{yu}(\omega)$, which is related to the stops. The clearances are somewhat overestimated most probably due to the underestimation of W_1. However, these estimates should be considered reasonable as differences are not significant. It is also assuring from the practical view point that results obtained using 10 samples are very close to those obtained using 100 samples.

The case described above was very close to symmetric. Asymmetric cases and cases with soft support springs were also studied using ten samples from the mechanical experiment which were used together to estimate clearance. The results for estimation of nonidentical clearances with strong springs in Table 8, row 2 indicate a good agreement. Two samples of y(t) of this case are shown in Figure 37. The y(t) in Figure 37(a) is normal. Even when only this sample of y(t) is used a reasonably good estimation of clearances can be obtained. But the y(t) in Figure 37(b) shows a nonlinear phenomenon of "drawing" the motion of mass to the stop at one side. If only such a sample is used, an inaccurate estimation would be inevitably obtained. However, such effects would be greatly reduced when more pieces of samples are used in estimation.

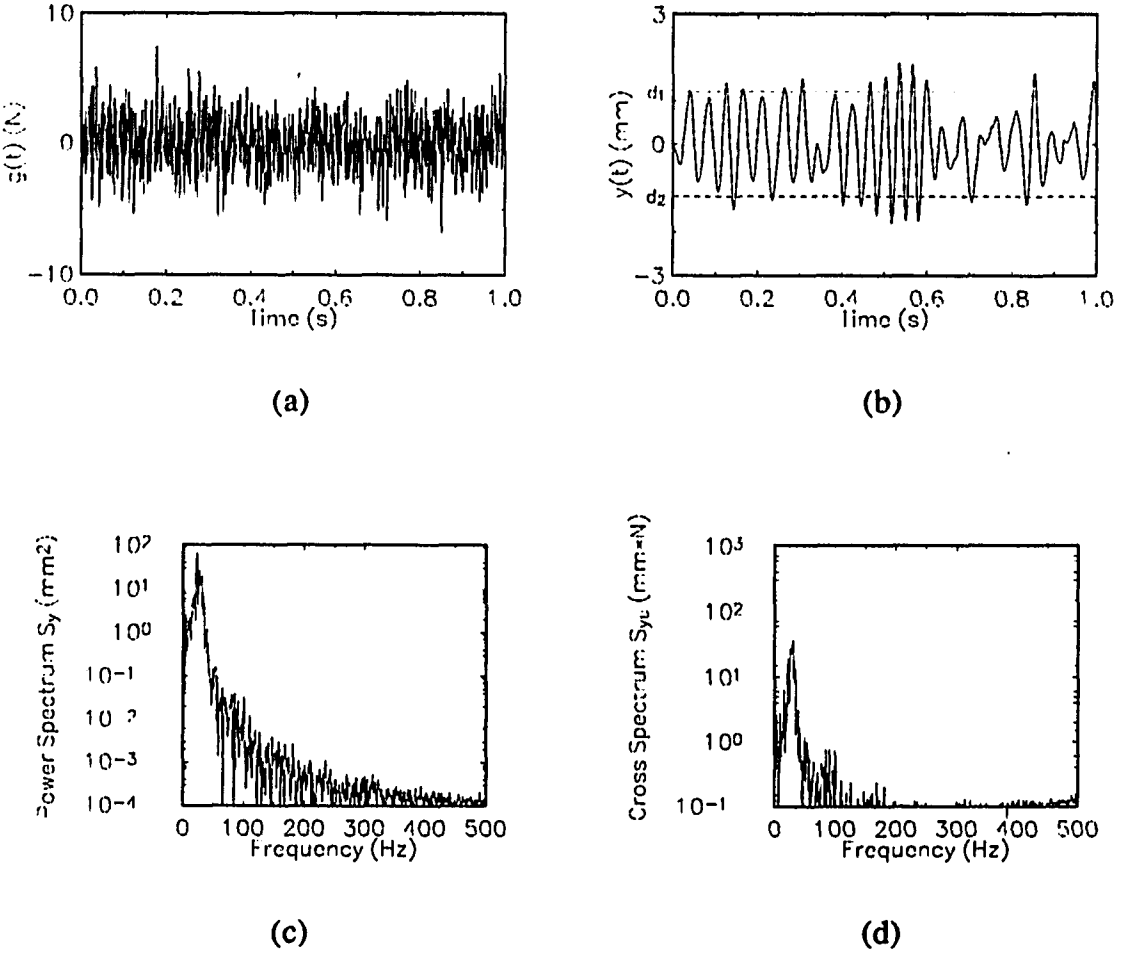

Figure 35. (a) Force excitation g(t), (b) system response y(t), and spectra (c) $S_y(\omega)$ and (d) $S_{yu}(\omega)$ using 1 sample from computer simulation. The system parameters were m = 0.1061 kg, k_0 = 1746 N/m, c = 0.7127 Ns/m, $k_1 = k_2$ = 11600 N/m, d_1 = 1.22 mm and d_2 = 1.19 mm.

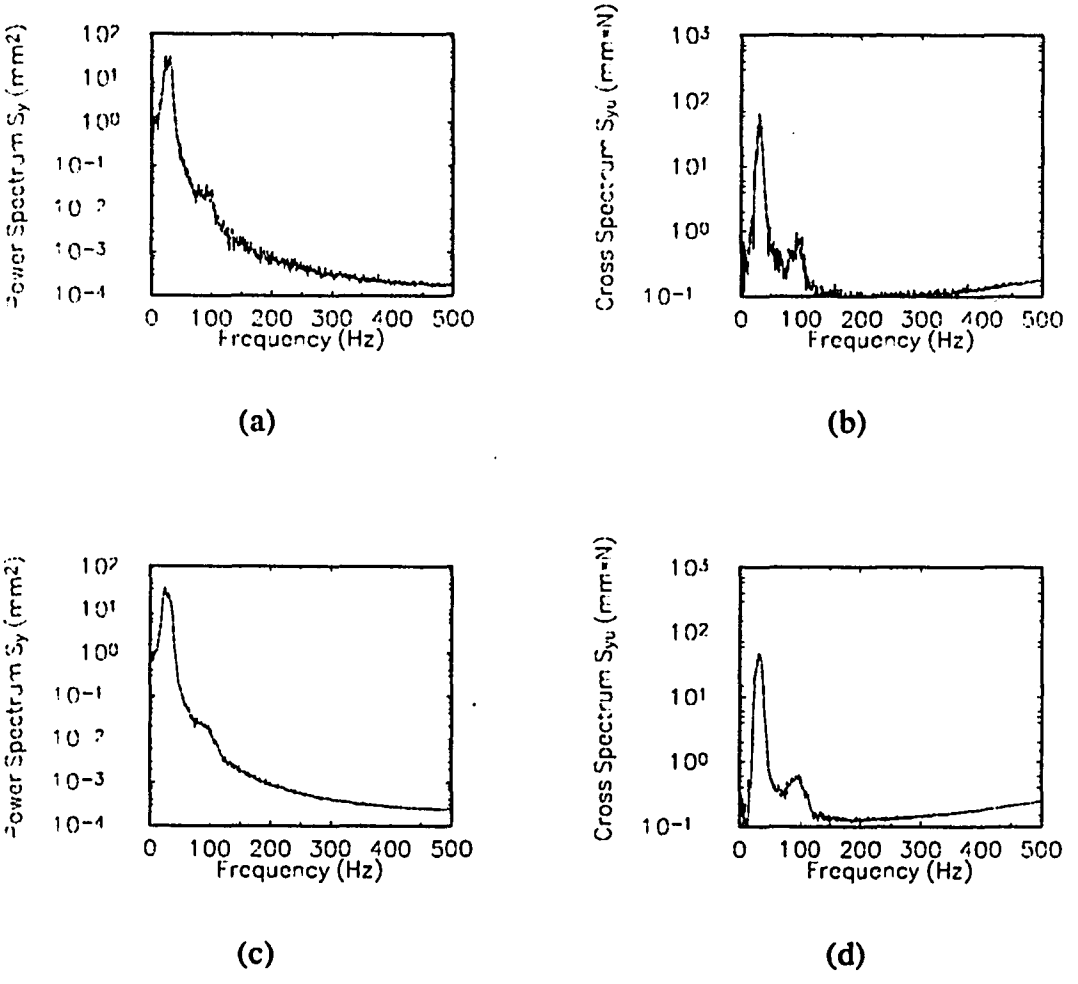

Figure 36. The spectra from computer simulation. (a) $S_y(\omega)$ and (b) $S_{yu}(\omega)$ using 10 records, (c) $S_y(\omega)$ and (d) $S_{yu}(\omega)$ using 100 records. The system parameters were the same as those of Figure 35.

TABLE 8

Comparison of actual clearances to its estimates based on data from mechanical experiments.

k_1 (N/m)	k_2 (N/m)	Actual Clearances		Estimated Clearances	
		d_1(mm)	d_2(mm)	d_1(mm)	d_2(mm)
11600±100	11600±100	0.99±0.05	1.40±0.05	1.20	1.48
1750±50	1750±50	0.79±0.05	0.79±0.05	0.77	0.82
1750±50	1750±50	0.81±0.05	1.52±0.05	0.76	1.13
1750±50	11600±100	0.81±0.05	1.45±0.05	0.45	1.58

The estimates of clearances with soft identical support springs, $k_0 \approx k_1 \approx k_2$ and identical gaps presented in Table 8, row 3 are quite accurate. The results for the case of nonidentical clearances with soft springs presented in row 4 indicate that the small clearance estimation is good, however larger clearance is underestimated. A typical system response y(t) of this case together with a corresponding y(t) from computer simulation are shown in Figure 38. Similarity between these two y(t)s can be observed. Figure 39 shows the power and cross spectra estimated using 10 samples from mechanical experiment and from computer simulation. These two groups of spectra are very similar.

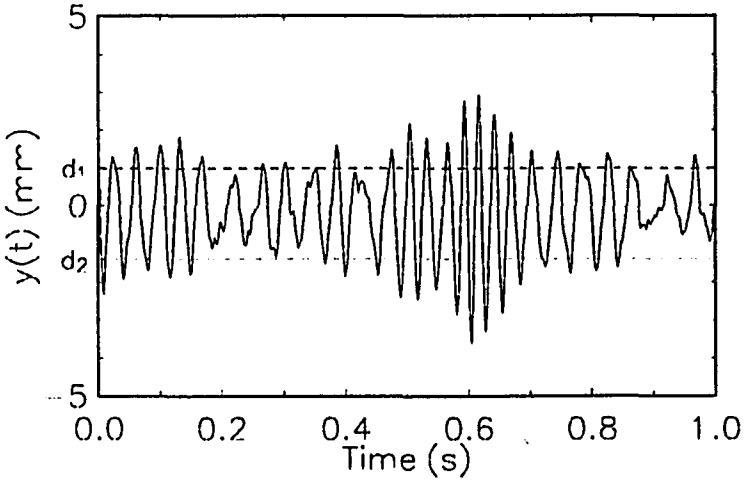

(a)

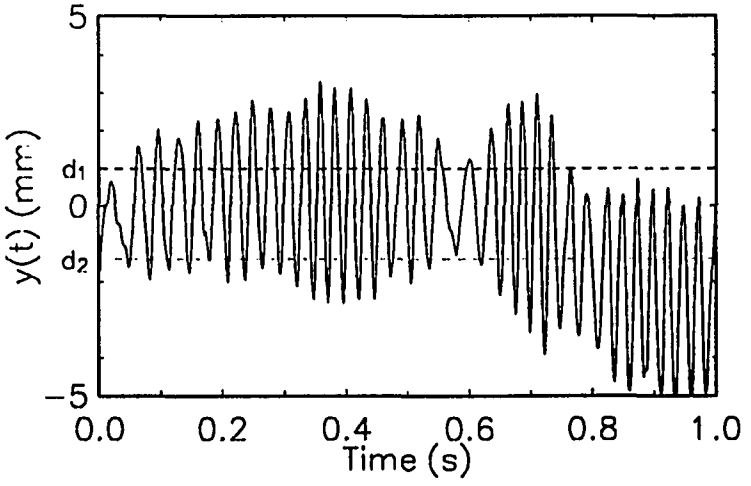

(b)

Figure 37. Sample records of system response y(t) of the case in Table 8, row 2.

(a)

(b)

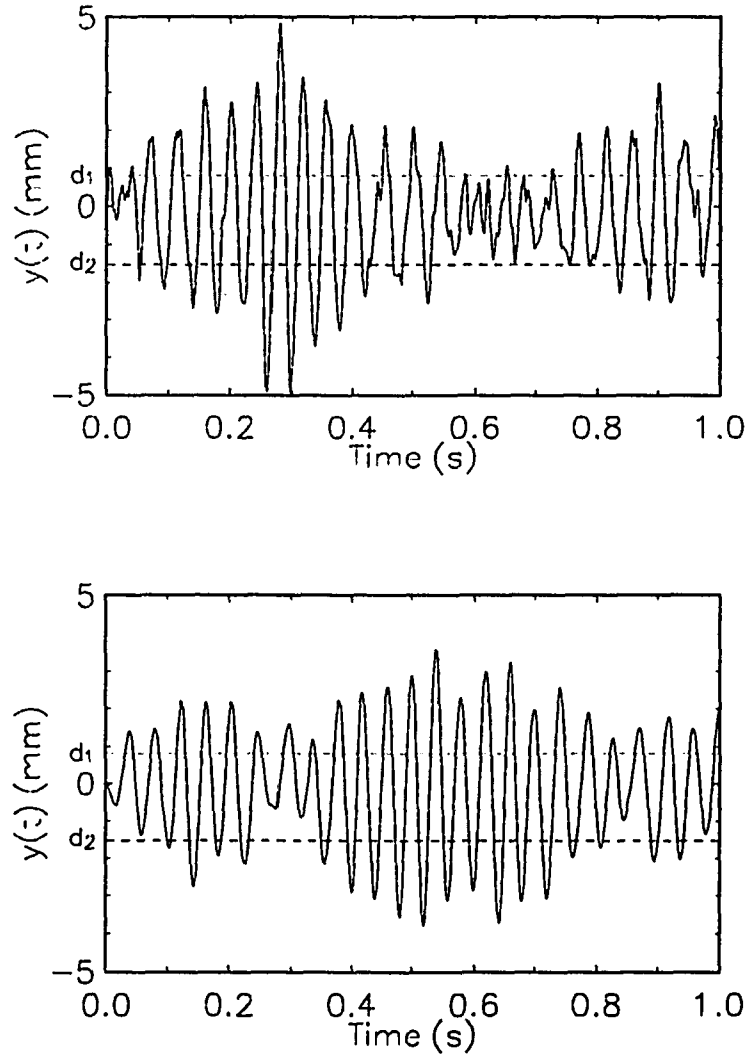

Figure 38. Sample records of system response y(t). (a) Mechanical experiment and (b) Computer simulation. The system parameters were m = 0.1061 kg, k_0 = 1746 N/m, c = 0.7127 Ns/m, $k_1 = k_2$ = 1750 N/m, d_1 = 0.81 mm and d_2 = 1.52 mm.

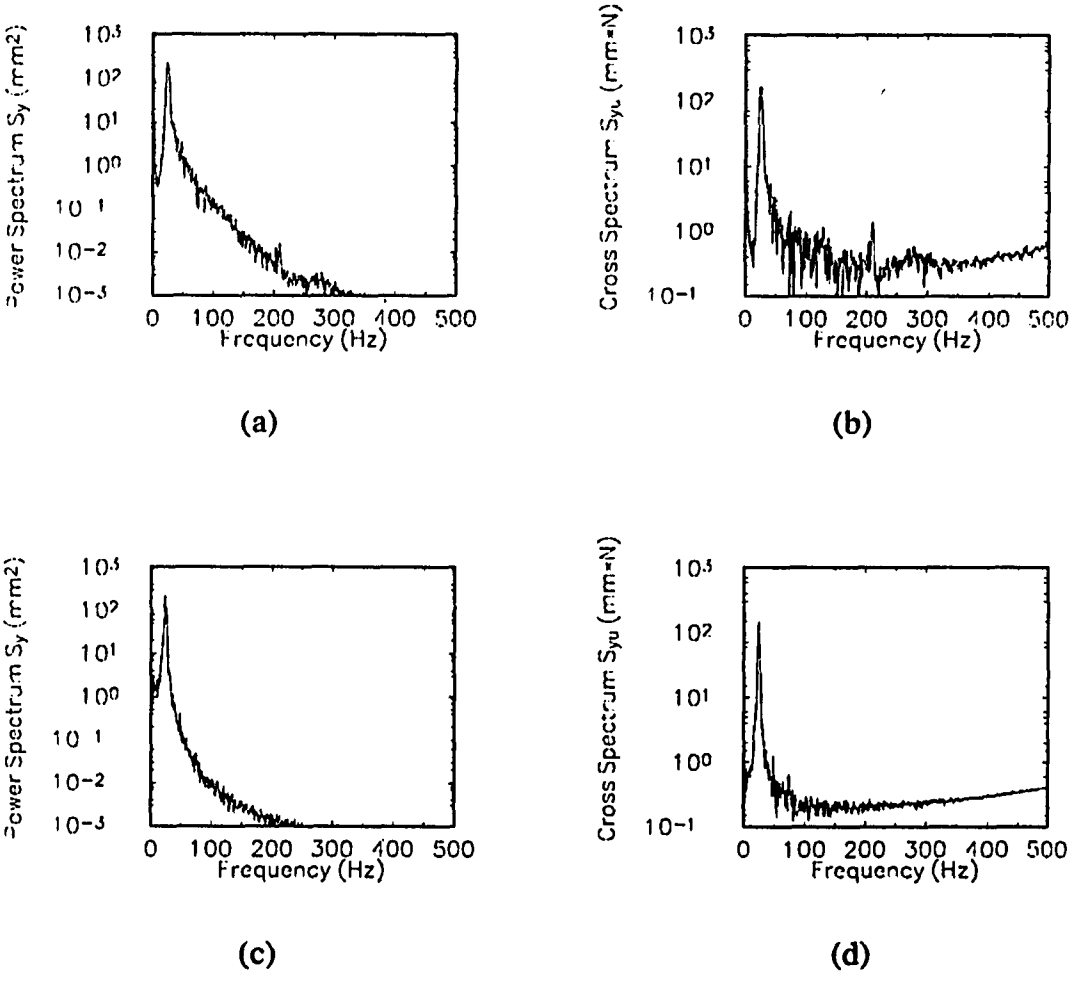

Figure 39. The spectra of the same system of Figure 38 estimated using 10 records. (a) $S_y(\omega)$ and (b) $S_{yu}(\omega)$ from mechanical experiments, (c) $S_y(\omega)$ and (d) $S_{yu}(\omega)$ from computer simulation.

The results for the case of asymmetric clearances and spring stiffnesses reported in Table 8, row 5 indicate more reasonable agreement on the strong support spring side than that on the soft support spring side. One probable reason is that when the mass hits the soft spring the change in the combined stiffness is small and hence its effects on the y(t) is small and less pronounced and is not reflected to that extent. A sample of y(t) of this case

accompanied with a y(t) obtained from computer simulation is shown in Figure 40. Figure 41 shows the cross spectra $S_{yu}(\omega)$ estimated using 10 samples from mechanical experiments and using 10 and 100 samples from computer simulation. Two small peaks are found in Figure 41 (b) and (c) due to the two different stop springs, while there is only one second peak in Figure 36 (b) and (d) because the stop springs were identical.

The corresponding estimates for all these cases based on computer generated data are reported in Table 9, and generally the agreement is good.

The author believes that the case of identical clearances and spring stiffnesses is important from the practical point of view. Hence effects of excitation amplitude, spring stiffness and damping on the clearance estimation were studied using a computer simulation approach and results are presented next. The effect of the intensity of excitation on the estimation represented in Figure 42 was studied by computer simulated experiments where the standard deviation σ_g of the input force was increased from 0 to 20 N in a step of 0.2 N. Ten records of g(t) and y(t) each of 1 second duration were used for each estimation. Figure 42 indicates that when σ_g is small (i.e. $\sigma_g < 0.7$ N) the mass rarely makes contact with the stops which results in underestimation of clearance. However, when excitation is strong enough to ensure that the mass hit the stops the intensity has negligible effect on the accuracy of the estimation.

The effect of support stiffness on the clearance estimation is presented in Figure 43. The estimation for the cases of very small values of stiffnesses was inaccurate. It is understandable that very soft stops have negligible effect, the system is close to a simple oscillator without stops and the clearances are almost unobservable. Estimates are quite accurate for relatively strong spring cases.

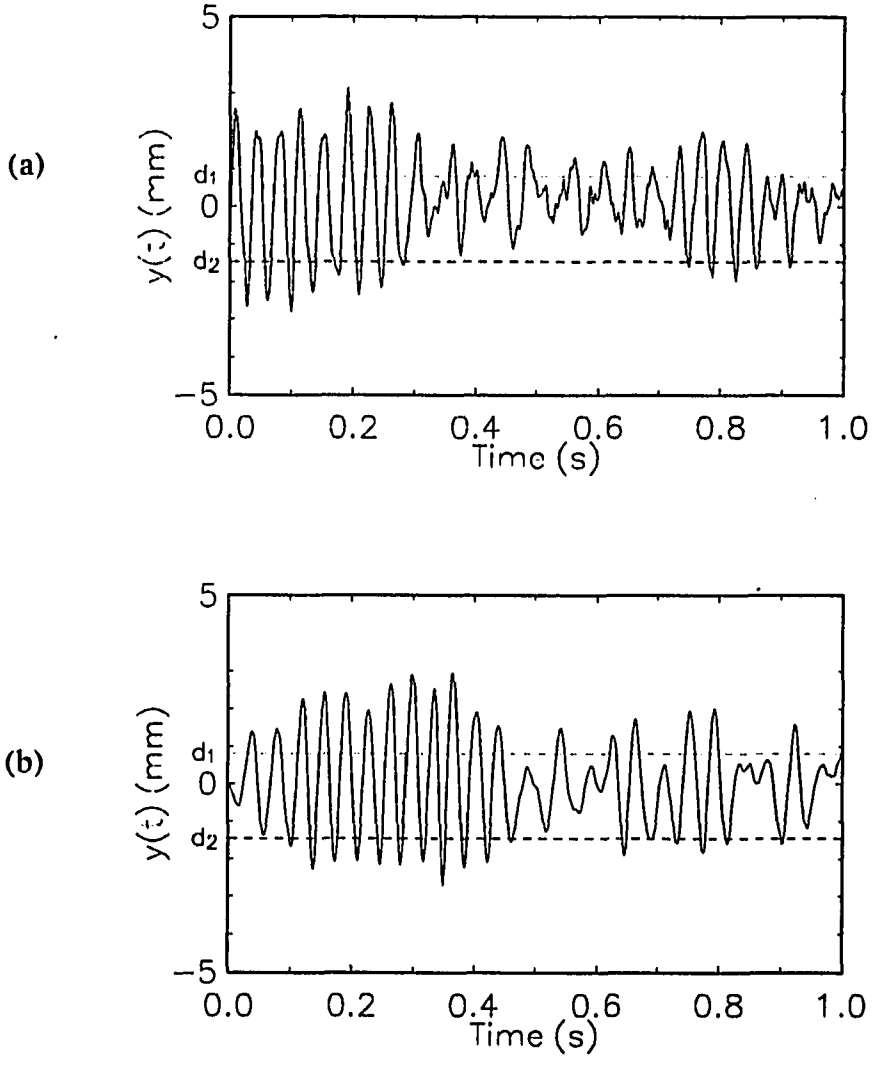

Figure 40. Sample records of system response y(t). (a) Mechanical experiment and (b) Computer simulation. The system parameters were m = 0.1061 kg, k_0 = 1746 N/m, c = 0.7127 Ns/m, k_1 = 1750 N/m, k_2 = 11600 N/m, d_1 = 0.81 mm and d_2 = 1.45 mm.

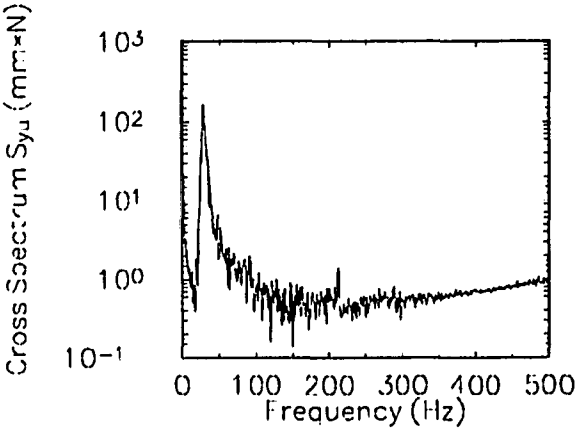

(a)

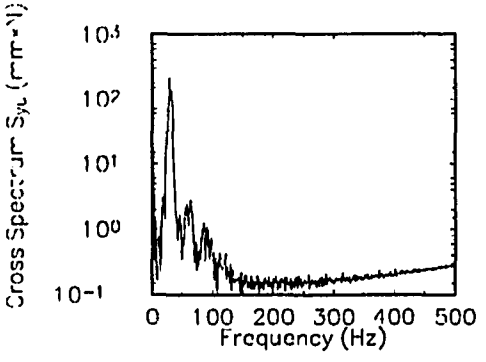

(b)

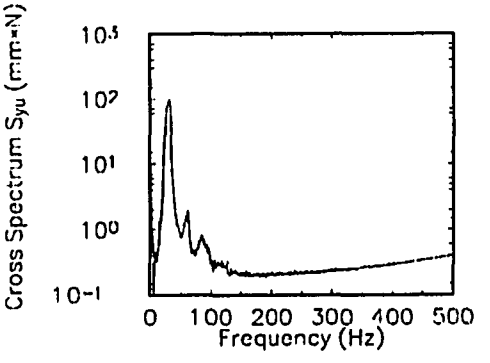

(c)

Figure 41. The cross spectra $S_{yu}(\omega)$ of the same system of Figure 40. (a) Estimated using 10 records from mechanical experiments, (b) Estimated using 10 records from computer simulation and (c) Estimated using 100 records from computer simulation.

TABLE 9

Comparison of actual clearances to its estimates based on data from computer simulation.

k_1 (N/m)	k_2 (N/m)	Actual Clearances		Estimated Clearances 10 Records Used		Estimated Clearances 100 Records Used	
		d_1(mm)	d_2(mm)	d_1(mm)	d_2(mm)	d_1(mm)	d_2(mm)
11600	11600	0.99	1.40	1.09	1.47	1.07	1.46
1750	1750	0.79	0.79	0.63	0.64	0.59	0.58
1750	1750	0.81	1.52	0.67	1.33	0.67	1.25
1750	11600	0.81	1.45	0.71	1.59	0.69	1.57

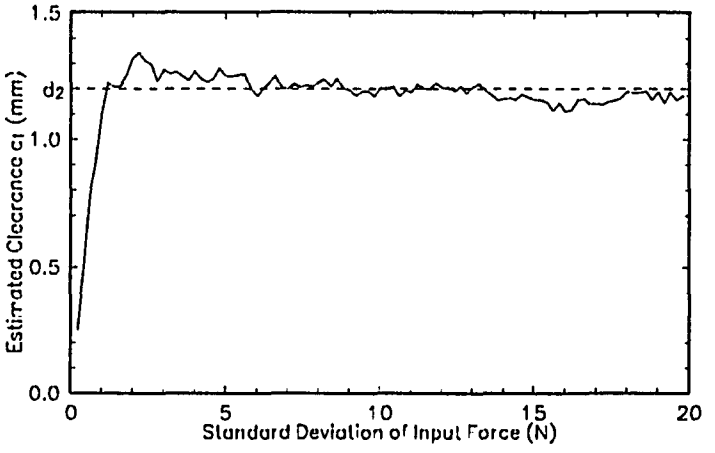

(a)

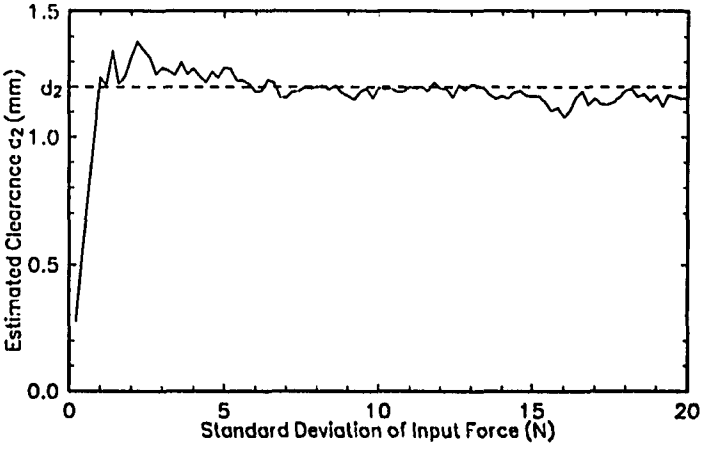

(b)

Figure 42. The effect of varying the intensity of random excitation on the clearance estimation.

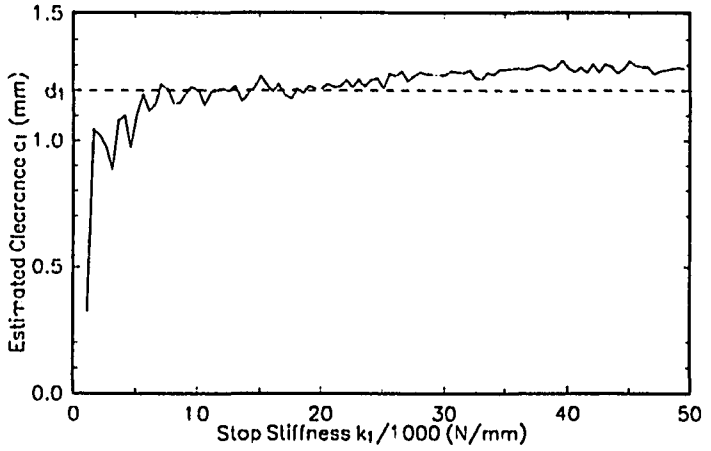

(a)

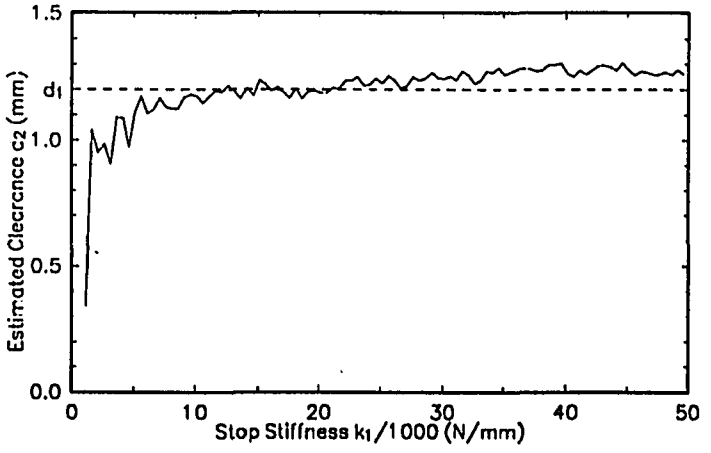

(b)

Figure 43. The effect of identical spring stiffnesses of stops on the clearance estimation. The $d_1 = d_2 = 1.2$ mm and $\sigma_s = 10$ N.

Clearances generally increase with time. Hence the effect was studied by generating data using increasing clearances in steps and the results are presented by comparing estimated clearances with actual ones in Figure 44. To ensure contacts the σ_g was also linearly increased with the gap to produce the necessary output y(t). The comparison indicates that the clearances were very well estimated and hence the estimation by using this approach will at least give a hint to the ever-increasing clearance in actual practice. The effect of different damping coefficients on the clearance estimation was also studied and the results are presented in Figure 45 which indicates that damping has little effect on the clearance estimation.

3.5 CONCLUSIONS

A novel approach to estimate clearances which utilizes the response of the vibroimpact system under random excitation has been developed in this chapter. The estimates of clearances obtained using data from mechanical experiments and computer simulations were compared with actual clearances and indicate a good agreement. Estimation is more accurate for symmetric systems and estimation associated with strong springs is more accurate than that associated with soft springs. Reasonable number of samples are necessary to obtain smooth power spectrum $S_y(\omega)$ and cross spectrum $S_{yu}(\omega)$ as it ensures more reliable estimates. In the next chapter, the clearance estimation approaches developed in this and the last chapter will be applied to a continuous beam-stop system.

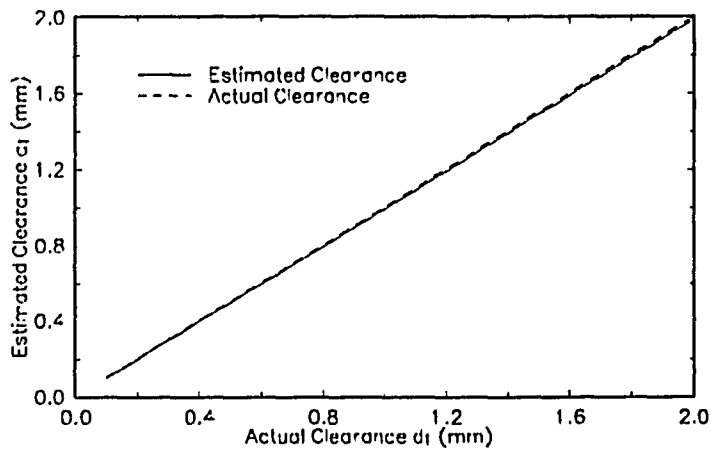

(a)

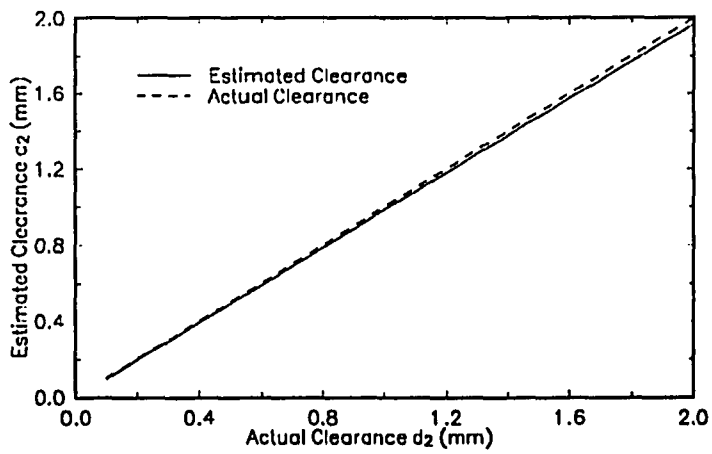

(b)

Figure 44. The effect of clearance size on the clearance estimation. The clearances were identical i.e. $d_1 = d_2$ and the input was $\sigma_g = 3d_1k_0$ N.

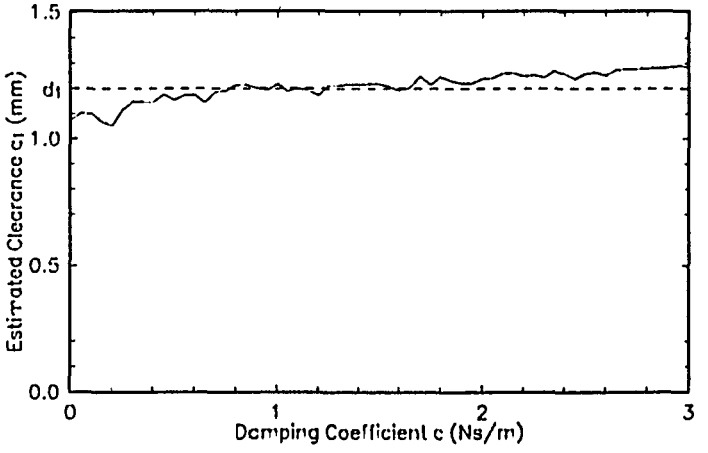

(a)

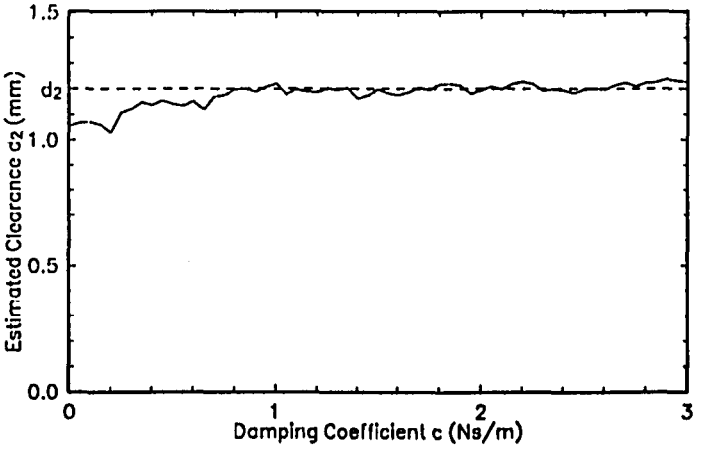

(b)

Figure 45. The effect of varying damping coefficient on the clearance estimation. The clearances were $d_1 = d_2 = 1.2$ mm and $\sigma_g = 10$ N.

CHAPTER IV

ESTIMATION OF CLEARANCES AND IMPACT FORCES FOR A BEAM-STOP SYSTEM

4.1 INTRODUCTION

The three clearance and impact force estimation approaches have been developed and tested in the last two chapters using an impact oscillator as an example. These approaches also could be directly extended to other vibro-impact systems with clearances. To illustrate such an extension, these estimation approaches will be applied to a continuous system - a beam-stop system in this chapter. A beam-stop system is chosen intentionally because it has practical applications. It is an idealized model for heat exchanger tubes and piping systems in nuclear plants. Many investigators have conducted studies on the dynamic behavior of beam-stop systems. For a beam-stop system with only one stop, analytic solution has been obtained by using Bernoulli-Euler beam theory [68-71]. Takamara et al [70] used only two modes in their calculation and concluded that higher modes should be included. Results with 5, 10 and 15 modes were obtained numerically by Lo [71]. Normal mode approach and numerical solution were also used to solve the beam stop system [72]. The finite element method has been employed to study more general cases such as the tube/baffle interaction in multi-span heat exchanger tubes [73-76]. Experimental study is a direct and reliable mean to determine the effects of various system parameters on dynamic behavior and to verify the validity of various analytical and numerical methods. Masri's group in the University of Southern California [26,31,33,69] and Lo [71] in Bell Telephone Laboratories conducted experiments on a

cantilever beam with one motion limiting stop. Moretti and Lowery [77,78] reported experimental results on 1 to 5-span models, illustrating the effects of tube-support condition on tube natural frequency and damping. A series of comprehensive experiments have been performed in the Argonne National Laboratory to determine the effects of tube/support parameters on the vibration of heat exchanger tubes [79-83]. The importance of estimating clearances in beam-stop systems is stated in Chapter 1 using an example of a heat exchanger tube. A few references on this topic are also mentioned there.

A beam-stop system will be formulated in Section 4.2. The clearance and impact force estimation approaches for this system are presented in Section 4.3. Experiments were performed using a mechanical analogue. Comparison of estimated clearances and impact forces with actual ones indicated a good agreement and is reported in Section 4.4.

4.2 MODEL OF A BEAM-STOP SYSTEM

Consider a uniform cantilever beam of length L having 1 pair of stops with clearances d_1 and d_2 at location x_1 and excited at the base as shown in Figure 46. A displacement at another location x_2 will be measured and is considered the response of the system. This is an inherently nonlinear system because of clearances and stops. The same strategy used to formulate the impact oscillator can be used here, i.e., instead of treating the nonlinear system as a whole, it will be decomposed into two parts: a linear subsystem and a relative simple nonlinear element.

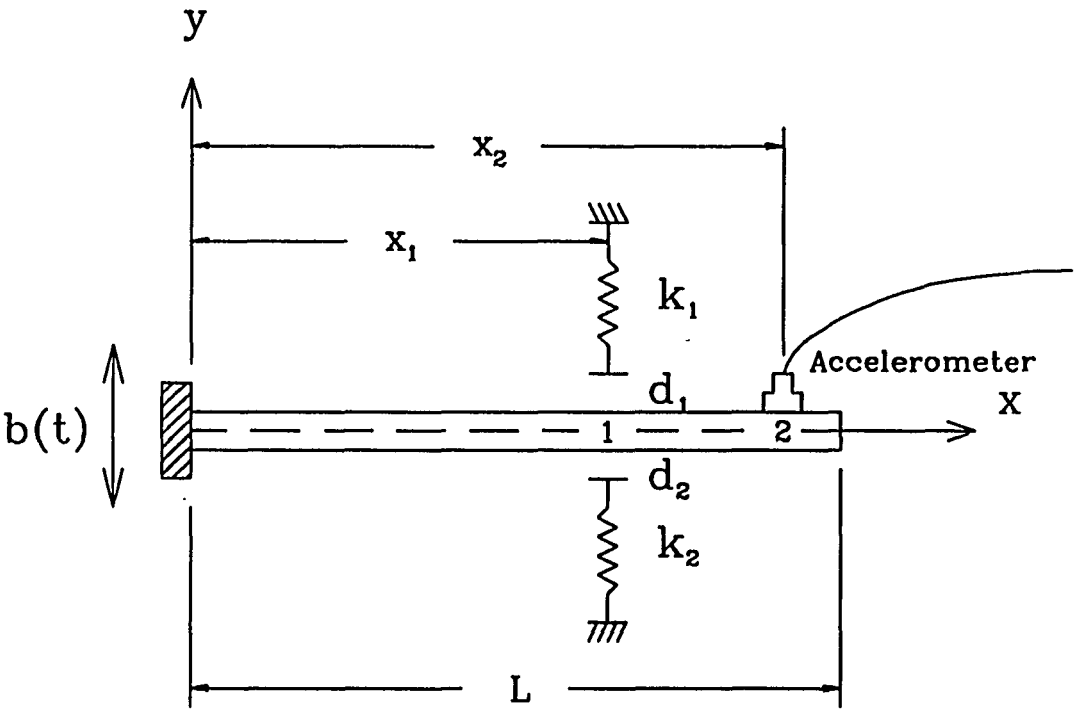

Figure 46. A cantilever beam with a pair of stops.

The effect of a pair of motion limiting stops at x_1 can be considered equivalent to that of an impact force u(t) acting at that location. The developed impact force is a function of displacement y_1 at x_1 and can be expressed as

$$u(t) = u[y_1(t)] = \begin{cases} k_2(y_1 + d_2) & -\infty < y_1 \le -d_2 \\ 0 & -d_2 < y_1 < d_1 \\ k_1(y_1 - d_1) & d_1 < y_1 < \infty \end{cases} . \qquad (4.1)$$

The above equation defining a dead-zone nonlinearity is identical to equation (2.4) of the impact oscillator. If these motion limiting stops are removed and their effect is replaced by the impact force (which can be considered as an external excitation) the beam becomes a

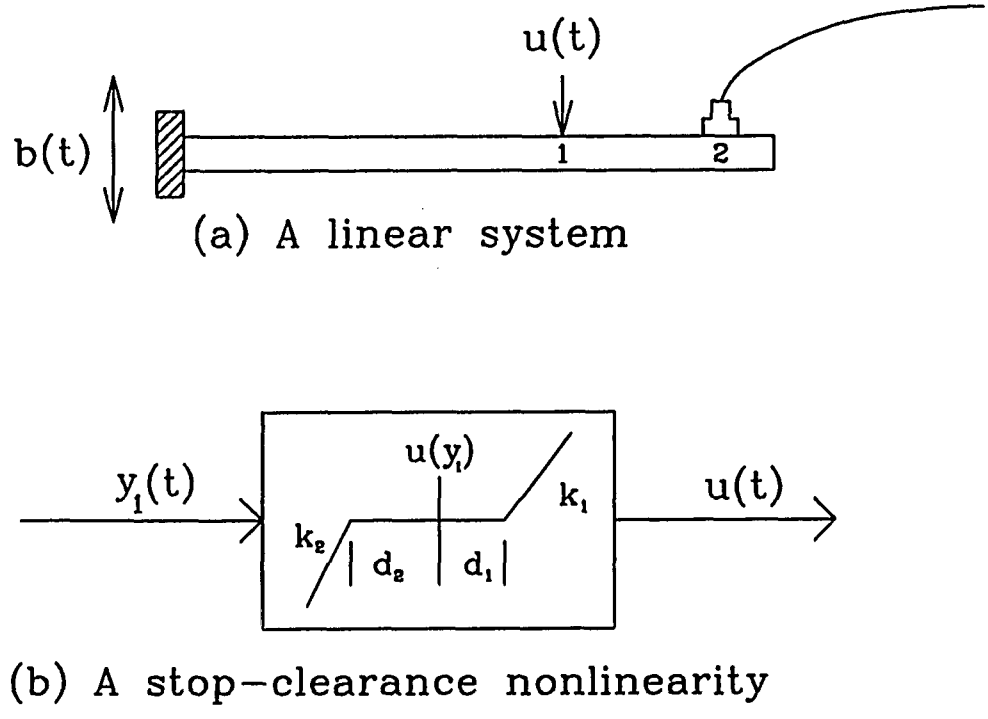

Figure 47. Decomposition of the beam-stop system into two systems (a) and (b).

linear system under two excitations. Figure 47 shows the decomposition of the beam-stop system into a beam and a clearance-stop nonlinearity. The superposition principle holds true for the linear part and the displacement $y_i(t)$ at location x_i could be found as

$$y_i(t) = y_{ib}(t) + y_{i1}(t), \qquad i = 1 \quad \text{or} \quad 2 \tag{4.2}$$

where y_{ib} is the displacement response at x_i due to the base excitation b(t) and y_{i1} is the response at x_i due to a concentrated impact force at x_1. In frequency domain, equation (4.2) becomes

$$Y_i(\omega) = Y_{ib}(\omega) + Y_{i1}(\omega), \qquad i = 1 \quad \text{or} \quad 2 \tag{4.3}$$

$Y_{ib}(\omega)$ and $Y_{i1}(\omega)$ can be found by

$$Y_{ib}(\omega) = B(\omega)H_{bi}(\omega) \quad \text{and} \quad Y_{i1}(\omega) = -U(\omega)H_{1i}(\omega), \tag{4.4}$$

where $H_{bi}(\omega)$ and $H_{1i}(\omega)$ are the frequency response functions due to the base excitation and the impact force respectively. The negative sign is used for the second term as for positive displacement $y_1(t)$ impact force will be negative. Substituting equation (4.4) into (4.3), yields the transformed displacement at point x_i as

$$Y_i(\omega) = B(\omega)H_{bi}(\omega) - U(\omega)H_{1i}(\omega). \tag{4.5}$$

Coupled equations (4.5) and (4.1) totally define the beam-stop system because the frequency response functions $H_{bi}(\omega)$ and $H_{1i}(\omega)$ can be determined for a given beam. Equation (4.5) represents the linear part of the system and equation (4.1) defines a nonlinear element with $y_1(t)$ being the input and u(t) the corresponding output. Figure 48 shows the block diagram of the beam-stop system and its decomposition. Comparing Figure 48 with Figure 4, one can see the similarity between the block diagram representations of these two different systems. This suggests that such a representation and decomposition may be equally applicable to other systems with clearances. The remaining problem is to find the frequency response functions $H_{bi}(\omega)$ and $H_{1i}(\omega)$. Generally, only a relatively simple system can be solved analytically and a close form frequency response function can be obtained. A more general method of finding the response involves using a numerical approach, by which a frequency response function in discrete form will be obtained. A more practical way to find the frequency response function is to actually measure the excitation and response and find the ratio. For example, the needed frequency response functions of a heat exchanger tube can be measured before its installation or during its maintenance when it is unplugged.

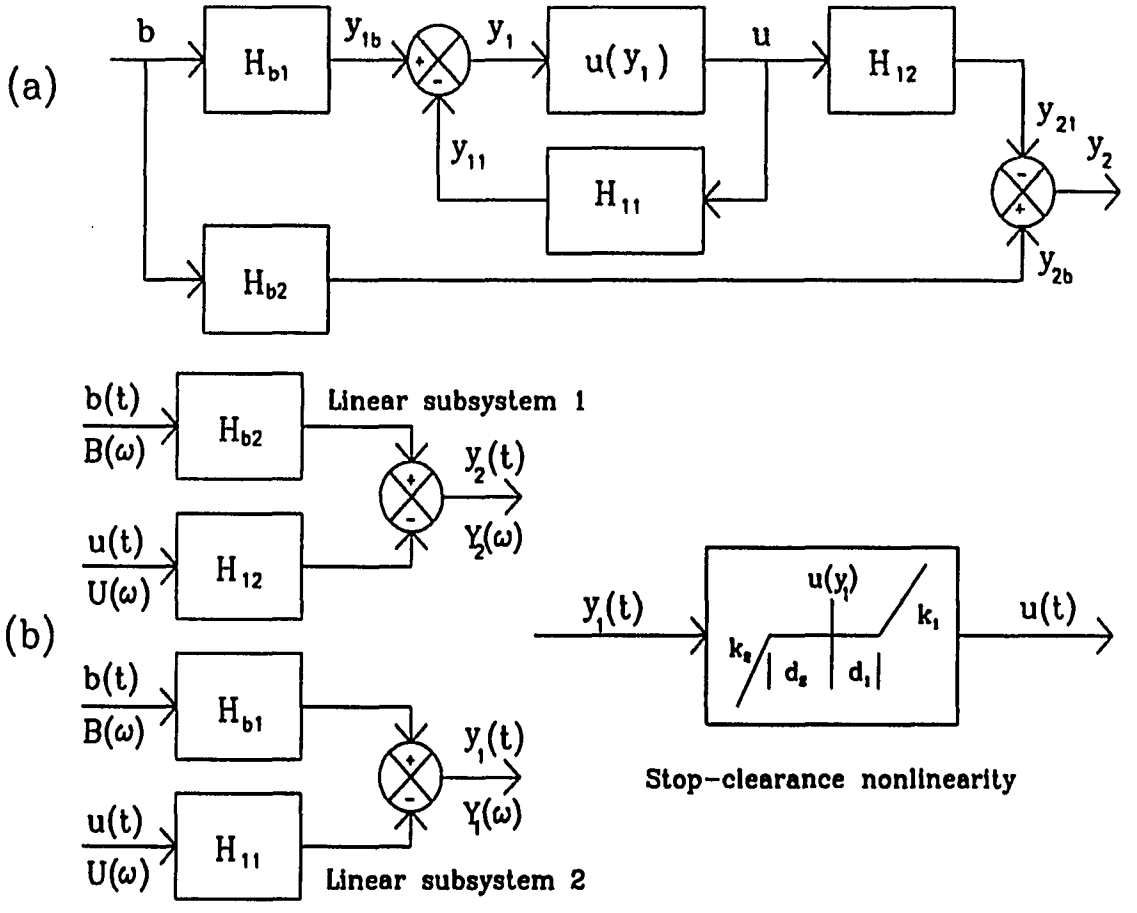

Figure 48. (a) Block diagram of the beam-stop system and (b) its decomposition.

Recently an exact approach was developed to study the free vibration of a straight beam supported at many locations and with non-classical boundary conditions including concentrated masses [84,85]. This was based on connecting the coefficients of the general

solution of the forth order differential equation of two adjacent beam sections, based on the Euler beam theory, by a transfer matrix. This approach is extended in Appendix A to predict the steady state forced vibration of a beam made up of n different but uniform sections. The exact closed form forced vibration response of the ith section subjected to a concentrated force excitation or a base excitation can be written as

$$y_i(x,t) = Y_i(x_i)\sin(\Omega t), \tag{4.6}$$

where

$$Y_i(x_i) = A_i\cos\lambda_i x_i + B_i\sin\lambda_i x_i + C_i\cosh\lambda_i x_i + D_i\sinh\lambda_i x_i. \tag{4.7}$$

The Ω is the frequency of excitation and $\lambda_i^4 = \Omega^2(A_i\rho_i/E_iI_i)$ is known, however A_i, B_i, C_i and D_i are unknowns and the procedure to determine these constants is described in Appendix A. Computer programs based on this approach are developed to generate the frequency response functions $H_{bi}(\omega)$ and $H_{1i}(\omega)$ and are listed in Appendix C.

In the next section, the three previously presented clearances estimation approaches will be used to predict the clearances and impact forces of the beam-stop system. A common feature of these approaches is that the linear relation of equation (4.5) is first used to find the needed information of $y_1(t)$ and u(t) and then clearances d_1 and d_2 will be estimated by considering only the isolated nonlinearity $u(y_1)$.

4.3 ESTIMATION OF CLEARANCE AND IMPACT FORCES

Assume all the system parameters except the clearances d_1 and d_2 are known. The base excitation b(t) and displacement $y_2(t)$ at x_2 are assumed available. Consider the linear subsystem 1 in the Figure 48(b) first. All its elements are known, and among its two inputs and one output, only one input, the impact force u(t), is unknown. This system can be

solved to find the unknown u(t) as follows. Solving equation (4.5) with i=2, gives the impact force U(ω) in frequency domain and u(t) in time domain as

$$U(\omega)=\frac{1}{H_{12}(\omega)}[B(\omega)H_{b2}(\omega)-Y_2(\omega)] \quad \text{and} \quad u(t)=F^{-1}[U(\omega)]. \qquad (4.8,4.9)$$

At this stage, the problem of estimating impact forces of the beam-stop system is complete. As explained in Chapter 2, the small amplitude high frequency noise is greatly amplified when equation (4.8) is used, hence the optimal estimate of impact force, $\hat{u}(t)$, obtained after clearances have been estimated is a much better estimate of the impact force than that obtained using equation (4.9). The $Y_1(\omega)$ and $y_1(t)$ can be found by considering the second linear subsystem shown in Figure 48(b). As U(ω) and B(ω) are known, the output $Y_1(\omega)$ in frequency domain or $y_1(t)$ in time domain can be found by using equation (4.5) and using i=1 as

$$Y_1(\omega)=B(\omega)H_{b1}(\omega)-U(\omega)H_{11}(\omega) \quad \text{and} \quad y_1(t)=F^{-1}[Y_1(\omega)]. \qquad (4.10,4.11)$$

The stop-clearance nonlinearity in Figure 48(b) can be studied as an isolated element. The input $y_1(t)$ and the output u(t) of this element are all known, and the unknown clearances d_1 and d_2 can be estimated using approaches developed in Chapters 2 and 3.

The describing function approach is used for the case when the base motion, b(t)=Bsin(Ω), is sinusoidal and the motion of the beam has reached a steady state. Evaluate equations (4.8) and (4.10) at frequencies ω=0 and ω=Ω to get U(0), U(Ω), $Y_1(0)$ and $Y_1(\Omega)$ respectively. The describing functions N_0 and N_1 can be expressed as (see equations (2.19) and (2.20))

$$N_0=\frac{U(0)}{|Y_1(\Omega)|}=\frac{1}{2\pi}\{k_1[(2\theta_1-\pi)\sin\theta_1+2\cos\theta_1]-k_2[(2\theta_2-\pi)\sin\theta_2+2\cos\theta_2]\} \qquad (4.12)$$

and

$$N_1 = \frac{U(\Omega)}{Y_1(\Omega)} = \frac{1}{2\pi}[k_1(\pi - 2\theta_1 - \sin 2\theta_1) + k_2(\pi - 2\theta_2 - \sin 2\theta_2)]. \tag{4.13}$$

The θ_1 and θ_2 in above equations satisfy (see equation (2.15))

$$d_1 = Y(0) + |Y_1(\Omega)| \sin\theta_1, \quad \text{and} \quad d_2 = -Y(0) + |Y_1(\Omega)| \sin\theta_2, \tag{4.14}$$

respectively. The procedure to estimate d_1 and d_2 is the same as that stated in Section 2.3, namely, substitute the values of experimentally obtained N_0 and N_1 into equations (4.12) and (4.13), solve the nonlinear equations numerically for θ_1 and θ_2, and use θ_1 and θ_2 to obtain d_1 and d_2 by using equation (4.14).

The optimization approach can also be used to estimate clearances when excitation b(t) is sinusoidal. The needed impact forces u(t) and the displacement at stop location $y_1(t)$ are give by equations (4.9) and (4.11) respectively. Clearances d_1 and d_2 can now be estimated as the values which minimize the objective function J defined by (see equation (2.33))

$$J(\hat{d}_1, \hat{d}_2) = \begin{cases} \frac{1}{T}\int_0^T \{\hat{u}[y_1(t), \hat{d}_1, \hat{d}_2] - u(t)\}^2 dt + [k_1(\hat{d}_1 - y_{1\max})]^2 & \hat{d}_1 > y_{1\max}, \\ \frac{1}{T}\int_0^T \{\hat{u}[y_1(t), \hat{d}_1, \hat{d}_2] - u(t)\}^2 dt & \hat{d}_1 \le y_{1\max} \text{ and } \hat{d}_2 \le -y_{1\min}, \\ \frac{1}{T}\int_0^T \{\hat{u}[y_1(t), \hat{d}_1, \hat{d}_2] - u(t)\}^2 dt + [k_2(\hat{d}_2 + y_{1\min})]^2 & \hat{d}_2 > -y_{1\min}, \end{cases} \tag{4.15}$$

where $y_{1\max}$ and $y_{1\min}$ are the maximum and minimum values of $y_1(t)$, $t \in [0,T]$, respectively. The $\hat{u}[y_1(t), \hat{d}_1, \hat{d}_2]$ can be obtained by substituting $y_1(t)$ and assumed $\hat{d}_1$ and $\hat{d}_2$ in equation (4.1).

The spectral analysis approach is used when the system is under random excitation. It is assumed that b(t) is a stationary ergotic stochastic process and the impact forces and displacements of the beam-stop system are also stationary and ergotic. The first two

coefficients W_0 and W_1 of the Chebyshev-Hermite expansion of $u(y_1)$ relate to the unknown clearances, d_1 and d_2, by (see equations (3.14) and (3.15))

$$W_0=\frac{\sigma_{y1}}{\sqrt{2\pi}}\left[k_1\exp\left(-\frac{(d_1-m_{y1})^2}{2\sigma_{y1}^2}\right)-k_2\exp\left(-\frac{(d_2+m_{y1})^2}{2\sigma_{y1}^2}\right)\right]+$$

$$\frac{1}{2}\left[k_2(m_{y1}+d_2)erfc\left(\frac{d_2+m_{y1}}{\sqrt{2}\sigma_{y1}}\right)+k_1(m_{y1}-d_1)erfc\left(\frac{d_1-m_{y1}}{\sqrt{2}\sigma_{y1}}\right)\right] \tag{4.16}$$

and

$$W_1=\frac{\sigma_{y1}}{2}\left[k_2erfc\left(\frac{d_2+m_{y1}}{\sqrt{2}\sigma_{y1}}\right)+k_1erfc\left(\frac{d_1-m_{y1}}{\sqrt{2}\sigma_{y1}}\right)\right]. \tag{4.17}$$

These W_0 and W_1 can be obtained experimentally as (see equations (3.24) and (3.28))

$$W_0 = m_u \tag{4.18}$$

and

$$W_1=\sigma_{y1}\frac{\int_{\omega_1}^{\omega_2}S_{y1u}(\omega)d\omega}{\int_{\omega_1}^{\omega_2}S_{y1}(\omega)d\omega}. \tag{4.19}$$

To evaluate W_0 and W_1 by above equations, it is needed to find the m_{y1}, σ_{y1}, $S_{y1}(\omega)$, m_u and $S_{y1u}(\omega)$ from experimentally obtained b(t) and $y_2(t)$. Corresponding to equation (4.8), an equation relating the mean value m_u of the impact force with the mean value m_{y2} of the measured displacement and the m_b of the base excitation can be written as

$$m_u=\frac{1}{H_{12}(0)}[m_bH_{b2}(0)-m_{y2}]. \tag{4.20}$$

Similarly, corresponding to equation (4.10), an equation relating the mean value m_{y1} of displacement at the stop location with m_u and m_b can be written as

$$m_{y1}=m_bH_{b1}(0)-m_uH_{11}(0). \tag{4.21}$$

Since input b(t) and measured outputs $y_2(t)$ are known, m_b and m_{y2} could be computed directly from the time history records using the ergotic property. So m_u can be found by equation (4.20) and then m_{y1} can be calculated by equation (4.21).

The Fourier transform of impact force of a finite duration T, $U(\omega,T)$ can be found by equation (4.8) from $B(\omega,T)$ and $Y_2(\omega,T)$ which are known from direct Fourier transform of measured time history records. The transformed displacement $Y_1(\omega,T)$ at stop location can be found by equation (4.10). The power and cross spectral density functions can be calculated using

$$S_{y1}(\omega) = \lim_{T\to\infty} \frac{1}{T} E\{| Y_1(\omega,T) |^2\} \tag{4.22}$$

and

$$S_{y1u}(\omega) = \lim_{T\to\infty} \frac{1}{T} E\{Y_1^*(\omega,T)U(\omega,T)\}. \tag{4.23}$$

The variance σ_{y1}^2 can be computed by

$$\sigma_{y1}^2 = \lim_{T\to\infty} \frac{1}{T} \int_0^T y_1(t)^2 dy_1 - m_{y1}^2, \tag{4.24}$$

after m_{y1} is calculated and $y_1(t)$ is found by inverse Fourier transforming $Y_1(\omega,T)$.

When m_{y1}, σ_{y1}, $S_{y1}(\omega)$, m_u and $S_{y1u}(\omega)$ have been found, the clearances d_1 and d_2 could be estimated by the following procedure which is exactly the same as that explained in Section 3.2. Find the first two coefficients W_0 and W_1 of the Chebyshev-Hermite expansion of $u(y_1)$ by using the experimentally obtained values in equations (4.18) and (4.19), respectively. Then substitute the values of W_0 and W_1 into the left hand sides of equations (4.16) and (4.17) respectively. Finally, solve these two coupled nonlinear equations for unknown d_1 and d_2 using numerical iteration.

4.4 EXPERIMENTS

Experiments were conducted using a mechanical analogue to test the performance of the three presented estimation approaches on the beam-stop system.

4.4.1 EXPERIMENTAL SETUP

A mechanical analogue of the system was built and is shown in Figure 49. It consisted of an uniform aluminum beam clamped rigidly at one end on the electromagnetic shaker. Two stop springs were mounted on a frame with clearances between springs and the beam. These clearances can be adjusted using two screws. The beam had a rectangular cross-section (6.32 mm × 25.73 mm), which gives a cross-section area A = 163 mm^2 and a moment of inertia I = 542 mm^4, length L = 570 mm, elasticity modulus E = 6.895×10^{10} Pa and mass density ρ = 2713 kg/m^3. An accelerometer was mounted near the tip of the beam 549 mm away from the base to measure the absolute displacement of that point. The accelerometer together with the wire made up a concentrated mass of 23 g. The base input, b(t), was measured using another accelerometer which was mounted on the fixed end of the beam. A force transducer was connected to one of the stop springs to measure the impact force. The measurement and other instrumentation was the same as that described in Section 2.5.2 and Section 3.3.2 for sinusoidal and random excitation respectively.

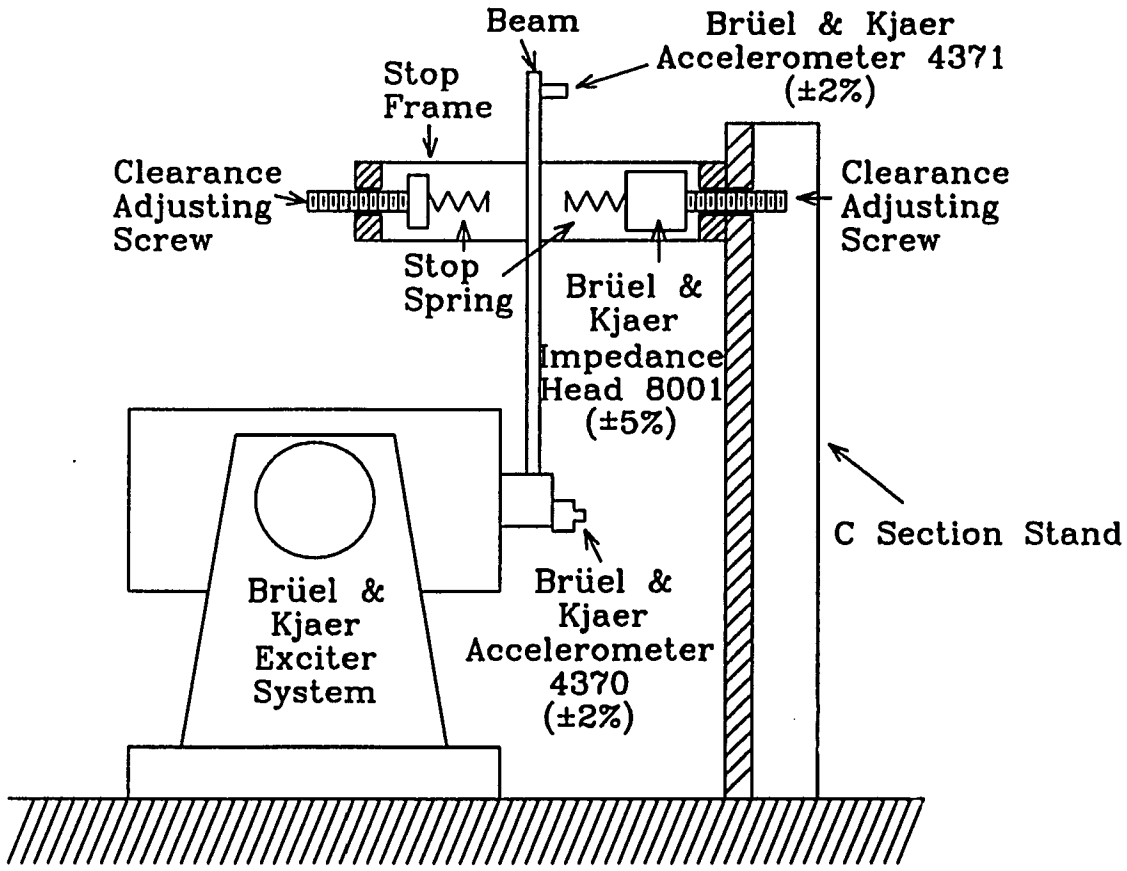

Figure 49. Experimental setup for the beam-stop system.

4.4.2 FREQUENCY RESPONSE FUNCTIONS

The success of the estimation of clearance depends greatly on the accuracy of the needed frequency response functions. Experiments were conducted on the cantilever beam without motion limiting springs to verify the frequency response function $H_{b2}(\omega)$

obtained by the approach described in the Appendix A.

The beam shown in Figure 49 without stops was excited at various frequencies between 5 Hz to 110 Hz using a sinusoidal base excitation. The frequency response function $H_{b2}(\omega)$ in form of $H_{b2}(f)$ ($f = \omega/2\pi$) was obtained experimentally by measuring the base displacement b(t) and the beam displacement $y_2(t)$ at point x_2 and finding the ratio of their amplitudes. The $H_{b2}(f)$ obtained experimentally is shown in Figure 50(a) together with the corresponding $H_{b2}(f)$ calculated theoretically and agreement between them is good. The natural frequencies of the beam obtained are listed in Table 10. The frequency response function was also obtained experimentally using a random excitation. In the experiment the beam was excited by a random base motion and 25 samples of b(t) and $y_2(t)$ were taken. The spectra $S_{by2}(f)$ and $S_{y2}(f)$ were estimated using these records. The frequency response function $H_{b2}(f)$ was found as $H_{b2}(f)=S_{y2}(f)/S_{by2}(f)$ [22] and is shown in Figure 50(b). The agreement between theoretical and experimental $H_{b2}(f)$ is good.

Most of the experiments were conducted with stop location x_1 = 435 mm and accelerometer location x_2 = 549 mm. The $H_{b1}(f)$, $H_{b2}(f)$, $H_{11}(f)$ and $H_{12}(f)$ for this setting were calculated theoretically without consideration of damping. But in reality small damping is inevitable. The effect of damping on the vibration of the beam near resonant frequencies is considered in Appendix B. The theoretically predicted infinite peaks in the frequency response functions were suppressed by using $\zeta = 0.01$, which seems to be the average damping as can be seen from Figure 50(a). To avoid difficulty in the division process indicated by equation (4.8) the very small amplitudes of $H_{12}(f)$ were averaged to the nearby values. The modified frequency response functions are shown in Figure 51 and were used in the clearances and impact forces estimation.

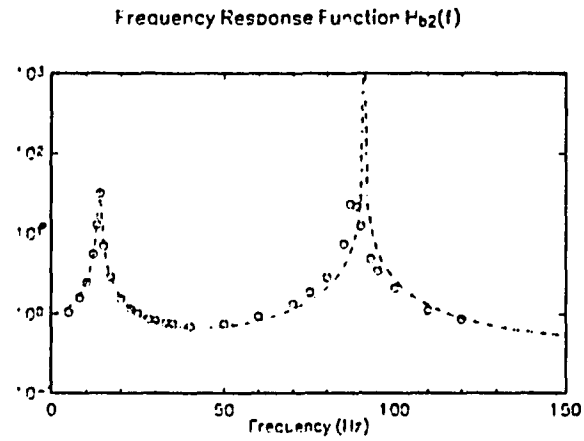

(a)

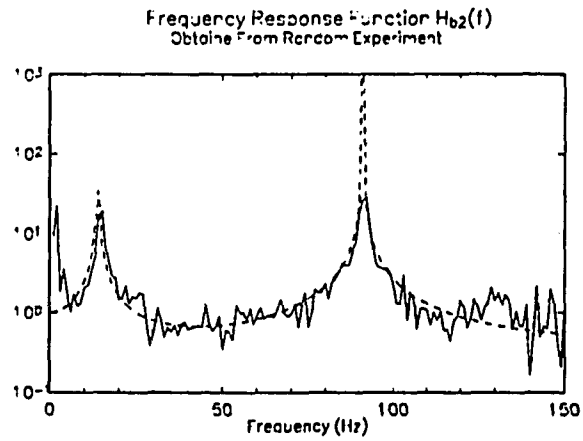

(b)

Figure 50. Frequency response function $H_{b2}(f)$. (a) From deterministic experiment, O , and from calculations, - - - -. (b) From random experiment, —— .

TABLE 10

Comparison of natural frequencies obtained from experiments and calculations.

	Natural Frequencies (Hz)			
	1st	2nd	3rd	4th
Experiment	14±0.5	90±0.5		
Calculation	13.7	91.0	262.8	525.7

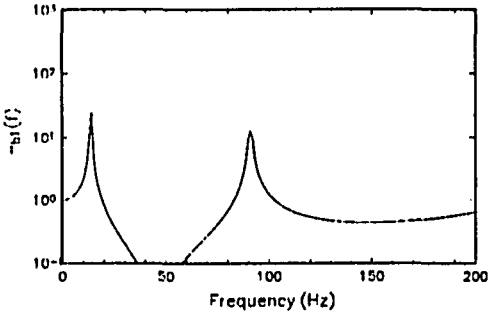

(a) $H_{b1}(f)$

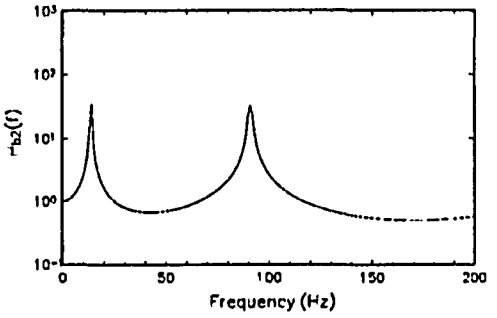

(b) $H_{b2}(f)$

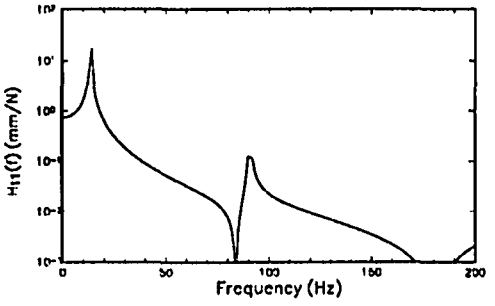

(c) $H_{11}(f)$

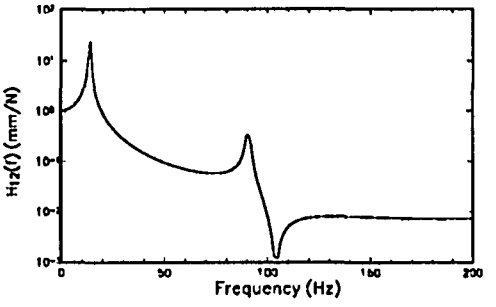

(d) $H_{12}(f)$

Figure 51. Frequency response functions.

4.4.3 ESTIMATION PROCEDURE

During experiments, the amplitude of the excitation was adjusted to ensure impacts occur between the beam and the stops. The base excitation b(t) and beam displacement $y_2(t)$ at x_2 were measured by two accelerometers and were amplified using a vibration meter and a charge amplifier respectively. The signals were digitized using an A/D converter and were stored on a floppy disk. As explained before, the sampled discrete data were $b_n = b(n\nabla t)$ and $y_{2n} = y_2(n\nabla t + \nabla t/2)$. The sampling rate ∇t was taken as 1/1024 second and the sample duration chosen was 1 second. So the Nyquist frequency was 512 Hz and the frequency resolution was 1 Hz for all spectral quantities. The finite frequency resolution also justify the smoothening of the peaks and valleys of the frequency response functions. During the experiments using a random excitation, 10 samples were taken for each case. The data was transferred to a VAXstation 2000 workstation and all computations were performed there. The needed frequency response functions were pre-calculated and stored in the computer.

The procedure of estimation of clearances and impact forces based on the describing function approach and the optimization approach which uses deterministic excitation is described first. The Fourier transforms $B(\omega)$ and $Y_2(\omega)$ were obtained from the digitized b(t) and $y_2(t)$ using a FFT subroutine. To reduce the effects of high frequency noise, the $B(\omega)$ and $Y_2(\omega)$ were filtered above a cutoff frequency. The cutoff frequency was chosen automatically by the computer program as fifteen times the exciting frequency or the frequency above which no signal components were larger than 1 thousandths of the main frequency component. The filtering process was used to reduce noise which otherwise will get amplified by $1/H_{12}(\omega)$ when equation (4.8) was used to calculate $U(\omega)$. The $U(\omega)$ was used to calculate $Y_1(\omega)$ using equation (4.10). The $Y_1(0)$, $Y_1(\Omega)$, U(0) and $U(\Omega)$

needed for the describing function approach were obtained from $Y_1(\omega)$ and $U(\omega)$. The describing functions N_0 and N_1 were obtained by substituting $Y_1(\Omega)$, $U(0)$ and $U(\Omega)$ into equations (4.12) and (4.13). Equations (4.12) and (4.13) were two nonlinear equations in two unknowns θ_1 and θ_2. These equations were iteratively solved until the differences between the right and the left hand sides was minimum. The estimates of d_1 and d_2 were obtained using calculated θ_1, θ_2, $Y_1(0)$ and $Y_1(\Omega)$ into equation (4.14). The impact force could be estimated equation (4.1) after the clearances have been estimated.

When the optimization approach was used, the impact force u(t) and displacement $y_1(t)$ at the stop location were obtained by inverse Fourier transforming $U(\omega)$ and $Y_1(\omega)$ respectively. The optimal estimates $\hat{d}_1$ and $\hat{d}_2$ were found by searching for the minimum of J given by equation (4.15) by the Powell method and the search was started using $\hat{d}_1 = \hat{d}_2 = 0$.

The procedure of estimation of clearances based on the spectral analysis approach which uses random excitation consisted of the following steps.

1. Find the mean values m_{y1} and m_u.

The m_b and m_{y2} were computed directly from the time history records of b(t) and $y_2(t)$. Using the m_b and m_{y2}, m_u was then found by equation (4.20) and m_{y1} was calculated by equation (4.21).

2. Estimate the power and cross spectral density functions $S_{y1}(\omega)$ and $S_{y1u}(\omega)$.

From each b(t) and $y_2(t)$ record, find $B(\omega,T)$ and $Y_2(\omega,T)$, find $U(\omega,T)$ using equation (4.8) from $B(\omega,T)$ and $Y_2(\omega,T)$, and then find $Y_1(\omega,T)$ using equation (4.10). The spectra $S_{y1}(\omega)$ and $S_{y1u}(\omega)$ were obtained form $Y_1(\omega,T)$ and $U(\omega,T)$ using equations (4.22) and (4.23) respectively. The expected value was estimated using spectral quantities for each sample of the collection of 10 records and by averaging the results.

3. Find the variance σ^2_{y1}.

The $y_1(t)$ was found by inverse Fourier transforming $Y_1(\omega,T)$. Then σ^2_{y1} was found using equation (4.24).

4. Calculate the W_0 and W_1 from above experimentally obtained quantities.

The W_0 and W_1 were obtained using equations (4.18) and (4.19), respectively. The frequency range ω_1 through ω_2, $\omega_1 = 2\pi$ and $\omega_2 = 100 \times 2\pi$, was considered in evaluating equation (4.19) and the integrals were replaced by sums. This frequency range was chosen to avoid the effects of the valley in the frequency response function $H_{12}(\omega)$.

5. Estimate clearances d_1 and d_2 optimally.

Substituting the calculated W_0 and W_1 into the left hand sides of equations (4.16) and (4.17) respectively. Solve these two nonlinear equations in two unknowns d_1 and d_2 iteratively using the Powell method to obtain the estimates of d_1 and d_2.

4.5 RESULTS AND DISCUSSION

The comparison of estimated clearances of the beam-stop system with actual ones is presented here. A typical case is presented first to show the step by step detail of these approaches. As an example, consider the beam-stop system shown in Figure 49 under a sinusoidal excitation, $b(t) = 0.98\sin(38\pi t)$ mm, contacting stops located at $x_1 = 435$ mm with support springs constants $k_1 = k_2 = 11600 \pm 100$ N/m and gaps $d_1 = d_2 = 0.64 \pm 0.05$ mm. The b(t) and $y_2(t)$ at $x_2 = 549$ mm are shown in Figure 52. Clearances were estimated using b(t) and $y_2(t)$ of Figure 52 by the computer programs (Appendix C) based on the describing function approach and the optimization approach. The B(f) and $Y_2(f)$, $f = \omega/2\pi$, shown in Figure 53 were found first. They were filtered out above 248 Hz as it was found that above that frequency no components were larger then one thousandths of the main

frequency component at 19 Hz. The U(f) and $Y_1(f)$ were then calculated from the B(f) and $Y_2(f)$ and are shown in Figure 54. For comparison the $\hat{U}(f)$ which was the Fourier transform of the optimal estimates of impact force $\hat{u}(t)$, is also shown in Figure 54. The similarity in the low frequency rage between U(f) and $\hat{U}(f)$ is visible. The U(0), U(19), $Y_1(0)$ and $Y_1(19)$ needed for the application of the describing function approach were obtained from U(f) and $Y_1(f)$. They were:

$$U(0) = 0.023 \text{ N}, \qquad U(19) = 2.28 - i1.01 \text{ N},$$

$$Y_1(0) = -0.020 \text{ mm}, \qquad Y_1(19) = 0.86 - i0.44 \text{ mm}.$$

N_0 and N_1 were then found by equations (4.12) and (4.13) as

$$N_0 = 24 \text{ N/m}, \qquad N_1 = 2578 - i140 \text{ N/m}.$$

In theory N_1 should be real. However, a small imaginary part of N_1 seen above was due to the experimental noise and errors. Its effect on the estimation of clearances was found to be negligible. The estimates were obtained using the real part of N_1. The N_0 was close to zero as this response was symmetric. The estimates of d_1 and d_2 by the describing function approach were $d_1 = 0.60$ mm and $d_2 = 0.69$ mm. The estimates of clearances were very accurate. The estimation of clearances based on the optimization approach needs inverse transforming of spectra of Figure 54 to obtain the time traces u(t) and $y_1(t)$, which is presented in Figure 55. An objective function $J(\hat{d}_1, \hat{d}_2)$ was constructed using the u(t) and its minimum was searched to find the optimal estimates of clearances $d_1 = 0.63$ mm and $d_2 = 0.68$ mm. The estimates of clearances were also very accurate. Figure 56 shows the comparison between the estimated and the measured impact forces and indicates that the estimate is reasonable. Only one impedance head was used and hence only impact force trace due to the stop spring on the positive displacement side was obtained.

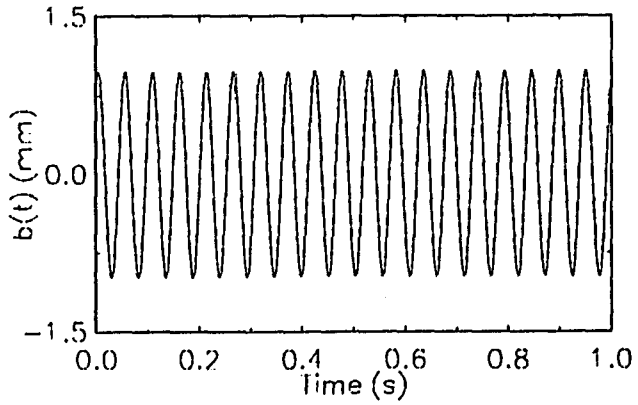

(a) b(t)

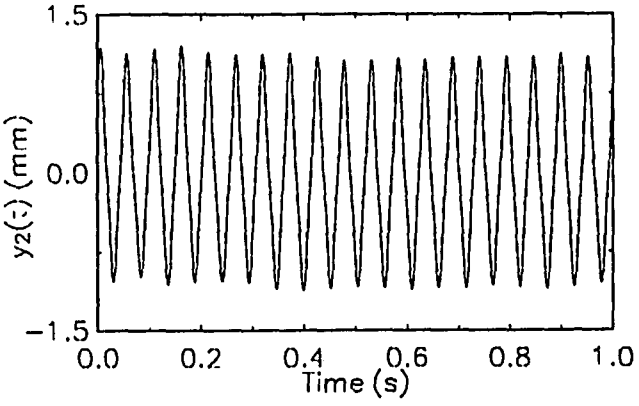

(b) $y_2(t)$

Figure 52. The traces of b(t) and $y_2(t)$. The system parameters were $x_1 = 435$ mm, $x_2 = 549$ mm, $k_1 = k_2 = 11600 \pm 100$ N/m, $d_1 = d_2 = 0.64 \pm 0.05$ mm and $b(t) = 0.98\sin(38\pi t)$ mm.

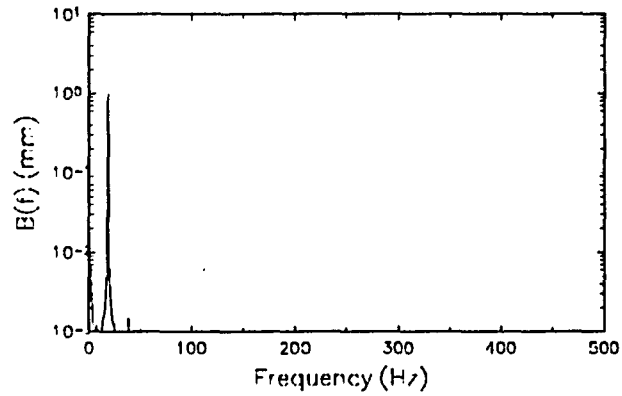

(a) B(f)

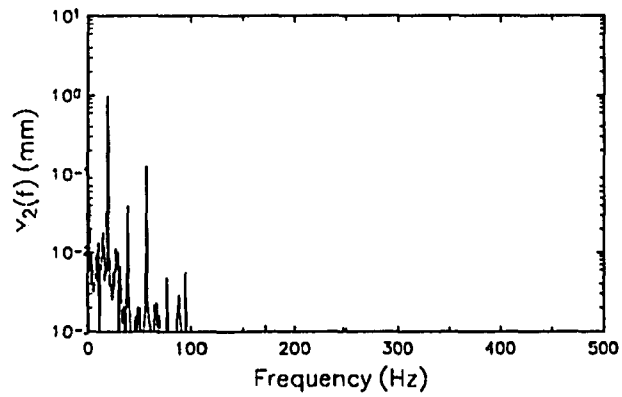

(b) $Y_2(f)$

Figure 53. The frequency spectra B(f) and $Y_2(f)$. The system parameters were identical to those reported in Figure 52.

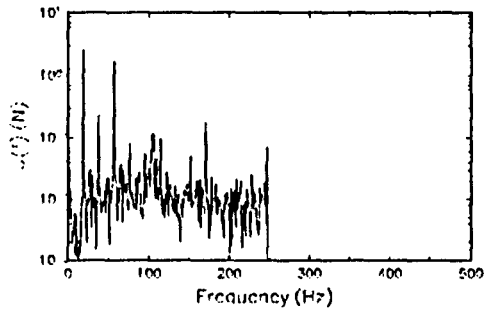

(a) U(f)

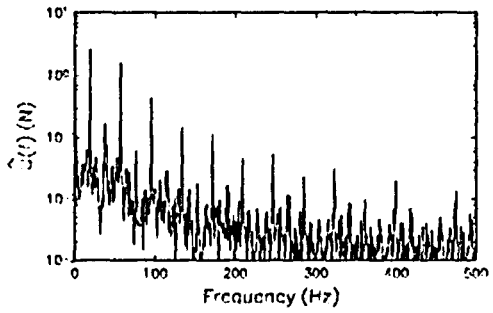

(b) $\hat{U}$(f)

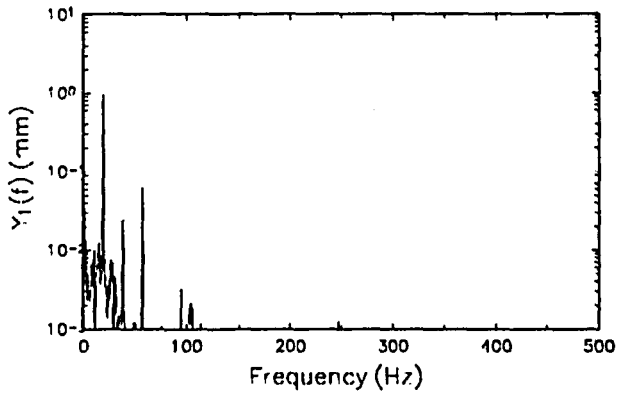

(c) Y_1(f)

Figure 54. The frequency spectra U(f), $\hat{U}$(f) and Y_1(f). The system parameters were identical to those reported in Figure 52.

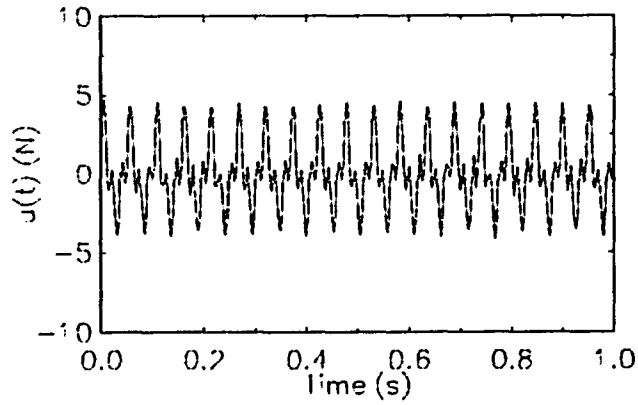

(a) u(t)

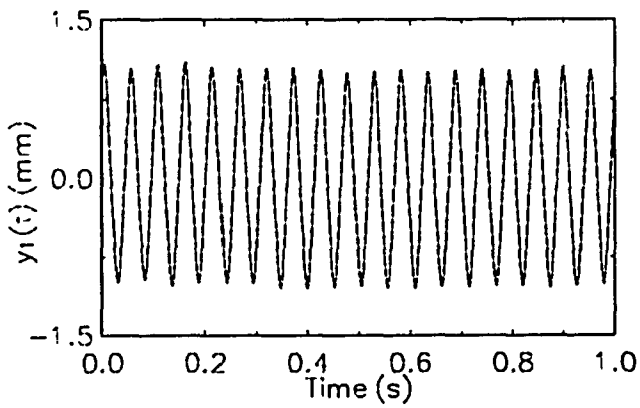

(b) $y_1(t)$

Figure 55. The traces of u(t) and $y_1(t)$. The system parameters were identical to those reported in Figure 52.

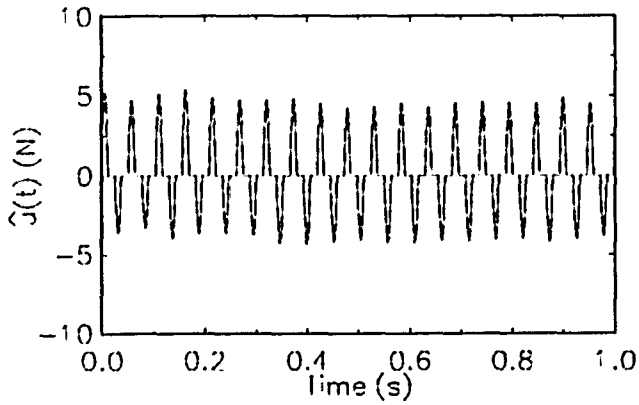

(a)

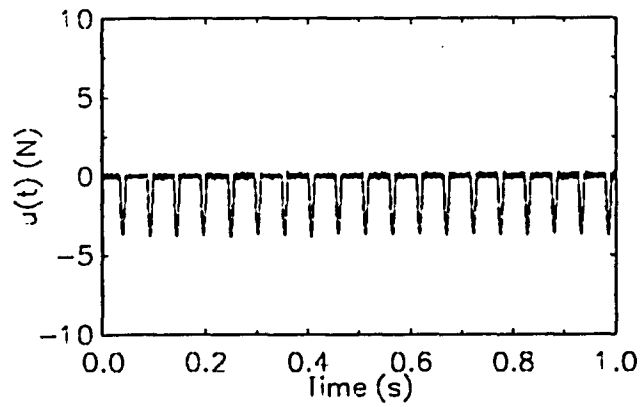

(b)

Figure 56. The estimated and measured impact forces u(t). (a) Estimated using experimental data and the optimization approach. (b) Measured using an impedance head. The system parameters were identical to those reported in Figure 52.

Excitations with various amplitudes and frequencies were used in the experiments and estimates of clearances using vibroimpact response under those excitations are reported in Table 11. The frequencies chosen were not far away from the first natural frequency of the cantilever beam so the beam was excited enough to hit the stops. Compared with the actual clearances, which were measured by a feeler gauge, the estimates are generally accurate. The describing function approach worked as good as the optimization approach did. The reason is that almost all responses were dominated by their fundamental harmonic and the assumption of the describing function was well satisfied. The comparison of estimated and measured impact forces for a few cases where input frequencies and amplitudes was varied is shown in Figure 57 and indicates a good agreement.

Experiments with smaller clearances, $d_1 = d_2 = 0.25 \pm 0.05$ mm, were conducted using sinusoidal and random excitation. The results of sinusoidal excitation are reported in Table 12. These estimates were reasonable, but somewhat overestimated. The system responses under random excitation were used to estimate the clearances by the spectral analysis approach. A typical sample of random base displacement b(t) and measured beam displacement $y_2(t)$ is shown in Figure 58 together with B(f) and $Y_2(f)$. The power and cross spectrum $S_{y1}(f)$ and $S_{y1u}(f)$ needed for the spectral analysis approach are shown in Figure 59. These were estimated using 10 samples. The W_0 and W_1 were found as -0.0024 and 3.16 respectively and the estimates of clearances obtained were $d_1 = 0.23$ mm and $d_2 = 0.21$ mm. Comparing these estimates with actual values of clearances, the results are quite accurate.

TABLE 11

Estimates of clearances based on data from mechanical experiments under sinusoidal excitation. The system parameters were $x_1 = 435$ mm, $x_2 = 549$ mm, $k_1 = k_2 = 11600 \pm 100$ N/m and $d_1 = d_2 = 0.64 \pm 0.05$ mm.

Excitation Frequency (Hz)	Base Amplitude (mm)	Describing Function Approach		Optimization Approach	
		d_1(mm)	d_2(mm)	d_1(mm)	d_2(mm)
8	0.56	0.61	0.57	0.78	0.68
8	0.97	0.50	0.61	0.65	0.82
10	1.41	0.69	0.52	0.54	0.92
12	0.97	0.68	0.63	0.84	0.65
17	0.42	0.58	0.63	0.63	0.63
17	0.72	0.44	0.63	0.64	0.62
19	0.70	0.61	0.68	0.65	0.68
19	0.98	0.60	0.69	0.63	0.68
19	1.42	0.47	0.48	0.60	0.56

Continued on the next page.

TABLE 11

(Continued)

Excitation Frequency (Hz)	Base Amplitude (mm)	Describing Function Approach		Optimization Approach	
		d_1(mm)	d_2(mm)	d_1(mm)	d_2(mm)
21	0.70	0.64	0.65	0.68	0.69
21	1.00	0.57	0.69	0.64	0.71
21	1.41	0.42	0.81	0.56	0.77
23	2.84	0.50	0.70	0.57	0.66
23	3.66	0.62	0.51	0.60	0.55
25	2.79	0.50	0.68	0.56	0.63
25	4.18	0.61	0.48	0.59	0.55
27	2.80	0.58	0.66	0.60	0.65
29	1.42	0.64	0.57	0.63	0.60
Average		0.57	0.62	0.63	0.67

f = 17 Hz

|b(t)|=0.42 mm

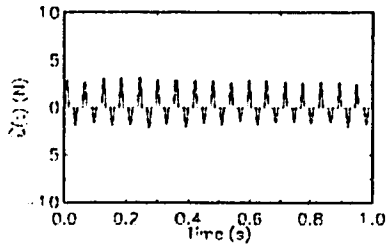

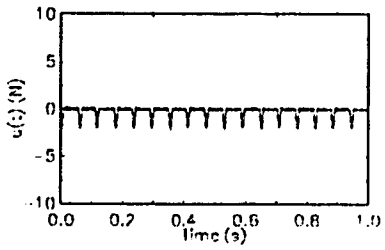

f = 17 Hz

|b(t)|=0.72 mm

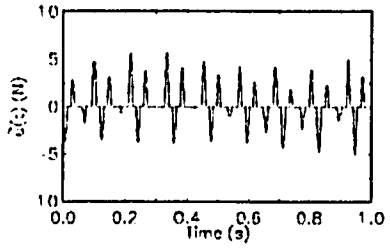

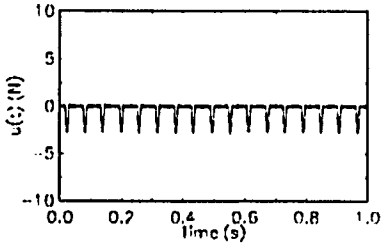

f = 19 Hz

|b(t)|=0.70 mm

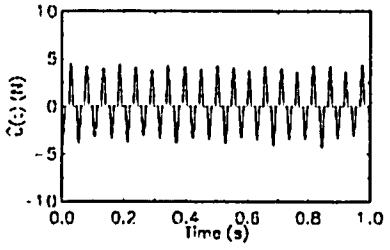

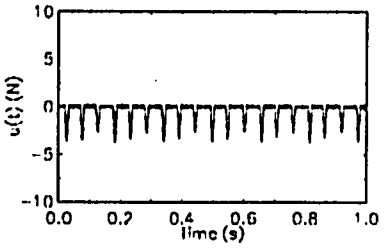

(a) (b)

Continued on the next page.

f = 21 Hz

|b(t)|=0.70 mm

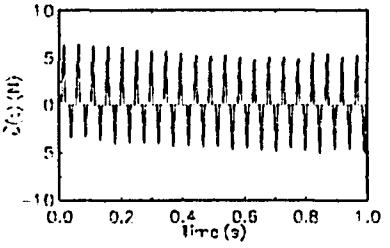

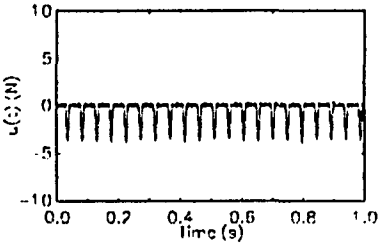

f = 21 Hz

|b(t)|=1.00 mm

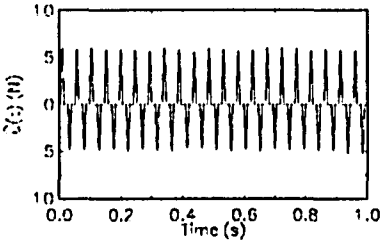

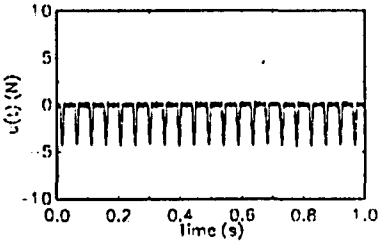

f = 23 Hz

|b(t)|=2.84 mm

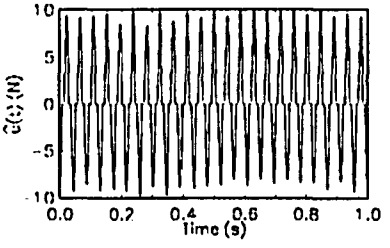

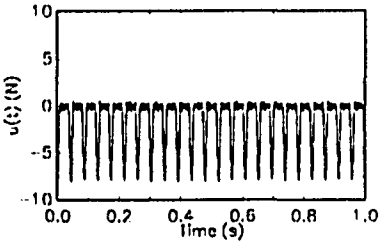

(a) (b)

Figure 57. (a) Estimated impact force $\hat{u}(t)$ from the optimization approach. (b) Measured impact force. The system parameters were identical to those given in Table 11.

TABLE 12

Estimates of clearances based on data from mechanical experiments under sinusoidal excitation. The system parameters were $x_1 = 435$ mm, $x_2 = 549$ mm, $k_1 = k_2 = 11600 \pm 100$ N/m and $d_1 = d_2 = 0.25 \pm 0.05$ mm.

Excitation Frequency (Hz)	Base Amplitude (mm)	Describing Function Approach		Optimization Approach	
		d_1(mm)	d_2(mm)	d_1(mm)	d_2(mm)
8	0.56	0.34	0.21	0.48	0.28
17	0.14	0.33	0.37	0.36	0.36
19	0.69	0.28	0.26	0.29	0.26
21	0.55	0.37	0.25	0.36	0.31
23	0.84	0.30	0.38	0.33	0.36
25	1.40	0.40	0.25	0.38	0.29
27	1.37	0.26	0.38	0.30	0.35
Average		0.33	0.30	0.36	0.32

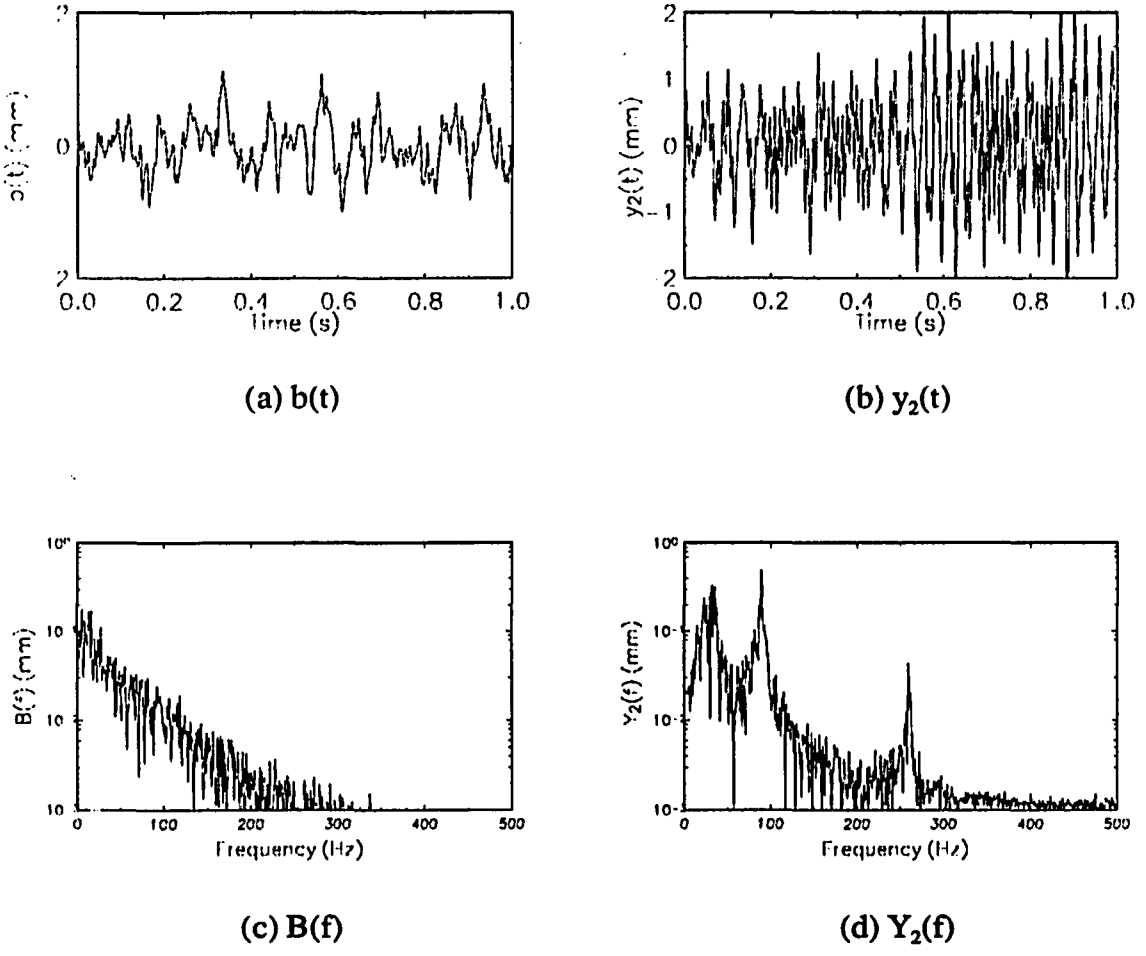

(a) b(t)

(b) $y_2(t)$

(c) B(f)

(d) $Y_2(f)$

Figure 58. Typical measured system excitation b(t) and response $y_2(t)$ and their spectra. The system parameters were identical to those given in Table 12.

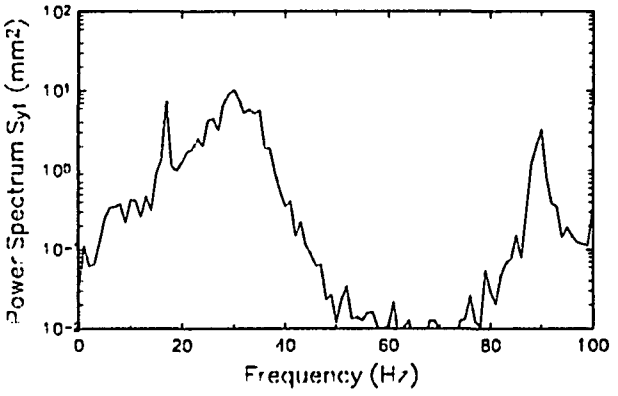

(a)

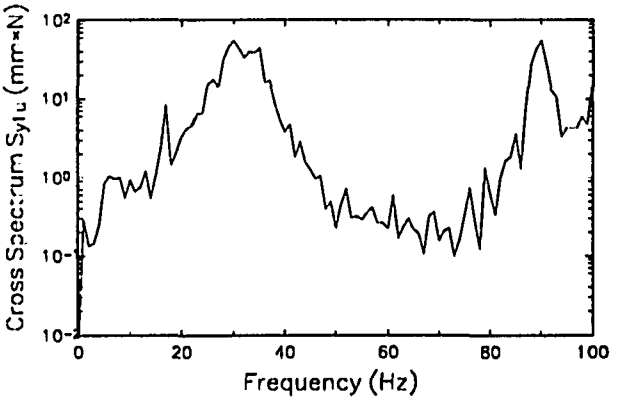

(b)

Figure 59. (a) The power spectrum $S_{y1}(f)$ and (b) The cross spectrum $S_{y1u}(f)$. The system parameters were identical to those reported in Table 12.

The cases described above were symmetric. The results of estimation obtained using sinusoidal excitation for systems where gaps were significantly asymmetric are presented in Table 13. Figure 60 shows a sample of b(t) and $y_2(t)$ of one case reported in Table 13. The estimates of overall clearance indicate a very reasonable agreement with actual values, but the estimation fails to indicate the asymmetry. The estimates of clearances obtained using the random system response and the spectral analysis approach were $d_1 = d_1$ = 0.37 mm i.e. an overall estimate d_1+d_2 = 0.74 mm. Again the overall estimation was reasonable, but asymmetry was not detected. Figure 61 shows typical random excitation and response sample records. Carefully checking the measured system excitation and system response (see Figure 60), it is found that even the system was asymmetric, the measured responses were essentially symmetric.

Experiments were also conducted when the stop springs were moved to another position x_1 = 346 mm. Table 14 shows the results and the agreement between the estimated and actual clearances is reasonable.

TABLE 13

Estimates of clearances based on data from mechanical experiments under sinusoidal excitation. The system parameters were $x_1 = 435$ mm, $x_2 = 549$ mm, $k_1 = k_2 = 11600 \pm 100$ N/m and asymmetric clearances $d_1 = 0.25 \pm 0.05$ mm and $d_2 = 0.64 \pm 0.05$ mm, i.e. a overall clearance $d_1+d_2 = 0.89 \pm 0.1$ mm.

Excitation Frequency (Hz)	Base Amplitude (mm)	Describing Function Approach			Optimization Approach		
		d_1(mm)	d_2(mm)	d_1+d_2(mm)	d_1(mm)	d_2(mm)	d_1+d_2(mm)
8	0.69	0.50	0.34	0.84	0.37	0.73	1.10
17	0.28	0.47	0.52	0.99	0.51	0.51	1.02
19	0.69	0.39	0.57	0.96	0.45	0.53	0.98
21	0.55	0.48	0.45	0.93	0.50	0.49	0.99
23	0.84	0.46	0.49	0.95	0.47	0.49	0.96
25	2.79	0.41	0.42	0.83	0.40	0.42	0.82
27	2.11	0.46	0.43	0.89	0.46	0.45	0.91
29	1.39	0.49	0.45	0.94	0.49	0.47	0.96
Average		0.46	0.46	0.92	0.46	0.51	0.97

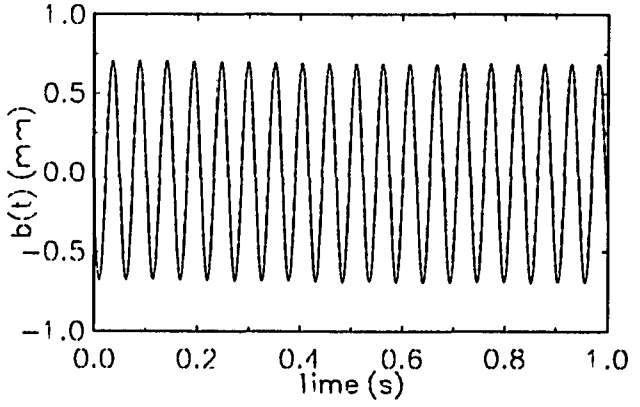

(a)

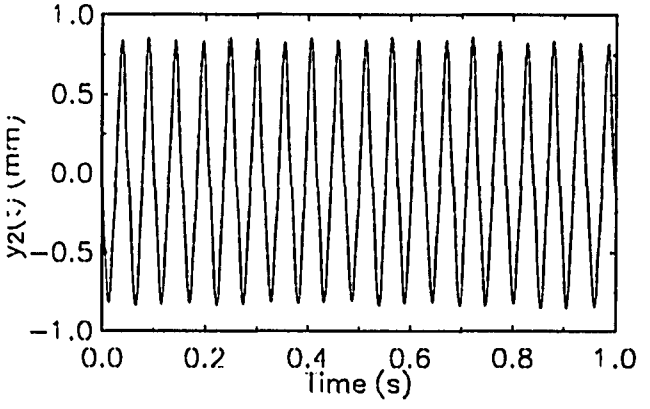

(b)

Figure 60. (a) The sinusoidal excitation b(t) and (b) the response $y_2(t)$ of a beam-stop system with asymmetric clearances. The system parameters were identical to those reported in Table 13 and $b(t) = 0.69\sin(38\pi t)$ mm.

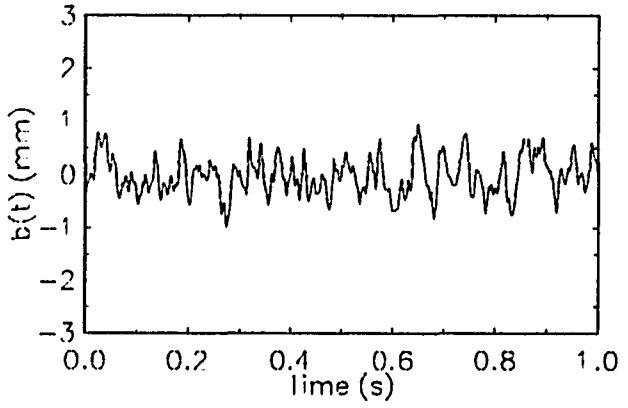

(a)

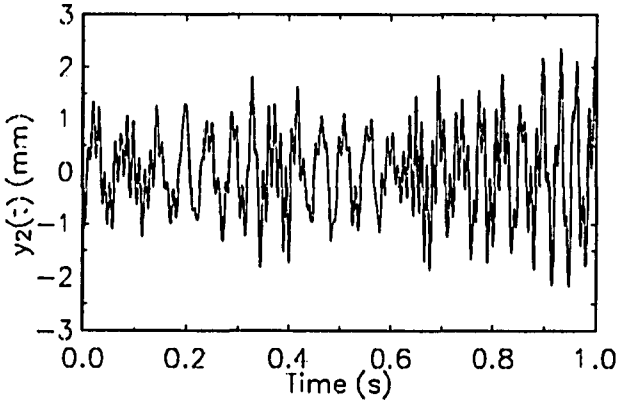

(b)

Figure 61. (a) The random excitation b(t) and (b) the response $y_2(t)$ of a beam-stop system with asymmetric clearances. The system parameters were identical to those reported in Table 13.

TABLE 14

Estimates of clearances based on data from mechanical experiments under sinusoidal excitation. The system parameters were $x_1 = 361$ mm, $x_2 = 549$ mm, $k_1 = k_2 = 11600 \pm 100$ N/m and $d_1 = d_2 = 0.71 \pm 0.05$ mm.

Excitation Frequency (Hz)	Base Amplitude (mm)	Describing Function Approach		Optimization Approach	
		d_1(mm)	d_2(mm)	d_1(mm)	d_2(mm)
8	0.98	0.83	0.70	0.78	0.89
12	0.98	0.89	0.79	0.89	0.84
17	0.70	1.01	0.48	0.89	0.61
19	2.83	0.70	0.66	0.61	0.63
21	6.87	0.79	0.64	0.75	0.73
Average		0.84	0.65	0.78	0.74

4.6 CONCLUSIONS

The clearances and impact forces estimation approaches developed in Chapter 2 and Chapter 3 for an impact oscillator can be easily extended to other systems with clearances. The three novel clearance and impact force estimation approaches can be applied successfully to a beam-stop system. The estimates of clearances and impact forces obtained using data from mechanical experiments were compared with actual clearances and impact forces and indicate a good agreement.

CHAPTER V.
CONCLUSIONS

Three novel clearance and impact force estimation approaches using vibroimpact signals are presented in this dissertation. Two approaches, the describing function approach and the optimization approach are developed for systems under a deterministic excitation. A third approach, the spectral analysis approach, is developed specially for systems under random excitation. These three approaches are first presented and tested using a single degree of freedom impact oscillator model, and later applied to a continuous beam-stop system to illustrate that these estimation approaches can be used for other more complex systems with clearances. Both computer simulated experiments and physical experiments were conducted to test these approaches. The estimates obtained using vibroimpact responses from the mechanical analogues of an impact oscillator and a beam-stop system and from a computer program simulating an impact oscillator were shown to agree with actual clearances and impact forces.

The describing function approach works only for a harmonically excited vibroimpact system. Estimation using this approach will be more reliable for a response dominated by the fundamental harmonic and this limits the use of the approach to systems with moderate nonlinearity. To estimate clearances the describing function approach requires only the constant and fundamental components of the response when the system is asymmetric and only the fundamental component when the system is symmetrical. This makes it possible to estimate clearances in the case of a symmetric system with the use of a vibration meter and a hand calculator and makes this approach promising for the on site in situ application.

Estimation relying only on one or two frequency components is also less susceptible to wide band noise and so the describing function approach can work well even when a highly polluted signal is used.

The optimization approach works well for simple as well as complex motions. It requires the complete time record of the vibroimpact response in order to estimate the clearances and impact forces. Generally, it provides more accurate estimation than the describing function approach. However this approach is susceptible to wide band noise.

The spectrum analysis approach utilizes the response of the vibroimpact system under random excitation to estimate clearances. Since the excitation to an operating system is more likely to be random than deterministic, a potential advantage of this approach is that it might be used to estimate clearances using a vibration signal of a normal operating condition. Reasonable numbers of vibro-impact samples are necessary to obtain smooth power spectrum and cross spectrum which are needed in the spectrum analysis approach, and this ensures more reliable estimates.

The effects of various system parameters on the estimation were also studied. Proper adjustment of the input frequency and/or amplitude which produces response with medium intensity impacts coupled with averaging estimates obtained under different excitations seems to be the best approach to estimate unknown clearances and impact forces.

APPENDIX A.

FORCED VIBRATION OF A BEAM SUPPORTED AT MANY LOCATIONS

Recently an exact approach was developed to study the free vibration of a straight beam. This was based on connecting the coefficients of two adjacent beam sections of the general solution of the forth order differential equation, based on the Euler beam theory, by a transfer matrix [84]. This study was restricted to free vibrations of beams consisting of many uniform sections having different cross-sections. In this Appendix, the above mentioned exact approach will be extended to predict the steady state forced vibration of a beam on many supports under a base excitation and a concentrated force excitation. The exact closed form solution of forced vibration of the above mentioned system which consists of the sum of four elementary functions is believed to be the first such solution.

Consider a beam made up of n different but uniform sections with the elasticity modulus, moment of inertia, area, mass density, end points and length of the ith section as E_i, I_i, A_i, ρ_i and l_i respectively. The beam is connected to fixed wall at n+1 points, and the corresponding translational and rotational spring stiffness and rigidly attached concentrated mass at the ith point are K_i, T_i and m_i respectively. The differential equation of motion of the ith section can be written as,

$$E_i I_i \frac{\partial^4 y_i}{\partial x_i^4} + \rho_i A_i \frac{\partial^2 y_i}{\partial t^2} = 0, \qquad (A1)$$

where $y_i = y_i(x_i, t)$ is the lateral deflection of the point on the ith section, located at distance x_i from the ith point. The forced vibration response of the ith section can be written as

$$y_i(x,t) = Y_i(x_i)\sin(\Omega t) \tag{A2}$$

where

$$Y_i(x_i) = A_i\cos\lambda_i x_i + B_i\sin\lambda_i x_i + C_i\cosh\lambda_i x_i + D_i\sinh\lambda_i x_i. \tag{A3}$$

The Ω is the frequency of excitation and $\lambda_i^4 = \Omega^2(A_i\rho_i/E_iI_i)$ is known, however A_i, B_i, C_i and D_i are unknowns and the procedure to determine these constants is given below.

The continuity of slope and deflection and the relations between shear forces and bending moments at every point i, can be written as,

$$Y_{(i-1)}(l_{i-1}) = Y_i(0), \tag{A4}$$

$$\frac{dY_{(i-1)}(l_{i-1})}{dx_{i-1}} = \frac{dY_i(0)}{dx_i}, \tag{A5}$$

$$E_{i-1}I_{i-1}\frac{d^3Y_{(i-1)}(l_{i-1})}{dx_{i-1}^3} = K_iY_i(0) - m_i\Omega^2Y_i(0) + E_iI_i\frac{d^3Y_i(0)}{dx_i^3}, \tag{A6}$$

$$E_{i-1}I_{i-1}\frac{d^2Y_{(i-1)}(l_{i-1})}{dx_{i-1}^2} = -T_i\frac{dY_i(0)}{dx_i} + E_iI_i\frac{d^2Y_i(0)}{dx_i^2}. \tag{A7}$$

Substituting equation (A3) into equation (A4) through (A7), it can be shown that,

$$[A_i, B_i, C_i, D_i]^T = M_i[A_{(i-1)}, B_{(i-1)}, C_{(i-1)}, D_{(i-1)}]^T, \tag{A8}$$

where M_i is a 4×4 matrix. The elements of M_i are found as

$$M(1,1)_i = \frac{1}{2}([\lambda_{(i-1)}s_{(i-1)}T_i + r_{(i-1)}c_{(i-1)}]/r_i + c_{(i-1)})$$

$$M(1,2)_i = \frac{1}{2}([-\lambda_{(i-1)}c_{(i-1)}T_i + r_{(i-1)}s_{(i-1)}]/r_i + s_{(i-1)})$$

$$M(1,3)_i = \frac{1}{2}(-[\lambda_{(i-1)}sh_{(i-1)}T_i + r_{(i-1)}ch_{(i-1)}]/r_i + ch_{(i-1)})$$

$$M(1,4)_i = \frac{1}{2}(-[\lambda_{(i-1)} ch_{(i-1)} T_i + r_{(i-1)} sh_{(i-1)}]/r_i + sh_{(i-1)})$$

$$M(2,1)_i = \frac{1}{2}(-[q_{(i-1)} s_{(i-1)} - h_i c_{(i-1)}]/q_i - \lambda_{(i-1)} s_{(i-1)}/\lambda_i)$$

$$M(2,2)_i = \frac{1}{2}(-[-q_{(i-1)} c_{(i-1)} - h_i s_{(i-1)}]/q_i + \lambda_{(i-1)} c_{(i-1)}/\lambda_i)$$

$$M(2,3)_i = \frac{1}{2}(-[q_{(i-1)} sh_{(i-1)} - h_i ch_{(i-1)}]/q_i + \lambda_{(i-1)} sh_{(i-1)}/\lambda_i)$$

$$M(2,4)_i = \frac{1}{2}(-[q_{(i-1)} ch_{(i-1)} - h_i sh_{(i-1)}]/q_i + \lambda_{(i-1)} ch_{(i-1)}/\lambda_i),$$

(A9)

where

$c_i = \cos(\lambda_{(i-1)} l_{i-1})$, $s_i = \sin(\lambda_{(i-1)} l_{i-1})$, $ch_i = \cosh(\lambda_{(i-1)} l_{i-1})$, $sh_i = \sinh(\lambda_{(i-1)} l_{i-1})$,

$q_i = E_i I_i \lambda_i^3$, $r_i = E_i I_i \lambda_i^2$, $h_i = k_i - m_i \lambda_i^4 E_i I_i/(A_i \rho_i)$.

The values $M(3,e)_i$ and $M(4,e)_i$ are obtained respectively from $M(1,e)_i$ and $M(2,e)_i$, e=1, 2, 3 and 4, by changing the sign before the rectangular bracket.

Equation (A8) can be repeatedly used to relate coefficients of the last span to the first one as

$$[A_n, B_n, C_n, D_n]^T = M_T [A_1, B_1, C_1, D_1]^T, \qquad (A10)$$

where $M_T = M_n \cdot M_{(n-1)} \cdots M_2$.

A1. UNDER A BASE EXCITATION

Assume the first point of the beam undergoes a sinusoidal motion b(t)=Bsin(Ωt). The boundary condition at point 1 is

$$Y_1(0)=B \quad i.e. \quad A_1+C_1=B. \tag{A11}$$

Using equation (A10) and boundary condition (A11) and other boundary conditions (A6) and (A7) at points 1 and (n+1) results in an equation,

$$\begin{bmatrix} 1 & 0 & 1 & 0 \\ -r_1 & -T_1\lambda_1 & r_1 & -T_1\lambda_1 \\ W_1 & W_2 & W_3 & W_4 \\ V_1 & V_2 & V_3 & V_4 \end{bmatrix} \begin{bmatrix} A_1 \\ B_1 \\ C_1 \\ D_1 \end{bmatrix} = \begin{bmatrix} B \\ 0 \\ 0 \\ 0 \end{bmatrix}, \tag{A12}$$

where

$$W_i=\sum_{k=1}^{k=4} R1(k)M_T(k,i) \quad \text{and} \quad V_i=\sum_{k=1}^{k=4} R2(k)M_T(k,i) \quad i=1,2,3,4$$

with

$$R1(1)=q_n s_n-h_{(n+1)}c_n, \quad R1(2)=-q_n c_n-h_{(n+1)}s_n,$$

$$R1(3)=q_n sh_n-h_{(n+1)}ch_n, \quad R1(4)=q_n ch_n-h_{(n+1)}sh_n,$$

$$R2(1)=-r_n c_n-T_{n+1}s_n\lambda_n, \quad R2(2)=-r_n s_n+T_{n+1}c_n\lambda_n,$$

$$R2(3)=r_n ch_n+T_{n+1}sh_n\lambda_n, \quad R2(4)=r_n sh_n+T_{n+1}ch_n\lambda_n.$$

Equation (A12) is a system of 4 linear equations in 4 unknowns and was solved using the lower and upper triangular decomposition of the 4×4 matrix. Coefficients A_i, B_i, C_i and D_i for other sections could be obtained by using equation (A8).

A2. UNDER A CONCENTRATED FORCE EXCITATION [85]

A single force $f(t) = F\sin(\Omega t)$ acting at point z on the beam is considered. The response due to multiple inputs could be obtained by superposition.

The relations based on continuity of displacement and slope and between shear forces and bending moments across support point i for i≠z are given by equations (A4) through (A7). However, equation (A6) relating the shear force across point i=z changes to,

$$E_{z-1}I_{z-1}\frac{d^3Y_{z-1}(l_{z-1})}{dx_{z-1}^3}+F_z = K_zY_z(0)-m_z\omega_z^2Y_z(0)+E_zI_z\frac{d^3Y_z(0)}{dx_z^3}. \qquad (A13)$$

The relation between the coefficients A_{i-1}, B_{i-1} etc. of the (i-1)th section and A_i, B_i etc. of the ith section could be obtained using equation (A3) and equations (A4) through (A7). However, for i=z equation (A13) should be used instead of equation (A6). These relations for points $i \neq z$ and point i=z can be expressed as,

$$[A_i, B_i, C_i, D_i]^T = M_i[A_{i-1}, B_{i-1}, C_{i-1}, D_{i-1}]^T, \quad i \neq z \qquad (A14)$$

and

$$[A_z, B_z, C_z, D_z]^T = M_z[A_{z-1}, B_{z-1}, C_{z-1}, D_{z-1}]^T + [0, -F/2q_z, 0, F/2q_z]^T, \quad i = z, \qquad (A15)$$

respectively. The relation between the coefficients of the μTh section to the first section can be obtained by repeatedly use of (A14) and (A15) as

$$[A_\mu, B_\mu, C_\mu, D_\mu]^T = M_{T\mu}[A_1, B_1, C_1, D_1]^T + M_{Fz}[0, -F/2q_z, 0, F/2q_z]^T, \qquad (A16)$$

where

$$M_{T\mu} = M_{\mu}M_{\mu-1}\cdots M_2 \quad \text{and} \quad M_{Fz} = \begin{Bmatrix} [I] & for\ \mu = z \\ M_{\mu}M_{\mu-1}\cdots M_{z+1} & for\ \mu > z \\ [0] & for\ \mu < z \end{Bmatrix}, \tag{A17}$$

and [I] and [0] indicate an identity matrix and a null matrix, respectively. The relation between the coefficients of the nth section and the 1st section can be obtained by substituting μ=n in equation (A16) and (A17). The boundary conditions relating bending moments and shear forces, i.e. equations (A6) and (A7), at points 1 and n+1 together with equations (A16) and (A17) give,

$$\begin{bmatrix} h_1 & -q_1 & h_1 & q_1 \\ -r_1 & -T_1\lambda_1 & r_1 & -T_1\lambda_1 \\ W_1 & W_2 & W_3 & W_4 \\ V_1 & V_2 & V_3 & V_4 \end{bmatrix} \begin{bmatrix} A_1 \\ B_1 \\ C_1 \\ D_1 \end{bmatrix} = \begin{bmatrix} 0 \\ 0 \\ u_1 \\ u_2 \end{bmatrix}, \tag{A18}$$

where

$$[u_1, u_2]^T = -QM_{Fn}[0, -F/2q_z, 0, F/2q_z]^T, \tag{A19}$$

and

$$Q = \begin{bmatrix} R1(1) & R1(2) & R1(3) & R1(4) \\ R2(1) & R2(2) & R2(3) & R2(4) \end{bmatrix}. \tag{A20}$$

Equation (A18) is a system of 4 linear equations in 4 unknowns and was solved using the lower and upper triangular decomposition of the 4×4 matrix. Coefficients A_i, B_i, C_i and D_i for other sections could be obtained by using equations (A16) and (A17).

APPENDIX B.

THE EFFECT OF DAMPING ON VIBRATION OF BEAM AT RESONANCE

When the lateral vibration of beam is studied by the Euler beam theory, the damping effect is not considered. However, damping is of great importance in limiting the amplitude of vibration at resonance. The effect of damping on vibration of beams at resonance will be studied in this appendix. Base excitation and concentrated force excitation will be considered.

B1. UNDER A BASE EXCITATION

Assume a uniform beam undergoes a known base motion b(t). The equation of motion of the beam, including the effects of damping can be written in terms of relative displacement w(x,t) as

$$EI\frac{\partial^4 w}{\partial x^4}+C\frac{\partial w}{\partial t}+\rho A\frac{\partial^2 w}{\partial t^2}=-\rho A\ddot{b}(t), \qquad (B1)$$

where E is Young's modulus, I is the moment of inertia, ρ is the mass density, A is the cross-sectional area of the beam and C is the effective viscous damping coefficient. Assume the base excitation is sinusoidal with one of the resonant frequencies of the beam, and can be written in a form as

$$b(t)=Be^{i\omega_i t} \quad , \qquad (B2)$$

where ω_i is the ith natural frequency of the beam.

It is reasonable to assume that the response w(x,t) is dominated by its ith mode and can be written as

$$w(x,t) = q_i(t)\phi_i(x), \tag{B3}$$

where $\phi_i(x)$ is the ith normal mode and satisfy the equation

$$EI\frac{\partial^4\phi}{\partial x^4} - \omega_i^2 \rho A \phi_i = 0. \tag{B4}$$

By substituting equations (B2) and (B3) into equation (B1) and using relation (B4), the equation of motion can be rendered similar to the equation of a single-degree-of-freedom system under a sinusoidal excitation as

$$\ddot{q}_i(t) + 2\zeta_i\omega_i\dot{q}_i(t) + \omega_i^2 q_i = \frac{\rho AB\omega_i^2}{M_i}\int_0^l \phi_i(x)dx e^{i\omega_i t}, \tag{B5}$$

where ζ_i is the equivalent damping ratio defined as

$$\zeta_i = \frac{C}{2\rho A\omega_i} \tag{B6}$$

and M_i is the generalized mass defined as

$$M_i = \int_0^l \rho A\phi_i^2(x)dx. \tag{B7}$$

The steady state solution $q_i(t)$ is also sinusoidal and with the same frequency as the excitation. It can be obtained by solving equation (B5) as

$$q_i(t) = \frac{\rho AB\omega_i^2}{2\zeta_i\omega_i^2 M_i i}\int_0^l \phi_i(x)dx e^{i\omega_i t}. \tag{B8}$$

The absolute motion y(x,t) of any point of the beam is obtained by adding the base motion b(t) to the relative motion w(x,t) as

$$y(x,t) = w(x,t) + b(t)$$

$$= \left(\frac{\rho A \omega_i^2 \phi_i(x) \int_0^l \phi_i(x) dx}{2\zeta_i \omega_i^2 M_i i} + 1 \right) B e^{i\omega_i t}. \qquad (B9)$$

The amplitude value at ω_i of the frequency response function $H_{b1}(\omega)$ of the beam system when the base motion is considered as the input and the displacement motion of the beam at an arbitrary location x_1 as the output then is

$$H_{b,1}(\omega_i) = \left| \frac{y(x_1,t)}{B} \right| = \left| \frac{\rho A \omega_i^2 \phi_i(x_1) \int_0^l \phi_i(x) dx + 2\zeta_i \omega_i^2 M_i i}{2\zeta_i \omega_i^2 M_i i} \right|. \qquad (B10)$$

The ζ_i usually is very small, so approximately

$$H_{b,1}(\omega_i) \cong \frac{\rho A \phi_i(x_1) \int_0^l \phi_i(x) dx}{2\zeta_i M_i}. \qquad (B11)$$

It can be seen from equations (B10) and (B11) that damping is the main factor to limiting the amplitude of vibration at resonance.

B2. UNDER THE EXCITATION OF A CONCENTRATED FORCE

Considered the same beam but under the excitation of a concentrated lateral force f(t) at location x_1 instead of a base location. The force is sinusoidal and with a frequency equal to the ith natural frequency ω_i of the beam. It take the form as

$$f(t) = F e^{i\omega_i t} \quad . \qquad (B12)$$

The equation of motion in this case is

$$EI \frac{\partial^4 y}{\partial x^4} + C \frac{\partial y}{\partial t} + \rho A \frac{\partial^2 y}{\partial t^2} = F e^{i\omega_i t} \delta(x - x_1), \qquad (B13)$$

where $\delta(x)$ represent a Dirac's delta function in space domain.

The y(x,t) is dominated by the ith mode and can be written as

$$y(x,t) = q_i(t)\phi_i(x). \tag{B 14}$$

The equation of motion in term of $q_i(t)$ becomes

$$\ddot{q}_i(t) + 2\zeta_i\omega_i\dot{q}_i(t) + \omega_i^2 q_i = \frac{F}{M_i}\int_0^l \phi_i(x)\delta(x - x_1)dx e^{i\omega_i t}$$

$$= \frac{F}{M_i}\phi_i(x_1)e^{i\omega_i t}. \tag{B 15}$$

The steady state solution of above equation take the form as

$$q_i(t) = \frac{F\phi_i(x_1)}{2\zeta_i\omega_i^2 M_i i}e^{i\omega_i t}. \tag{B 16}$$

The displacement at point x_2 is

$$y(x_2,t) = q_i(t)\phi_i(x_2) \tag{B 17}$$

and the frequency response function $H_{12}(\omega)$ with the concentrated lateral force at point x_1 as the input and the displacement motion of the beam at point x_2 as the output then is

$$H_{12}(\omega_i) = \left|\frac{y(x_2,t)}{f(t)}\right| = \frac{\phi_i(x_1)\phi_i(x_2)}{2\zeta_i\omega_i^2 M_i}. \tag{B 18}$$

APPENDIX C.

COMPUTER PROGRAMS

Ten computer programs and four subroutines used in these computer programs are listed here.

C1. Program IOSIMU

Program IOSIMU simulate the motion of an impact oscillator under a sinusoidal base excitation using an exact piecewise linear solution.

```
C
C     PROGRAM IOSIMU
C
C     A PROGRAM TO SIMULATE THE MOTION OF
C     AN IMPACT OSCILLATOR UNDER THE EXCITATION
C     OF A SINUSOIDAL BASE MOTION
C
      IMPLICIT REAL*8(A-H,O-Z)
      REAL*8 Y(2050)
      COMMON RR,CC,AA,DD,QQ,BB,D1,D2,OM,DDE1,DDE2,
     &IS,FO1,FO2,AF
C
C     FIRST PHASE OF THIS PROGRAM
C     CALCULATE THE CHANGE OVER CONDITIONS OF
C     THE PIECEWISE LINEAR SOLUTION
C
C     INPUT DATA FILE SYSPARA.DAT PROVIDE ALL NEEDED
C     SYSTEM PARAMETERS
C
C     IOOUT.DAT WILL BE USED TO STORE THE CHANGE OVER
C     CONDITIONS FOUND FOR EACH LINEAR REGION
C
C     AM = MASS OF THE IMPACT OSCILLATOR
C     C = DAMPING COEFFICIENT OF THE IMPACT OSCILLATOR
C     S1,S2 = STIFFNESS OF THE STOPS
C     D1,D2 = SIZE OF THE CLEARANCES
C     OM = FREQUENCY OF THE BASE EXCITATION
C     AF = AMPLITUDE OF THE BASE EXCITATION
C     TMAX = LENGTH OF TIME HISTORY
```

```
C     N = NUMBER OF SAMPLING POINTS
C
      OPEN (UNIT=1, FILE='SYSPARA.DAT', STATUS='OLD')
      OPEN (UNIT=2, FILE='IOOUT.DAT', STATUS='NEW')
      READ (1,*) AM,C,S0,S1,S2,D1,D2,OM,TMAX,N,AF
C
C     CALCULATE SOME CONSTANTS FOR ALL LINEAR REGIONS
C
      PAI=4.0D0*DATAN(1.0D0)
      PAI2=PAI*2.0D0
      OM=PAI2*OM
      DT=TMAX/N
      B=C/2.0/AM
      S0=S0/AM
      S1=S1/AM
      S2=S2/AM
      OM2=OM*OM
      AFF=AF
      AF=AF*OM2
      SS1=S0+S1
      SS2=S0+S2
      DDE1=-D1/SS1
      DE1=-S1*DDE1
      DDE1=S0*DDE1
      DDE2=D2/SS2
      DE2=S2*DDE2
      DDE2=S0*DDE2
      DD0=DSQRT(S0-B*B)
      DD1=DSQRT(SS1-B*B)
      DD2=DSQRT(SS2-B*B)
      FS0=DMAX1(OM,DD0)
      FS1=DMAX1(OM,DD1)
      FS2=DMAX1(OM,DD2)
      C0=DSQRT((S0-OM2)**2+4*B*B*OM2)
      C1=DSQRT((SS1-OM2)**2+4*B*B*OM2)
      C2=DSQRT((SS2-OM2)**2+4*B*B*OM2)
      DT0=0.1D0/FS0
      DT1=0.1D0/FS1
      DT2=0.1D0/FS2
      T=0.0D0
      IS=1
      IF(X.GT.-D1) IS=0
      IF(X.GT.D2) IS=2
      K=0
 4    FORMAT(1x,I3,1X,I2,4(1X,F17.10))
C
C     START SEARCH THE CHANGE OVER CONDITIONS FOR
C     EACH LINEAR REGION FROM A ZERO INITIAL CONDITION
C
      ISTOP=0
```

```
PHI=0.0
X=0.0
V=0.0
TOT=0.0
DO 11 K=1,1000
IT=1
IF(K.GT.400) TOT=TOT+T
IF(TOT.GT.TMAX) ISTOP=ISTOP+1
T=0.0D0
LIMIT=0
IF(IS.EQ.0) THEN
CC=C0
DD=DD0
SS=S0
DX=DT0
BB=B
FO1=X+D1
FO2=D2-X
F=DMIN1(FO1,FO2)
ELSE
IF(IS.EQ.1) THEN
CC=C1
DD=DD1
SS=SS1
DX=DT1
BB=B
X=X+DE1
F=DDE1-X
ELSE
CC=C2
DD=DD2
SS=SS2
DX=DT2
BB=B
X=X-DE2
F=X-DDE2
END IF
END IF
SI=SS-OM2
RR=PHI-DATAN(2*BB*OM/SI)
IF(SI.LT.0.0) RR=RR-PAI
XX=X-AF*DSIN(RR)/CC
VV=V-AF*OM*DCOS(RR)/CC
AA=DSQRT((VV+BB*XX)**2/(DD*DD)+XX*XX)
SI=VV+BB*XX
QQ=DATAN(XX*DD/SI)
IF(SI.LE.0.0) QQ=QQ+PAI
DO 10 IL=1,400
T=T+DX
F1=F
```

```
      IF(IT.EQ.1) XI=X
      CALL CALFUN(X,F,T)
      IF(IT.EQ.1) GOTO 14
      IF(F1*F.LT.0.0) THEN
C
C     FIND CHANGE OVER CONDITIONS WITH
C     AN ERROR OF 1.0D-13
C
 13   IF(DABS(F).LT.1.0D-13) GOTO 12
      T=T-DX
 15   DX2=DX
      F2=F
      DX=DABS(F1)/(DABS(F1)+DABS(F))*DX
      LIMIT=LIMIT+1
      IF(LIMIT.GE.350) GOTO 122
      T=T+DX
      CALL CALFUN(X,F,T)
      IF(F1*F.LT.0.0) GOTO 13
      IF(DABS(F).LT.1.D-13) GOTO 12
      F1=F
      F=F2
      DX=DX2-DX
      GOTO 15
      ELSE
      END IF
      GOTO 17
 14   XII=XI
      XI=X-XI
      IF(XI*V.LT.0.0) THEN
      F=F1
      T=T-DX
      DX=DX/2.0D0
      X=XII
      GOTO 10
      ELSE
      IF(IS.GT.0.1) GOTO 17
      IF(((XII.LT.0.0).AND.(X.GE.D2)).OR.
     &((XII.GT.0.0).AND.(X.LE.-D1))) THEN
      F=F1
      T=T-DX
      DX=DX/2.0D0
      X=XII
      GOTO 10
      ELSE
      END IF
      END IF
 17   IT=IT+1
 10   CONTINUE
C
C     CALCULATE THE VELOCITY OF CHANGE OVER
```

```
C
 12   EE=AA*DEXP(-BB*T)
      V=AF*OM*DCOS(OM*T+RR)/CC-BB*EE*DSIN(DD*T+QQ)
     &+EE*DD*DCOS(DD*T+QQ)
      PHI=PHI+T*OM
      PP=PHI/PAI2
      PHI=PHI-IFIX(SNGL(PP))*PAI2
C
C     AFTER 400 TIMES CHANGE STATUS, WRITE
C     THE CHANGE OVER CONDITIONS INTO FILE IOOUT.DAT
C
      IF(IS.EQ.0) THEN
      IF(X*V.LT.0.0) GOTO 138
      IF(F.EQ.FO1) IS=1
      IF(F.EQ.FO2) IS=2
      IF(K.GT.400) WRITE(2,4) K,IS,X,V,PHI,T
      ELSE
      IF(IS.EQ.1) X=X-DE1
      IF(IS.EQ.2) X=X+DE2
      IS=0
      IF(K.GT.400) WRITE(2,4) K,IS,X,V,PHI,T
      IF(X*V.GT.0.0) GOTO 138
      END IF
      IF(ISTOP.EQ.4) GO TO 199
 11   CONTINUE
      TOT=TOT+T
 199  WRITE(2,*) 'TOTAL TIME =',TOT
      GOTO 122
 138  WRITE(6,*) 'ERROR, CHECK A AND V.'
 122  CLOSE (UNIT=1, STATUS='KEEP')
      CLOSE (UNIT=2, STATUS='KEEP')
C
C     SECOND PHASE OF THIS PROGRAM
C     GENERATE A PIECE OF STEADY STATE RESPONSE
C     USING THE CHANGE OVER CONDITIONS OBTAINED
C     IN THE FIRST PHASE OF THIS PROGRAM
C
C     FILE IOTHOUT.DAT IS USED TO STORE THE RESULTING
C     TIME HISTORY RESPONSE TOGETHER WITH THE KNOWN
C     BASE EXCITATION
C
      OPEN (UNIT=3, FILE='IOOUT.DAT', STATUS='OLD')
      OPEN (UNIT=2, FILE='IOTHOUT.DAT', STATUS='NEW')
      TT=0.0D0
      TOT=0.0D0
      I=0
C
C     READ THE FIRST GROUP OF CHANGE OVER CONDITIONS
C
      READ(3,4) K,IS,X,V,PHI,T
```

```
      PHII=PHI
 37   IF(IS.EQ.0) THEN
      CC=C0
      DD=DD0
      ISS=0
      SS=S0
      ELSE
      IF(IS.EQ.1) THEN
      CC=C1
      DD=DD1
      SS=SS1
      ISS=1
      X=X+DE1
      ELSE
      CC=C2
      DD=DD2
      SS=SS2
      ISS=2
      X=X-DE2
      END IF
      END IF
      SI=SS-OM2
      IF(DABS(SI).LT.1.0D-20) THEN
      RR=PHI-PAI/2.0
      ELSE
      RR=PHI-DATAN(2*B*OM/SI)
      END IF
      IF(SI.LT.0.0) RR=RR-PAI
      XX=X-AF*DSIN(RR)/CC
      VV=V-AF*OM*DCOS(RR)/CC
      AA=DSQRT((VV+B*XX)**2/(DD*DD)+XX*XX)
      SI=VV+B*XX
      QQ=DATAN(XX*DD/SI)
      IF(SI.LE.0.0) QQ=QQ+PAI
C
C     READ THE NEXT GROUP OF CHANGE OVER CONDITIONS
C
      READ(3,4) K,IS,X,V,PHI,T
 49   TT=TT+DT
      IF(TT.GE.T) THEN
      TOT=TOT+T
      TT=TT-T-DT
      GOTO 37
      ELSE
      END IF
      I=I+1
      IF(I.GT.N) GOTO 222
C
C     CALCULATE THE DISPLACEMENT WITHIN EACH LINEAR REGION
C
```

```
      Y(I)=AF*DSIN(OM*TT+RR)/CC+AA*DEXP(-B*TT)*DSIN(DD*TT+QQ)
      IF(ISS.EQ.1) Y(I)=Y(I)-DE1
      IF(ISS.EQ.2) Y(I)=Y(I)+DE2
      GOTO 49
 222  TE=0.0
      DO 55 I=1,N
      TE=TE+DT
      BT=AFF*SIN(OM*TE+PHII)
C
C     WRITE BASE DISPLACEMENT AND MASS DISPLACEMENT
C     INTO FILE IOTHOUT.DAT
C
 55   WRITE(2,*) BT,Y(I)
      CLOSE (UNIT=1, STATUS='KEEP')
      CLOSE (UNIT=3, STATUS='DELETE')
      CLOSE (UNIT=2, STATUS='KEEP')
      STOP
      END
C
C     A SUBROUTINE TO FIND THE DISPLACEMENT AND
C     THE DIFFERENCE BETWEEN THE DISPLACEMENT
C     AND THE CLEARANCE
C
      SUBROUTINE CALFUN(X,F,T)
      IMPLICIT REAL*8(A-H,O-Z)
      COMMON RR,CC,AA,DD,QQ,BB,D1,D2,OM,DDE1,DDE2,
     &IS,FO1,FO2,AF
      X=AF*DSIN(OM*T+RR)/CC+AA*DEXP(-BB*T)*DSIN(DD*T+QQ)
      IF(IS.EQ.0) THEN
      FO1=X+D1
      FO2=D2-X
      F=DMIN1(FO1,FO2)
      ELSE
      IF(IS.EQ.1) F=DDE1-X
      IF(IS.EQ.2) F=X-DDE2
      END IF
      RETURN
      END
```

C2. Program DFA

Program DFA estimate the clearances based on the simulated vibroimpact response generated by Program IOSIMU or measured response from mechanical experiments using the describing function approach.

```
C
C     PROGRAM DFA
C
C     A PROGRAM TO ESTIMATE CLEARANCES OF AN IMPACT
C     OSCILLATOR BY THE DESCRIBING FUNCTION APPROACH
C
      DIMENSION X1(2050,2),X2(2050,2),IG(11),Y1(2050),Y2(2050),L(2050,2)
      DIMENSION D(2),ED(2)
      COMMON PAI,TN0,TN1,S1,S2
C
C     INPUT FILE SYSPARA.DAT PROVIDE ALL NEEDED
C     SYSTEM PARAMETERS
C
C     INPUT FILE IOTH.DAT PROVIDES THE EXCITATION B(T)
C     AND RESPONSE Y(T)
C
C     DFA.DAT IS USED TO STORE RESULTS OF
C     ESTIMATION BY THE DESCRIBING FUNCTION APPROACH
C
C     AM = MASS OF THE IMPACT OSCILLATOR
C     C = DAMPING COEFFICIENT OF THE IMPACT OSCILLATOR
C     S0 = STIFFNESS OF THE MAIN SPRING
C     S1,S2 = STIFFNESS OF THE STOPS
C     D1,D2 = SIZE OF THE CLEARANCES
C     OM = FREQUENCY OF THE BASE EXCITATION
C     T = LENGTH OF TIME HISTORY
C     N = NUMBER OF SAMPLING POINTS
C     CO1,CO2 = COEFFICIENTS TO CALIBRATE SIGNALS
C           OBTAINED FROM MECHANICAL EXPERIMENTS
C
      OPEN (UNIT=1, FILE='SYSPARA.DAT', STATUS='OLD')
      OPEN (UNIT=2, FILE='IOTH.DAT', STATUS='OLD')
      OPEN (UNIT=4, FILE='DFA.DAT', STATUS='NEW')
      READ (1,*) AM,C,S0,S1,S2,D1,D2,OM,T,N,CO1,CO2
      WRITE(4,*) 'SYSTEM PARAMETERS'
      WRITE(4,*) 'MASS=',AM,'KG'
      WRITE(4,*) 'MAIN SPRING COEFFECIENT=',S0,'N/M'
      WRITE(4,*) 'STOP 1 SPRING COEFFECIENT=',S1,'N/M'
      WRITE(4,*) 'STOP 2 SPRING COEFFECIENT=',S2,'N/M'
      WRITE(4,*) 'DAMPING COEFFECIENT=',C,'N*S/M'
      WRITE(4,*) 'CLEARANCE 1 =',D1,'M'
```

```
      WRITE(4,*) 'CLEARANCE 2 =',D2,'M'
      WRITE(4,*) 'SAMPLING RATE=',N/T,'1/S'
      WRITE(4,*) 'LENGTH OF RECORD=',T,'S'
      WRITE(4,*) 'BASE EXCITATION FREQUENCY=',OM,'1/S'
      WRITE(4,*) 'BASE EXCITATION AMPLITUDE=',AF,'M'
      IPA=LOG(FLOAT(N))/LOG(2.0)+.001
      NN=N+1
      B=C/2.0
      CALL MAIN (AM,S0,B,D1,D2,OM,IPA,T,N,NN,X1,X2,IG,
     &Y1,Y2,L,CO1,CO2)
      STOP
      END
      SUBROUTINE MAIN (AM,S0,B,D1,D2,OM,IPA,T,N,NN,X1,X2,
     &IG,Y1,Y2,L,CO1,CO2)
      DIMENSION X1(NN,2),X2(NN,2),IG(IPA),Y1(NN),Y2(NN)
     &,L(NN,2)
      DIMENSION D(2),ED(2)
      COMMON PAI,TN0,TN1,S1,S2
      PAI=4.0*ATAN(1.0)
      XNI=OM*T+1.5
      OM=OM*2.0*PAI
      NI=IFIX(XNI)
      N2=N/2
      DT=T/N
      DT2=DT/2.0
      DF=1.0/T
      DFA=DF*2.0*PAI
      FE=-DFA
      N21=N2+1
C
C     READ IN THE EXCITATION B(T) AND
C     RESPONSE Y(T)
C
      DO 5 I=1,N
  5   READ (2,*) X1(I,1),X1(I,2)
      DO 10 I=1,N
C
C     THE FOLLOWING TWO COMMENTED LINES ARE NEEDED
C     TO CALIBRATE THE SIGNALS OBTAINED FROM
C     MECHANICAL EXPERIMENTS
C
C     X1(I,1)=X1(I,1)/CO1
C     X1(I,2)=X1(I,2)/CO2
      X2(I,1)=0.0
 10   X2(I,2)=0.0
      ISIGN=-1
      NUM=1
C
C     FOURIER TRANSFORMING BOTH EXCITATION AND RESPONSE
C
```

```
      CALL FFT (IPA,X1,X2,N,NN,Y1,Y2,ISIGN,NUM,IG,L,K1,K2)
C
C     THE FOLLOWING COMMENDED LINES ARE NEEDED FOR
C     SAMPLED DATA FROM MECHANICAL EXPERIMENTS
C     WHERE THE X(T) IS SHIFTED DT/2.
C
C     DO 30 I=1,N21
C     FE=FE+DFA
C     TH=-FE*DT2
C     HI=SIN(TH)
C     HR=COS(TH)
C     IN=N-I+2
C     RR=X1(I,K2)*HR-X2(I,K2)*HI
C     RI=X1(I,K2)*HI+X2(I,K2)*HR
C     X1(I,2)=RR
C     X2(I,2)=RI
C     X1(IN,2)=X1(I,2)
C 30  X2(IN,2)=-X2(I,2)
C     X2(N21,2)=-X2(N21,2)
C
C     THE RESPONSE MEASURED FROM THE MECHANICAL
C     EXPERIMENTS ARE ABSOLUTE DISPLACEMENT X(T)
C     SO THE FOLLOWING THREE COMMENTED LINES ARE NEEDED
C     TO FIND THE RELATIVE DISPLACEMENT Y(T)
C
C     DO 35 I=1,N
C     X1(I,1)=X1(I,2)-Y1(I)
C 35  X2(I,1)=X2(I,2)-Y2(I)
      H0=S0
      AMOM=AM*OM*OM
      HR=S0-AMOM
      WRITE(4,*) 'RESULTS OF DESCRIBING FUNCTION METHOD'
      WRITE(4,*) 'B0RE=',Y1(1)/N,'B0IM=',Y2(1)/N
      WRITE(4,*) 'B1RE=',Y1(NI)/N2,'B1IM=',Y2(NI)/N2
      WRITE(4,*) 'YORE=',X1(1,1)/N,'Y0IM=',X2(1,1)/N
      WRITE(4,*) 'Y1RE=',X1(NI,1)/N2,'Y1IM=',X2(NI,1)/N2
      Y1A=X1(NI,1)*X1(NI,1)+X2(NI,1)*X2(NI,1)
      Y1AS=SQRT(Y1A)
      Y0=X1(1,1)/2.0
C
C     CALCULATE THE DESCRIBING FUNCTION VALUES
C
      TN0=-Y0*H0/Y1AS
      TN1=AMOM*(Y1(NI)*X1(NI,1)+Y2(NI)*X2(NI,1))/Y1A-HR
      WRITE(4,*) 'N00=',TN0,'N01=',TN1
      TN0=2.0*PAI*TN0
      TN1=PAI*(S1+S2)/2.0-PAI*TN1
C
C     SEARCH FOR THETA1 AND THETA2
C
```

```
      D(1)=1.5
      D(2)=1.5
      CALL POWELL(D,ED,FY,2,5000,ICOVG,0.0001,0.0001,1)
      WRITE(4,1)ED,FY,ICOVG
C
C     CALCULATE THE ESTIMATED VALUES OF CLEARANCES
C
      ED(1)=(Y1AS*SIN(ED(1))-Y0)/N2
      ED(2)=(Y1AS*SIN(ED(2))+Y0)/N2
      WRITE(4,*) 'ESTIMATED VALUES OF CLEARANCES'
      WRITE(4,2)ED
      ER1=ABS(D1-ED(1))/D1
      ER2=ABS(D2-ED(2))/D2
      WRITE(4,*) 'RELATIVE ERROR OF ESTIMATION'
    1 FORMAT(5X,3E21.10,2X,I5//)
    2 FORMAT(5X,3E21.10/)
   70 CLOSE (UNIT=1, STATUS='KEEP')
      CLOSE (UNIT=2, STATUS='KEEP')
      CLOSE (UNIT=4, STATUS='KEEP')
      RETURN
      END
C
C     A SUBROUTINE TO GENERATE AN OBJECTIVE FUNCTION
C     USED IN THE SUBROUTINE POWELL WHERE ROOTS
C     OF NONLINEAR EQUATIONS ARE FOUND BY SEARCHING
C     THE MINIMUM OT THE OBJECTIVE FUNCTION
C
      SUBROUTINE OBF(X,FX)
      DIMENSION X(2)
      COMMON PAI,TN0,TN1,S1,S2
      SZ1=SIN(X(2))
      CZ1=COS(X(2))
      SZ2=SIN(X(1))
      CZ2=COS(X(1))
      Z1=ATAN(SZ1/CZ1)
      Z2=ATAN(SZ2/CZ2)
      PAI2=2.*PAI
      FX=(S2*(-SZ1*(PAI-2.0*Z1)+2.0*CZ1)+S1*(SZ2*
     &(PAI-2.0*Z2)-2.*CZ2)-TN0)**2
      FX=FX+(S2*(Z1+SZ1*CZ1)+S1*(Z2+SZ2*CZ2)-TN1)**2
      RETURN
      END
```

C3. Program OPA

Program OPA estimate the clearances and impact forces based on the simulated vibroimpact response generated by Program IOSIMU or measured response from mechanical experiments using the optimization approach.

```
C
C     PROGRAM OPA
C
C     A PROGRAM TO ESTIMATE CLEARANCES OF AN IMPACT
C     OSCILLATOR BY THE OPTIMIZATION APPROACH
C
      DIMENSION BYU(2048,8)
      DIMENSION X1(2050,2),X2(2050,2),IG(11),Y1(2050),
     &Y2(2050),L(2050,2)
      DIMENSION D(3),ED(3)
      COMMON /P/PAI /O/S0,S1,S2,N21,YMIN,YMAX
C
C     INPUT FILE SYSPARA.DAT PROVIDE ALL NEEDED
C     SYSTEM PARAMETERS
C
C     INPUT FILE IOTH.DAT PROVIDES THE EXCITATION B(T)
C     AND RESPONSE Y(T)
C
C     BYU.DAT IS USED TO STORE TIME HISTORIES OF
C     B(T), Y(T), U(T) AND UHAT(T)
C
C     BYUF.DAT IS USED TO STORE SPECTRA
C     B(F), Y(F), U(F) AND UHAT(F)
C
C     OPA.DAT IS USED TO STORE RESULTS OF
C     ESTIMATION BY THE OPTIMIZATION APPROACH
C
C     AM = MASS OF THE IMPACT OSCILLATOR
C     C = DAMPING COEFFICIENT OF THE IMPACT OSCILLATOR
C     S0 = STIFFNESS OF THE MAIN SPRING
C     S1,S2 = STIFFNESS OF THE STOPS
C     D1,D2 = SIZE OF THE CLEARANCES
C     OM = FREQUENCY OF THE BASE EXCITATION
C     T = LENGTH OF TIME HISTORY
C     N = NUMBER OF SAMPLING POINTS
C     CO1,CO2 = COEFFICIENTS TO CALIBRATE SIGNALS
C          OBTAINED FROM MECHANICAL EXPERIMENTS
C
      OPEN (UNIT=1, FILE='SYSPARA.DAT', STATUS='OLD')
      OPEN (UNIT=2, FILE='IOTH.DAT', STATUS='OLD')
      OPEN (UNIT=3, FILE='BYU.DAT', STATUS='NEW')
```

```
      OPEN (UNIT=8, FILE='BYUF.DAT', STATUS='NEW')
      OPEN (UNIT=4, FILE='OPA.DAT', STATUS='NEW')
      READ (1,*) AM,C,S0,S1,S2,D1,D2,OM,T,N,CO1,CO2
      IPA=LOG(FLOAT(N))/LOG(2.0)+.001
      NN=N+1
      B=C/2.0
      CALL MAIN (AM,B,D1,D2,OM,IPA,T,N,NN,X1,X2,
     &IG,Y1,Y2,L,CO1,CO2,BYU)
      STOP
      END
      SUBROUTINE MAIN (AM,B,D1,D2,OM,IPA,T,N,NN,X1,X2,
     &IG,Y1,Y2,L,CO1,CO2,BYU)
      DIMENSION BYU(N,8)
      DIMENSION X1(NN,2),X2(NN,2),IG(IPA),Y1(NN),
     &Y2(NN),L(NN,2)
      DIMENSION D(3),ED(3)
      COMMON /P/PAI /O/S0,S1,S2,N21,YMIN,YMAX
      PAI=4.0*ATAN(1.0)
      OM=OM*2.0*PAI
      N2=N/2
      DT=T/N
      DT2=DT/2.0
      DF=1.0/T
      DFA=DF*2.0*PAI
      FE=-DFA
      N21=N2+1
C
C     READ IN THE EXCITATION B(T) AND
C     RESPONSE Y(T)
C
      DO 5 I=1,N
  5   READ (2,*) X1(I,1),X1(I,2)
      DO 10 I=1,N
C
C     THE FOLLOWING TWO COMMENTED LINES ARE NEEDED
C     TO CALIBRATE THE SIGNALS OBTAINED FROM
C     MECHANICAL EXPERIMENTS
C
C     X1(I,2)=X1(I,2)/CO2
C     X1(I,1)=X1(I,1)/CO1
      BYU(I,1)=X1(I,1)*1000.0
      X2(I,1)=0.0
 10   X2(I,2)=0.0
      ISIGN=-1
      NUM=1
C
C     FOURIER TRANSFORMING BOTH B(T) AND Y(T)
C
      CALL FFT (IPA,X1,X2,N,NN,Y1,Y2,ISIGN,NUM,IG,L,K1,K2)
C
```

```
C     THE FOLLOWING COMMENDED LINES ARE NEEDED FOR
C     SAMPLED DATA FROM MECHANICAL EXPERIMENTS
C     WHERE THE X(T) IS SHIFTED DT/2.
C
C     DO 30 I=1,N21
C     FE=FE+DFA
C     TH=-FE*DT2
C     HI=SIN(TH)
C     HR=COS(TH)
C     IN=N-I+2
C     RR=X1(I,K2)*HR-X2(I,K2)*HI
C     RI=X1(I,K2)*HI+X2(I,K2)*HR
C     X1(I,2)=RR
C     X2(I,2)=RI
C     X1(IN,2)=X1(I,2)
C 30  X2(IN,2)=-X2(I,2)
C     X2(N21,2)=-X2(N21,2)
C
C     THE RESPONSE MEASURED FROM THE MECHANICAL
C     EXPERIMENTS ARE ABSOLUTE DISPLACEMENT X(T)
C     SO THE FOLLOWING THREE COMMENTED LINES ARE NEEDED
C     TO FIND THE RELATIVE DISPLACEMENT Y(T)
C
C     DO 35 I=1,N
C     X1(I,1)=X1(I,2)-Y1(I)
C 35  X2(I,1)=X2(I,2)-Y2(I)
      DO 401 I=1,N21
      BYU(I,5)=SQRT((Y1(I)*Y1(I)+Y2(I)*Y2(I)))/N2*1000.0
 401  BYU(I,6)=SQRT((X1(I,1)*X1(I,1)+X2(I,1)*X2(I,1)))/
     &N2*1000.0
C
C     CALCULATE TRANSFORMED IMPACT FORCE U(F)
C
      FE=-DFA
      DO 33 I=1,N21
      FE=FE+DFA
      FE2=FE*FE*AM
      HI=2.0*B*FE
      HR=S0-FE*FE*AM
      IN=N-I+2
      RR=FE2*Y1(I)-X1(I,1)*HR+X2(I,1)*HI
      RI=FE2*Y2(I)-X1(I,1)*HI-X2(I,1)*HR
      X1(I,2)=RR
      X2(I,2)=RI
      X1(IN,2)=X1(I,2)
 33   X2(IN,2)=-X2(I,2)
      X2(N21,2)=-X2(N21,2)
      DO 402 I=1,N21
 402  BYU(I,7)=SQRT((X1(I,2)*X1(I,2)+X2(I,2)*X2(I,2)))/N2
      NUM=1
```

```
      ISIGN=1
C
C     FIND U(T) BY INVERSE FOURIER TRANSFORMATION
C
      CALL FFT (IPA,X1,X2,N,NN,Y1,Y2,ISIGN,NUM,IG,L,K1,K2)
      DO 25 I=1,N
      BYU(I,2)=Y1(I)*1000.0
      Y2(I)=Y1(I)
 25   CONTINUE
C
C     FIND THE MAXIMUM AND MINIMUM OF Y(T)
C
      YMIN=0.0
      YMAX=0.0
      DO 37 I=1,N
      IF(Y2(I).LT.YMIN) YMIN=Y2(I)
      IF(Y2(I).GT.YMAX) YMAX=Y2(I)
 37   CONTINUE
      DO 365 I=1,N
 365  Y1(I)=X1(I,K2)
      D(1)=0.0
      D(2)=0.0
      D(3)=0.0
C
C     USE POWELL METHOD THE SEARCH THE MINIMUM
C     OF OBJECTIVE FUNCTION J
C
      CALL POWELL(D,ED,FY,3,5000,ICOVG,0.0001,0.0001,
     &1,NN,Y2,Y1)
C
C     CALCULATE THE OPTIMALLY ESTIMATED
C     IMPACT FORCES UHAT(T)
C
      EU=S0*D(3)
      DO 367 I=1,N
 367  BYU(I,3)=Y1(I)-EU
      DO 901 I=1,N
      YY2=Y2(I)+D(3)
      IF(YY2.LE.-D(1)) UT=S1*(YY2+D(1))
      IF((YY2.GT.-D(1)).AND.(YY2.LT.D(2))) UT=0.0
      IF(YY2.GE.D(2)) UT=S2*(YY2-D(2))
      X1(I,1)=UT
      X2(I,1)=0.0
 901  BYU(I,4)=UT
      NUM=0
      ISIGN=-1
      CALL FFT (IPA,X1,X2,N,NN,Y1,Y2,ISIGN,NUM,IG,L,K1,K2)
      DO 403 I=1,N21
 403  BYU(I,8)=SQRT((X1(I,K2)*X1(I,K2)+X2(I,K2)*
     &X2(I,K2)))/N2
```

```
      WRITE(4,*) 'RESULTS OF OPTIMAL METHODS'
      WRITE(4,1)ED,FY,ICOVG
      WRITE(4,*) 'ESTIMATED VALUES OF CLEARANCES'
      WRITE(4,2)ED
      ER1=ABS(D1-ED(1))/D1
      ER2=ABS(D2-ED(2))/D2
      WRITE(4,*) 'RELATIVE ERROR OF ESTIMATION'
      WRITE(4,2)ER1,ER2
      DO 404 I=1,N
  404 WRITE(3,3) (BYU(I,J),J=1,4)
      DO 406 I=1,N21
  406 WRITE(8,3) (BYU(I,J),J=5,8)
    1 FORMAT(5X,4E21.10,2X,I5//)
    2 FORMAT(5X,3E21.10/)
    3 FORMAT(1X,4(1X,E15.7))
   70 CLOSE (UNIT=1, STATUS='KEEP')
      CLOSE (UNIT=2, STATUS='KEEP')
      CLOSE (UNIT=3, STATUS='KEEP')
      CLOSE (UNIT=4, STATUS='KEEP')
      CLOSE (UNIT=8, STATUS='KEEP')
      RETURN
      END
C
C     A SUBROUTINE TO CALCULATE THE OBJECTIVE
C     FUNCTION J
C
C     SUBROUTINE OBF(X,FX,NN,Y2,Y1)
      COMMON /P/PAI /O/S0,S1,S2,N21,YMIN,YMAX
      DIMENSION X(3),Y2(NN),Y1(NN)
      SUM=0.0
      N=NN-1
      N1=N/16
      N2=N-N1
      DO 10 I=N1,N2
      EU=X(3)*S0
      YY2=Y2(I)+X(3)
      IF(YY2.LE.-X(1)) T=Y1(I)-EU-S1*(YY2+X(1))
      IF((YY2.GT.-X(1)).AND.(YY2.LT.X(2))) T=Y1(I)-EU
      IF(YY2.GE.X(2)) T=Y1(I)-EU-S2*(YY2-X(2))
   10 SUM=SUM+T*T
      FX=SUM/(N2-N1)
      YMIN1=YMIN+X(3)
      YMAX1=YMAX+X(3)
      IF(-X(1).LT.YMIN1) FX=FX+(S1*(YMIN1+X(1)))**2
      IF(X(2).GT.YMAX1) FX=FX+(S2*(YMAX1-X(2)))**2
      RETURN
      END
```

C4. Program SPASIMU

Program SPASIMU first simulate the response of an impact oscillator under a random excitation by solving the nonlinear equation of motion using the fourth-order Runge-Kutta method, and then use this response to estimate clearances by the spectrum analysis approach.

```
C
C     PROGRAM SPASIMU
C
C     A PROGRAM TO SIMULATE THE MOTION OF
C     AN IMPACT OSCILLATOR UNDER A RANDOM EXCITATION
C     AND THEN USING THE RESPONSE TO ESTIMATE
C     THE CLEARANCES BY THE SPECTRUM ANALYSIS APPROACH
C
      IMPLICIT REAL*8(A-H,O-Z)
      DIMENSION X1(2048,2),X2(2048,2),IG(11),Y1(2048),
     &Y2(2048),L(2048,2)
      DIMENSION A(2048),B(2,2048)
      COMMON/DD/ D(2),ED(2)
      COMMON PAI,EW0,EW1,AM,C,S0,S1,S2,D1,D2,EV,EM
C
C     INPUT FILE RANEX.DAT PROVIDE ALL NEEDED
C     SYSTEM PARAMETERS
C
C     REXREZ.DAT IS USED TO STORE RESULTS OF
C     ESTIMATION BY THE SPECTRUM ANALYSIS APPROACH
C
C     TI.DAT IS USED TO STORE TYPICAL SAMPLE OF
C     EXCITATION AND RESPONSE
C
C     SP.DAT IS USED TO STORE THE POWER AND CROSS SPECTRUM
C
C     AM = MASS OF THE IMPACT OSCILLATOR
C     C = DAMPING COEFFICIENT OF THE IMPACT OSCILLATOR
C     S0 = STIFFNESS OF THE MAIN SPRING
C     S1,S2 = STIFFNESS OF THE STOPS
C     D1,D2 = SIZE OF THE CLEARANCES
C     FA = STANDARD DERIVATION OF RANDOM EXCITATION
C     TMAX = LENGTH OF A PIECE OF TIME HISTORY SAMPLE
C     M = NUMBER OF SAMPLE RECORDS
C     N = NUMBER OF SAMPLING POINTS
C
      OPEN (UNIT=2, FILE='RANEX.DAT', STATUS='OLD')
      OPEN (UNIT=1, FILE='REXREZ.DAT', STATUS='NEW')
      OPEN (UNIT=3, FILE='TI.DAT', STATUS='NEW')
```

```
      OPEN (UNIT=8, FILE='SP.DAT', STATUS='NEW')
      READ (2,*) AM,M,N,C,S0,S1,S2,D1,D2,FA,TMAX
      WRITE(1,*) 'NUMBER OF SAMPLE =',M
      WRITE(1,*) 'POINT OF EACH SAMPLE =',N
      WRITE(1,*) 'SPRING COEFFICIENTS =',S1,S2
      WRITE(1,*) 'CLEARANCES =',D1,D2
      WRITE(1,*) 'AMPLITUDE OF INPUT =',FA
      IPA=LOG(FLOAT(N))/LOG(2.0)+.001
      N=2**IPA
      WRITE(1,*) 'N =',N
      CALL MAIN (IPA,X1,X2,N,M,Y1,Y2,IG,L,A,B,FA,TMAX)
      STOP
      END
      SUBROUTINE MAIN (IPA,X1,X2,N,M,Y1,Y2,IG,L,A,B,FA,TMAX)
      IMPLICIT REAL*8(A-H,O-Z)
      DIMENSION X1(N,2),X2(N,2),IG(IPA),Y1(N),Y2(N),L(N,2)
      DIMENSION A(N),B(2,N)
      COMMON/DD/ D(2),ED(2)
      COMMON PAI,EW0,EW1,AM,C,S0,S1,S2,D1,D2,EV,EM
      PAI=4.0D0*DATAN(1.0D0)
      IX=0
      SIGN=-1.
      MN=M*N
      NUM=1
      N2=N/2.0
      DF=1.0/TMAX
      DFA=DF*2.0*PAI
      DT=TMAX/N
      N21=N2+1
      N1=N-1
      DO 11 I=1,N
      A(I)=0.0
      B(1,I)=0.0
11    B(2,I)=0.0
      EM=0.0
      EV=0.0
      EMU=0.0
      DO 50 J=1,M
      FE=-DFA
      YI=0.0
      VI=0.0
      EM=EM+YI
      EV=EV+YI*YI
      X1(1,2)=YI
      Y1(1)=VI
C
C     GENERATE RANDOM EXCITATION G(T)
C
      DO 5 II=1,N
      X2(II,2)=0.0
```

```
      CALL RANDS2(IX,YEL,FA,0.0,RA)
      X1(II,1)=RA
 5    X2(II,1)=RA
C
C     CALCULATE THE RESPONSE USING THE 4TH-ORDER
C     RUNGE-KUTTA METHOD
C
      DO 10 III=1,N1
      AK1=Y1(III)
      AL1=FG(X1(III,2),Y1(III),X1(III,1))
      AK2=Y1(III)+AL1*DT/2.0
      P2=X1(III,2)+DT*AK1/2.0
      P3=Y1(III)+DT*AL1/2.0
      AL2=FG(P2,P3,X2(III,1))
      AK3=Y1(III)+AL2*DT/2.0
      P2=X1(III,2)+DT*AK2/2.0
      P3=Y1(III)+DT*AL2/2.0
      AL3=FG(P2,P3,X2(III,1))
      AK4=Y1(III)+AL3*DT
      P2=X1(III,2)+DT*AK3
      P3=Y1(III)+DT*AL3
      I1=III+1
      AL4=FG(P2,P3,X1(I1,1))
      X1(I1,2)=X1(III,2)+(AK1+2.0*AK2+2.0*AK3+AK4)*DT/6.0
      Y1(I1)=Y1(III)+(AL1+2.0*AL2+2.0*AL3+AL4)*DT/6.0
      EM=EM+X1(I1,2)
      EV=EV+X1(I1,2)*X1(I1,2)
      X2(III,1)=0.0
 10   CONTINUE
      X2(N,1)=0.0
      IF(J.GE.2) GOTO 17
C
C     WRITE TYPICAL EXCITATION AND RESPONSE TO
C     FILE TI.DAT
C
      DO 38 I=1,N
 38   WRITE(3,3) X1(I,1),X1(I,2)*1000.0
 17   SIGN=-1.
      NUM=1
C
C     FOURIER TRANSFORMING EXCITATION G(T)
C     AND RESPONSE Y(T)
C
      CALL FFT (IPA,X1,X2,N,Y1,Y2,SIGN,NUM,IG,L,K1,K2)
C
C     CALCULATE THE TRANSFORMED IMPACT FORCE U(F)
C
      DO 30 IV=1,N21
      FE=FE+DFA
      HI=C*FE
```

```
      FE2=FE*FE*AM
      HR=S0-FE2
      RR=Y1(IV)-X1(IV,K2)*HR+X2(IV,K2)*HI
      RI=Y2(IV)-X1(IV,K2)*HI-X2(IV,K2)*HR
      Y1(IV)=RR
30    Y2(IV)=RI
      DO 35 IW=2,N2
      IN=N-IW+2
      Y1(IN)=Y1(IW)
35    Y2(IN)=-Y2(IW)
      EMU=EMU+Y1(1)
      DO 33 IZ=1,N
      BR=Y1(IZ)*X1(IZ,K2)+Y2(IZ)*X2(IZ,K2)
      BI=Y1(IZ)*X2(IZ,K2)-Y2(IZ)*X1(IZ,K2)
      B(1,IZ)=B(1,IZ)+BR
      B(2,IZ)=B(2,IZ)+BI
      AA=X1(IZ,K2)*X1(IZ,K2)+X2(IZ,K2)*X2(IZ,K2)
33    A(IZ)=A(IZ)+AA
50    CONTINUE
      EM=EM/MN
      EMU=EMU/MN
      EV=(EV-MN*EM*EM)/(MN-1)
      EV=SQRT(EV)
      WRITE(1,*) 'ESTIMATE OF MEAN VALUE OF Y =',EM
      WRITE(1,*) 'ESTIMATE OF MEAN VALUE OF U =',EMU
      WRITE(1,*) 'ESTIMATE OF VARIANCE=',EV
      DN1R=(D1+EM)/(1.414213562*EV)
      DN2R=(D2-EM)/(1.414213562*EV)
      DN1=DN1R*DN1R
      DN2=DN2R*DN2R
      EPS=1.0E-8
      WRITE(1,*) 'DN1R=',DN1R,'DN2R=',DN2R
      ERFC1=1.0-ER(DN1R,EPS)
      ERFC2=1.0-ER(DN2R,EPS)
      WRITE(1,*) 'ER1=',1.0-ERFC1
      WRITE(1,*) 'ERFC1=',ERFC1
      WRITE(1,*) 'ERFC2=',ERFC2
C
C     CALCULATE W0 AND W1 USING ACTUAL CLEARANCES
C     THIS IS NOT NEEDED FOR ESTIMATION PURPOSE
C     ONLY FOR STUDY PURPOSE
C
      W0=EV*(S2*EXP(-DN2)-S1*EXP(-DN1))/SQRT(2.0*PAI)-
     &(S2*(D2-EM)*ERFC2-S1*(D1+EM)*ERFC1)/2.0
      WRITE(1,*) 'W0=',W0
      W1=EV*(S2*ERFC2+S1*ERFC1)/2.0
      WRITE(1,*) 'W1=',W1
      DO 55 I=1,N
      A(I)=A(I)/MN
      B(1,I)=B(1,I)/MN
```

```
 55   B(2,I)=B(2,I)/MN
      DO 56 I=1,N2
      BAMP=SQRT(B(1,I)*B(1,I)+B(2,I)*B(2,I))*1000.0
 56   WRITE(8,3) A(I)*1000000.0,BAMP
      SUMD=0.0
      SUMN=0.0
      DO 60 I=2,N
      BB=B(1,I)*B(1,I)+B(2,I)*B(2,I)
      BB=SQRT(BB)
      SUMD=SUMD+A(I)
      SUMN=SUMN+BB
 60   CONTINUE
C
C     ESTIMATE W0 AND W1
C
      EW1=EV*SUMN/SUMD
      WRITE(1,*) 'ESTIMATE OF W1=',EW1
      EW0=EMU
      WRITE(1,*) 'ESTIMATE OF W0=',EW0
      D(1)=0.0
      D(2)=0.0
C
C     ESTIMATE CLEARANCES USING ESTIMATED W0 & W1
C
      CALL POWELL(D,ED,FY,2,5000,ICOVG,0.001,0.001,1)
      WRITE(1,*)ED,FY,ICOVG
      WRITE(1,*) 'ESTIMATED VALUES OF CLEARANCES'
      WRITE(1,*)ED
      ER1=ABS(D1-ED(1))/D1
      ER2=ABS(D2-ED(2))/D2
      WRITE(1,*) 'RELATIVE ERROR OF ESTIMATION'
      WRITE(1,*)ER1,ER2
 3    FORMAT(1X,2(1X,E15.7))
      CLOSE (UNIT=1, STATUS='KEEP')
      CLOSE (UNIT=2, STATUS='KEEP')
      CLOSE (UNIT=3, STATUS='KEEP')
      CLOSE (UNIT=8, STATUS='KEEP')
      RETURN
      END
C
C     A SUBROUTINE TO SIMULATE
C     NORMAL DISTRIBUTED RANDOM FUNCTION
C
      SUBROUTINE RANDS2(IX,YEL,S,AM,V)
      IMPLICIT REAL*8(A-H,O-Z)
      A=0.0
      DO 1 I=1,12
      YEL=RAN(IX)
 1    A=A+YEL
      V=(A-6.0)*S+AM
```

```
      RETURN
      END
C
C     A SUBROUTINE TO GENERATE AN OBJECTIVE FUNCTION
C     USED IN THE SUBROUTINE POWELL WHERE ROOTS
C     OF NONLINEAR EQUATIONS ARE FOUND BY SEARCHING
C     THE MINIMUM OT THE OBJECTIVE FUNCTION
C
      SUBROUTINE OBF(X,FX)
      IMPLICIT REAL*8(A-H,O-Z)
      DIMENSION X(2)
      COMMON PAI,EW0,EW1,AM,C,S0,S1,S2,D1,D2,EV,EM
      DN1R=(X(1)+EM)/(1.414213562*EV)
      DN2R=(X(2)-EM)/(1.414213562*EV)
      DN1=DN1R*DN1R
      DN2=DN2R*DN2R
      EPS=1.0E-8
      ERFC1=1.0-ER(DN1R,EPS)
      ERFC2=1.0-ER(DN2R,EPS)
      W0=EV*(S2*EXP(-DN2)-S1*EXP(-DN1))/SQRT(2.0*PAI)-
     &(S2*(X(2)-EM)*ERFC2-S1*(X(1)+EM)*ERFC1)/2.0
      W1=EV*(S2*ERFC2+S1*ERFC1)/2.0
      FX=(EW1-W1)**2+(EW0-W0)**2
      XMAX=3.0*EV-EM
      XMIN=3.0*EV+EM
      IF(X(1).LT.0) FX=FX+S1*X(1)*X(1)
      IF(X(2).LT.0) FX=FX+S2*X(2)*X(2)
      IF(X(1).GT.XMIN) FX=FX+S1*(X(1)-XMIN)*(X(1)-XMIN)
      IF(X(2).GT.XMAX) FX=FX+S2*(X(2)-XMAX)*(X(2)-XMAX)
      RETURN
      END
C
C     A FUNCTION NEEDED TO SOLVE THE EQUATION
C     OF MOTION BY RUNGE-KUTTA METHOD
C
      FUNCTION FG(Y,V,R)
      IMPLICIT REAL*8(A-H,O-Z)
      COMMON PAI,EW0,EW1,AM,C,S0,S1,S2,D1,D2,EV,EM
      IF(Y.LE.-D1) SY=S0*Y+(Y+D1)*S1
      IF((Y.GT.-D1).AND.(Y.LT.D2)) SY=S0*Y
      IF(Y.GE.D2) SY=S0*Y+(Y-D2)*S2
      FG=(-C*V-SY+R)/AM
      RETURN
      END
```

C5. Program SPAEX

Program SPAEX estimate clearances by the spectrum analysis approach using random vibro-impact responses measured from mechanical experiments.

```
C
C     PROGRAM SPAEX
C
C     A PROGRAM USING THE RESPONSE OF
C     AN IMPACT OSCILLATOR UNDER A RANDOM EXCITATION
C     TO ESTIMATE THE CLEARANCES
C     BY THE SPECTRUM ANALYSIS APPROACH
C

      IMPLICIT REAL*8(A-H,O-Z)
      DIMENSION X1(2048,2),X2(2048,2),IG(11),Y1(2048)
     &,Y2(2048),L(2048,2)
      DIMENSION A(2048),B(2,2048)
      COMMON/DD/ D(2),ED(2)
      COMMON PAI,EW0,EW1,AM,C,S0,S1,S2,D1,D2,EV,EM
C
C     INPUT FILE RANEX.DAT PROVIDE ALL NEEDED
C     SYSTEM PARAMETERS
C
C     INPUT FILE IN.DAT PROVIDE THE NEEDED
C     SAMPLED RECORDS OF RANDOM EXCITATION
C     AND RESPONSE
C
C     SPA.DAT IS USED TO STORE RESULTS OF
C     ESTIMATION BY THE SPECTRUM ANALYSIS APPROACH
C
C     TI.DAT IS USED TO STORE TYPICAL SAMPLE OF
C     EXCITATION AND RESPONSE
C
C     SP.DAT IS USED TO STORE THE POWER AND CROSS SPECTRUM
C
C     AM = MASS OF THE IMPACT OSCILLATOR
C     C = DAMPING COEFFICIENT OF THE IMPACT OSCILLATOR
C     S0 = STIFFNESS OF THE MAIN SPRING
C     S1,S2 = STIFFNESS OF THE STOPS
C     D1,D2 = SIZE OF THE CLEARANCES
C     FA = STANDARD DERIVATION OF RANDOM EXCITATION
C     TMAX = LENGTH OF A PIECE OF TIME HISTORY SAMPLE
C     M = NUMBER OF SAMPLE RECORDS
C     N = NUMBER OF SAMPLING POINTS
C     CO1,CO2 = COEFFICIENTS TO CALIBRATE SIGNALS
C           OBTAINED FROM MECHANICAL EXPERIMENTS
C
```

```
      OPEN (UNIT=2, FILE='RANEX.DAT', STATUS='OLD')
      OPEN (UNIT=3, FILE='TI.DAT', STATUS='NEW')
      OPEN (UNIT=8, FILE='SP.DAT', STATUS='NEW')
      OPEN (UNIT=1, FILE='IN.DAT', STATUS='OLD')
      OPEN (UNIT=4, FILE='SPA.DAT', STATUS='NEW')
      READ (2,*) AM,C,S0,S1,S2,D1,D2,TMAX,M,N,CO1,CO2
      WRITE(4,*) 'SYSTEM PARAMETERS'
      WRITE(4,*) 'MASS=',AM,'KG'
      WRITE(4,*) 'MAIN SPRING COEFFECIENT=',S0,'N/M'
      WRITE(4,*) 'STOP 1 SPRING COEFFECIENT=',S1,'N/M'
      WRITE(4,*) 'STOP 2 SPRING COEFFECIENT=',S2,'N/M'
      WRITE(4,*) 'DAMPING COEFFECIENT=',C,'N*S/M'
      WRITE(4,*) 'CLEARANCE 1 =',D1,'M'
      WRITE(4,*) 'CLEARANCE 2 =',D2,'M'
      WRITE(4,*) 'SAMPLING RATE=',N/TMAX,'1/S'
      WRITE(4,*) 'LENGTH OF RECORD=',TMAX,'S'
      WRITE(4,*) 'NUMBER OF SAMPLE =',M
      WRITE(4,*) 'POINT OF EACH SAMPLE =',N
      IPA=LOG(FLOAT(N))/LOG(2.0)+.001
      N=2**IPA
      WRITE(6,*) 'N =',N
      CALL MAIN (IPA,X1,X2,N,M,Y1,Y2,IG,L,A,B,TMAX,CO1,CO2)
      STOP
      END
      SUBROUTINE MAIN (IPA,X1,X2,N,M,Y1,Y2,IG,L,A,B,
     &TMAX,CO1,CO2)
      IMPLICIT REAL*8(A-H,O-Z)
      DIMENSION X1(N,2),X2(N,2),IG(IPA),Y1(N),Y2(N),L(N,2)
      DIMENSION A(N),B(2,N)
      COMMON/DD/ D(2),ED(2)
      COMMON PAI,EW0,EW1,AM,C,S0,S1,S2,D1,D2,EV,EM
      PAI=4.0D0*DATAN(1.0D0)
      IX=0
      SIGN=-1.
      MN=M*N
      NUM=1
      N2=N/2.0
      DF=1.0/TMAX
      DFA=DF*2.0*PAI
      DT=TMAX/N
      DT2=DT/2.0
      N21=N2+1
      N1=N-1
      DO 11 I=1,N
      A(I)=0.0
      B(1,I)=0.0
11    B(2,I)=0.0
      EM=0.0
      EV=0.0
      EMU=0.0
```

```
      DO 50 J=1,M
      FE=-DFA
C
C     READ IN A SAMPLE RECORD OF
C     BASE EXCITATION B(T) AND
C     ABSOLUTE DISPLACEMENT OF MASS X(T)
C
      DO 5 I=1,N
    5 READ (1,*) X1(I,1),X1(I,2)
      DO 10 I=1,N
      X1(I,1)=X1(I,1)/CO1
      X2(I,1)=0.0
      X2(I,2)=0.0
   10 X1(I,2)=X1(I,2)/CO2
      SIGN=-1
      NUM=1
C
C     FOURIER TRANSFORMING EXCITATION B(T)
C     AND RESPONSE X(T)
C
      CALL FFT (IPA,X1,X2,N,Y1,Y2,SIGN,NUM,IG,L,K1,K2)
C
C     SHIFT X(T) BY DT/2 IN FREQUENCY DOMAIN
C
      FE=-DFA
      DO 30 I=1,N21
      FE=FE+DFA
      TH=-FE*DT2
      HI=SIN(TH)
      HR=COS(TH)
      IN=N-I+2
      RR=X1(I,K2)*HR-X2(I,K2)*HI
      RI=X1(I,K2)*HI+X2(I,K2)*HR
      X1(I,2)=RR
      X2(I,2)=RI
      X1(IN,2)=X1(I,2)
   30 X2(IN,2)=-X2(I,2)
      X2(N21,2)=-X2(N21,2)
C
C     FIND RELATIVE DISPLACEMENT Y(T)
C
      DO 35 I=1,N
      X1(I,1)=X1(I,2)-Y1(I)
      X2(I,1)=X2(I,2)-Y2(I)
      X1(I,2)=Y1(I)
   35 X2(I,2)=Y2(I)
      SIGN=1
      NUM=1
C
C     GET Y(T) BY INVERSE FOURIER TRANSFORMATION
```

```
C
      CALL FFT (IPA,X1,X2,N,Y1,Y2,SIGN,NUM,IG,L,K1,K2)
C
C     CALCULATE MEAN VALUES AND VARIANCE OF Y(T)
C
      DO 37 I=1,N
      EM=EM+Y1(I)
      EV=EV+Y1(I)*Y1(I)
      X1(I,1)=X1(I,K2)
      X2(I,1)=X2(I,K2)
      X1(I,2)=Y1(I)
 37   X2(I,2)=Y2(I)
      IF(J.GE.2) GOTO 17
C
C     WRITE TYPICAL EXCITATION AND RESPONSE TO
C     FILE TI.DAT
C
      DO 38 I=1,N
 38   WRITE(3,3) X1(I,1)*1000.0,X1(I,2)*1000.0
 17   SIGN=-1.
      NUM=1
C
C     FOURIER TRANSFORMING EXCITATION B(T)
C     AND RESPONSE Y(T)
C
      CALL FFT (IPA,X1,X2,N,Y1,Y2,SIGN,NUM,IG,L,K1,K2)
C
C     CALCULATE THE TRANSFORMED IMPACT FORCE U(F)
C
      FE=-DFA
      DO 130 IV=1,N21
      FE=FE+DFA
      HI=C*FE
      FE2=FE*FE*AM
      HR=S0-FE2
      RR=Y1(IV)*FE2-X1(IV,K2)*HR+X2(IV,K2)*HI
      RI=Y2(IV)*FE2-X1(IV,K2)*HI-X2(IV,K2)*HR
      Y1(IV)=RR
 130  Y2(IV)=RI
      DO 135 IW=2,N2
      IN=N-IW+2
      Y1(IN)=Y1(IW)
 135  Y2(IN)=-Y2(IW)
      EMU=EMU+Y1(1)
      DO 33 IZ=1,N
      BR=Y1(IZ)*X1(IZ,K2)+Y2(IZ)*X2(IZ,K2)
      BI=Y1(IZ)*X2(IZ,K2)-Y2(IZ)*X1(IZ,K2)
      B(1,IZ)=B(1,IZ)+BR
      B(2,IZ)=B(2,IZ)+BI
      AA=X1(IZ,K2)*X1(IZ,K2)+X2(IZ,K2)*X2(IZ,K2)
```

```
 33   A(IZ)=A(IZ)+AA
 50   CONTINUE
      EM=EM/MN
      EMU=EMU/MN
      EV=(EV-MN*EM*EM)/(MN-1)
      EV=SQRT(EV)
      WRITE(4,*) 'ESTIMATE OF MEAN VALUE OF Y =',EM
      WRITE(4,*) 'ESTIMATE OF MEAN VALUE OF U =',EMU
      WRITE(4,*) 'ESTIMATE OF VARIANCE=',EV
      DN1R=(D1+EM)/(1.414213562*EV)
      DN2R=(D2-EM)/(1.414213562*EV)
      DN1=DN1R*DN1R
      DN2=DN2R*DN2R
      EPS=1.0E-8
      ERFC1=1.0-ER(DN1R,EPS)
      ERFC2=1.0-ER(DN2R,EPS)
      WRITE(4,*) 'ERFC1=',ERFC1
      WRITE(4,*) 'ERFC2=',ERFC2
C
C     CALCULATE W0 AND W1 USING ACTUAL CLEARANCES
C     THIS IS NOT NEEDED FOR ESTIMATION PURPOSE
C     ONLY FOR STUDY PURPOSE
C
      W0=EV*(S2*EXP(-DN2)-S1*EXP(-DN1))/SQRT(2.0*PAI)-
     &(S2*(D2-EM)*ERFC2-S1*(D1+EM)*ERFC1)/2.0
      WRITE(4,*) 'W0=',W0
      W1=EV*(S2*ERFC2+S1*ERFC1)/2.0
      WRITE(4,*) 'W1=',W1
      DO 55 I=1,N
      A(I)=A(I)/MN
      B(1,I)=B(1,I)/MN
 55   B(2,I)=B(2,I)/MN
      DO 56 I=1,N2
      BAMP=SQRT(B(1,I)*B(1,I)+B(2,I)*B(2,I))*1000.0
 56   WRITE(8,3) A(I)*1000000.0,BAMP
      SUMD=0.0
      SUMN=0.0
      DO 60 I=2,N
      BB=B(1,I)*B(1,I)+B(2,I)*B(2,I)
      BB=SQRT(BB)
      SUMD=SUMD+A(I)
      SUMN=SUMN+BB
 60   CONTINUE
C
C     ESTIMATE W0 AND W1
C
      EW1=EV*SUMN/SUMD
      WRITE(4,*) 'ESTIMATE OF W1=',EW1
      EW0=EMU
      WRITE(4,*) 'ESTIMATE OF W0=',EW0
```

```
      D(1)=EV
      D(2)=EV
C
C     ESTIMATE CLEARANCES USING ESTIMATED W0 & W1
C
      CALL POWELL(D,ED,FY,2,5000,ICOVG,0.001,0.001,1)
      WRITE(4,*)ED,FY,ICOVG
      WRITE(4,*) 'ESTIMATED VALUES OF CLEARANCES'
      WRITE(4,*)ED
      ER1=ABS(D1-ED(1))/D1
      ER2=ABS(D2-ED(2))/D2
      WRITE(4,*) 'RELATIVE ERROR OF ESTIMATION'
      WRITE(4,*)ER1,ER2
    3 FORMAT(1X,2(1X,E15.7))
      CLOSE (UNIT=1, STATUS='KEEP')
      CLOSE (UNIT=2, STATUS='KEEP')
      CLOSE (UNIT=3, STATUS='KEEP')
      CLOSE (UNIT=8, STATUS='KEEP')
      CLOSE (UNIT=4, STATUS='KEEP')
      RETURN
      END
C
C     A SUBROUTINE TO GENERATE AN OBJECTIVE FUNCTION
C     USED IN THE SUBROUTINE POWELL WHERE ROOTS
C     OF NONLINEAR EQUATIONS ARE FOUND BY SEARCHING
C     THE MINIMUM OT THE OBJECTIVE FUNCTION
C
      SUBROUTINE OBF(X,FX)
      IMPLICIT REAL*8(A-H,O-Z)
      DIMENSION X(2)
      COMMON PAI,EW0,EW1,AM,C,S0,S1,S2,D1,D2,EV,EM
      DN1R=(X(1)+EM)/(1.414213562*EV)
      DN2R=(X(2)-EM)/(1.414213562*EV)
      DN1=DN1R*DN1R
      DN2=DN2R*DN2R
      EPS=1.0E-8
      ERFC1=1.0-ER(DN1R,EPS)
      ERFC2=1.0-ER(DN2R,EPS)
      W0=EV*(S2*EXP(-DN2)-S1*EXP(-DN1))/SQRT(2.0*PAI)-
     &(S2*(X(2)-EM)*ERFC2-S1*(X(1)+EM)*ERFC1)/2.0
      W1=EV*(S2*ERFC2+S1*ERFC1)/2.0
      FX=(EW1-W1)**2+(EW0-W0)**2
      XMAX=3.0*EV-EM
      XMIN=3.0*EV+EM
      IF(X(1).LT.0) FX=FX+S1*X(1)*X(1)
      IF(X(2).LT.0) FX=FX+S2*X(2)*X(2)
      IF(X(1).GT.XMIN) FX=FX+S1*(X(1)-XMIN)*(X(1)-XMIN)
      IF(X(2).GT.XMAX) FX=FX+S2*(X(2)-XMAX)*(X(2)-XMAX)
      RETURN
      END
```

C6. Program HB

Program HB calculate the frequency response function $H_{ij}(\omega)$ of a multi-section beam, when the beam is considered as a single input and single output system with the base motion being the input and the displacement motion of the beam at an arbitrary location x_i being the output. Such frequency response functions are needed in estimating clearances of beam-stop systems.

```
C
C      PROGRAM HB
C
C      A PROGRAM TO CALCULATE THE FREQUENCY RESPONSE
C      FUNCTION OF A N-SECTION BEAMS
C      UNDER A BASE EXCITATION
C
     IMPLICIT REAL*8(A-H,O-Z)
     REAL*8 X(1),F(1),AM(10),AME(10),AKT(10)
     REAL*8 H(4,4),Z(514),Y(514)
     COMMON/AB/AK(10),T(10),E(10),AI(10),RHO(10),AL(10),A(10)
     COMMON/AC/AP(10),BP(10),CP(10),DP(10)
     COMMON/AD/H1(10)
     COMMON/B/N,NN
C
C    AK(I)=TRANSVERSE STIFFNESS AT THE I-TH POINT
C    AM(I)=MASS AT THE I-TH POINT
C    T(I)=ROTATIONAL STIFFNESS AT THE I-TH POINT
C    E(I)=ELADTICITY MODULUS OF I-TH SECTION
C    AI(I)=MOMENT OF INERTIA
C    RHO(I)=DENSITY OF THE I-TH MATERIAL
C    AL(I)=LENGTH OF THE I-TH BEAM
C    A(I)=AREA OF THE I-TH BEAM
C
     WRITE(6,111)
111  FORMAT(' N=THE NUMBER OF SPANS',I4)
     WRITE(6,112)
112  FORMAT('  AK(I)=TRANSVERSE STIFFNESS AT THE I-TH POINT')
     WRITE(6,113)
113  FORMAT('  T(I)=ROTATIONAL STIFFNESS AT THE I-TH POINT')
     WRITE(6,114)
114  FORMAT('  AL(I)=LENGTH OF THE I-TH BEAM')
     READ ,N,FA,FMAX,DF,XL
C
C      N = NUMBER OF SECTION
C    FA= AMPLITUDE OF APPLIED FORCE
```

```
C    FMAX = UP-LIMIT FREQUENCY
C      DF = FREQUENCY STEP
C      XL = POSITION WHERE THE DISPLACEMENT
C         IS CONSIDERED AS SYSTEM RESPONSE
C
     PRINT ,'X=',XL
     WRITE(6,111) N
     NN=N+1
C
C       READ BEAM PARAMETERS
C
     DO 50 I=1,NN
     READ , AK(I),T(I),AL(I),AM(I),AKT(I)
     WRITE(6,7)
7    FORMAT(6X,'AK(I)',12X,'T(I)',18X,'AL(I)',15X,'AM(I)',15X,'AKT(I)')
     WRITE(6,4) AK(I),T(I),AL(I),AM(I),AKT(I)
4    FORMAT(F15.5,2X,F15.5,2X,F15.5,2X,F15.5,2X,F15.5)
     E(I)=68.95D9
     AI(I)=5.42000D-10
     RHO(I)=2713
50   A(I)=1.63000D-4
     N99=0.0
     DF=DF*6.283185307
     FF=-DF+0.0000001
     FMAX=FMAX*6.283185307
328  IF((FF*FF).LT.1.0D-11) FF=FF-0.0000001
     FF=FF+DF
     ZZ=FF*FF
     DO 127 I=1,NN
     IF(AM(I).EQ.0.0) GOTO 129
     AME(I)=AM(I)*AKT(I)/(AKT(I)-AM(I)*ZZ)
     GOTO 127
129  AME(I)=0.0
127  CONTINUE
C
C       FIND AN EXACT SOLUTION UNDER A
C       PARTICULAR FREQUENCY
C
     CALL FORCEB(FA,FF,PHA,AME)
     N99=N99+1
     Z(N99)=FF/6.283185307
     R2=FF*DSQRT(RHO(1)*A(1)/(E(1)*AI(1)))
     R=DSQRT(R2)*XL
     Y(N99)=AP(1)*DCOS(R)+BP(1)*DSIN(R)+CP(1)*DCOSH(R)
    &+DP(1)*DSINH(R)
C    Y(N99)=DLOG10(DABS(Y(N99)))
     IF(FF.LE.FMAX)  GOTO 328
123  PRINT ,'  SPECTRUM'
     DO 223 I=1,N99
223  WRITE(6,224) Y(I)
```

```
224  FORMAT(1X,F20.10)
220  STOP
     END
C
C       A SUBROUTINE TO FIND AN EXACT SOLUTION
C       FOR A N-SECTION BEAM UNDER A SINUSOIDAL
C       BASE EXCITATION
C
     SUBROUTINE FORCEV(FA,FF,PHA,AM)
     IMPLICIT REAL*8(A-H,O-Z)
     REAL*8 X(1),F(1),Z(15),C1(15),S1(15),V1(15),T1(15),AZ(4,4)
     REAL*8 AM(10),R(10),Q(10),BB(4,4),UU(4,4),AA(4,4),H(4,4)
     REAL*8 T2(4),T3(4),UL(4,4),BF(4,4),AF(4,4),BF1(4)
     COMMON/AB/AK(10),T(10),E(10),AI(10),RHO(10),AL(10),A(10)
     COMMON/AC/AP(10),BP(10),CP(10),DP(10)
     COMMON/AD/H1(10)
     COMMON/B/N,NN
     CO1=1.0
     CO2=1.0
     Z(1)=RHO(1)*A(1)/(E(1)*AI(1))*FF*FF
     Z(1)=DSQRT(DSQRT(Z(1)))
     DO 10 I=1,N
     Z(I)=E(1)*AI(1)/(E(I)*AI(I))*Z(1)**4
     Z(I)=Z(I)*RHO(I)*A(I)/(RHO(1)*A(1))
     Z(I)=DSQRT(DSQRT(Z(I)))
     R(I)=Z(I)*Z(I)*E(I)*AI(I)
     Q(I)=Z(I)*Z(I)*Z(I)*E(I)*AI(I)
     Z(I)=Z(I)*AL(I)
     S1(I)=DSIN(Z(I))
     C1(I)=DCOS(Z(I))
     T1(I)=DSINH(Z(I))
     V1(I)=DCOSH(Z(I))
10   Z(I)=Z(I)/AL(I)
     DO 18 I=1,NN
     IF(I.EQ.NN) THEN
     VV=Z(I-1)**4
     ELSE
     VV=Z(I)**4
     END IF
18   H1(I)=AK(I)-AM(I)*VV*E(I)*AI(I)/(A(I)*RHO(I))
     DO 25 I=1,4
     DO 25 J=1,4
     BB(I,J)=0.0
     IF(I.EQ.J) BB(I,J)=1.0
25   CONTINUE
     IF(N.EQ.1) GO TO 33
     DO 30 I=2,N
     L=I-1
     SS=(Z(L)*S1(L)*T(I)+R(L)*C1(L))/R(I)
     UU(1,1)=(SS+C1(L))/2
```

```
      UU(3,1)=(-SS+C1(L))/2
      SS=(-Z(L)*C1(L)*T(I)+R(L)*S1(L))/R(I)
      UU(1,2)=(SS+S1(L))/2
      UU(3,2)=(-SS+S1(L))/2
      SS=-(Z(L)*T1(L)*T(I)+R(L)*V1(L))/R(I)
      UU(1,3)=(SS+V1(L))/2
      UU(3,3)=(-SS+V1(L))/2
      SS=-(Z(L)*V1(L)*T(I)+R(L)*T1(L))/R(I)
      UU(1,4)=(SS+T1(L))/2
      UU(3,4)=(-SS+T1(L))/2
      SS=-(Q(L)*S1(L)-H1(I)*C1(L))/Q(I)
      UU(2,1)=(SS-Z(L)*S1(L)/Z(I))/2
      UU(4,1)=(-SS-Z(L)*S1(L)/Z(I))/2
      SS=-(-Q(L)*C1(L)-H1(I)*S1(L))/Q(I)
      UU(2,2)=(SS+Z(L)*C1(L)/Z(I))/2
      UU(4,2)=(-SS+Z(L)*C1(L)/Z(I))/2
      SS=-(Q(L)*T1(L)-H1(I)*V1(L))/Q(I)
      UU(2,3)=(SS+Z(L)*T1(L)/Z(I))/2
      UU(4,3)=(-SS+Z(L)*T1(L)/Z(I))/2
      SS=-(Q(L)*V1(L)-H1(I)*T1(L))/Q(I)
      UU(2,4)=(SS+Z(L)*V1(L)/Z(I))/2
      UU(4,4)=(-SS+Z(L)*V1(L)/Z(I))/2
      DO 11 II=1,4
      DO 11 J=1,4
      AA(II,J)=0.0
      AF(II,J)=0.0
      DO 11 K1=1,4
      AA(II,J)=AA(II,J)+UU(II,K1)*BB(K1,J)
11    CONTINUE
      DO 12 II=1,4
      DO 12 J=1,4
      BB(II,J)=AA(II,J)
12    CONTINUE
30    CONTINUE
33    CONTINUE
      H(1,1)=1.0
      H(1,2)=0.0
      H(1,3)=1.0
      H(1,4)=0.0
      H(2,1)=-E(1)*AI(1)*Z(1)
      H(2,2)=-T(1)
      H(2,3)=-H(2,1)
      H(2,4)=H(2,2)
      IF (T(1).GT.100) GO TO 83
      GO TO 64
83    DO 24 I1=1,4
24    H(2,I1)=H(2,I1)/T(1)
64    CONTINUE
      TT=Q(N)
      T3(1)=TT*S1(N)-H1(N+1)*C1(N)
```

```
      T3(2)=-TT*C1(N)-H1(N+1)*S1(N)
      T3(3)=TT*T1(N)-H1(N+1)*V1(N)
      T3(4)=TT*V1(N)-H1(N+1)*T1(N)
      DO 21  I1=1,4
      H(3,I1)=0.0
      DO 21 J=1,4
   21  H(3,I1)=H(3,I1)+T3(J)*BB(J,I1)
      IF(H1(N+1).GT.100) GO TO 84
      GO TO 65
   84  DO 26 I1=1,4
   26  H(3,I1)=H(3,I1)/H1(N+1)
   65  CONTINUE
   37  TT=E(N)*AI(N)*Z(N)
      T3(1)=-TT*C1(N)-T(N+1)*S1(N)
      T3(2)=-TT*S1(N)+T(N+1)*C1(N)
      T3(3)=TT*V1(N)+T(N+1)*T1(N)
      T3(4)=TT*T1(N)+T(N+1)*V1(N)
      DO 27 I1=1,4
      H(4,I1)=0.0
      DO 27 J=1,4
   27  H(4,I1)=H(4,I1)+T3(J)*BB(J,I1)
      IF (T(N+1).GT.100) GO TO 85
      GO TO 66
   85  DO 28 I1=1,4
   28  H(4,I1)=H(4,I1)/T(N+1)
   66  CONTINUE
   39  DO 110 I=1,4
  110  UL(I,1)=H(I,1)
      DO 120 I=2,4
  120  UL(1,I)=H(1,I)/UL(1,1)
      I=2
  130  I1=I-1
      DO 140 J=I,4
      SU=0.0
      DO 135 II=1,I1
  135  SU=SU+UL(J,II)*UL(II,I)
  140  UL(J,I)=H(J,I)-SU
      IF(I-3) 150,160,170
  150  DO 155 J=3,4
  155  UL(I,J)=(H(I,J)-UL(I,1)*UL(1,J))/UL(2,2)
      GOTO 165
  160  UL(3,4)=(H(3,4)-UL(3,1)*UL(1,4)-UL(3,2)*UL(2,4))
     &/UL(3,3)
  165  I=I+1
      GOTO 130
  170  CONTINUE
      AP(1)=FA/UL(1,1)
      BP(1)=-AP(1)*UL(2,1)/UL(2,2)
      CP(1)=-(AP(1)*UL(3,1)+BP(1)*UL(3,2))/UL(3,3)
      DP(1)=-(AP(1)*UL(4,1)+BP(1)*UL(4,2)+CP(1)*UL(4,3))
```

```
     &/UL(4,4)
      CP(1)=CP(1)-UL(3,4)*DP(1)
      BP(1)=BP(1)-(CP(1)*UL(2,3)+DP(1)*UL(2,4))
      AP(1)=AP(1)-(BP(1)*UL(1,2)+CP(1)*UL(1,3)+DP(1)
     &*UL(1,4))
      IF(N.EQ.1) GO TO 233
      DO 230 I=2,N
      L=I-1
      SS=(Z(L)*S1(L)*T(I)+R(L)*C1(L))/R(I)
      UU(1,1)=(SS+C1(L))/2
      UU(3,1)=(-SS+C1(L))/2
      SS=(-Z(L)*C1(L)*T(I)+R(L)*S1(L))/R(I)
      UU(1,2)=(SS+S1(L))/2
      UU(3,2)=(-SS+S1(L))/2
      SS=-(Z(L)*T1(L)*T(I)+R(L)*V1(L))/R(I)
      UU(1,3)=(SS+V1(L))/2
      UU(3,3)=(-SS+V1(L))/2
      SS=-(Z(L)*V1(L)*T(I)+R(L)*T1(L))/R(I)
      UU(1,4)=(SS+T1(L))/2
      UU(3,4)=(-SS+T1(L))/2
      SS=-(Q(L)*S1(L)-H1(I)*C1(L))/Q(I)
      UU(2,1)=(SS-Z(L)*S1(L)/Z(I))/2
      UU(4,1)=(-SS-Z(L)*S1(L)/Z(I))/2
      SS=-(-Q(L)*C1(L)-H1(I)*S1(L))/Q(I)
      UU(2,2)=(SS+Z(L)*C1(L)/Z(I))/2
      UU(4,2)=(-SS+Z(L)*C1(L)/Z(I))/2
      SS=-(Q(L)*T1(L)-H1(I)*V1(L))/Q(I)
      UU(2,3)=(SS+Z(L)*T1(L)/Z(I))/2
      UU(4,3)=(-SS+Z(L)*T1(L)/Z(I))/2
      SS=-(Q(L)*V1(L)-H1(I)*T1(L))/Q(I)
      UU(2,4)=(SS+Z(L)*V1(L)/Z(I))/2
      UU(4,4)=(-SS+Z(L)*V1(L)/Z(I))/2
      DO 261 K1=1,4
      SUM=UU(K1,1)*AP(L)+UU(K1,2)*BP(L)+UU(K1,3)*CP(L)+UU(K1,4)
     &*DP(L)
      IF(K1-2) 180,190,200
180   AP(I)=SUM
      GOTO 261
190   BP(I)=SUM
      GOTO 261
200   IF(K1-3) 261,210,220
210   CP(I)=SUM
      GOTO 261
220   DP(I)=SUM
261   CONTINUE
230   CONTINUE
 233 CONTINUE
C     PRINT,' '
C     PRINT,' FORCE VIBRATION PARAMETER '
C     DO 118 K1=1,N
```

```
C    PRINT,' VECTOR NO. ', K1
C    WRITE(6,117) AP(K1),BP(K1),CP(K1),DP(K1)
C117  FORMAT(1X,4(2X,F15.10))
118  CONTINUE
     RETURN
     END
```

C7. Program HF

Program HF calculate the frequency response function $H_{1i}(\omega)$ of a multi-section beam, when the beam is considered as a single input and single output system with the concentrated external lateral force excitation at position x_1 being the input and the displacement motion of the beam at location x_i being the output. Such frequency response functions are needed in estimating clearances of beam-stop systems.

```
C
C      PROGRAM HF
C
C      A PROGRAM TO CALCULATE THE FREQUENCY RESPONSE
C      FUNCTION OF A N-SECTION BEAMS
C      UNDER A CONCENTRATED FORCE EXCITATION
C
    IMPLICIT REAL*8(A-H,O-Z)
    REAL*8 X(1),F(1),AM(10),AME(10),AKT(10)
    REAL*8 H(4,4),Z(514),Y(514)
    COMMON/AB/AK(10),T(10),E(10),AI(10),RHO(10),AL(10),A(10)
    COMMON/AC/AP(10),BP(10),CP(10),DP(10)
    COMMON/AD/H1(10)
    COMMON/B/N,NN
C
C    AK(I)=TRANSVERSE STIFFNESS AT THE I-TH POINT
C    AM(I)=MASS AT THE I-TH POINT
C    T(I)=ROTATIONAL STIFFNESS AT THE I-TH POINT
C    E(I)=ELADTICITY MODULUS OF I-TH SECTION
C    AI(I)=MOMENT OF INERTIA
C    RHO(I)=DENSITY OF THE I-TH MATERIAL
C    AL(I)=LENGTH OF THE I-TH BEAM
C    A(I)=AREA OF THE I-TH BEAM
C
    WRITE(6,111)
111  FORMAT(' N=THE NUMBER OF SPANS',I4)
    WRITE(6,112)
112  FORMAT(' AK(I)=TRANSVERSE STIFFNESS AT THE I-TH POINT')
    WRITE(6,113)
113  FORMAT(' T(I)=ROTATIONAL STIFFNESS AT THE I-TH POINT')
    WRITE(6,114)
114  FORMAT(' AL(I)=LENGTH OF THE I-TH BEAM')
    READ ,N,NR,FA,FMAX,DF,XL
C
C      N = NUMBER OF SECTION
C    NR= THE POINT WHERE THE FORCE IS APPLIED
```

```
C    FA= AMPLITUDE OF APPLIED FORCE
C    FMAX = UP-LIMIT FREQUENCY
C      DF = FREQUENCY STEP
C      XL = POSITION WHERE THE DISPLACEMENT
C         IS CONSIDERED AS SYSTEM RESPONSE
C
     PRINT ,'X=',XL
     WRITE(6,111) N
     NN=N+1
C
C       READ BEAM PARAMETERS
C
     DO 50 I=1,NN
     READ , AK(I),T(I),AL(I),AM(I),AKT(I)
     WRITE(6,7)
7    FORMAT(6X,'AK(I)',12X,'T(I)',18X,'AL(I)',15X,
    &'AM(I)',15X,'AKT(I)')
     WRITE(6,4) AK(I),T(I),AL(I),AM(I),AKT(I)
4    FORMAT(F15.5,2X,F15.5,2X,F15.5,2X,F15.5,2X,F15.5)
     E(I)=68.95D9
     AI(I)=5.42000D-10
     RHO(I)=2713
50   A(I)=1.63700D-4
     N99=0.0
     DF=DF*6.283185307
     FF=-DF+0.0001
     FMAX=FMAX*6.283185307
328  IF((FF*FF).LT.1.0D-5) FF=FF-0.0001
     FF=FF+DF
     ZZ=FF*FF
     DO 127 I=1,NN
     IF(AM(I).EQ.0.0) GOTO 129
     AME(I)=AM(I)*AKT(I)/(AKT(I)-AM(I)*ZZ)
     GOTO 127
129  AME(I)=0.0
127  CONTINUE
C
C       FIND AN EXACT SOLUTION FOR
C       A PARTICULAR FREQUENCY
C
     CALL FORCEV(NR,FA,FF,PHA,AME)
     N99=N99+1
     Z(N99)=FF/6.283185307
     R2=FF*DSQRT(RHO(2)*A(2)/(E(2)*AI(2)))
     R=DSQRT(R2)*XL
     Y(N99)=AP(2)*DCOS(R)+BP(2)*DSIN(R)+CP(2)*DCOSH(R)
    &+DP(2)*DSINH(R)
     IF(FF.LE.FMAX)  GOTO 328
123  PRINT ,'  SPECTRUM'
     DO 125 I=1,N99
```

```
      WRITE(6,126) Y(I)
  125 CONTINUE
  126 FORMAT(1X,F23.15)
  220 STOP
      END
C
C       A SUBROUTINE TO FIND AN EXACT SOLUTION
C       FOR A N-SECTION BEAM UNDER A SINUSOIDAL
C       CONCENTRATED FORCE EXCITATION
C
      SUBROUTINE FORCEV(NR,FA,FF,PHA,AM)
      IMPLICIT REAL*8(A-H,O-Z)
      REAL*8 X(1),F(1),Z(15),C1(15),S1(15),V1(15),
     &T1(15),AZ(4,4)
      REAL*8 AM(10),R(10),Q(10),BB(4,4),UU(4,4),AA(4,4),
     &H(4,4)
      REAL*8 T2(4),T3(4),UL(4,4),BF(4,4),AF(4,4),BF1(4)
      COMMON/AB/AK(10),T(10),E(10),AI(10),RHO(10),AL(10),
     &A(10)
      COMMON/AC/AP(10),BP(10),CP(10),DP(10)
      COMMON/AD/H1(10)
      COMMON/B/N,NN
      CO1=1.0
      CO2=1.0
      Z(1)=RHO(1)*A(1)/(E(1)*AI(1))*FF*FF
      Z(1)=DSQRT(DSQRT(Z(1)))
      DO 10 I=1,N
      Z(I)=E(1)*AI(1)/(E(I)*AI(I))*Z(1)**4
      Z(I)=Z(I)*RHO(I)*A(I)/(RHO(1)*A(1))
      Z(I)=DSQRT(DSQRT(Z(I)))
      R(I)=Z(I)*Z(I)*E(I)*AI(I)
      Q(I)=Z(I)*Z(I)*Z(I)*E(I)*AI(I)
      Z(I)=Z(I)*AL(I)
      S1(I)=DSIN(Z(I))
      C1(I)=DCOS(Z(I))
      T1(I)=DSINH(Z(I))
      V1(I)=DCOSH(Z(I))
   10 Z(I)=Z(I)/AL(I)
      DO 18 I=1,NN
      IF(I.EQ.NN) THEN
      VV=Z(I-1)**4
      ELSE
      VV=Z(I)**4
      END IF
   18 H1(I)=AK(I)-AM(I)*VV*E(I)*AI(I)/(A(I)*RHO(I))
      DO 25 I=1,4
      DO 25 J=1,4
      BB(I,J)=0.0
      IF(I.EQ.J) BB(I,J)=1.0
      BF(I,J)=BB(I,J)
```

```
25  CONTINUE
    IF(N.EQ.1) GO TO 33
    DO 30 I=2,N
    L=I-1
    SS=(Z(L)*S1(L)*T(I)+R(L)*C1(L))/R(I)
    UU(1,1)=(SS+C1(L))/2
    UU(3,1)=(-SS+C1(L))/2
    SS=(-Z(L)*C1(L)*T(I)+R(L)*S1(L))/R(I)
    UU(1,2)=(SS+S1(L))/2
    UU(3,2)=(-SS+S1(L))/2
    SS=-(Z(L)*T1(L)*T(I)+R(L)*V1(L))/R(I)
    UU(1,3)=(SS+V1(L))/2
    UU(3,3)=(-SS+V1(L))/2
    SS=-(Z(L)*V1(L)*T(I)+R(L)*T1(L))/R(I)
    UU(1,4)=(SS+T1(L))/2
    UU(3,4)=(-SS+T1(L))/2
    SS=-(Q(L)*S1(L)-H1(I)*C1(L))/Q(I)
    UU(2,1)=(SS-Z(L)*S1(L)/Z(I))/2
    UU(4,1)=(-SS-Z(L)*S1(L)/Z(I))/2
    SS=-(-Q(L)*C1(L)-H1(I)*S1(L))/Q(I)
    UU(2,2)=(SS+Z(L)*C1(L)/Z(I))/2
    UU(4,2)=(-SS+Z(L)*C1(L)/Z(I))/2
    SS=-(Q(L)*T1(L)-H1(I)*V1(L))/Q(I)
    UU(2,3)=(SS+Z(L)*T1(L)/Z(I))/2
    UU(4,3)=(-SS+Z(L)*T1(L)/Z(I))/2
    SS=-(Q(L)*V1(L)-H1(I)*T1(L))/Q(I)
    UU(2,4)=(SS+Z(L)*V1(L)/Z(I))/2
    UU(4,4)=(-SS+Z(L)*V1(L)/Z(I))/2
    DO 11 II=1,4
    DO 11 J=1,4
    AA(II,J)=0.0
    AF(II,J)=0.0
    DO 11 K1=1,4
    AA(II,J)=AA(II,J)+UU(II,K1)*BB(K1,J)
    IF(I.LE.NR) GOTO 11
    AF(II,J)=AF(II,J)+UU(II,K1)*BF(K1,J)
11  CONTINUE
    DO 12 II=1,4
    DO 12 J=1,4
    BB(II,J)=AA(II,J)
    IF(I.LE.NR) GOTO 12
    BF(II,J)=AF(II,J)
12  CONTINUE
30  CONTINUE
33  CONTINUE
    H(1,1)=H1(1)
    H(1,2)=-Q(1)
    H(1,3)=H1(1)
    H(1,4)=Q(1)
    IF(H1(1).GT.100) GO TO 82
```

```
      GO TO 63
82    DO 23 I1=1,4
23    H(1,I1)=H(1,I1)/H1(1)
63    CONTINUE
      H(2,1)=-E(1)*AI(1)*Z(1)
      H(2,2)=-T(1)
      H(2,3)=-H(2,1)
      H(2,4)=H(2,2)
      IF (T(1).GT.100) GO TO 83
      GO TO 64
83    DO 24 I1=1,4
24    H(2,I1)=H(2,I1)/T(1)
64    CONTINUE
      DO 34 II=1,4
34    BF1(II)=BF(II,2)-BF(II,4)
      TT=Q(N)
      T3(1)=TT*S1(N)-H1(N+1)*C1(N)
      T3(2)=-TT*C1(N)-H1(N+1)*S1(N)
      T3(3)=TT*T1(N)-H1(N+1)*V1(N)
      T3(4)=TT*V1(N)-H1(N+1)*T1(N)
      DO 21  I1=1,4
      H(3,I1)=0.0
      DO 21 J=1,4
21    H(3,I1)=H(3,I1)+T3(J)*BB(J,I1)
      IF(H1(N+1).GT.100) GO TO 84
      GO TO 65
84    DO 26 I1=1,4
26    H(3,I1)=H(3,I1)/H1(N+1)
      CO1=CO1*H1(N+1)
65    CONTINUE
      IF(NR-NN) 437,537,537
537   R1=FA
      GOTO 37
437   R1=0.0
      FA1=FA/(Q(NR)*2.0)
      DO 36 J=1,4
36    R1=R1+T3(J)*BF1(J)
      R1=-FA1*R1/CO1
37    TT=E(N)*AI(N)*Z(N)
      T3(1)=-TT*C1(N)-T(N+1)*S1(N)
      T3(2)=-TT*S1(N)+T(N+1)*C1(N)
      T3(3)=TT*V1(N)+T(N+1)*T1(N)
      T3(4)=TT*T1(N)+T(N+1)*V1(N)
      DO 27 I1=1,4
      H(4,I1)=0.0
      DO 27 J=1,4
27    H(4,I1)=H(4,I1)+T3(J)*BB(J,I1)
      IF (T(N+1).GT.100) GO TO 85
      GO TO 66
85    DO 28 I1=1,4
```

```
28   H(4,I1)=H(4,I1)/T(N+1)
     CO2=CO2*T(N+1)
66   CONTINUE
     IF(NR-NN) 438,538,538
538  R2=0.0
     GOTO 39
438  R2=0.0
     DO 38 J=1,4
38   R2=R2+T3(J)*BF1(J)
     R2=-FA1*R2/CO2
39   DO 110 I=1,4
110  UL(I,1)=H(I,1)
     DO 120 I=2,4
120  UL(1,I)=H(1,I)/UL(1,1)
     I=2
130  I1=I-1
     DO 140 J=I,4
     SU=0.0
     DO 135 II=1,I1
135  SU=SU+UL(J,II)*UL(II,I)
140  UL(J,I)=H(J,I)-SU
     IF(I-3) 150,160,170
150  DO 155 J=3,4
155  UL(I,J)=(H(I,J)-UL(I,1)*UL(1,J))/UL(2,2)
     GOTO 165
160  UL(3,4)=(H(3,4)-UL(3,1)*UL(1,4)-UL(3,2)*UL(2,4))/UL(3,3)
165  I=I+1
     GOTO 130
170  CONTINUE
     CP(1)=R1/UL(3,3)
     DP(1)=(R2-CP(1)*UL(4,3))/UL(4,4)
     CP(1)=CP(1)-UL(3,4)*DP(1)
     BP(1)=-(CP(1)*UL(2,3)+DP(1)*UL(2,4))
     AP(1)=-(BP(1)*UL(1,2)+CP(1)*UL(1,3)+DP(1)*UL(1,4))
     IF(N.EQ.1) GO TO 233
     DO 230 I=2,N
     L=I-1
     SS=(Z(L)*S1(L)*T(I)+R(L)*C1(L))/R(I)
     UU(1,1)=(SS+C1(L))/2
     UU(3,1)=(-SS+C1(L))/2
     SS=(-Z(L)*C1(L)*T(I)+R(L)*S1(L))/R(I)
     UU(1,2)=(SS+S1(L))/2
     UU(3,2)=(-SS+S1(L))/2
     SS=-(Z(L)*T1(L)*T(I)+R(L)*V1(L))/R(I)
     UU(1,3)=(SS+V1(L))/2
     UU(3,3)=(-SS+V1(L))/2
     SS=-(Z(L)*V1(L)*T(I)+R(L)*T1(L))/R(I)
     UU(1,4)=(SS+T1(L))/2
     UU(3,4)=(-SS+T1(L))/2
     SS=-(Q(L)*S1(L)-H1(I)*C1(L))/Q(I)
```

```
      UU(2,1)=(SS-Z(L)*S1(L)/Z(I))/2
      UU(4,1)=(-SS-Z(L)*S1(L)/Z(I))/2
      SS=-(-Q(L)*C1(L)-H1(I)*S1(L))/Q(I)
      UU(2,2)=(SS+Z(L)*C1(L)/Z(I))/2
      UU(4,2)=(-SS+Z(L)*C1(L)/Z(I))/2
      SS=-(Q(L)*T1(L)-H1(I)*V1(L))/Q(I)
      UU(2,3)=(SS+Z(L)*T1(L)/Z(I))/2
      UU(4,3)=(-SS+Z(L)*T1(L)/Z(I))/2
      SS=-(Q(L)*V1(L)-H1(I)*T1(L))/Q(I)
      UU(2,4)=(SS+Z(L)*V1(L)/Z(I))/2
      UU(4,4)=(-SS+Z(L)*V1(L)/Z(I))/2
      DO 261 K1=1,4
      SUM=UU(K1,1)*AP(L)+UU(K1,2)*BP(L)+UU(K1,3)*CP(L)+UU(K1,4)
     &*DP(L)
      IF(K1-2) 180,190,200
180   AP(I)=SUM
      GOTO 261
190   BP(I)=SUM
      GOTO 261
200   IF(K1-3) 261,210,220
210   CP(I)=SUM
      GOTO 261
220   DP(I)=SUM
261   CONTINUE
      IF(I-NR) 230,231,230
231   BP(I)=BP(I)+FA1
      DP(I)=DP(I)-FA1
230   CONTINUE
 233 CONTINUE
C     PRINT, ' '
C     PRINT,' FORCE VIBRATION PARAMETER '
C     DO 118 K1=1,N
C     PRINT,' VECTOR NO. ', K1
C     WRITE(6,117) AP(K1),BP(K1),CP(K1),DP(K1)
C117  FORMAT(1X,4(2X,F15.10))
118   CONTINUE
      RETURN
      END
```

C8. Program BMDFA

Program BMDFA estimate the clearances of a beam-stop system using experimentally obtained data by the describing function approach.

```
C
C     PROGRAM BMDFA
C
C     A PROGRAM TO ESTIMATE CLEARANCES OF A BEAM-STOP
C     SYSTEM BY THE DESCRIBING FUNCTION APPROACH
C

      DIMENSION X1(2050,2),X2(2050,2),IG(11),Y1(2050),Y2(2050),L(2050,2)
      DIMENSION D(2),ED(2)
      COMMON PAI,TN0,TN1,S1,S2
C
C     INPUT FILE SYSPARA.DAT PROVIDE ALL NEEDED
C     SYSTEM PARAMETERS
C
C     INPUT FILE IN.DAT PROVIDES THE EXCITATION B(T)
C     AND RESPONSE Y2(T)
C
C     FILE HB1.DAT, HB2.DAT, HF1.DAT AND HF2.DAT
C     PROVIDE THE NEEDED FREQUENCY RESPONSE FUNCTIONS
C
C     DFA.DAT IS USED TO STORE RESULTS OF
C     ESTIMATION BY THE DESCRIBING FUNCTION APPROACH
C
      OPEN (UNIT=1, FILE='SYSPARA.DAT', STATUS='OLD')
      OPEN (UNIT=2, FILE='IN.DAT', STATUS='OLD')
      OPEN (UNIT=3, FILE='HB1.DAT', STATUS='OLD')
      OPEN (UNIT=7, FILE='HB2.DAT', STATUS='OLD')
      OPEN (UNIT=8, FILE='HF1.DAT', STATUS='OLD')
      OPEN (UNIT=9, FILE='HF2.DAT', STATUS='OLD')
      OPEN (UNIT=4, FILE='DFA.DAT', STATUS='NEW')
C
C     S1,S2 = STIFFNESS OF THE STOPS
C     D1,D2 = SIZE OF THE CLEARANCES
C     OM = FREQUENCY OF THE BASE EXCITATION
C     FLIM = LOW PASS FREQUENCY LIMIT
C     T = LENGTH OF TIME HISTORY
C     N = NUMBER OF SAMPLING POINTS
C     CO1,CO2 = COEFFICIENTS TO CALIBRATE SIGNALS
C           OBTAINED FROM MECHANICAL EXPERIMENTS
C
      READ (1,*) S1,S2,D1,D2,OM,FLIM,T,N,CO1,CO2
      WRITE(4,*) 'SYSTEM PARAMETERS'
      WRITE(4,*) 'STOP 1 SPRING COEFFECIENT=',S1,'N/M'
```

```
      WRITE(4,*) 'STOP 2 SPRING COEFFECIENT=',S2,'N/M'
      WRITE(4,*) 'CLEARANCE 1 =',D1,'M'
      WRITE(4,*) 'CLEARANCE 2 =',D2,'M'
      WRITE(4,*) 'SAMPLING RATE=',N/T,'1/S'
      WRITE(4,*) 'LENGTH OF RECORD=',T,'S'
      WRITE(4,*) 'EXCITATION FREQUENCY=',OM,'1/S'
      WRITE(4,*) 'FILTER FREQUENCY=',FLIM,'1/S'
      IPA=LOG(FLOAT(N))/LOG(2.0)+.001
      NN=N+1
      CALL MAIN (D1,D2,OM,IPA,T,N,NN,X1,X2,IG,Y1,Y2,L,CO1,CO2)
      STOP
      END
      SUBROUTINE MAIN
(D1,D2,OM,IPA,T,N,NN,X1,X2,IG,Y1,Y2,L,CO1,CO2)
      DIMENSION X1(NN,2),X2(NN,2),IG(IPA),Y1(NN),Y2(NN),L(NN,2)
      DIMENSION D(2),ED(2)
      COMMON PAI,TN0,TN1,S1,S2
      PAI=4.0*ATAN(1.0)
      XNI=OM*T+1.5
      OM=OM*2.0*PAI
      NI=IFIX(XNI)
      N2=N/2
      DT=T/N
      DT2=DT/2.0
      DF=1.0/T
      DFA=DF*2.0*PAI
      FE=-DFA
      N21=N2+1
C
C     READ IN THE EXCITATION B(T) AND
C     RESPONSE Y2(T)
C
      DO 5 I=1,N
 5    READ (2,*) X1(I,1),X1(I,2)
      DO 10 I=1,N
      X1(I,1)=X1(I,1)/CO1
      X2(I,1)=0.0
      X2(I,2)=0.0
10    X1(I,2)=-X1(I,2)/CO2
      ISIGN=-1
      NUM=1
C
C     FOURIER TRANSFORMING BOTH EXCITATION AND RESPONSE
C
      CALL FFT (IPA,X1,X2,N,NN,Y1,Y2,ISIGN,NUM,IG,L,K1,K2)
C
C     SHIFT Y2(T) BY DT/2
C
      DO 30 I=1,N21
      FE=FE+DFA
```

```
      TH=-FE*DT2
      HI=SIN(TH)
      HR=COS(TH)
      IN=N-I+2
      RR=X1(I,K2)*HR-X2(I,K2)*HI
      RI=X1(I,K2)*HI+X2(I,K2)*HR
      X1(I,2)=RR
      X2(I,2)=RI
      X1(IN,2)=X1(I,2)
 30   X2(IN,2)=-X2(I,2)
      X2(N21,2)=-X2(N21,2)
      WRITE(4,*) 'RESULTS OF DESCRIBING FUNCTION METHOD'
      WRITE(4,*) 'B0RE=',Y1(1)/N,'B0IM=',Y2(1)/N
      WRITE(4,*) 'B1RE=',Y1(NI)/N2,'B1IM=',Y2(NI)/N2
      WRITE(4,*) 'Y2ORE=',X1(1,2)/N,'Y20IM=',X2(1,2)/N
      WRITE(4,*) 'Y21RE=',X1(NI,2)/N2,'Y21IM=',X2(NI,2)/N2
C
C     READ IN THE NEEDED FREQUENCY RESPONSE
C     FUNCTION VALUES
C
      DO 35 I=1,NI
      READ (3,*) THB1
      READ (7,*) THB2
      READ (8,*) THF1
      READ (9,*) THF2
      IF(I.EQ.1) THEN
      THB10=THB1
      THB20=THB2
      THF10=THF1
      THF20=THF2
      ELSE
      END IF
 35   CONTINUE
      WRITE(4,*) 'HB10 AND HB11=',THB10, THB1
      WRITE(4,*) 'HB20 AND HB21=',THB20, THB2
      WRITE(4,*) 'HF10 AND HF11=',THF10, THF1
      WRITE(4,*) 'HF20 AND HF21=',THF20, THF2
C
C     CALCULATE THE CONSTANT AND FUNDAMENTAL
C     COMPONENTS OF U AND Y1
C
      U0=(-X1(1,2)+Y1(1)*THB10)/THF10
      URE=(-X1(NI,2)+Y1(NI)*THB1)/THF1
      UIM=(-X2(NI,2)+Y2(NI)*THB1)/THF1
      Y20=THB20*Y1(1)-U0*THF20
      Y2RE=THB2*Y1(NI)-URE*THF2
      Y2IM=THB2*Y2(NI)-UIM*THF2
      Y2A=Y2RE*Y2RE+Y2IM*Y2IM
      Y2AS=SQRT(Y2A)
C
```

```
C     CALCULATE THE DESCRIBING FUNCTION VALUES
C
      TN0=U0/Y2AS/2.0
      TN1RE=(URE*Y2RE+UIM*Y2IM)/Y2A
      TN1IM=(UIM*Y2RE-URE*Y2IM)/Y2A
      TN1A=SQRT(TN1RE*TN1RE+TN1IM*TN1IM)
      WRITE(4,*) 'U0=',U0/N,'U1RE=',URE/N2,'U1IM=',UIM/N2
      WRITE(4,*) 'Y10=',Y20/N,'Y11RE=',Y2RE/N2,'Y11IM=',Y2IM/N2
    WRITE(4,*) 'Y1A=',Y2AS/N2
      WRITE(4,*) 'N0=',TN0,'N1RE=',TN1RE,'N1IM=',TN1IM,'N1A=',TN1A
    IF(TN1RE.LT.0.0) TN1RE=0.0
      TN0=2.0*PAI*TN0
      TN1=PAI*(S1+S2)/2.0-PAI*TN1RE
      D(1)=1.5
      D(2)=1.5
C
C     SEARCH FOR THETA1 AND THETA2
C
      CALL POWELL(D,ED,FY,2,5000,ICOVG,0.0001,0.0001,1)
      WRITE(4,1)ED,FY,ICOVG
C
C     CALCULATE THE ESTIMATED VALUES OF CLEARANCES
C
      ED(1)=(Y2AS*SIN(ED(1))-Y20)/N2
      ED(2)=(Y2AS*SIN(ED(2))+Y20)/N2
      WRITE(4,*) 'ESTIMATED VALUES OF CLEARANCES'
      WRITE(4,2)ED
      ER1=ABS(D1-ED(1))/D1
      ER2=ABS(D2-ED(2))/D2
      WRITE(4,*) 'RELATIVE ERROR OF ESTIMATION'
      WRITE(4,2)ER1,ER2
 1    FORMAT(5X,3E21.10,2X,I5//)
 2    FORMAT(5X,3E21.10/)
 70   CLOSE (UNIT=1, STATUS='KEEP')
      CLOSE (UNIT=2, STATUS='KEEP')
      CLOSE (UNIT=3, STATUS='KEEP')
      CLOSE (UNIT=4, STATUS='KEEP')
      CLOSE (UNIT=7, STATUS='KEEP')
      CLOSE (UNIT=9, STATUS='KEEP')
      CLOSE (UNIT=8, STATUS='KEEP')
      RETURN
      END
C
C     A SUBROUTINE TO GENERATE AN OBJECTIVE FUNCTION
C     USED IN THE SUBROUTINE POWELL WHERE ROOTS
C     OF NONLINEAR EQUATIONS ARE FOUND BY SEARCHING
C     THE MINIMUM OT THE OBJECTIVE FUNCTION
C
      SUBROUTINE OBF(X,FX)
      DIMENSION X(2)
```

```
      COMMON PAI,TN0,TN1,S1,S2
      SZ1=SIN(X(2))
      CZ1=COS(X(2))
      SZ2=SIN(X(1))
      CZ2=COS(X(1))
      Z1=ATAN(SZ1/CZ1)
      Z2=ATAN(SZ2/CZ2)
      PAI2=2.*PAI
      FX=(S2*(-SZ1*(PAI-2.0*Z1)+2.0*CZ1)+S1*(SZ2*(PAI-2.0*Z2)-2.*CZ2)
     &-TN0)**2
      FX=FX+(S2*(Z1+SZ1*CZ1)+S1*(Z2+SZ2*CZ2)-TN1)**2
      RETURN
      END
```

C9. Program BMOPA

Program BMOPA estimate the clearances and impact forces of a beam-stop system using experimentally obtained data by the optimization approach.

```
C
C     PROGRAM BMOPA
C
C     A PROGRAM TO ESTIMATE CLEARANCES OF A BEAM-STOP
C     SYSTEM BY THE OPTIMIZATION APPROACH
C
      DIMENSION BWUY(2048,10)
      DIMENSION X1(2050,2),X2(2050,2),IG(11),Y1(2050),Y2(2050),L(2050,2)
      DIMENSION D(2),ED(2)
      COMMON /P/PAI /O/S1,S2,N21,YMIN,YMAX
C
C     INPUT FILE SYSPARA.DAT PROVIDE ALL NEEDED
C     SYSTEM PARAMETERS
C
C     INPUT FILE IN.DAT PROVIDES THE EXCITATION B(T)
C     AND RESPONSE Y2(T)
C
C     FILE HB1.DAT, HB2.DAT, HF1.DAT AND HF2.DAT
C     PROVIDE THE NEEDED FREQUENCY RESPONSE FUNCTIONS
C
C     BYU.DAT IS USED TO STORE TIME HISTORIES OF
C     B(T), Y2(T), U(T),Y1(T) AND UHAT(T)
C
C     BYUF.DAT IS USED TO STORE SPECTRA
C     B(F), Y2(F), U(F), Y1(F) AND UHAT(F)
C
C     OPA.DAT IS USED TO STORE RESULTS OF
C     ESTIMATION BY THE OPTIMIZATION FUNCTION APPROACH
C
      OPEN (UNIT=1, FILE='SYSPARA.DAT', STATUS='OLD')
      OPEN (UNIT=2, FILE='IN.DAT', STATUS='OLD')
      OPEN (UNIT=3, FILE='BYU.DAT', STATUS='NEW')
      OPEN (UNIT=8, FILE='BYUF.DAT', STATUS='NEW')
      OPEN (UNIT=9, FILE='HB1.DAT', STATUS='OLD')
      OPEN (UNIT=10, FILE='HB2.DAT', STATUS='OLD')
      OPEN (UNIT=11, FILE='HF1.DAT', STATUS='OLD')
      OPEN (UNIT=12, FILE='HF2.DAT', STATUS='OLD')
      OPEN (UNIT=4, FILE='OPA.DAT', STATUS='NEW')
C
C     S1,S2 = STIFFNESS OF THE STOPS
C     D1,D2 = SIZE OF THE CLEARANCES
C     OM = FREQUENCY OF THE BASE EXCITATION
C     FLIM = LOW PASS FREQUENCY LIMIT
```

```
C     T = LENGTH OF TIME HISTORY
C     N = NUMBER OF SAMPLING POINTS
C     CO1,CO2 = COEFFICIENTS TO CALIBRATE SIGNALS
C           OBTAINED FROM MECHANICAL EXPERIMENTS
C
      READ (1,*) S1,S2,D1,D2,OM,FLIM,T,N,CO1,CO2
      IPA=LOG(FLOAT(N))/LOG(2.0)+.001
      NN=N+1
      CALL MAIN
(D1,D2,OM,IPA,T,N,NN,X1,X2,IG,Y1,Y2,L,CO1,CO2,BWUY,FLIM)
      STOP
      END
      SUBROUTINE MAIN (D1,D2,OM,IPA,T,N,NN,X1,X2,IG,Y1,Y2,L,CO1,
     &CO2,BWUY,FLIM)
      DIMENSION BWUY(N,10)
      DIMENSION X1(NN,2),X2(NN,2),IG(IPA),Y1(NN),Y2(NN),L(NN,2)
      DIMENSION D(2),ED(2)
      COMMON /P/PAI /O/S1,S2,N21,YMIN,YMAX
      PAI=4.0*ATAN(1.0)
      OM=OM*2.0*PAI
      N2=N/2
      DT=T/N
      NLIM=FLIM*T+1.01
      DT2=DT/2.0
      DF=1.0/T
      DFA=DF*2.0*PAI
      FE=-DFA
      N21=N2+1
      IF(NLIM.GT.N21) NLIM=N21
C
C     READ IN THE EXCITATION B(T) AND
C     RESPONSE Y2(T)
C
      DO 5 I=1,N
  5   READ (2,*) X1(I,1),X1(I,2)
      DO 10 I=1,N
      X1(I,1)=X1(I,1)/CO1
      BWUY(I,1)=X1(I,1)*1000.0
      X2(I,1)=0.0
      X2(I,2)=0.0
      X1(I,2)=-X1(I,2)/CO2
 10   BWUY(I,2)=X1(I,2)*1000.0
      ISIGN=-1
      NUM=1
C
C     FOURIER TRANSFORMING BOTH B(T) AND Y2(T)
C
      CALL FFT (IPA,X1,X2,N,NN,Y1,Y2,ISIGN,NUM,IG,L,K1,K2)
C
C     SHIFT Y2 BY DT/2
```

```
C
      DO 30 I=1,N21
      FE=FE+DFA
      TH=-FE*DT2
      HI=SIN(TH)
      HR=COS(TH)
      IN=N-I+2
      RR=X1(I,K2)*HR-X2(I,K2)*HI
      RI=X1(I,K2)*HI+X2(I,K2)*HR
      X1(I,2)=RR
      X2(I,2)=RI
      X1(IN,2)=X1(I,2)
 30   X2(IN,2)=-X2(I,2)
      X2(N21,2)=-X2(N21,2)
      DO 401 I=1,N21
      BWUY(I,6)=SQRT((Y1(I)*Y1(I)+Y2(I)*Y2(I)))/N2*1000.0
401   BWUY(I,7)=SQRT((X1(I,2)*X1(I,2)+X2(I,2)*X2(I,2)))
     &/N2*1000.0
      Y1M=0.0
      DO 411 I=1,N21
      IF(BWUY(I,7).GT.Y1M) Y1M=BWUY(I,7)
      IF(BWUY(I,7).GT.(0.001*Y1M)) LIM=I
411   CONTINUE
      IF(NLIM.GT.LIM) NLIM=LIM
C
C     READ IN THE FREQUENCY RESPONSE FUNCTIONS
C
      DO 35 I=1,NLIM
      READ (9,*) THB1
      READ (10,*) THB2
      READ (11,*) THF1
      READ (12,*) THF2
C
C     CALCULATE TRANSFORMED IMPACT FORCE U(F)
C     AND Y1(F)
C
      IN=N-I+2
      URE=(-X1(I,2)+Y1(I)*THB1)/THF1
      UIM=(-X2(I,2)+Y2(I)*THB1)/THF1
      X1(I,1)=THB2*Y1(I)-URE*THF2
      X2(I,1)=THB2*Y2(I)-UIM*THF2
      X1(I,2)=URE
      X2(I,2)=UIM
      X1(IN,1)=X1(I,1)
      X2(IN,1)=-X2(I,1)
      X1(IN,2)=X1(I,2)
 35   X2(IN,2)=-X2(I,2)
      IF(NLIM.EQ.N21) GOTO 536
      NLIM1=NLIM+1
      DO 535 I=NLIM1,N21
```

```
      IN=N-I+2
      X1(I,1)=0.0
      X1(I,2)=0.0
      X2(I,1)=0.0
      X2(I,2)=0.0
      X1(IN,1)=0.0
      X1(IN,2)=0.0
      X2(IN,1)=0.0
 535  X2(IN,2)=0.0
 536  X2(N21,2)=-X2(N21,2)
      X2(N21,1)=-X2(N21,1)
      DO 402 I=1,N21
      BWUY(I,8)=SQRT((X1(I,2)*X1(I,2)+X2(I,2)*X2(I,2)))/N2
 402  BWUY(I,9)=SQRT((X1(I,1)*X1(I,1)+X2(I,1)*X2(I,1)))/
     &N2*1000.0
      NUM=1
      ISIGN=1
C
C     FIND U(T) AND Y1(T)
C     BY INVERSE FOURIER TRANSFORMATION
C
      CALL FFT (IPA,X1,X2,N,NN,Y1,Y2,ISIGN,NUM,IG,L,K1,K2)
      DO 25 I=1,N
      BWUY(I,4)=Y1(I)*1000.0
      Y2(I)=Y1(I)
 25   CONTINUE
C
C     FIND THE MAXIMUM AND MINIMUM OF Y1(T)
C
      YMIN=0.0
      YMAX=0.0
      DO 37 I=1,N
      IF(Y2(I).LT.YMIN) YMIN=Y2(I)
      IF(Y2(I).GT.YMAX) YMAX=Y2(I)
 37   CONTINUE
      DO 365 I=1,N
    BWUY(I,3)=X1(I,K2)
 365  Y1(I)=X1(I,K2)
      D(1)=0.0
      D(2)=0.0
C
C     USE POWELL METHOD THE SEARCH THE MINIMUM
C     OF OBJECTIVE FUNCTION J
C
      CALL POWELL(D,ED,FY,2,5000,ICOVG,0.0001,0.0001,1,
     &NN,Y2,Y1)
C
C     CALCULATE THE OPTIMALLY ESTIMATED
C     IMPACT FORCES UHAT(T)
C
```

```
      DO 901 I=1,N
      YY2=Y2(I)
      IF(YY2.LE.-D(1)) UT=S1*(YY2+D(1))
      IF((YY2.GT.-D(1)).AND.(YY2.LT.D(2))) UT=0.0
      IF(YY2.GE.D(2)) UT=S2*(YY2-D(2))
      X1(I,1)=UT
      X2(I,1)=0.0
 901  BWUY(I,5)=UT
      NUM=0
      ISIGN=-1
      CALL FFT (IPA,X1,X2,N,NN,Y1,Y2,ISIGN,NUM,IG,L,K1,K2)
      DO 403 I=1,N21
 403  BWUY(I,10)=SQRT((X1(I,K2)*X1(I,K2)+X2(I,K2)*
     &X2(I,K2)))/N2
      WRITE(4,*) 'RESULTS OF OPTIMAL METHODS'
      WRITE(4,*) 'NLIM=',NLIM
      WRITE(4,1)ED,FY,ICOVG
      WRITE(4,*) 'ESTIMATED VALUES OF CLEARANCES'
      WRITE(4,2)ED
      ER1=ABS(D1-ED(1))/D1
      ER2=ABS(D2-ED(2))/D2
      WRITE(4,*) 'RELATIVE ERROR OF ESTIMATION'
      WRITE(4,2)ER1,ER2
      DO 404 I=1,N
 404  WRITE(3,3) (BWUY(I,J),J=1,5)
      DO 406 I=1,N21
 406  WRITE(8,3) (BWUY(I,J),J=6,10)
 1    FORMAT(5X,3E21.10,2X,I5//)
 2    FORMAT(5X,2E21.10/)
 3    FORMAT(1X,5(1X,E15.7))
 70   CLOSE (UNIT=1, STATUS='KEEP')
      CLOSE (UNIT=2, STATUS='KEEP')
      CLOSE (UNIT=3, STATUS='KEEP')
      CLOSE (UNIT=4, STATUS='KEEP')
      CLOSE (UNIT=8, STATUS='KEEP')
      CLOSE (UNIT=12, STATUS='KEEP')
      CLOSE (UNIT=9, STATUS='KEEP')
      CLOSE (UNIT=10, STATUS='KEEP')
      CLOSE (UNIT=11, STATUS='KEEP')
      RETURN
      END
C
C     A SUBROUTINE TO CALCULATE THE OBJECTIVE
C     FUNCTION J
C
      SUBROUTINE OBF(X,FX,NN,Y2,Y1)
      COMMON /P/PAI /O/S1,S2,N21,YMIN,YMAX
      DIMENSION X(2),Y2(NN),Y1(NN)
      SUM=0.0
      N=NN-1
```

```
      N1=N/16
      N2=N-N1
      DO 10 I=N1,N2
      YY2=Y2(I)
      IF(YY2.LE.-X(1)) T=Y1(I)-S1*(YY2+X(1))
      IF((YY2.GT.-X(1)).AND.(YY2.LT.X(2))) T=Y1(I)
      IF(YY2.GE.X(2)) T=Y1(I)-S2*(YY2-X(2))
10    SUM=SUM+T*T
      FX=SUM/(N2-N1)
      IF(-X(1).LT.YMIN) FX=FX+(S1*(YMIN+X(1)))**2
      IF(X(2).GT.YMAX) FX=FX+(S2*(YMAX-X(2)))**2
      RETURN
      END
```

C10. Program BMSPA

Program BMSPA estimate the clearances of a beam-stop system using experimentally obtained data by the spectrum analysis approach.

```
C
C     PROGRAM BMSPA
C
C     A PROGRAM USING THE RESPONSE OF
C     A BEAM-STOP SYSTEM UNDER A RANDOM EXCITATION
C     TO ESTIMATE THE CLEARANCES
C     BY THE SPECTRUM ANALYSIS APPROACH
C
      IMPLICIT REAL*8(A-H,O-Z)
      DIMENSION X1(2048,2),X2(2048,2),IG(11),Y1(2048),
     &Y2(2048),L(2048,2)
      DIMENSION TB1(1024),TB2(1024),TF1(1024),TF2(1024)
      DIMENSION A(2048),B(2,2048)
      COMMON/DD/ D(2),ED(2)
      COMMON PAI,EW0,EW1,S1,S2,D1,D2,EV,EM
C
C     INPUT FILE SYSPARA.DAT PROVIDE ALL NEEDED
C     SYSTEM PARAMETERS
C
C     INPUT FILE IN.DAT PROVIDE THE NEEDED
C     SAMPLED RECORDS OF RANDOM EXCITATION B(T)
C     AND RESPONSE Y2(T)
C
C     FILE HB1.DAT, HB2.DAT, HF1.DAT AND HF2.DAT
C     PROVIDE THE NEEDED FREQUENCY RESPONSE FUNCTIONS
C
C     TI.DAT IS USED TO STORE TYPICAL SAMPLE OF
C     EXCITATION AND RESPONSE
C
C     FTI.DAT IS USED TO STORE THE FOURIER
C     TRANSFORM OF THE EXCITATION AND RESPONSE
C
C     SP.DAT IS USED TO STORE THE POWER AND CROSS SPECTRUM
C
C     SPA.DAT IS USED TO STORE RESULTS OF
C     ESTIMATION BY THE SPECTRUM ANALYSIS APPROACH
C
      OPEN (UNIT=2, FILE='RANEX.DAT', STATUS='OLD')
      OPEN (UNIT=3, FILE='TI.DAT', STATUS='NEW')
      OPEN (UNIT=13, FILE='FTI.DAT', STATUS='NEW')
      OPEN (UNIT=8, FILE='SP.DAT', STATUS='NEW')
      OPEN (UNIT=9, FILE='HB1.DAT', STATUS='OLD')
      OPEN (UNIT=10, FILE='HB2.DAT', STATUS='OLD')
```

```
      OPEN (UNIT=11, FILE='HF1.DAT', STATUS='OLD')
      OPEN (UNIT=12, FILE='HF2.DAT', STATUS='OLD')
      OPEN (UNIT=1, FILE='IN.DAT', STATUS='OLD')
      OPEN (UNIT=4, FILE='SPA.DAT', STATUS='NEW')
C
C     S1,S2 = STIFFNESS OF THE STOPS
C     D1,D2 = SIZE OF THE CLEARANCES
C     OM = FREQUENCY OF THE BASE EXCITATION
C     FLIM = LOW PASS FREQUENCY LIMIT
C     TMAX = LENGTH OF A PIECE OF TIME HISTORY SAMPLE
C     M = NUMBER OF SAMPLE RECORDS
C     N = NUMBER OF SAMPLING POINTS
C     CO1,CO2 = COEFFICIENTS TO CALIBRATE SIGNALS
C           OBTAINED FROM MECHANICAL EXPERIMENTS
C
      READ (2,*) S1,S2,D1,D2,TMAX,M,N,CO1,CO2,FLIM
      WRITE(4,*) 'SYSTEM PARAMETERS'
      WRITE(4,*) 'STOP 1 SPRING COEFFECIENT=',S1,'N/M'
      WRITE(4,*) 'STOP 2 SPRING COEFFECIENT=',S2,'N/M'
      WRITE(4,*) 'CLEARANCE 1 =',D1,'M'
      WRITE(4,*) 'CLEARANCE 2 =',D2,'M'
      WRITE(4,*) 'SAMPLING RATE=',N/TMAX,'1/S'
      WRITE(4,*) 'LENGTH OF RECORD=',TMAX,'S'
      WRITE(4,*) 'NUMBER OF SAMPLE =',M
      WRITE(4,*) 'POINT OF EACH SAMPLE =',N
      WRITE(4,*) 'FILTER FREQUENCY =', FLIM
      IPA=LOG(FLOAT(N))/LOG(2.0)+.001
      N=2**IPA
      WRITE(6,*) 'N =',N
      CALL MAIN (IPA,X1,X2,N,M,Y1,Y2,IG,L,A,B,TMAX,
     &CO1,CO2,TB1,TB2,TF1,TF2,FLIM)
      STOP
      END
      SUBROUTINE MAIN (IPA,X1,X2,N,M,Y1,Y2,IG,L,A,B,TMAX,
     &CO1,CO2,TB1,TB2,TF1,TF2,FLIM)
      IMPLICIT REAL*8(A-H,O-Z)
      DIMENSION X1(N,2),X2(N,2),IG(IPA),Y1(N),Y2(N),L(N,2)
      DIMENSION TB1(N),TB2(N),TF1(N),TF2(N)
      DIMENSION A(N),B(2,N)
      COMMON/DD/ D(2),ED(2)
      COMMON PAI,EW0,EW1,S1,S2,D1,D2,EV,EM
      PAI=4.0D0*DATAN(1.0D0)
      SIGN=-1.
      MN=M*N
      NUM=1
      N2=N/2.0
      DF=1.0/TMAX
      DFA=DF*2.0*PAI
      DT=TMAX/N
      NLIM=FLIM*TMAX+1.01
```

```
      WRITE(6,*) 'NLIM=',NLIM
      DT2=DT/2.0
      N21=N2+1
      IF(NLIM.GT.N21) NLIM=N21
C
C     READ IN THE NEEDED FREQUENCY RESPONSE
C     FUNCTIONS
C
      DO 7 I=1,N21
      READ (9,*) BH1
      READ (10,*) BH2
      READ (11,*) FH1
      READ (12,*) FH2
      TB1(I)=BH1
      TB2(I)=BH2
      TF1(I)=FH1
    7 TF2(I)=FH2
      N1=N-1
      DO 11 I=1,N
      A(I)=0.0
      B(1,I)=0.0
   11 B(2,I)=0.0
      EM=0.0
      EV=0.0
      EMU=0.0
      DO 50 J=1,M
C
C     READ IN A SAMPLE RECORD OF
C     BASE EXCITATION B(T) AND
C     DISPLACEMENT AT POINT 2 Y2(T)
C
      DO 5 I=1,N
    5 READ (1,*) X1(I,1),X1(I,2)
      DO 10 I=1,N
      X1(I,1)=X1(I,1)/CO1
      X2(I,1)=0.0
      X2(I,2)=0.0
      X1(I,2)=-X1(I,2)/CO2
   10 CONTINUE
      SIGN=-1
      NUM=1
C
C     FOURIER TRANSFORMING EXCITATION B(T)
C     AND RESPONSE Y2(T)
C
      CALL FFT (IPA,X1,X2,N,Y1,Y2,SIGN,NUM,IG,L,K1,K2)
C
C     SHIFT Y2(T) BY DT/2 IN FREQUENCY DOMAIN
C
      FE=-DFA
```

```
      DO 30 I=1,N21
      FE=FE+DFA
      TH=-FE*DT2
      HI=SIN(TH)
      HR=COS(TH)
      IN=N-I+2
      RR=X1(I,K2)*HR-X2(I,K2)*HI
      RI=X1(I,K2)*HI+X2(I,K2)*HR
      X1(I,K2)=RR
      X2(I,K2)=RI
      IF(IN.GT.N) GOTO 30
      X1(IN,K2)=X1(I,K2)
      X2(IN,K2)=-X2(I,K2)
 30   CONTINUE
      X2(N21,K2)=-X2(N21,K2)
      IF(J.GE.2) GOTO 17
      DO 35 I=1,N
      X1(I,1)=X1(I,K2)
      X2(I,1)=X2(I,K2)
      X1(I,2)=Y1(I)
 35   X2(I,2)=Y2(I)
      WRITE(4,*) 'B0=',Y1(1)/N
      WRITE(4,*) 'Y20=',X1(1,1)/N
      SIGN=1
      NUM=1
      CALL FFT (IPA,X1,X2,N,Y1,Y2,SIGN,NUM,IG,L,K1,K2)
      DO 37 I=1,N
      X1(I,1)=X1(I,K2)
      X2(I,1)=X2(I,K2)
      X1(I,2)=Y1(I)
 37   X2(I,2)=Y2(I)
      DO 38 I=1,N
 38   WRITE(3,3) X1(I,1)*1000.0,X1(I,2)*1000.0
      SIGN=-1.
      NUM=1
      CALL FFT (IPA,X1,X2,N,Y1,Y2,SIGN,NUM,IG,L,K1,K2)
      DO 39 IV=1,N2
      BA=SQRT(Y1(IV)*Y1(IV)+Y2(IV)*Y2(IV))/N2*1000.0
      Y1A=SQRT(X1(IV,K2)*X1(IV,K2)+X2(IV,K2)*X2(IV,K2))
     &/N2*1000.0
 39   WRITE(13,3) BA,Y1A
C
C     CALCULATE THE TRANSFORMED IMPACT FORCE U(F)
C     AND DISPLACEMENT AT STOP LOCATION Y1(F)
C
 17   DO 130 IV=1,NLIM
      URE=(-X1(IV,K2)+Y1(IV)*TB1(IV))/TF1(IV)
      UIM=(-X2(IV,K2)+Y2(IV)*TB1(IV))/TF1(IV)
      X1(IV,K2)=TB2(IV)*Y1(IV)-URE*TF2(IV)
      X2(IV,K2)=TB2(IV)*Y2(IV)-UIM*TF2(IV)
```

```
      Y1(IV)=URE
  130 Y2(IV)=UIM
      DO 135 IW=2,N2
      IN=N-IW+2
      Y1(IN)=Y1(IW)
  135 Y2(IN)=-Y2(IW)
      EM=EM+X1(1,K2)
      EMU=EMU+Y1(1)
      DO 33 IZ=1,NLIM
      BR=Y1(IZ)*X1(IZ,K2)+Y2(IZ)*X2(IZ,K2)
      BI=Y1(IZ)*X2(IZ,K2)-Y2(IZ)*X1(IZ,K2)
      B(1,IZ)=B(1,IZ)+BR
      B(2,IZ)=B(2,IZ)+BI
      AA=X1(IZ,K2)*X1(IZ,K2)+X2(IZ,K2)*X2(IZ,K2)
   33 A(IZ)=A(IZ)+AA
      DO 137 IZ=2,NLIM
      IN=N-IZ+2
      X1(IZ,1)=X1(IZ,K2)
      X2(IZ,1)=X2(IZ,K2)
      X1(IN,1)=X1(IZ,1)
  137 X2(IN,1)=-X2(IZ,1)
      X1(1,1)=X1(1,K2)
      X2(1,1)=X2(1,K2)
      IF(NLIM.EQ.N21) GOTO 139
      NLIM1=NLIM+1
      DO 147 IZ=NLIM1,N21
      IN=N-IZ+2
      X1(IZ,1)=0.0
      X2(IZ,1)=0.0
      X1(IN,1)=0.0
  147 X2(IN,1)=0.0
  139 X2(N21,1)=-X2(N21,1)
      SIGN=1
      NUM=0
C
C     FIND Y1(T) BY INVERSE FOURIER TRANSFORM
C
      CALL FFT (IPA,X1,X2,N,Y1,Y2,SIGN,NUM,IG,L,K1,K2)
C
C     CALCULATE VARIANCE OF Y1(T)
C
      DO 237 I=1,N
  237 EV=EV+X1(I,K2)*X1(I,K2)
   50 CONTINUE
      EM=EM/MN
      EMU=EMU/MN
      EV=(EV-MN*EM*EM)/(MN-1)
      EV=SQRT(EV)
      WRITE(4,*) 'ESTIMATE OF MEAN VALUE OF Y1 =',EM
      WRITE(4,*) 'ESTIMATE OF MEAN VALUE OF U =',EMU
```

```
      WRITE(4,*) 'ESTIMATE OF VARIANCE OF Y1 =',EV
      DN1R=(D1+EM)/(1.414213562*EV)
      DN2R=(D2-EM)/(1.414213562*EV)
      DN1=DN1R*DN1R
      DN2=DN2R*DN2R
      EPS=1.0E-8
      ERFC1=1.0-ER(DN1R,EPS)
      ERFC2=1.0-ER(DN2R,EPS)
      WRITE(4,*) 'ERFC1=',ERFC1
      WRITE(4,*) 'ERFC2=',ERFC2
C
C     CALCULATE W0 AND W1 USING ACTUAL CLEARANCES
C     THIS IS NOT NEEDED FOR ESTIMATION PURPOSE
C     ONLY FOR STUDY PURPOSE
C
      W0=EV*(S2*EXP(-DN2)-S1*EXP(-DN1))/SQRT(2.0*PAI)-
     &(S2*(D2-EM)*ERFC2-S1*(D1+EM)*ERFC1)/2.0
      WRITE(4,*) 'W0=',W0
      W1=EV*(S2*ERFC2+S1*ERFC1)/2.0
      WRITE(4,*) 'W1=',W1
      DO 55 I=1,N2
      A(I)=A(I)/MN
      B(1,I)=B(1,I)/MN
 55   B(2,I)=B(2,I)/MN
      DO 56 I=1,NLIM
      BAMP=SQRT(B(1,I)*B(1,I)+B(2,I)*B(2,I))*1000.0
 56   WRITE(8,3) A(I)*1000000.0,BAMP
      SUMD=0.0
      SUMN=0.0
      DO 60 I=11,NLIM
      BB=B(1,I)*B(1,I)+B(2,I)*B(2,I)
      BB=SQRT(BB)
      SUMD=SUMD+A(I)
      SUMN=SUMN+BB
 60   CONTINUE
C
C     ESTIMATE W1 FROM POWER AND CROSS SPECTRA
C     ESTIMATE W0 BY MEAN VALUE OF U(T)
C
      EW1=EV*SUMN/SUMD
      WRITE(4,*) 'ESTIMATE OF W1=',EW1
      EW0=EMU
      WRITE(4,*) 'ESTIMATE OF W0=',EW0
      D(1)=EV
      D(2)=EV
C
C     ESTIMATE CLEARANCES USING ESTIMATED W0 & W1
C
      CALL POWELL(D,ED,FY,2,5000,ICOVG,0.001,0.001,1)
      WRITE(4,*)ED,FY,ICOVG
```

```
      WRITE(4,*) 'ESTIMATED VALUES OF CLEARANCES'
      WRITE(4,*)ED
      ER1=ABS(D1-ED(1))/D1
      ER2=ABS(D2-ED(2))/D2
      WRITE(4,*) 'RELATIVE ERROR OF ESTIMATION'
      WRITE(4,*)ER1,ER2
    3 FORMAT(1X,2(1X,E15.7))
      CLOSE (UNIT=1, STATUS='KEEP')
      CLOSE (UNIT=2, STATUS='KEEP')
      CLOSE (UNIT=3, STATUS='KEEP')
      CLOSE (UNIT=13, STATUS='KEEP')
      CLOSE (UNIT=8, STATUS='KEEP')
      CLOSE (UNIT=4, STATUS='KEEP')
      CLOSE (UNIT=9, STATUS='KEEP')
      CLOSE (UNIT=10, STATUS='KEEP')
      CLOSE (UNIT=11, STATUS='KEEP')
      CLOSE (UNIT=12, STATUS='KEEP')
      RETURN
      END
C
C     A SUBROUTINE TO GENERATE AN OBJECTIVE FUNCTION
C     USED IN THE SUBROUTINE POWELL WHERE ROOTS
C     OF NONLINEAR EQUATIONS ARE FOUND BY SEARCHING
C     THE MINIMUM OT THE OBJECTIVE FUNCTION
C
      SUBROUTINE OBF(X,FX)
      IMPLICIT REAL*8(A-H,O-Z)
      DIMENSION X(2)
      COMMON PAI,EW0,EW1,S1,S2,D1,D2,EV,EM
      DN1R=(X(1)+EM)/(1.414213562*EV)
      DN2R=(X(2)-EM)/(1.414213562*EV)
      DN1=DN1R*DN1R
      DN2=DN2R*DN2R
      EPS=1.0E-8
      ERFC1=1.0-ER(DN1R,EPS)
      ERFC2=1.0-ER(DN2R,EPS)
      W0=EV*(S2*EXP(-DN2)-S1*EXP(-DN1))/SQRT(2.0*PAI)-
     &(S2*(X(2)-EM)*ERFC2-S1*(X(1)+EM)*ERFC1)/2.0
      W1=EV*(S2*ERFC2+S1*ERFC1)/2.0
      FX=(EW1-W1)**2+(EW0-W0)**2
      XMAX=3.0*EV-EM
      XMIN=3.0*EV+EM
      IF(X(1).LT.0) FX=FX+S1*X(1)*X(1)
      IF(X(2).LT.0) FX=FX+S2*X(2)*X(2)
      IF(X(1).GT.XMIN) FX=FX+S1*(X(1)-XMIN)*(X(1)-XMIN)
      IF(X(2).GT.XMAX) FX=FX+S2*(X(2)-XMAX)*(X(2)-XMAX)
      RETURN
      END
```

C11. Function ER

A function used in the Programs SPASIMU, SPAEX and BMSPA to calculate the error function.

```
C
C     A FUNCTION TO CALCULATE THE ERROR FUNCTION
C
      FUNCTION ER(B,EPS)
      IMPLICIT REAL*8(A-H,O-Z)
      IF(B.LT.0.0) THEN
      SGN=-1.0
      B=-B
      ELSE
      SGN=1.0
      ENDIF
      IF(B.LT.6.0) GOTO 7
      ER=1.0*SGN
      RETURN
 7    IF(B.GE.1.0) GOTO 20
      X=B
      BI=3.0
      AI=1.0
      AC=-1.0
      AX=X*X
      AB=AX*X/BI
      ER=X-AB
 10   AI=AI+1.0
      BI=BI+2.0
      AC=-AC
      AB=AB/BI*AX*(BI-2.0)/AI
      ER=ER+SIGN(AB,AC)
      IF(ABS(AB).GE.EPS) GOTO 10
      ER=ER*1.128379167*SGN
      RETURN
 20   V=0.5/B/B
      XE=B*EXP(B*B)
      P0=1.0
      Q0=1.0
      P1=1.0
      ER0=1.0
      N=2
      Q1=1.0+V
 30   RN=N
      AN=RN*V
      PN=P1+AN*P0
      QN=Q1+AN*Q0
      P0=P1
```

```
      Q0=Q1
      P1=PN
      Q1=QN
      N=N+1
      ER=PN/QN
      IF(ABS(ER-ER0).LT.EPS) GOTO 40
      ER0=ER
      GOTO 30
40    ER=(1.0-ER/XE*0.5641895835)*SGN
      RETURN
      END
```

C12. Subroutine FFT

Subroutine FFT is used in above estimation programs to perform forward and inverse Fourier transform.

```
C
C     SUBROUTINE FFT
C
C     A SUBROUTINE TO PERFORM FORWARD AND
C     INVERSE FOURIER TRANSFORM
C
      SUBROUTINE FFT (IPA,X1,X2,N,NN,Y1,Y2,ISIGN,NUM,IG,L,K1,K2)
      DIMENSION X1(NN,2),X2(NN,2),IG(IPA),Y1(NN),Y2(NN),L(NN,2)
      COMMON PAI,TN0,TN1,S1,S2
      AG=2.0D0*PAI/N
      IF (NUM.EQ.0) GOTO 4
      DO 5 I=1,N
      Y1(I)=X1(I,2)
 5    Y2(I)=X2(I,2)
 4    MM=NUM
 6    ME=1
      K1=1
      K2=2
      DO 7 K=1,IPA
      IG(K)=N/2**K
      IGK=IG(K)
      IAS=IGK
      M2=(2**K)
      IP=2**(K-1)
      LA=-IP
      DO 8 I=1,IAS
      LA=LA+IP
      MX=-IGK*2
      DO 8 M=ME,M2,2
      MX=MX+IGK*2
      IPX=I+MX
      IPM=IPX+IGK
      AGP=LA*AG
      BB1=COS(AGP)
      BB2=ISIGN*SIN(AGP)
      X1(IPX,K2)=X1(IPX,K1)+X1(IPM,K1)
      X2(IPX,K2)=X2(IPX,K1)+X2(IPM,K1)
      AA1=X1(IPX,K1)-X1(IPM,K1)
      AA2=X2(IPX,K1)-X2(IPM,K1)
      X1(IPM,K2)=BB1*AA1-BB2*AA2
      X2(IPM,K2)=BB2*AA1+BB1*AA2
 8    CONTINUE
      K3=K2
```

```
      K2=K1
      K1=K3
7     CONTINUE
      NP=2
      NG=IPA
      DO 9 I=1,N
9     L(I,1)=I-1
      N1=1
      N2=2
      LEN=N*NP
      NGM=NG-1
      DO 10 M1=1,NGM
      N3=N2
      N2=N1
      N1=N3
      LEN=LEN/NP
      J1=LEN/NP
      I=0
      IX=NP**(M1-1)
      DO 11 I1=1,IX
      DO 11 J=1,NP
      DO 11 K=1,J1
      I=I+1
      KK=(I1-1)*LEN+J+(K-1)*NP
11    L(I,N1)=L(KK,N2)
10    CONTINUE
      IF(MM.EQ.0) GOTO 12
      DO 13 I=1,N
      J=L(I,N1)+1
      X1(I,K2)=Y1(I)
      X2(I,K2)=Y2(I)
      Y1(I)=X1(J,K1)
13    Y2(I)=X2(J,K1)
      DO 17 I=1,N
      X1(I,1)=X1(I,K2)
17    X2(I,1)=X2(I,K2)
      MM=0
      GOTO 6
12    DO 14 I=1,N
      J=L(I,N1)+1
      X1(I,K2)=X1(J,K1)
14    X2(I,K2)=X2(J,K1)
      IF(ISIGN.LT.0) RETURN
      XN=N
      WRITE(6,*) 'N=',XN
      DO 15 I=1,N
      Y1(I)=Y1(I)/XN
      Y2(I)=Y2(I)/XN
      X1(I,K2)=X1(I,K2)/XN
```

```
15    X2(I,K2)=X2(I,K2)/XN
      RETURN
      END
```

C13. Subroutine POWELL

Subroutine POWELL is used in above estimation programs to search the minimum of objective functions by POWELL method.

```
C
C     SUBROUTINE POWELL
C
C     A SUBROUTINE TO SEARCH THE MINIMUM OF
C     A FUNCTION WITH MULTIPLE VARIABLES
C     BY THE POWELL METHOD
C
      SUBROUTINE POWELL(X,Y,FY,N,IMOS,ICOVG,XT,FT,IT)
      DIMENSION X(N),Y(N),DIR(20,20),S(20),W(20),BEF(20)
      COMMON PAI,TN0,TN1,S1,S2
      ITER=0
      IF(IT.GT.0) GOTO 101
      XT=0.001
      FT=0.001
  101 ICOVG=0
      N1=N-1
      TD=FT*0.1
      DO 2 I=1,N
      DO 1 J=1,N
    1 DIR(I,J)=0.0
    2 DIR(I,I)=1.0
      CALL OBF(X,FX)
      STEP=1.0
  102 IF(ITER.EQ.IMOS) GOTO 22
      DO 4 I=1,N
    4 BEF(I)=X(I)
      F1=FX
      SUM=0.0
      DO 9 I=1,N
      DO 5 J=1,N
    5 S(J)=DIR(J,I)
      CALL DSCPOW(X,FX,Y,FY,S,S,N,2,TD,1,ITER,IEX)
      IF(IEX.EQ.1) GOTO 21
      A=FX-FY
      IF(A-SUM) 7,7,6
    6 ISUM=I
      SUM=A
    7 DO 8 J=1,N
    8 X(J)=Y(J)
    9 FX=FY
      F2=FX
      DO 10 I=1,N
   10 W(I)=X(I)-BEF(I)
```

```
      CALL DSCPOW(X,FX,Y,FY,W,W,N,2,TD,1,ITER,IEX)
      IF(IEX.EQ.1) GOTO 21
      DO 41 I=1,N
      IF(W(I).EQ.0.) GOTO 41
      ALPH=ABS((Y(I)-X(I))/W(I))
      GOTO 42
41    CONTINUE
42    IF(ALPH+1.-SQRT((F1-FY)/SUM)) 49,12,12
12    IF(ISUM-N) 13,15,15
13    DO 14 I=ISUM,N1
      I1=I+1
      DO 14 J=1,N
14    DIR(J,I)=DIR(J,I1)
15    A=0.0
      DO 16 J=1,N
      DIR(J,N)=X(J)-BEF(J)
16    A=DIR(J,N)**2+A
      A=1.0/SQRT(A)
      DO 17 J=1,N
      DIR(J,N)=DIR(J,N)*A
17    S(J)=DIR(J,N)
49    FX=FY
      DO 18 I=1,N
18    X(I)=Y(I)
      ITER=ITER+1
19    IF(ABS(F1-FX).GT.(ABS(F1)+1.)*FT) GOTO 102
      DO 20 I=1,N
      IF(ABS(BEF(I)-X(I)).GT.(ABS(BEF(I))+1.)*XT) GOTO 102
20    CONTINUE
      ICOVG=1
      GOTO 23
21    ICOVG=-1
      GOTO 23
22    ICOVG=0
23    RETURN
      END
```

C14. Subroutine DSCPOW

Subroutine DSCPOW is used in Subroutine POWELL to perform one dimensional search for minimum.

```
C
C       SUBROUTINE DSCPOW
C
C       A SUBROUTINE PERFORMING ONE DIMENSIONAL SEARCH
C       OF MINIMUM USED IN SUBROUTINE POWELL
C
        SUBROUTINE
DSCPOW(X,FX,Y,FY,S,DELX,N,INDIC,TOL,ITOL,ITER,IEX)
        DIMENSION X(N),Y(N),S(N),DELX(N)
        IF(ITOL.EQ.1) GOTO 110
        TOL=.001
 110    FTOL2=TOL/100.
        IEX=1
        K=-2
        M=0
        FA=FX
        DA=0.
        STEP=1.0
        D=STEP
        IF(INDIC.EQ.2) GOTO 1
        IF(ITER.EQ.0) GOTO 1
        DXNORM=0.
        SNORM=0.
        DO 102 I=1,N
        DXNORM=DXNORM+DELX(I)*DELX(I)
 102    SNORM=SNORM+S(I)*S(I)
        IF(INDIC.NE.1) GOTO 103
        IF(DXNORM.GE.SNORM) GOTO 1
 103    RATIO=DXNORM/SNORM
        STEP=SQRT(RATIO)
        D=STEP
 1      DO 2 I=1,N
 2      Y(I)=X(I)+D*S(I)
        CALL OBF(Y,F)
        K=K+1
        IF(F-FA) 5,3,6
 3      D=0.5*(DA+D)
        DO 4 I=1,N
 4      Y(I)=X(I)+D*S(I)
        CALL OBF(Y,F)
        IF(F-FA) 204,202,205
 202    DO 203 I=1,N
 203    Y(I)=X(I)+DA*S(I)
```

```
      FY=FA
      GOTO 326
204   FC=FA
      DC=DA+2.*(D-DA)
      FB=F
      DB=D
      GOTO 21
205   STEP=0.5*STEP
      IF(K) 7,8,206
206   DC=D
      D=DA
      DA=DB
      DB=D
      FC=F
      F=FA
      FA=FB
      FB=F
      GOTO 10
5     FC=FB
      FB=FA
      FA=F
      DC=DB
      DB=DA
      DA=D
      D=2.0*D+STEP
      GOTO 1
6     IF(K) 7,8,9
7     FB=F
      DB=D
      D=-D
      STEP=-STEP
      GOTO 1
8     FC=FB
      FB=FA
      FA=F
      DC=DB
      DB=DA
      DA=D
      GOTO 21
9     DC=DB
      DB=DA
      DA=D
      FC=FB
      FB=FA
      FA=F
10    D=0.5*(DA+DB)
      DO 11 I=1,N
11    Y(I)=X(I)+D*S(I)
      CALL OBF(Y,F)
12    IF((DC-D)*(D-DB)) 15,13,18
```

```
 13   DO 14 I=1,N
 14   Y(I)=X(I)+DB*S(I)
      FY=FB
      IF(IEX.EQ.0) GOTO 32
      GOTO 326
 15   IF(F-FB) 16,13,17
 16   FC=FB
      FB=F
      DC=DB
      DB=D
      GOTO 21
 17   FA=F
      DA=D
      GOTO 21
 18   IF(F-FB) 19,13,20
 19   FA=FB
      FB=F
      DA=DB
      DB=D
      GOTO 21
 20   FC=F
      DC=D
 21   IF(ABS(DA-DB).GE.ABS(DC-DB)) GOTO 50
      D=DA
      DA=DC
      DC=D
      F=FA
      FA=FC
      FC=F
 50   IF(ABS((DC-DB)/(DA-DB)).GT.0.25) GOTO 26
      D=0.5*(DA+DB)
      DO 51 I=1,N
 51   Y(I)=X(I)+D*S(I)
      CALL OBF(Y,F)
      IF(F-FB) 52,13,53
 52   FC=FB
      FB=F
      DC=DB
      DB=D
      GOTO 26
 53   FA=F
      DA=D
 26   A=FA*(DB-DC)+FB*(DC-DA)+FC*(DA-DB)
      IF(A) 22,30,22
 22
D=0.5*((DB*DB-DC*DC)*FA+(DC*DC-DA*DA)*FB+(DA*DA-DB*DB)*FC)/A
      IF((DA-D)*(D-DC)) 13,13,23
 23   DO 24 I=1,N
 24   Y(I)=X(I)+D*S(I)
      CALL OBF(Y,F)
```

```
      IF(ABS(FB-F)-(ABS(FB)+FTOL2)*TOL) 28,28,12
28    IEX=0
      IF(F-FB) 29,13,13
29    FY=F
      GOTO 32
30    IF(M) 31,31,13
31    M=M+1
      GOTO 10
32    DO 99 I=1,N
      IF(Y(I).NE.X(I)) GOTO 326
99    CONTINUE
33    IF(NTOL.EQ.5) GOTO 34
      IEX=1
      NTOL=NTOL+1
      TOL=TOL/10.
      GOTO 12
34    IEX=1
      GOTO 35
326   IF(FY.LT.FX) GOTO 36
      IEX=1
      GOTO 35
36    IF(IEX.EQ.0) GOTO 35
      IEX=2
35    RETURN
      END
```

REFERENCES

1. 1978 *Standards of Tubular Exchanger Manufactures Association, Sixth Edition.* New York: The Association.

2. A. Y. KOBRINSKIY 1969 *NASA Technical Translation TTF-534.* Mechanisms with elastic couplings, dynamics and stability.

3. R. I. KUTCHEV and A. G. PAVLOV 1973 *Russian Engineering Journal* 53, 32-35. Influence of a roller-bearing clearance on vibration.

4. J. W. KANNEL and D. K. SNEDIKER 1977 *Machine Design* 49(8), 78-82. The hidden cause of bearing failure.

5. V. I. BABITSKII *1978 Theory of Vibroimpact Systems* (in Russian). Moscow: Nauka.

6. P. ESCHMANN, L. HASBRGER and WEIGAND 1985 *Ball and Roller Bearing Theory, Design and Applications.* New York: Wiley.

7. P. A. ENGEL 1977 *Machine Design* 49(12), 100-105. Predicting impact wear.

8. J. ROSEN 1989 *Mechanical Engineering* Oct. 92-96. On-line monitoring of wear.

9. A. SZCZEPANIK, I. ROY and B. T. KUHNELL 1990 *Journal of Vibration and Acoustics, Transactions of the American Society of Mechanical Engineers* 112, 268-273. Vibration and stress analysis for condition monitoring of symon cone crushers.

10. H. HALLE, J. M. CHENOWETH and M. W. WAMBSGANSS 1980 *Argonne National Laboratory, Argonne Illinois, Report ANL-CT-80-3.* DOE/ANL/HTRI heat exchanger tube vibration data bank.

11. H. A. NELMS and C. L. SEGASER 1969 *ORNL-4399.* Survey of nuclear reactor system primary circuit heat exchangers.

12. Y. S. SHIN and M. W. WAMBSGANSS 1975 *Argonne National Laboratory, Argonne Illinois, Report ANL-75-16,* 26-29. Flow-induced vibration in LMFBR steam generators: A state-of-the-art review.

13. M. G. HARE 1977 *Nuclear Safety* 18, 355-364. Steam generator tube failures: World experience in water-cooled nuclear reactors in 1975.

14. D. S. TATONE and R. S. PATHANIA 1981 *Nuclear Safety* 22, 636-656. Steam generator tube performance: World experience with water-cooled nuclear power reactors during 1979.

15. G. S. WHISTON 1984 *Journal of Sound and Vibration* **97**, 35-51. Remote impact analysis by use of propagated acceleration signals, I: Theoretical methods.

16. R. W. JORDAN and G. S. WHISTON 1984 *Journal of Sound and Vibration* **97**, 53-63. Remote impact analysis by use of propagated acceleration signals, II: Comparison between theory and experiment.

17. Y. BARD 1974 *Nonlinear Parameter Estimation*. New York and London: Academic Press.

18. J. V. BECK 1977 *Parameter Estimation in Engineering and Science*. New York and London: John Wiley & Sons, Inc.

19. N. E. NAHI 1969 *Estimation Theory and Applications*. New York and London: John Wiley & Sons, Inc.

20. N. MOHANTY 1986 *Random Signals Estimation and Identification: Analysis and Applications*. New York: Van Nostrand Reinhold Company.

21. J. S. BENDAT and A. G. PIERSOL 1971 *Random Data: Analysis and Measurement Procedures*. New York: Wiley-Interscience.

22. J. S. BENDAT and A. G. PIERSOL 1980 *Engineering Applications of Correlation and Spectral Analysis*. New York: Wiley-Interscience.

23. C. CEMPEL 1978 *Journal of Sound and Vibration* **60**, 411-416. Detection of clearances in machine kinematic pairs by a coherence method.

24. C. CEMPEL 1979 *Proceedings of the 5th Theory of Machines and Mechanisms conference, Published by the American society of Mechanical Engineers*, 1368-1371. A simple method of clearance detection in kinematic pairs.

25. C. N. BAPAT and N. POPPLEWELL 1987 *Journal of Sound and Vibration* **113**, 17-28. Several similar vibroimpact systems.

26. S. F. MASRI 1978 *Journal of Mechanical Design, Transactions of the American Society of Mechanical Engineers* **100**, 480-486. Analytical and experimental studies of a dynamic system with a gap.

27. S. W. SHAW and P. J. HOLMES 1983 *Journal of Applied Mechanics, Transactions of the American Society of Mechanical Engineers* **50**, 849-850. A periodically forced impact oscillator with large dissipation.

28. S. W. SHAW and P. J. HOLMES 1983 *Physical Review Letters* **51**, 623-626. Periodically forced linear oscillator with impacts: Chaos and long period motion.

29. S. W. SHAW 1985 *Journal of Applied Mechanics, Transactions of the American Society of Mechanical Engineers* **52**, 453-464. The dynamics of a harmonically excited system having rigid amplitude constraints.

30. S. W. SHAW and P. J. HOLMES 1983 *Journal of Sound and Vibration* **90**, 129-155. A periodically forced piecewise linear oscillator.

31. J. C. ANDERSON and S. F. MASRI 1979 *University of Southern California, Los Angeles, Report CE79-07*. Analytical/experimental correlation of a nonlinear system subjected to a dynamic load.

32. S. S. CHEN, G. S. ROSENBERG and M. W. WAMBSGANASS 1970 *Argonne National Laboratory, Argonne Illinois, Report ANL-76-19*. Vibration of a beam with motion-constraint stops.

33. L. E. GALHEND, S. F. MASRI and J. C. ANDERSON 1987 *Journal of Applied Mechanics* 54, 215-225. Transfer function of a class of nonlinear multidegree of freedom oscillators.

34. S. DUBOWSKY and F. FREUDENSTEIN 1971 *Journal of Engineering for Industry, Trans. ASME*, Series D, 93(1), 305-309. Dynamic Analysis of Mechanical Systems with Clearances, Part 1: Formation of Dynamic Model.

35. S. DUBOWSKY and F. FREUDENSTEIN 1971 *Journal of Engineering for Industry, Trans. ASME*, Series D, 93(1), 310-316. Dynamic analysis of mechanical systems with clearances, Part 2: Dynamic response.

36. A. YE. KOBRINSKIY 1964 *Mechanisms with Elastic Couplings: Dynamics and Stability*. Moscow: Nauka Press.

37. J. M. T. THOMPSON and R. GHAFFARI 1982 *Physics Letters* **93** A, 5-8. Chaos after period-doubling bifurcations in the response of an impact oscillator.

38. J. M. T. THOMPSON, A. R. BOKAIAN and R. GHAFFARI 1983 *IMA Journal of Applied Mathematics* **31**, 207-234. Subharmonic resonance and chaotic motions of a bilinear oscillator.

39. G. S. WISTON 1979 *Journal of Sound and Vibration* **67**, 179-186. Impacting under harmonic excitation.

40. D. T. NGUYEN, S. T. NOAH and C. F. KETTLEBOROUGH 1986 *Journal of Sound and Vibration* **109**, 293-307. Impact behavior of an oscillator with limiting stops - Part I: A parametric study.

41. D. T. NGUYEN, S. T. NOAH and C. F. KETTLEBOROUGH 1986 *Journal of Sound and Vibration* **109**, 309-325. Impact behavior of an oscillator with limiting stops - Part II: Dimensionless design parameters.

42. W. T. THOMSON 1960 *Laplace Transformations*. New Jersey: Prentice-Hall, Inc.

43. S. S. RAO 1986 *Mechanical Vibration*. Massachusetts: Addison-Wesley Publishing Company.

44. D. GRAHAM and D. MCRUER 1961 *Analysis of Nonlinear Control Systems.* New York and London: John Wiley & Sons.

45. A. BLAQUIERE 1966 *Nonlinear System Analysis.* New York and London: Academic Press.

46. 1984 *DASH-8 Manual.* Massachusetts: Metrabyte Corporation.

47. W. T. THOMSON 1981 *Theory of Vibration with Application.* New Jersey: Prentice-Hall, Inc.

48. E. O. BRIGHAM 1974 *The Fast Fourier Transform.* New Jersey: Prentice-Hall Inc.

49. R. W. RAMIREZ 1985 *The FFT, Fundamentals and Concepts.* New Jersey: Prentice-Hall, Inc.

50. C. S. BURRUS and T. W. PARKS 1985 *DFT/FFT and Convolution Algorithms: Theory and Implementation.* New York: Wiley.

51. M. J. D. POWELL 1964 *Computer Journal* 7, 155-162. An efficient method for finding the minimum of a function of several variables without calculating derivatives.

52. M. J. D. POWELL 1965 *Computer J*ournal 7, 303-307. A method for minimizing a sum of squares of nonlinear functions without calculating derivatives.

53. J. W. DANIEL 1971 *The Approximate Minimization of Functions.* New Jersey: Prentice-Hall, Inc.

54. Y. BARD 1970 *SIAM J. Numer. Anal.* 7(1). Comparison of gradient methods for the solution on nonlinear parameter estimation.

55. R. D. BLEVINS 1977 *Flow-induced Vibration.* New York: Van Nostrand Rein Co.

56. S. CHEN 1987 *Flow-induced Vibration of Circular Cylindrical Structures.* Washington: Hemisphere Pub. Corp.

57. A. PAPOULIS 1984 *Probability, Random Variables, and Stochastic Processes.* New York: McGraw-Hill Book Company.

58. T. T. SOONG 1973 *Random Differential Equations in Science and Engineering.* New York: Academic Press.

59. A. V. OPPENHEIM and R. W. SCHAFER 1975 *Digital Signal Processing.* New Jersey: Prentice-Hall, Inc.

60. S. M. KAY and S. L. MARPLE 1981 *Proceeding of the IEEE,* 69(11), 1380-1419. Spectrum Analysis - A Modern Perspective.

61. SH. A. ASSAF and L. D. ZIRKLE 1976 *Int. J. Control.* 23(4), 477-492. Approximate analysis of non-linear stochastic systems.

62. S. H. CRANDALL 1980 *Int. J. Non-linear Mechanics*, 15, 303-313. Non-Gaussian closure for random vibration of non-linear oscillators.

63. S. H. CRANDALL 1985 *Int. J. Non-linear Mechanics*, 20(1), 1-8. Non-Gaussian closure techniques for stationary random vibration.

64. R. A. IBRAHIM, A. SOUNDARAJAN and A. HEO 1985 *Journal of Applied Mechanics*, 52, 965-970. Stochastic response of nonlinear dynamic systems based on a non-Gaussian closure.

65. I. I. ORABI and G. AHMADI 1987 *Int. J. Non-linear Mechanics*, 22(6), 451-465. A functional series expansion method for response analysis of non-linear systems subjected to random excitations.

66. R. L. FANTE 1988 *Signal analysis and Estimation, an Introduction.* New York and London: John Wiley & Sons.

67. B. CARNAHAN, H. A. LUTHER and J. O. WILKES 1969 *Applied Numerical Methods.* New York and London: John Wiley & Sons.

68. T. WATANABE 1978 *ASME Journal of Mechanical Design* 100(3), 487-491. Forced vibration of continuous systems with nonlinear boundary conditions.

69. S. F. MASRI, Y. A. MARIAMY and J. C. ANDERSON 1981 *ASME Journal of Applied Mechanics* 48, 404-410. Dynamic response of a beam with a geometric nonlinearity.

70. M. TAKAMURA, T. MATINA and S. YAMAZAKI 1966 *Review of Electrical Communication Laboratory* 14, 13-26. Study on rebound displacement of vibratory system.

71. C. C. LO 1980 *Journal of Sound and Vibration* 69(2), 245-255. A cantilever beam chattering against a stop.

72. Y. S. SHIN, D. E. SASS and M. W. WAMBSGANASS 1975 *Argonne National Laboratory, Argonne Illinois, Report ANL-CT-76-06.* Preliminary studies on dynamics of beam/stop impact: numerical analysis.

73. G. J. BOHM and A. N. NAHAVANDI 1972 *Nucl. Sci. Eng.* 47, 391-408. Dynamic analysis of reactor internal structures with impact between components.

74. R. J. RAGERS and R. J. PICK 1976 *Nuclear Engineering and Design* 36, 81-90. On the dynamic spatial response of a heat exchanger tube with intermittent baffle contacts.

75. Y. S. SHIN, D. E. SASS and J. A. JENDRZEJCZYK 1978 *Argonne National Laboratory, Argonne Illinois, Report ANL-CT-78-11.* Vibro-impact responses of a tube with tube-baffle interaction.

76. P. L. KO and R. J. ROGERS 1981 *Nuclear Engineering and Design* 65, 399-409. Analytical and experimental studies of tube/support interaction in multi-span heat exchanger tubes.

77. P. M. MORETTI and R. L. LOWERY Mar. 11-15, 1973 *AICHE 74th National Meeting, New Orleans, Louisiana.* Natural frequencies and damping of tubes in shell-and-tube heat exchangers.

78. R. L. LOWERY and P. M. MORETTI Aug. 1975 *AICHE 15th National Heat Transfer Conference, San Francisco, Ca.* Natural frequencies and damping of tubes on multiple supports.

79. Y. S. SHIN, J. A. JENDRZEJCZYK and M. W. WAMBSGANSS 1977 *Argonne National Laboratory, Argonne Illinois, Report ANL-CT-77-5.* Effect of tube/support interaction on the vibration of a tube on multiple support.

80. Y. S. SHIN, J. A. JENDRZEJCZYK and M. W. WAMBSGANSS Sept. 12-18, 1977 *ASME Joint Power Generation Conference, Long Beach, Ca.* Vibration of a heat exchanger tube with tube/support impact.

81. S. S. CHEN, J. A. JENDRZEJCZYK and M. W. WAMBSGANSS 1985 *Journal of Pressure Vessel Technology* **107**, 7-17. Dynamics of tubes in fluid with tube-baffle interaction.

82. J. A. JENDRZEJCZYK 1986 *Journal of Pressure Vessel Technology* **108**, 256-266. Dynamics characteristics of heat exchanger tubes vibrating in a tube support plate inactive mode.

83. J. A. JENDRZEJCZYK 1984 *Argonne National Laboratory, Argonne Illinois, Report ANL-84-39* Dynamics characteristics of heat exchanger tubes vibrating in a tube support plate inactive mode.

84. C. N. BAPAT and C. BAPAT 1987 *Journal of Sound and Vibration* **112**(1), 177-182. Natural frequencies of a beam with non-classical boundary conditions and concentrated masses.

85. S. Q. LIN and C. N. BAPAT 1990 *Journal of Sound and Vibration* **142**, 343-354. Free and forced vibration of a beam supported at many locations.